

**Decellularised dental pulp tissue as a potential biological
scaffold for endodontic tissue regeneration**

Hayat Abdulaziz Alghutaimel

Submitted in accordance with the requirements for the degree of

Doctor of Philosophy

The University of Leeds

School of Dentistry

February 2021

Declaration

The candidate confirms that the work submitted is her own and that appropriate credit has been given where reference has been made to the work of others. This copy has been supplied on the understanding that it is a copyright material and that no quotation from the thesis may be published without proper acknowledgement. The right of Hayat Abdulaziz Alghutaimel to be identified as an author of this work has been asserted by her in accordance with the Copyright, Designs and Patents Act 1988.

This thesis contains research work from a jointly-authored publication:

Alghutaimel, H., Yang, X., Drummond, B., Nazzal, H., Duggal, M. and Raïf, E., 2021. Investigating the vascularization capacity of a decellularized dental pulp matrix seeded with human dental pulp stem cells: *in vitro* and preliminary *in vivo* evaluations. *International Endodontic Journal*. DOI: 10.1111/iej.13510.

I was responsible for all the laboratory work and manuscript drafting. The remaining co-authors reviewed the manuscript and provided guidance on its final layout.

© 2021 The University of Leeds and Hayat Abdulaziz Alghutaimel

Acknowledgements

This PhD project has been a life-enriching experience and a transformative journey for me as a clinician. It has endured academic highs and lows and would have been impossible without god's blessings followed by constant support from people to whom I would like to express my sincere gratitude and appreciation.

From an academic perspective, I would like to thank my supervisors; Dr El Mostafa Raïf, Dr Xuebin Yang, Professor Bernadette Drummond, Dr Hani Nazzal and Professor Monty Duggal for guiding me through this project with patience, considerable expertise and unconditional assistance and support. Special thank goes to Dr Raïf, my lead supervisor, whose assistance and support has been invaluable throughout.

I would also like to extend my thanks to Mrs Sue Keat, Dr Mannaa Aldowsari and Dr Abdulwadood Sharqawi for their assistance in bovine tissue procurement, Dr Filomena Esteves for the training in histological and immunohistochemical staining techniques and microscopy, Dr Jehan El-Jawhari for the training in cell characterisation and flowcytometry, Mr Matthew Percival for the training in teeth sectioning and root slices preparation, Dr Sarah Myers for the training in cell culture and general laboratory use and Mrs Jaqueline Hudson for the training in scanning electron microscopy. Extended thanks go to all the staff and colleagues at the oral biology department for their support and friendship and to all the staff at the animal facility at St. James Biomedical Services for making my *in vivo* research experience delightful.

I would also like to extend my thanks to all the staff and colleagues at the paediatric dentistry department for their support and friendship, with special

thanks to Dr Jinous Tahmassebi for her continuous encouragement, unlimited kindness and unconditional support throughout the course of this project. Extended thank goes to my dear friend Dr Manal Matoug-Elwerfelli for sharing her valuable experience in tissue decellularisation and for her constant support, motivation and willingness to help.

I would also like to thank King Saud Bin Abdulaziz University for Health Sciences in Saudi Arabia for funding my research project and for the financial support to undertake my postgraduate study.

Finally, I have to mention the enduring support from my family, parents (Abdulaziz and Aziza) and siblings (Hamad, Hanan, Hatem, Hosam, Sahar and May), who supported me along the way and are now delighted that the end is approaching.

I would say thank you from the bottom of my heart to my family, but my heart has no bottom for them.

Dedication

To all patients, may the fruits of this research be of service to you.

Abstract

Background: There is an unmet need for regenerating functional dental pulp, particularly in non-vital immature permanent teeth where dental pulp necrosis arrests further radicular maturation, putting young patients at risk of tooth loss. Despite the progress achieved over recent decades, dental pulp regeneration still faces challenges in promoting post-implantation vascularisation and inducing odontoblast-like cell differentiation.

Aim: The overall aim of the research presented in this thesis was to investigate the potential of a decellularised dental pulp matrix (DDP) of bovine origin to facilitate vascularisation and support dental pulp regeneration.

Methods: Bovine dental pulp tissues were retrieved and decellularised. The efficiency of the decellularisation method was evaluated using histological analysis, DNA quantification assay, immunohistochemical staining and scanning electron microscopy. Furthermore, the cytocompatibility of the developed DDPs were assessed using contact and extract cytotoxicity assays. DDPs were then recellularised with human dental pulp stem cells (hDPSCs) and analysed *in vitro* using scanning electron microscopy, fluorescent staining and confocal scanning laser microscopy, Live/Dead[®] cells assay, Quant-iT[™] PicoGreen[®] dsDNA assay and histology. The effect of DDPs on gene expression of markers involved in angiogenesis and odontogenesis in hDPSCs was evaluated *in vitro* using reverse-transcription quantitative polymerase chain reaction (RT-qPCR). A preliminary *in vivo* study was then conducted in which hDPSCs-seeded and unseeded DDPs were inserted in debrided human premolar root slices and implanted subcutaneously into immunodeficient mice. Samples were retrieved after 30 days and analysed using histological and immunohistochemical staining.

Results: Acellular dental pulp matrices retaining the native histoarchitecture, vasculature, essential extracellular matrix components and several growth factors were generated following bovine dental pulp decellularisation. The *in vitro* cytocompatibility evaluation of the developed DDPs revealed no apparent cytotoxic effect on the growth and morphology of the cells grown in direct contact with the DDPs, and on the viability of cells grown in an extract of DDPs. Upon recellularisation of the DDPs with hDPSCs, the *in vitro* analyses showed cell engraftment with progressive repopulation of the matrix and vasculature of the DDPs, and with enhanced gene expression of the markers involved in angiogenesis and odontogenesis. *In vivo* implantation of root slices with hDPSCs-seeded DDPs revealed apparent vascularisation enhancement, whilst those with unseeded DDPs showed host cell recruitment and infiltration.

Conclusions: The developed DDP is a cytocompatible, pro-angiogenic and pro-odontogenic scaffold characterised by the retention of native histoarchitecture, vasculature, essential extracellular matrix components and angiogenic and odontogenic growth factors in the matrix following decellularisation. Seeding of hDPSCs onto the DDP led to progressive cell repopulation of the matrix and vasculature, enhanced expression of the markers involved in angiogenesis and odontogenesis in hDPSCs and improved *in vivo* vascularisation capacity of the DDP. Moreover, the DDP has a chemotactic activity *in vivo*, enabling host cells mobilisation and recruitment. The findings of this research suggest that a combination of DDP and hDPSCs could provide a promising vascularisation promoting strategy for dental pulp regeneration via cell transplantation. Furthermore, the use of DDP, in its acellular form, could provide a strategy for dental pulp regeneration via cell homing.

Table of Contents

Title page	I
Declaration	II
Acknowledgements	III
Dedication	V
Abstract	VI
Table of Contents	VIII
List of Figures	XIII
List of Tables	XVII
List of Abbreviations	XVIII
Chapter 1 General introduction	1
1.1 Justification of the subject matter	1
1.2 Hypothesis	4
1.3 Scope of the research.....	4
1.4 Thesis structure	5
Chapter 2 Literature review	6
2.1 Dental pulp biology	6
2.1.1 Embryonic development of the dental pulp	7
2.1.2 Histological characteristics of the dental pulp	8
2.1.3 Physiological functions of the dental pulp	15
2.2 Dental pulp necrosis in young permanent teeth with developing roots	17
2.2.1 Interventions for treating immature permanent teeth with pulpal necrosis	19
2.3 Dental pulp tissue engineering.....	40
2.3.1 Challenges facing dental pulp tissue engineering	44
2.4 Decellularised biological scaffolds	46
2.4.1 Methods of tissue decellularisation	46
2.4.2 Evaluation of tissue decellularisation	52
2.4.3 Effects of decellularised scaffolds on stem cell behaviours	53
2.4.4 Decellularised scaffolds of dental origin.....	54
2.5 Summary.....	60
2.6 Aim and objectives.....	61
Chapter 3 Materials and Methods	62
3.1 Materials	62

3.1.1 Equipment.....	62
3.1.2 Consumables.....	64
3.1.3 Chemical reagents and kits.....	66
3.1.4 Antibodies.....	71
3.1.5 TaqMan gene expression assays.....	74
3.2 Methods.....	75
3.2.1 Acquisition of bovine dental pulps.....	75
3.2.2 Basic techniques for the histological and immunohistochemical staining methods.....	76
3.2.3 Histological staining methods.....	80
3.2.4 Immunohistochemical staining technique.....	84
3.2.5 Scanning electron microscopy.....	91
3.2.6 DNA extraction.....	91
3.2.7 DNA quantification.....	93
3.2.8 Cell culture techniques.....	95
3.2.9 Cell characterisation of human dental pulp stem cells.....	100
3.2.10 Cell seeding onto the scaffolds using a dynamic technique..	104
3.2.11 Cell viability analysis.....	105
3.2.12 Gene expression analysis using RT-qPCR.....	107
3.2.13 Statistical analysis.....	111
Chapter 4 Development of a decellularised bovine dental pulp matrix.....	112
4.1 Introduction.....	112
4.2 Aim and objectives.....	114
4.3 Experimental approach.....	115
4.4 Methods.....	116
4.4.1 Decellularisation protocols.....	116
4.4.2 Evaluation of decellularisation protocols efficiency.....	122
4.5 Results.....	123
4.5.1 Cell nuclei and DNA removal efficiency following bovine dental pulp decellularisation using protocol I.....	123
4.5.2 Cell nuclei and DNA removal efficiency following bovine dental pulp decellularisation using protocol II.....	127
4.6 Discussion.....	130
Chapter 5 Characterisation of the developed decellularised dental pulp matrix.....	134
5.1 Introduction.....	134

5.2 Aim and objectives.....	136
5.3 Experimental approach	137
5.4 Methods	137
5.4.1 Histological staining	137
5.4.2 Immunohistochemical staining	137
5.4.3 Scanning electron microscopy	138
5.5 Results.....	139
5.5.1 Retention of native pulpal histoarchitecture in the developed decellularised dental pulps	139
5.5.2 Retention of extracellular matrix components in the developed decellularised dental pulps	141
5.5.3 Retention of growth factors in the developed decellularised dental pulps.....	147
5.5.4 Elimination of alpha-gal epitope from the developed decellularised dental pulps	153
5.5.5 Surface topography of the developed decellularised dental pulps	153
5.6 Discussion.....	156
Chapter 6 <i>In vitro</i> performance of the developed decellularised dental pulp matrix	161
6.1 Introduction.....	161
6.2 Aim and objectives.....	164
6.3 Experimental approach	165
6.4 Methods	165
6.4.1 Cytocompatibility evaluation	166
6.4.2 Characterisation of hDPSCs prior to seeding onto the surface of decellularised dental pulps	168
6.4.3 Seeding of hDPSCs onto the surface of the decellularised dental pulps using a dynamic cell seeding technique.....	170
6.4.4 Scanning electron microscopy	171
6.4.5 Fluorescent staining and confocal scanning laser microscopy	172
6.4.6 Cell viability analysis.....	172
6.4.7 Cell proliferation analysis	173
6.4.8 Histological analysis.....	175
6.4.9 Gene expression analysis using RT-qPCR	175
6.4.10 Immunohistochemical staining.....	177
6.5 Results.....	178

6.5.1	Cytocompatibility evaluation using contact cytotoxicity assay.....	178
6.5.2	Cytocompatibility evaluation using extract cytotoxicity assay.....	179
6.5.3	The harvested populations of hDPSCs exhibited mesenchymal stem cell characteristics	181
6.5.4	hDPSCs attached to the surface of the decellularised dental pulp matrix.....	190
6.5.5	hDPSCs organised in tube-like structures following seeding onto the surface of the decellularised dental pulp matrix	190
6.5.6	hDPSCs maintained viability following seeding onto the surface of the decellularised dental pulp matrix	192
6.5.7	hDPSCs proliferated following seeding onto the surface of the decellularised dental pulp matrix	193
6.5.8	hDPSCs repopulated the matrix and vasculature of the decellularised dental pulp matrix	195
6.5.9	The effects of decellularised dental pulp on gene expression of markers involved in angiogenesis and odontogenesis in hDPSCs	199
6.5.10	Detection and localisation of CD31-positive cells in hDPSCs-seeded decellularised dental pulp matrix <i>in vitro</i>	210
6.5.11	Detection and localisation of DSPP in hDPSCs-seeded decellularised dental pulp matrix <i>in vitro</i>	212
6.6	Discussion.....	214
Chapter 7 <i>In vivo</i> performance of the developed decellularised dental pulp matrix		221
7.1	Introduction.....	221
7.2	Aim and objectives.....	223
7.3	Experimental approach	224
7.4	Methods	224
7.4.1	Preparation of the root slices	224
7.4.2	Preparation of the root slice/scaffold constructs.....	225
7.4.3	<i>In vivo</i> implantation	225
7.4.4	Histological and immunohistochemical analyses	226
7.4.5	Quantification of the blood-perfused vessels in the experimental samples	227
7.5	Results.....	229
7.5.1	Macroscopic analysis of the tissues-engineered <i>in vivo</i> using hDPSCs-seeded and unseeded decellularised dental pulps	229

7.5.2 Histological analysis of the tissues-engineered <i>in vivo</i> using hDPSCs-seeded and unseeded decellularised dental pulps	231
7.5.3 Detection and localisation of hDPSCs in the tissues-engineered <i>in vivo</i> using hDPSCs-seeded decellularised dental pulps	237
7.5.4 Quantification of the blood-perfused vessels in the tissues-engineered <i>in vivo</i> using hDPSCs-seeded and unseeded decellularised dental pulps	237
7.6 Discussion.....	240
Chapter 8 General discussion, conclusions and future directions	244
8.1 General discussion	244
8.2 Conclusions	254
8.3 Future directions	255
References.....	257
Appendices.....	296
Appendix A: Ethical approvals	296
Appendix B: Presentations and scientific awards.....	300

List of Figures

Figure 2-1: Gross anatomy of the tooth.....	6
Figure 2-2: Morphological zones of the dental pulp.	9
Figure 3-1: Bovine dental pulp harvesting.....	76
Figure 3-2: Representative image of the rotary dynamic seeding apparatus used in the scaffolds seeding process.....	105
Figure 4-1: Flowchart demonstrates decellularisation protocol I.....	120
Figure 4-2: Flowchart demonstrates decellularisation protocol II.....	121
Figure 4-3: Bright-field microscopic images of native and decellularised bovine dental pulps stained with H&E.....	125
Figure 4-4: Florescent microscopic images of native and decellularised bovine dental pulps stained with DAPI.....	125
Figure 4-5: Bar graph demonstrates the DNA content of native and decellularised bovine dental pulps as determined by the NanoDrop spectrophotometer.....	126
Figure 4-6: Bright-field microscopic images of native and decellularised bovine dental pulps stained with H&E.....	128
Figure 4-7: Florescent microscopic images of native and decellularised bovine dental pulps stained with DAPI.....	128
Figure 4-8: Bar graph demonstrates the DNA content of native and decellularised bovine dental pulps as determined by the NanoDrop spectrophotometer.....	129
Figure 5-1: Bright-field microscopic images of PicroSirius Red-stained tissue sections of native and decellularised bovine dental pulps.	140
Figure 5-2: Bright-field microscopic images of Alcian Blue-stained tissue sections of native and decellularised bovine dental pulps.	140
Figure 5-3: Bright-field microscopic images of native and decellularised bovine dental pulps labelled with anti-collagen I and the corresponding control isotype antibody.....	143
Figure 5-4: Bright-field microscopic images of native and decellularised bovine dental pulps labelled with anti-collagen III and the corresponding control isotype antibody.....	144
Figure 5-5: Bright-field microscopic images of native and decellularised bovine dental pulps labelled with anti-fibronectin and the corresponding control isotype antibody.....	145
Figure 5-6: Bright-field microscopic images of native and decellularised bovine dental pulps labelled with anti-laminin and the corresponding control isotype antibody.....	146

Figure 5-7: Bright-field microscopic images of native and decellularised bovine dental pulps labelled with an antibody against bovine VEGF-A and its corresponding control isotype.	149
Figure 5-8: Bright-field microscopic images of native and decellularised bovine dental pulps labelled with an antibody against bovine FGF-2 and its corresponding control isotype.....	150
Figure 5-9: Bright-field microscopic images of native and decellularised bovine dental pulps labelled with an antibody against bovine TGF-β1 and its corresponding isotype antibody.....	151
Figure 5-10: Bright-field microscopic images of native and decellularised bovine dental pulps labelled with an antibody against bovine BMP2 antigen and its corresponding control isotype.	152
Figure 5-11: Bright-field microscopic images of native and decellularised bovine dental pulps labelled with antibody against bovine alpha-gal epitope and the corresponding isotype antibody.	154
Figure 5-12: Scanning electron microscopic images of native and decellularised bovine dental pulps.	155
Figure 6-1: Cell seeding density determination.	171
Figure 6-2: A curve of Lambda DNA standards.....	174
Figure 6-3: Validation of GAPDH as a house keeping gene.	177
Figure 6-4: Contact cytotoxicity assay.....	179
Figure 6-5: Extract cytotoxicity assay.....	180
Figure 6-6: Images of hDPSCs cultured in monolayers and viewed using an inverted phase-contrast microscope.....	181
Figure 6-7: An example of the gating strategy used in analysing the expression of a single stem cell surface marker in hDPSCs.	183
Figure 6-8: Expression of CD105, CD146 and CD90 in hDPSCs cultured under basal conditions and analysed using a flowcytometer.	184
Figure 6-9: Expression of CD45 in hDPSCs cultured under basal conditions and analysed using a flowcytometer.	185
Figure 6-10: Bright-field microscopic images of hDPSCs stained with alizarin red after three weeks of culture under osteogenic conditions.....	187
Figure 6-11: Bright-field microscopic images of hDPSCs stained with Oil red after three weeks of culture under adipogenic conditions.	188
Figure 6-12: Bright-field microscopic images of hDPSCs stained with Alcian Blue after three weeks of culture under chondrogenic conditions.....	189

Figure 6-13: Images of hDPSCs after three days of seeding onto the surface of the decellularised dental pulps viewed using a conventional high vacuum SEM.	191
Figure 6-14: Images of hDPSCs after seven days of seeding onto the decellularised dental pulps stained using Alexa-Fluor® 488 Phalloidin and DAPI and visualised using a confocal scanning laser microscope.	192
Figure 6-15: Images of hDPSCs seeded onto the decellularised dental pulps and analysed using Live/Dead® staining and a confocal scanning laser microscope.....	193
Figure 6-16: Bar graph demonstrates the dsDNA content of decellularised dental pulps after seeding with hDPSCs as determined using Quant-iT™ PicoGreen® dsDNA assay.	194
Figure 6-17: Bright-field microscopic images of H&E-stained sections of decellularised dental pulps seeded with hDPSCs and cultured <i>in vitro</i> for 7 days.	196
Figure 6-18: Bright-field microscopic images of H&E-stained sections of decellularised dental pulps seeded with hDPSCs and cultured <i>in vitro</i> for 14 days.	197
Figure 6-19: Bright-field microscopic images of H&E-stained sections of decellularised dental pulps seeded with hDPSCs and cultured <i>in vitro</i> for 21 days.	198
Figure 6-20: Bar graphs demonstrate the changes in KDR gene expression in hDPSCs grown on the decellularised dental pulps relative to similar cells grown on the controls.	201
Figure 6-21: Bar graphs demonstrate the changes in PECAM-1 gene expression level in hDPSCs grown on the decellularised dental pulps compared to similar cells grown on the controls.	203
Figure 6-22: Bar graphs demonstrate the changes in DSPP gene expression in hDPSCs grown on the decellularised dental pulps relative to similar cells grown on the controls.	205
Figure 6-23: Bar graphs demonstrate the changes in DMP-1 gene expression in hDPSCs grown on the decellularised dental pulps compared to similar cells grown on the controls.	207
Figure 6-24: Bar graphs demonstrate the changes in MEPE gene expression in hDPSCs grown on the decellularised dental pulps compared to similar cells grown on the controls.	209
Figure 6-25: Detection and localisation of CD31-positive cells in hDPSCs-seeded decellularised dental pulps.	211
Figure 6-26: Detection and localisation of DSPP expression in hDPSCs-seeded decellularised dental pulps.....	213
Figure 7-1: Surgical implantation of the root slice/scaffold constructs in the dorsal subcutaneous space of SCID mice.	228
Figure 7-2: A representative image of a mouse at the samples' retrieval time.	229

Figure 7-3: Macroscopic images of the root slice/scaffold constructs at the retrieval time.	230
Figure 7-4: Bright-field microscopic images of H&E-stained sections of a root slice with native dental pulp.	233
Figure 7-5: Bright-field microscopic images of H&E-stained sections of the tissue-engineered <i>in vivo</i> in a root slice using unseeded decellularised dental pulp.....	234
Figure 7-6: Bright-field microscopic images of H&E-stained sections of the tissue-engineered <i>in vivo</i> in a root slice using hDPSCs-seeded decellularised dental pulp.....	235
Figure 7-7: Bright-field microscopic images of H&E-stained sections of the tissue grew in an empty root slice following implantation into SCID mouse.....	236
Figure 7-8: Bright-field microscopic images of the tissues-engineered <i>in vivo</i> using hDPSCs-seeded and unseeded decellularised dental pulps labelled with an antibody against human nuclei and the corresponding control isotype.	238
Figure 7-9: Box plot demonstrates the blood-perfused vessels density in the tissues-engineered <i>in vivo</i> using hDPSCs-seeded and unseeded decellularised dental pulps compared to native dental pulps.	239

List of Tables

Table 2-1: A summary of the studies comparing the outcomes of current clinical interventions for treating non-vital immature permanent teeth.....	33
Table 2-2: Biomaterials used as scaffolds in dental pulp regeneration.	42
Table 2-3: Methods of tissue decellularisation.....	47
Table 2-4: A summary of the studies on dental tissues-derived decellularised scaffolds.	56
Table 3-1: Details of the laboratory equipment used in the present study.	62
Table 3-2: Details of the laboratory consumables used in the present study.	64
Table 3-3: Details of the chemical reagents and kits used in the present study.	66
Table 3-4: Details of the primary and control isotype antibodies used in the immunohistochemical staining.	71
Table 3-5: Details of the fluorochrome-conjugated primary and isotype antibodies used in the flowcytometric analysis of the cell surface markers.....	73
Table 3-6: Details of TaqMan gene expression assays used in the RT-qPCR.	74
Table 3-7: Details of Leica TP1020's overnight tissue processing program.	78
Table 3-8: A summary of the antigen-unmasking techniques used in the immunohistochemical staining.	86
Table 3-9: A summary of the Immunohistochemical staining process of formalin-fixed paraffin-embedded tissue sections.	87
Table 3-10: A summary of cell types and cell specific culture media used in the study.	96
Table 3-11: Dilutions of the fluorochrome-conjugated primary and isotype antibodies used in the flowcytometric analysis of the cell surface markers.	102
Table 4-1: Decellularisation solutions.....	118
Table 6-1: Details of the donors of human dental pulp stem cells.	168

List of Abbreviations

%	Percentage
°C	Degree Celsius
rpm	Revolution per minute
mg	Milligram
Mg²⁺	Magnesium
mL	Millilitre
μ	Micron
μg	Microgram
μL	Microliter
μm	Micrometre
mm	Millimetre
U	Unites
w/v	Weight per volume
v/v	Volume per volume
Alpha MEM	Alpha modified eagle's medium
ANOVA	Analysis of variance
BMP-2	Bone morphogenic protein 2
Ca(OH)₂	Calcium hydroxide
Ca²⁺	Calcium
CD31	Cluster of differentiation 31
CO₂	Carbon dioxide
DAB	3,3'-diaminobenzidine
DAPI	4',6-diamidino-2-phenylindole
DDP	Decellularised dental pulp

DMEM	Dulbecco's modified Eagle's medium
DMP-1	Dentine matrix protein-1
DMSO	Dimethyl sulfoxide
DNA	Deoxyribonucleic acid
DNase	Deoxyribonuclease
DSPP	Dentine sialophosphoprotein
ECM	Extracellular matrix
EDTA	Ethylene-diamine-tetra-acetic acid
FBS	Foetal bovine serum
FGF-2	Fibroblast growth factor 2
GAGs	Glycosaminoglycans
GAPDH	Glyceraldehyde-3-phosphate dehydrogenase
H&E	Haematoxylin and eosin
hDPSCs	Human dental pulp stem cells
HERS	Hertwig's epithelial root sheath
KDR	Kinase insert domain receptor
KIU	Kallikrein inhibitor unit
MEPE	Matrix extracellular phosphoglycoprotein
mRNA	Messenger ribonucleic acid
MTA	Mineral trioxide aggregate
PAA	Peracetic acid
PBS	Phosphate buffered saline
PECAM-1	Platelet and endothelial cell adhesion molecule
PGA	Polyglycolic acid
PLA	Polylactic acid
PLGA	Copolymer of PGA and PLA
RET	Regenerative endodontic therapy

RNA	Ribonucleic acid
RNase	Ribonuclease
SCAP	Stem cells from apical papilla
SDS	Sodium dodecyl sulphate
SEM	Scanning electron microscope
SHED	Stem cells from exfoliated deciduous teeth
TBS	Tris-buffered saline
TGF-β1	Transforming growth factor β 1
VEGF	Vascular endothelial growth factor
VEGF-A	Vascular endothelial growth factor A

Chapter 1

General introduction

*This chapter justifies the purpose of the research presented in this thesis;
states the central hypothesis and the framework of the thesis.*

1.1 Justification of the subject matter

The occurrence of dental pulp necrosis in young permanent teeth with developing roots due to either traumatic dental injuries, caries or developmental anomalies often represents a challenging clinical situation (Nazzal and Duggal, 2017). Once the dental pulp tissue becomes necrotic, the natural process of root maturation comes to a halt, rendering the affected tooth weak with short and thin brittle root walls. This situation increases the probability of subsequent root fracture and puts the young patient at risk of tooth loss (Cvek, 1992). The loss of permanent teeth in children and young adolescents alters the growth of the jawbone, interferes with speech, mastication and smile aesthetics, and negatively impacts the quality of life (Thelen *et al.*, 2011, Diogenes *et al.*, 2016).

Dental pulp regeneration using a tissue engineering approach can circumvent the consequences of pulpal necrosis in young permanent teeth with developing roots (Sui *et al.*, 2019). It has been shown that seeding a scaffold with dental stem cells and transplanting the engineered construct *in vivo* could give rise to dental pulp-like tissue (Huang *et al.*, 2010, Rosa *et al.*, 2013, Zhu *et al.*, 2018). However, securing adequate blood supply, in order to maintain the viability and function of

the cells within the engineered construct post-implantation, remains a challenge (Dissanayaka and Zhang, 2017). At the time of *in vivo* implantation, the engineered construct represents a free graft with no direct connection to the host vasculature. The cells, at that time, are provided with nutrients and oxygen solely via diffusion from the nearby host microvessels (Rouwkema *et al.*, 2008). Since the diffusion of nutrients and oxygen only serves to a distance of 200 μm (Carmeliet and Jain, 2000), cells beyond this diffusional distance undergo rapid apoptosis rapidly post-implantation (Muschler *et al.*, 2004). Although host microvessels usually invade the engineered construct as a result of signals produced by the cells in response to hypoxia, this vascular ingrowth happens very slowly (Rouwkema *et al.*, 2008). Therefore, the development of a strategy to promote vascularisation of the engineered construct following *in vivo* implantation is critical for the success of dental pulp regeneration.

Several strategies have been suggested to enhance vascularisation during dental pulp regeneration. These include incorporating angiogenic growth factors into the transplanted construct (Richardson *et al.*, 2001, Mullane *et al.*, 2008, Yadlapati *et al.*, 2017), co-culturing endothelial cells with the target stem cells into the scaffold before transplantation (Dissanayaka *et al.*, 2014, Dissanayaka *et al.*, 2015), and using a scaffold with prefabricated microvessels (Athirasala *et al.*, 2017). Unfortunately, these strategies pose many limitations including poor control over the delivery of growth factors, challenging manipulation of endothelial cells and the translational hurdle of a scaffold with prefabricated microvessels (Dissanayaka and Zhang, 2017).

Another challenge that dental pulp regeneration approaches face is the lack of adequate signalling cues to promote odontoblast-like cell differentiation (Dissanayaka and Zhang, 2020, Huang *et al.*, 2020). Current approaches for

dental pulp regeneration have focused on the delivery of single or multiple growth factors to induce cell differentiation into dental pulp specific lineage (Vo *et al.*, 2012). However, the dosage of growth factors, time of delivery and long-term stability make the translational potential of these approaches difficult (Ravindran and George, 2015). During normal body development and repair, the extracellular matrix provides stem cells with numerous growth factors in a unique combination during each stage of growth and differentiation. Therefore, it is not realistic to expect that adding a single or multiple growth factors would generate the same effect as the complex extracellular matrix environment.

Tissue decellularisation is a strategy by which a tissue-specific acellular scaffold could be prepared with highly preserved extracellular matrix structure and composition, and, interestingly, retained native vasculature (Crapo *et al.*, 2011). The use of decellularised scaffolds in regenerative medicine applications has been shown to facilitate vascularisation of the engineered constructs (Menon *et al.*, 2003, Silverman *et al.*, 2004, Liu *et al.*, 2011, Pellegata *et al.*, 2018) and provide an instructive environment for stem cell differentiation (French *et al.*, 2012, Cheung *et al.*, 2014, Ning *et al.*, 2015, Zhang and Dong, 2015, Agmon and Christman, 2016, Swinehart and Badylak, 2016, Robb *et al.*, 2017). When a tissue is decellularised, the cellular components are eliminated leaving behind a relatively conserved extracellular matrix with retained vascular network and several structural and functional components and biological cues that interact naturally with the cells of that particular tissue (Hoshiba *et al.*, 2010). This makes decellularised scaffolds promising platforms to facilitate vascularisation and provide stem cells with a structural framework and biological signalling necessary to promote tissue-specific cell differentiation (Agmon and Christman, 2016, Pellegata *et al.*, 2018). Therefore, it can be hypothesised that a decellularised

dental pulp with retained native histoarchitecture, composition and vasculature might facilitate vascularisation during dental pulp regeneration and help in promoting cell differentiation into dental pulp-specific lineage.

1.2 Hypothesis

The central hypothesis of the research presented in this thesis states that:

“Decellularised dental pulp matrix with retained native histoarchitecture, composition and vasculature might has the potential to facilitate vascularisation during dental pulp regeneration, and might also help in providing proper signalling to stimulate stem cell differentiation into odontoblast-like cells”

1.3 Scope of the research

In this thesis, decellularised dental pulps (DDPs) were prepared through bovine dental pulp decellularisation. The DDPs were then characterised for the retention of native histoarchitecture, vasculature, composition and surface topography. The cytocompatibility of the DDPs was then assessed. The DDPs were seeded with human dental pulp stem cells (hDPSCs), and their vascularisation capacity in addition to their potential to promote odontoblast-like cell differentiation were investigated *in vitro*. Furthermore, the vascularisation capacity of DDPs seeded with hDPSCs and the regenerative potential of DDPs seeded or unseeded with hDPSCs were preliminary assessed *in vivo* using a semi-orthotopic dental pulp regeneration model.

The research work presented in this thesis represents a first step towards understanding the potential of a DDP to promote post-implantation vascularisation and support dental pulp regeneration. The findings of the research work presented in this thesis form a foundation for further future

research towards translating the DDP for clinical use in regenerative endodontic therapy.

1.4 Thesis structure

A detailed literature review is provided in Chapter 2, followed by the main aim and objectives of the research presented in this thesis. The general materials and methods that were used throughout the experimental work are then outlined in Chapter 3.

The experimental work is then described and discussed in Chapter 4, Chapter 5, Chapter 6 and Chapter 7. Chapter 4 describes and discusses the process of developing DDPs through bovine dental pulp decellularisation, followed by Chapter 5 about the characterisation of the developed DDPs. Chapter 6 describes and discusses the cytocompatibility testing and the *in vitro* performance of the developed DDPs. Chapter 7 presents and discusses the *in vivo* performance of the developed DDPs in a semi-orthotopic dental pulp regeneration model.

The general discussion, conclusions and future directions are then contained in Chapter 8.

Chapter 2

Literature review

2.1 Dental pulp biology

Dental pulp is a soft tissue residing within the pulp space and constituting the vital tissue component of the tooth (Figure 2-1). This tissue, which is most commonly referred to as “the nerve” by the general public, is scientifically described as a highly specialised loose connective tissue of ectomesenchymal origin rich with a heterogeneous population of cells and neuro-vascular supply.

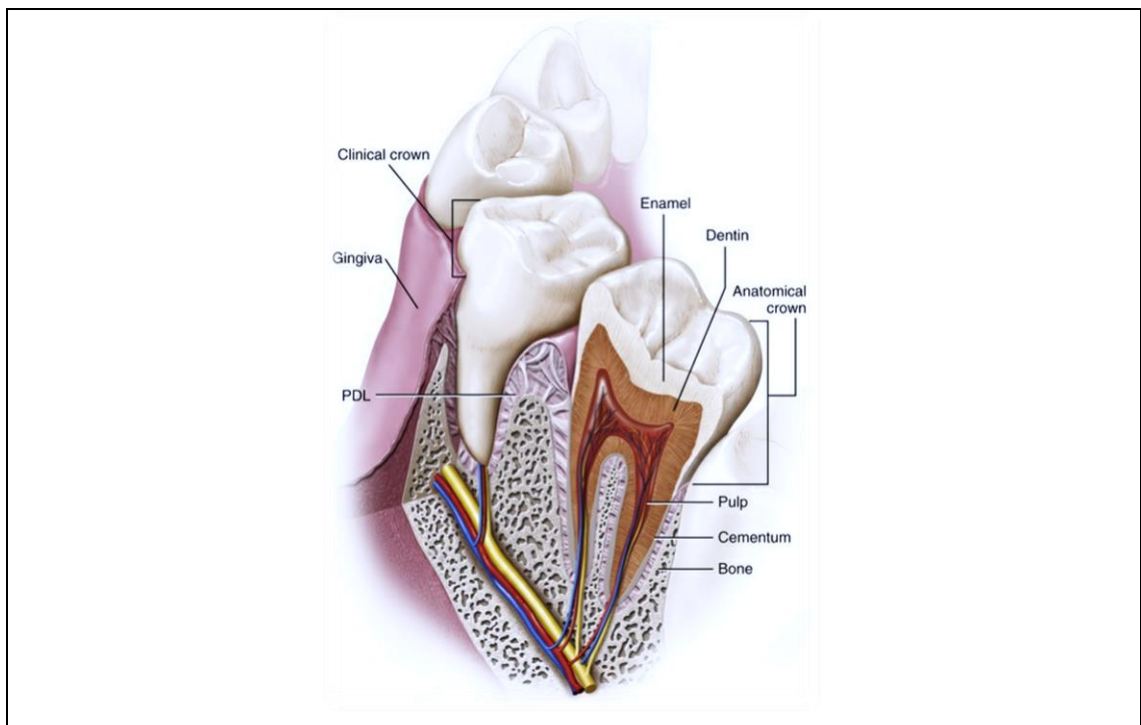


Figure 2-1: Gross anatomy of the tooth. Representative cross-sectional image of a molar tooth shows the dental pulp occupies the pulp space of the tooth and encompasses with the dentine, enamel and cementum. (PDL) Periodontal ligaments. The image is adapted from Nanci (2017).

2.1.1 Embryonic development of the dental pulp

The embryonic development of the dental pulp is initiated by the cells of the dental papilla which is a condensation of ectomesenchymal cells derived from the neural crest cells of the first pharyngeal arch (Moore *et al.*, 2018). The dental papilla appears in the oral region of the developing embryo below an aggregation of cells known as the enamel organ and surrounded by an aggregation of cells known as the dental follicle. The interaction between the cells of the enamel organ, dental papilla and dental follicle leads to tooth formation through a complex and multi-stages process known as the odontogenesis. Odontogenesis involves three main stages named as the bud stage, cap stage and bell stage.

During odontogenesis, a group of oral epithelial cells derived from the ectoderm of the first pharyngeal arch proliferate into the underlying ectomesenchyme and grow in size to form the enamel organ. The enamel organ becomes then invaginated with the dental papilla cells condensed within it. Dental pulp formation is then initiated when the outer ectomesenchymal cells of the dental papilla differentiate into odontoblasts in response to signals from the inner epithelial cells of the enamel organ (Thesleff and Nieminen, 1996, Lesot *et al.*, 2001, Lisi *et al.*, 2003). The odontoblasts then begin to secrete tooth crown dentine in a regular rhythm of about 4 – 8 μm per day and move downward in an apical direction leading to coronal dental pulp development (Kawasaki *et al.*, 1979).

Upon completion of crown formation, the cervical loop cells of the enamel organ proliferate apically into the underlying ectomesenchyme and become the Hertwig's epithelial root sheath (HERS). The HERS extends toward the apex of the future root, enclosing the dental papilla cells and interacting with them continuously leading to their differentiation into odontoblasts which secrete the root dentine and initiate radicular dental pulp development.

As tooth formation progresses, the dental papilla becomes more mature, confined within the hard tooth structures and is invaded with blood vessels and nerve fibres to complete dental pulp formation.

2.1.2 Histological characteristics of the dental pulp

The dental pulp appears microscopically as a vascularised loose connective tissue rich with heterogeneous cells that are organised in a unique pattern leading to the formation of four distinct morphological zones (Pashley *et al.*, 2002, Torabinejad *et al.*, 2014). These zones are the odontoblast layer, the cell-free zone, the cell-rich zone, and the pulp core (Figure 2-2).

The odontoblast layer represents the peripheral zone of the dental pulp that lies immediately subjacent to the predentine layer. This layer is characterised by the presence of the odontoblasts with their nuclei arranged in a staggered way that gives the appearance of a layer of multiple cells in thickness. The odontoblast layer also has dendritic cells and a network of vascular capillaries and nerve fibres branching among the odontoblasts (Torabinejad *et al.*, 2014).

Subjacent to the odontoblast layer, the cell-free zone (also known as the cell-poor zone or the zone of Weil) is sometimes observed (Pashley *et al.*, 2002). This zone, as indicated by its name, is relatively free of cells. Absence of the cell-free zone was reported in the young dental pulp during the process of active dentine formation, and in the old dental pulp as a result of the pulp space narrowing secondary to dentine deposition (Couve, 1986). The cell-free zone is traversed by a capillary network, unmyelinated nerve fibres, dendritic cells as well as the cytoplasmic processes of the fibroblasts that are present in the subjacent layer.

The cell-rich zone is situated internal to the cell-free zone (Pashley *et al.*, 2002). This zone contains a relatively higher number of fibroblasts as compared to the

central region of the dental pulp. In addition to the fibroblasts, this zone may include some macrophages, plasma cells, lymphocytes and undifferentiated mesenchymal stem cells (Harris and Griffin, 1969).

The central area of the dental pulp is known as the pulp core (Pashley *et al.*, 2002). This area has a heterogeneous population of cells including fibroblasts, undifferentiated mesenchymal stem cells, macrophages, lymphocytes and mast cells. In addition, the pulp core has the main neurovascular supply and lymphatic drainage of the dental pulp.

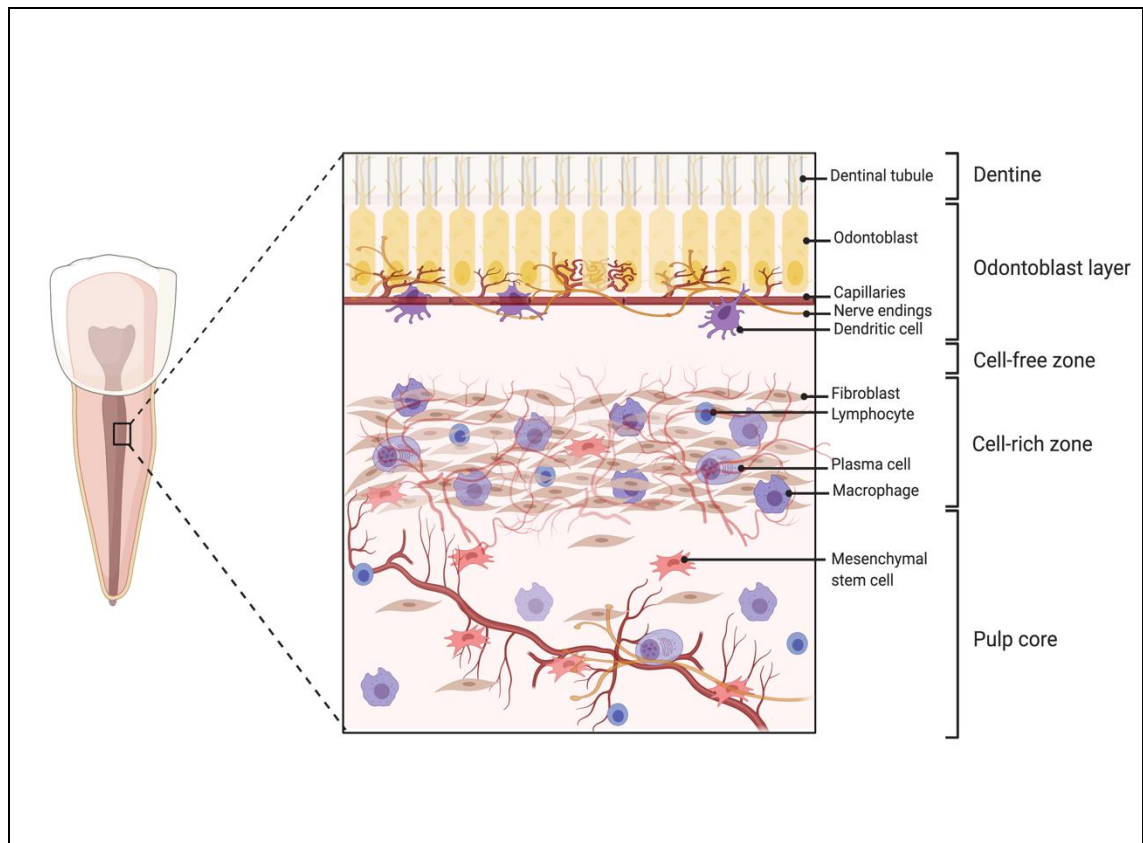


Figure 2-2: Morphological zones of the dental pulp. Schematic representation of the four morphological zones of the dental pulp, namely odontoblast layer, cell-free zone, cell-rich zone and pulp core.

2.1.2.1 Cells of the dental pulp:

Odontoblasts

The odontoblasts are terminally differentiated post-mitotic cells lining the periphery of the dental pulp and are responsible for dentine matrix secretion and mineralisation (Harris and Griffin, 1969, Hargreaves and Berman, 2015). The odontoblast consists of two parts: the cell body and cell process. The cell body lies against the predentine layer, whilst the cell process extends into a dentinal tubule (Sigal *et al.*, 1984, Holland, 1990, Hargreaves and Berman, 2015). The cell body is the synthesising part of the odontoblast. It contains a basally located nucleus and cytoplasmic organelles specific for protein-secreting cells (Ivanyi, 1972).

During active dentinogenesis, Golgi complex, rough endoplasmic reticulum, numerous mitochondria, lysosomes and secretory organelles become prominently visible in the cell body of the odontoblast. The odontoblast exhibits columnar morphology in the coronal pulp, and more flattened morphology towards the apical portion of the root. The odontoblast passes through multiple phases during the life cycle including functional phase, transitional phase and resting phase (Couve, 1986, Hargreaves and Berman, 2015). Each phase is marked by changes in cell size and organelles prominence. The odontoblasts synthesise and secrete collagen type I, proteoglycans, dentine sialoprotein, phosphophoryn and alkaline phosphatase (Pashley, 1996, Charadram *et al.*, 2013).

Fibroblasts

The fibroblasts are the most abundant cells in the dental pulp (Hargreaves and Berman, 2015). These cells handle the collagen synthesis and turnover. In

addition, the fibroblasts synthesise and secrete proteoglycans and glycosaminoglycans. The pulpal fibroblasts exhibit spindle-shape morphology and have the general characteristics of the protein-secreting cells (Martinez and Araujo, 2004). However, the prominence of the cytoplasmic organelles in the fibroblasts depends on their functional status.

Undifferentiated mesenchymal stem cells

Undifferentiated mesenchymal stem cells present throughout the dental pulp with more concentration in the pulp core (Shi *et al.*, 2005, Sloan and Smith, 2007, Sloan and Waddington, 2009). These precursor cells have the potential to migrate and differentiate into odontoblasts in response to injury and cell death (Smith, 2003). The undifferentiated mesenchymal cells of the dental pulp exhibit a spindle-shape fibroblastic morphology (Hargreaves and Berman, 2015).

Immune cells

The dental pulp contains several cells of the immune system including the dendritic cells, macrophages, lymphocytes and plasma cells (Hargreaves and Berman, 2015). These cells provide the necessary protective immune responses for the dental pulp.

2.1.2.2 Extracellular matrix of the dental pulp

The extracellular matrix (ECM) of the dental pulp comprises of a connective tissue fibres and ground substance within which the cells and other tissue components are organised (Linde, 1985, Hargreaves and Berman, 2015). The dental pulp ECM plays a pivotal role in supporting the cells and facilitating the diffusion of the nutrients and other substances from the blood vessels to the cells, and vice versa.

Connective tissue fibres of the dental pulp

Collagen

Collagen is the predominant type of protein in the pulpal ECM (Sloan, 2015). A single collagen molecule (i.e., Tropocollagen) is composed of three polypeptide chains. These chains are linked and organised in different ways leading to the formation of different collagen types (Linde, 1985).

Two types of collagen have been identified in the ECM of the dental pulp, each with a specific biological function (Shuttleworth *et al.*, 1978, Lukinmaa and Waltimo, 1992, Martinez *et al.*, 2000). Collagen type I constitutes about 55% of the collagen in the dental pulp, and presents as thick striated fibres (Van Amerongen *et al.*, 1983). These fibres play a role in providing the tissue with the required strength to withstand physical and mechanical forces. On the other hand, collagen type III represents around 45% of the collagen in the dental pulp ECM and appears as thin fibrils (Lechner and Kalnitsky, 1981). These fibrils contribute mainly to the elasticity of the dental pulp.

Elastin

Elastin fibres are characterised by their ability to contract and expand in response to the pressure. These fibres are confined to the walls of the blood vessels in the dental pulp (Linde, 1985).

Ground substance of the dental pulp

The ground substance of the dental pulp is amorphous gel-like substance within which the fibres, cells and other components of the dental pulp are embedded. This ground substance is mainly composed of glycosaminoglycans, glycoproteins and water .

Glycosaminoglycans

Glycosaminoglycans (GAGs) are essential components of the dental pulp ECM (Linde, 1970, 1972). GAGs can be classified according to their structure into four types: heparin sulphate, keratin sulphate, chondroitin/dermatan sulphate and hyaluronic acid. The concentration of each type of GAGs within the pulpal ECM is strongly affected by the age and the activity status of the dental pulp (Linde, 1973a). GAGs play a key role in maintaining the hydration of the pulpal ECM, thus contributing to its gel-like property. GAGs also provide binding sites for several types of cytokines and growth factors such as the fibroblast growth factor family and vascular endothelial growth factor family (Linde, 1973b, Mangkornkarn and Steiner, 1992).

Glycoproteins

The two main glycoproteins in the pulpal ECM are fibronectin and laminin. Fibronectin, an adhesion glycoprotein, presents as a reticular fibres throughout the dental pulp with increased concentration around the walls of the blood vessels (Linde *et al.*, 1982). Fibronectin plays a critical role in facilitating cell adhesion and promoting cell migration, proliferation and differentiation. Laminin, on the other hand, is a complex adhesion glycoprotein appearing mainly in the basement membrane of the pulpal ECM. Laminin has a prominent influence on cell attachment, migration and differentiation (Salmivirta *et al.*, 1997, Yuasa *et al.*, 2004).

Bioactive signalling molecules

The bioactive signalling molecules are proteins secreted by the cells of the dental pulp to initiate specific biological responses. Examples of these molecules are the chemokines, cytokines and growth factors. Vascular endothelial growth

factor-A (VEGF-A), fibroblast growth factor (FGF-2) and transforming growth factor- β (TGF- β) have all been identified in the pulpal ECM (Toyono *et al.*, 1997, Chen *et al.*, 2003, Wang *et al.*, 2007).

2.1.2.3 Vasculature of the dental pulp

Dental pulp is a highly vascular tissue with a special microcirculatory system consisting of arterioles that penetrate the apical foramen to form a capillary plexus in the peripheral zone of the dental pulp (Kim, 1985, Hargreaves and Berman, 2015). The dental pulp drains the blood out through arterio-venous anastomoses linked to venules located in the pulp core. The pulpal blood flow is controlled by a pre-capillary sphincter and a sympathetic innervation (Kim, 1990).

2.1.2.4 Nerve fibres of the dental pulp

Dental pulp is innervated with sensory and sympathetic nerve fibres (Pohto and Antila, 1968, Avery *et al.*, 1980, Silverman and Kruger, 1987). The sensory nerve fibres are responsible for pain perception and transduction. They enter the dental pulp through the apical foramen and form a plexus just beneath the cell-rich zone. This plexus is known as the Plexus of Raschkow. The Plexus of Raschkow is composed of large myelinated nerve fibres (A- δ and A- β fibres, 2 - 5 μm in diameter) and small unmyelinated nerve fibres (C fibres, 0.3 -1.2 μm in diameter) (Yu and Abbott, 2007). The myelinated nerve fibres lose their myelin and continue as free nerve endings through the cell-free zone and in-between the odontoblasts. Some free nerve endings penetrate the predentine layer and the dentine through the dentinal tubules. The sympathetic adrenergic nerve fibres play a role in regulating the pulpal blood flow through vasomotor control (Kim *et al.*, 1989).

2.1.3 Physiological functions of the dental pulp

Dental pulp has a primary formative function and many other secondary supportive functions (Pashley *et al.*, 2002). The primary formative function of the dental pulp involves the induction of enamel and cementum synthesis during the process of tooth development as well as the synthesis and deposition of dentine (Lisi *et al.*, 2003, Lesot *et al.*, 2001). The odontoblasts synthesise dentine throughout their life. They participate in dentine formation through the synthesis and deposition of the organic dentine matrix, the transportation of the inorganic components to the newly formed dentine matrix and the induction and control of dentine matrix mineralisation (Arana-Chavez and Massa, 2004). The odontoblasts deposit primary dentine during the process of tooth development following a rapid and symmetrical pattern. After tooth maturation, the odontoblasts deposit secondary dentine in a slower rate and in a less symmetrical pattern. In response to pathological and chemical stimuli, the odontoblasts tend to synthesise tertiary dentine to protect the dental pulp. This tertiary dentine may follow a tubular pattern (known as reactionary tertiary dentine) or have an atubular pattern (known as reparative tertiary dentine) (Smith *et al.*, 2001).

The secondary supportive functions of the dental pulp include the nutritional, defensive and conductive sensational roles. Dental pulp microcirculation supplies oxygen and nutrients that are essential to maintain the viability of the cells and eliminate metabolic wastes from the tissue. In addition, the cells of the dental pulp play an important role in identifying foreign substances such as microbial toxins and initiating a protective immune response against them (Nagaoka *et al.*, 1995). The pain sensation elicited by the nerve fibres of the dental pulp helps in the early detection of problems, thus protecting the tooth from further damage (Paphangkorakit and Osborn, 1998, Yu and Abbott, 2007).

Dental pulp is, therefore, very important in preserving the long-term viability of the tooth. It is when dental pulp vitality is lost due to an injury or infection that the integrity of the tooth is compromised.

2.2 Dental pulp necrosis in young permanent teeth with developing roots

Teeth undergo post-eruption radicular maturation (i.e. root development and apical closure) that takes up to three years to complete following crown eruption into the oral cavity (Kumar, 2015). During this period, the maintenance of dental pulp vitality is essential for the completion of radicular maturation.

In growing children, the loss of dental pulp vitality (i.e., dental pulp necrosis) in young permanent teeth with developing roots is not uncommon. Several factors including traumatic dental injuries, dental caries and developmental dental anomalies such as *dens invaginatus* and *dense evaginatus* can subsequently lead to dental pulp necrosis, thus disrupting the radicular maturation of the teeth (Levitan and Himel, 2006, Bjørndal, 2008, Andreasen and Kahler, 2015).

Traumatic dental injuries (TDI) frequently occur in growing children and are often associated with a risk of dental pulp necrosis (Andreasen and Kahler, 2015). Population-based studies from around the world have reported the prevalence of TDI falls between 4% - 59%, with the majority of TDI occurring in the young anterior permanent teeth of growing children (Glendor, 2008). In the United Kingdom, a national survey on children's oral health indicated around 5% of 8 year olds and 12% of 12 year olds had sustained TDI involving permanent anterior teeth (Harker and Morris, 2003, Pitts *et al.*, 2013). Furthermore, in another study, analysis of 10,673 young permanent teeth affected with TDI revealed pulpal necrosis in around 3% of concussion cases, 26% of extrusion cases, 58% of lateral luxation cases, 92% of avulsion cases and 94% of intrusion cases (Borum and Andreasen, 2001).

Dental caries is considered the second most prevalent infectious disease in the world (Islam *et al.*, 2007). A study on the global burden of disease, conducted by the World Health Organisation in 2016, reported oral diseases affecting half of the world's population with dental caries in the permanent dentition being the most prevalent disease assessed (Vos *et al.*, 2017). Advanced untreated dental caries can subsequently lead to dental pulp necrosis (Bjørndal, 2008).

Developmental defects such as *dense invaginatus* and *dense evaginatus* occur in the permanent teeth with a prevalence of around 0.3% to 10% for *dense invaginatus* and 0.1% to 7.7% for *dense evaginatus* (Levitan and Himel, 2006, Gallacher *et al.*, 2016). Failure to detect and manage these defects early could eventually lead to dental pulp necrosis.

Therefore, dental pulp necrosis occurrence in young permanent teeth with developing roots is relatively common. Unfortunately, pulpal necrosis prior to the full radicular maturation arrests further root development, rendering the affected immature teeth with thin and often short root/s, open apices and compromised crown to root ratios. This results in roots that are not developed enough to support the long-term survival of the teeth. Indeed, immature permanent teeth with pulpal necrosis are at increased risk of fracture and subsequent loss (Cvek, 1992).

In treating immature permanent teeth with pulpal necrosis, the desired clinical outcomes would be to resolve the signs and symptoms of periapical pathology, restore the functional competence of the dental pulp and promote the completion of the radicular maturation (Hargreaves *et al.*, 2008). These outcomes are likely to improve the long-term prognosis of affected teeth and promote their survival and retention.

2.2.1 Interventions for treating immature permanent teeth with pulpal necrosis

The treatment of immature permanent teeth with pulpal necrosis continues to be extremely challenging and technically demanding. Currently, three clinical interventions are utilised in treating immature permanent teeth with pulpal necrosis. These interventions are the apexification technique, apical plug technique and regenerative endodontic therapy (Duggal *et al.*, 2017). The outcomes of using these interventions in treating immature permanent teeth with pulpal necrosis are discussed below. Studies comparing the outcomes of using the interventions mentioned above in managing non-vital immature permanent teeth are highlighted in Table 2-1.

2.2.1.1 Apexification technique

The apexification technique involves removal of the necrotic pulpal tissue followed by debridement of the root canal space and placement of a biomaterial to resolve the signs and symptoms of periapical pathology and induce the generation of a calcified apical barrier against which the root canal obturation material can be placed (Rafter, 2005). The biomaterial that has gained the widest acceptance for use in the apexification technique is calcium hydroxide.

Calcium hydroxide (Ca(OH)_2) use in apexification technique was first proposed by Kaiser (1964), who suggested that a mixture of Ca(OH)_2 with camphorated parachlorophenol is capable of inducing a calcified barrier formation across the apices of the treated teeth (Rafter, 2005). Following this, further investigations were carried out in order to make the Ca(OH)_2 mixture less cytotoxic by using materials such as metacresylacetate instead of camphorated parachlorophenol

(Fava and Saunders, 1999). The use of Ca(OH)_2 mixed with saline, distilled water or methylcellulose was also evaluated with similar clinical success (Rafter, 2005). The two essential features of Ca(OH)_2 are the bactericidal effect and the hard-tissue inducing effect (Holland *et al.*, 1977, Safavi and Nichols, 1994). The bactericidal effect is related to release of hydroxyl ions, which denatures protein and causes damage to the bacterial cytoplasmic membrane and DNA (Safavi and Nichols, 1994, Barthel *et al.*, 1997, Mohammadi and Dummer, 2011). On the other hand, the hard tissue inducing effect of Ca(OH)_2 was shown to be associated with its high pH (12.5 -12.8) (Javelet *et al.*, 1985). Schroder (1971) postulated that the high pH of Ca(OH)_2 initiates a zone of necrosis in the adjacent apical tissues, resulting in a low-grade irritation of the underlying tissues adequate to produce a matrix that mineralised following the inclusion of the calcium molecules (Schroder, 1971). Analysis of this mineralised matrix revealed histological features similar to those found in cementum with multiple porosities traversed by blood vessels (Steiner and Van Hassel, 1971).

The apexification technique using Ca(OH)_2 has been carried out clinically through multiple and prolonged dressing of the root canal with Ca(OH)_2 until a calcified apical barrier appears radiographically. The average time length required for the calcified apical barrier formation ranged from five to twenty months (Rafter, 2005). Outcomes analysis of Ca(OH)_2 apexification-treated teeth revealed consistent results for the healing of periapical pathology and induction of calcified apical barrier formation (Best *et al.*, 2021). However, concerns about the prolonged dressing of the root canal with Ca(OH)_2 arisen when two retrospective studies (Cvek, 1992, Al-Jundi, 2004) reported a 40% and 32% incidence of late-stage crown-root fracture, respectively, in non-vital immature permanent teeth treated with Ca(OH)_2 apexification. The reported frequencies of crown-root fracture in the

treated teeth during a 4-year follow-up period ranged from 28% to 77%, with the highest frequency in teeth with root formation less than half of the final root development (Cvek, 1992). This suggested that the stage of root development is a predominant risk factor for late-stage crown-root fracture in non-vital immature permanent teeth treated with Ca(OH)_2 apexification. In Al-Jundi's study, the incidence of crown-root fracture during a 36-month follow-up period was spontaneous in 15% of the treated cases and associated with minor secondary injuries in the rest (Al-Jundi, 2004). Several laboratory studies have reported a time-dependant reduction in dentine fracture resistance following the application of Ca(OH)_2 (Andreasen *et al.*, 2002, Doyon *et al.*, 2005, Twati *et al.*, 2009b, Batur *et al.*, 2013). A significant decrease in the strength of Ca(OH)_2 -filled roots has been reported after two months, reaching approximately 50% lower fracture resistance after one year of application (Andreasen *et al.*, 2002). The application of Ca(OH)_2 in the root canals of permanent human incisor teeth reduced the fracture resistance by 43% after 84 days (Rosenberg *et al.*, 2007). Root cylinders, prepared from mature human teeth treated with Ca(OH)_2 for 30 days, required significantly less force until fracture than untreated root cylinders (Sahebi *et al.*, 2010). It has been suggested that due to the high pH, Ca(OH)_2 can cause degradation of dentinal proteins resulting in tooth structure weakening, thus increasing the susceptibility of immature teeth to crown-root fracture (Yassen and Platt, 2013).

The management of a young patient presenting with a crown-root fracture at, or just below, gingival margin level is often complex. Treatment difficulty is even compounded when the root is very immature with thin divergent walls and an open apex. The prognosis of such tooth may be regarded as poor, that extraction is prescribed followed by a prosthetic therapy. However, intentional root retention,

until the definitive restorative plan is made, has several benefits. Firstly, root retention preserves the alveolar bone, which has both functional and aesthetic importance. Indeed, resorption of the alveolar bone following tooth loss has been reported to complicate implant placement (Ledermann *et al.*, 1993, Agarwal *et al.*, 2016). The second benefit is that the root itself might potentially be able to support a post crown (Koyuturk and Malkoc, 2005, Arhun *et al.*, 2006, Canoglu *et al.*, 2007, Das and Muthu, 2013). The success rate of intentional root retention following crown loss has been reported to be around 91% over a 2-year follow-up period (Rodd *et al.*, 2002).

Given the limitations of the Ca(OH)_2 apexification technique, the routine use of this technique in treating non-vital immature permanent teeth has been discouraged recently by the European Academy of Paediatric Dentistry, and clinicians have been advised to consider alternative therapeutic strategies, such as apical plug technique or regenerative endodontic therapy (Duggal *et al.*, 2017). The outcomes of these techniques are discussed below.

2.2.1.2 Apical plug technique

The apical plug technique involves the use of a biomaterial at the open apices of immature permanent teeth with pulpal necrosis to create an apical plug for the immediate placement of the root canal filling material (Pradhan *et al.*, 2006). Following pulpal extirpation and root canal disinfection, the apical plug (i.e. barrier) can be established over one or two treatment visits using mineral trioxide aggregate (MTA) cement, thereby eliminating the need for multiple long-term applications of Ca(OH)_2 in the root canal to induce the formation of a calcified apical barrier (Bakland and Andreasen, 2012).

MTA was initially developed for use in sealing accidental root canal perforations (Lee *et al.*, 1993), and was then found suitable for use in creating an apical plug across the open apices of immature permanent teeth (Torabinejad *et al.*, 1995a, Shabahang and Torabinejad, 2000). MTA is a hydrophilic powder composed of fine particles of tricalcium silicate, tricalcium oxide and silicate oxide (Parirokh and Torabinejad, 2010). This powder, in the presence of moisture, forms a colloidal gel of high pH (pH 12.5) that solidifies into a hard structure. MTA has many favourable characteristics including excellent biocompatibility, good sealing ability, low solubility, antimicrobial properties and acceptable radiopacity (Torabinejad *et al.*, 1995a, Torabinejad *et al.*, 1995b).

The clinical efficacy and the outcomes of using the MTA apical plug technique in treating immature permanent teeth with pulpal necrosis has been demonstrated in multiple studies. Sarris *et al.* (2008) reported clinical success for the technique in 94.1% of the treated cases following a 12-month follow-up period. Similarly, Witherspoon *et al.* (2008) demonstrated clinical success for the technique in 93.5% of the cases treated in one visit and 90.5% of the cases treated in two visits. This is in line with the findings reported by Simon *et al.* (2007) showing one visit MTA apical plug technique is a reliable and predictable method for the management of immature permanent teeth with pulpal necrosis.

Studies evaluating the clinical efficacy and the outcomes of the MTA apical plug technique in comparison to Ca(OH)₂ apexification technique have also been performed. El Meligy and Avery (2006) reported the clinical and radiographic success of MTA apical plug technique in 100% of the cases twelve months after obturation in comparison to 87% of the cases in the Ca(OH)₂ apexification group. Similar higher clinical and radiographic success rates for the MTA apical plug technique in comparison to Ca(OH)₂ apexification were also reported by other

studies (Pradhan *et al.*, 2006, Damle *et al.*, 2012). This has made the MTA apical plug technique the 'gold standard' treatment option for immature permanent teeth with pulpal necrosis (Duggal *et al.*, 2017, Nicoloso *et al.*, 2017).

The use of the MTA apical plug technique in treating non-vital immature permanent teeth is not without limitations. The technique is neither capable of restoring the competency of pulpal functions nor able to induce the completion of root maturation, thus leaving the teeth at risk of fracture. Silujjai and Linsuwanont (2017) reported a fracture related-failure rate of 19.23% in teeth treated using the MTA apical plug technique over a 28 to 96-month follow-up period. Furthermore, Jamshidi *et al.* (2018) reported the lack of an increase in the fracture and impact resistance in simulated immature human teeth treated with the MTA apical plug technique and reinforced with a fibre post. Therefore, it was imperative for clinicians to look for an alternative treatment option, particularly for the management of non-vital immature permanent teeth with very short and thin roots, for which the use of the MTA apical plug technique often has a poor prognosis (Diogenes *et al.*, 2016).

2.2.1.3 Regenerative endodontic therapy

Regenerative endodontic therapy (RET) was introduced clinically to address the limitations of using Ca(OH)₂ apexification technique and MTA apical plug technique in treating immature permanent teeth with pulpal necrosis (Iwaya *et al.*, 2001, Banchs and Trope, 2004). This therapy aims to resolve the signs and symptoms of apical pathology, restore the functional competence of the dental pulp and promote the completion of root development in immature permanent teeth with pulpal necrosis (Kim *et al.*, 2018).

The term 'revascularisation' was initially used to describe this therapy (Iwaya *et al.*, 2001), and it was later suggested to be replaced with the term 'revitalisation' as the vital tissues regenerated in the root canal of the treated teeth were not merely blood vessels but also soft and hard tissues (Huang and Lin, 2008). The term 'regenerative endodontics' was then used by the American Association of Endodontists (2013), while the term 'revitalisation' was adopted by the European Society of Endodontology (2016). In the endodontic literature, all the terminologies mentioned above are used interchangeably to describe RET.

RET has been defined as "a biologically-based therapy designed to replace the damaged tooth structures, including dentine and root structures, as well as the cells of the pulp-dentine complex" (Murray *et al.*, 2007). This therapy is principally based on the combined application of the tissue engineering elements, namely a source of stem cells, suitable scaffold, signalling molecules and a sterile environment, to restore the functions and regenerate the structures of the necrotic pulps in immature permanent teeth (Nakashima and Akamine, 2005).

One current clinical form of RET involves disinfection of the root canal using a combination of intra-canal irrigants and medicaments followed by laceration of the periapical tissue to provoke apical bleeding into the root canal (Galler, 2016). The periapical tissue of the tooth is a source of stem cells originating from the apical dental papilla. These cells are referred to as stem cells of the apical papilla (SCAP) (Huang *et al.*, 2008, Sonoyama *et al.*, 2008). Delivery of these cells into the root canal of non-vital immature permanent teeth by the provoked apical bleeding has been evaluated by Lovelace *et al.* (2011). Their study demonstrated mobilisation and accumulation of mesenchymal stem cells in the root canal of treated teeth following apical bleeding induction. These cells become subsequently entrapped within the blood clot which acts as a fibrin scaffold

(Hargreaves *et al.*, 2013). During the regenerative process, the signalling molecules are derived from the dentinal walls of the root canal (Smith *et al.*, 1990, Roberts-Clark and Smith, 2000, Smith *et al.*, 2016, Kim, 2017, Schmalz *et al.*, 2017) as well as from the platelets in the provoked apical bleeding during the clotting cascade (Arora *et al.*, 2009, Alsousou *et al.*, 2009). Dentine conditioning using ethylenediaminetetraacetic acid (EDTA) has shown the ability to release growth factors from dentine matrix (Galler *et al.*, 2015), and is the technique used in the current clinical protocols of RET recommended by the American Association of Endodontists (2016) and the European Society of Endodontology (2016). In addition to EDTA, clinical materials including phosphoric acid and citric acid have shown the ability to liberate growth factors sequestered within dentine matrix (Zhao *et al.*, 2000, Smith *et al.*, 2011, Sadaghiani *et al.*, 2016).

Investigations on the role of the provoked apical bleeding in RET date back to the 1960s, when Nygaard Östby induced the apical bleeding in a debrided root canal space of dogs and human teeth (Östby, 1961). He observed deposition of fibrous connective tissue and cellular cementum in the apical third of the root canal space of the treated teeth. Following Nygaard Östby's observation, further experimental studies revealed the formation of repair tissue in the root canal space following provocation of the apical bleeding without any histological evidence of dental pulp regeneration (Östby and Hjortdal, 1971, Hørsted *et al.*, 1978). These observations shifted the focus of endodontic research during that period away from the regenerative objective towards the restorative objective, including root canal disinfection and filling, until the early 2000s.

Between 2000 and 2007, several case reports were published in which immature permanent teeth with pulpal necrosis were subjected to disinfection followed by provocation of apical bleeding into the root canal and placement of coronal

restorations (Iwaya *et al.*, 2001, Banchs and Trope, 2004, Chueh and Huang, 2006, Petrino, 2007, Thibodeau and Trope, 2007). The resulting clinical and radiographic outcomes of these case reports included apical healing with resolution of signs and symptoms of pathology and with an increase in radiographic root dimensions, occurring 6 – 12 months following the treatment. Based on these promising outcomes, the re-emergence of RET has been prompted (Murray *et al.*, 2007), with a plethora of studies published since then reporting variable outcomes following the use of RET in treating immature permanent teeth with pulpal necrosis.

Outcomes of RET in immature permanent teeth with pulpal necrosis

Clinical and radiographic outcomes

The American Association of Endodontists (2016) suggested measuring the degree of RET success in treating immature permanent teeth with pulpal necrosis based on the extent to which it is possible to achieve three clinical and radiographic outcomes. These outcomes were defined as the following:

- Primary outcome: Resolution of clinical signs and symptoms of pathology with periapical lesion healing.
- Secondary outcome: Radiographic evidence of increased root thickness and/or root length with apical closure.
- Tertiary outcome: Return of positive response to pulp sensibility testing.

The primary outcome was found to be generally achievable following RET in immature permanent teeth with pulpal necrosis (Chen *et al.*, 2012). This is in agreement with the results of two recent systematic reviews which demonstrated consistent reporting of complete resolution of clinical signs and symptoms of

pathology with radiographic evidence of periapical healing observed in 91% - 94% of the treated cases (Tong *et al.*, 2017, Torabinejad *et al.*, 2017).

Several investigators compared the success of RET in resolving the signs and symptoms of the disease and promoting periapical healing with Ca(OH)₂ apexification technique and MTA apical plug technique. Jeeruphan *et al.* (2012) indicated that both RET and MTA apical plug technique were highly effective in resolving the signs and symptoms of the disease and achieved periapical healing in 100% and 95% of patients, respectively, compared with 77% of patients in Ca(OH)₂ apexification group. This is consistent with the results reported by Nagy *et al.* (2014) showing RET and MTA apical plug technique equally effective in achieving periapical healing in 100% of the treated teeth. Similar results were reported by Lin *et al.* (2017) at the 12-month follow-up period. Findings from these studies together with several case series clearly indicated comparable outcome of RET or MTA apical plug technique with regards to resolution of signs and symptoms of the disease and apical healing.

The desired secondary outcome of increased root thickness and/or root length with apical closure was shown to be not always achievable following RET in immature permanent teeth with pulpal necrosis (Petrino *et al.*, 2010, Chen *et al.*, 2012). A prospective analysis of sixteen immature permanent teeth following 18 months of RET revealed variable patterns of root maturation with the percentage of change in preoperative root length and thickness varying between - 2.7% to 25.3% and - 1.9% to 72.6%, respectively (Kahler *et al.*, 2014). Similarly, a radiographic analysis of fifteen teeth, treated with RET, after an average of 40 months showed the mean percentage change in root length equalled $14.38 \pm 20.92\%$ and root thickness equalled $13.82 \pm 11.17\%$ (Linsuwanont *et al.*, 2017). These findings are in agreement with the results of a recent systematic review

and meta-analysis demonstrating inconsistent and unpredictable outcomes for continued root maturation and apical closure following RET in immature permanent teeth with pulpal necrosis (Tong *et al.*, 2017). Collectively, the studies mentioned above pointed to the potential of RET to promote root maturation in some cases, but not all.

The tertiary outcome of regaining a positive response to pulp sensibility testing following RET was reported in approximately 50% of the published cases (Diogenes *et al.*, 2013). However, a potential for a publication bias is likely to exist in the current literature as the successful cases are more often reported than the failed cases leading to an overestimation of the RET success rate. Furthermore, the return of a positive response to pulp sensibility testing does not necessarily indicate successful regeneration of the dental pulp. Any vital tissue grown in the root canal is vascularised and innervated, and therefore, capable of eliciting a positive response to pulp sensibility testing (Diogenes and Ruparel, 2017).

Histological outcomes

Thibodeau *et al.* (2007) reported the formation of new vital soft and hard tissues in the root canals of immature teeth of dogs treated with RET using a blood clot. These tissues were characterised in subsequent animal studies as periodontal ligament-like tissues, cementum-like tissues and bone-like tissues but not pulp-like tissues (Da Silva *et al.*, 2010, Wang *et al.*, 2010, Yamauchi *et al.*, 2011). Similar histological outcomes were observed in human studies following RET in non-vital immature permanent teeth (Shimizu *et al.*, 2012, Martin *et al.*, 2013, Shimizu *et al.*, 2013, Becerra *et al.*, 2014, Lei *et al.*, 2015). The newly-formed mineralised tissues include cementum-like tissues deposited in the apical region and along the dentinal walls and bone-like tissues forming islands within the root

canal (Gomes-Filho *et al.*, 2013, Lei *et al.*, 2015, Saoud *et al.*, 2015, Del Fabbro *et al.*, 2016). These mineralised tissues have been reported to distribute mechanical stress disadvantageously compared to the dentine (Bucchi *et al.*, 2019). Therefore, dentine formation continues to be an overarching goal after RET in order to enhance the biomechanical performance of the teeth and improve their fracture resistance and long-term survival.

RET, in its current clinical forms, is regarded as a reparative and not a regenerative process (Simon *et al.*, 2014), and the term “guided endodontic repair” has been suggested for this therapy (Diogenes and Ruparel, 2017).

Is RET successful in treating non-vital immature permanent teeth?

RET can only be considered successful if periapical healing is consistently achieved with a predictable quantitative increase in root length and thickness. Unfortunately, outcomes analysis of the current clinical forms of RET revealed limited success in most of the published studies with periapical healing consistently observed, but the induction of root maturation unpredictably observed (Kontakiotis *et al.*, 2014). Despite the growing use of RET in treating immature permanent teeth with pulpal necrosis, this therapy in its current clinical forms has led to inconsistent results with some teeth showing excellent outcomes while others are merely surviving with questionable long-term prognosis (Duggal *et al.*, 2017).

Disturbance of the biological interaction between the Hertwig’s Epithelial Root Sheath (HERS) and ectomesenchymal cells of the dental papilla and dental follicle is one of the suggested contributing factors to the inconsistent observation of root maturation following RET (Nazzal and Duggal, 2017). HERS is a sheath of epithelial cells derived from the cervical loop where the outer and inner enamel

epithelial cells fuse after the completion of crown formation. This sheath of epithelial cells plays a crucial role in determining the root morphology and stimulating the differentiation of ectomesenchymal cells into odontoblasts and cementoblasts (Li *et al.*, 2017). The viability of HERS cells is fundamental for obtaining an increase in root length and apical closure (Zeichner-David *et al.*, 2003). Damage to HERS cells due to traumatic dental injury or long-standing periapical infection could hinder the differentiation of ectomesenchymal cells into odontoblasts and cementoblasts, thus arresting further root lengthening and apex formation (Nazzal and Duggal, 2017).

Another factor that has been proposed to contribute to the inconsistent observation of root maturation following RET is the inadequate application of the tissue engineering principles required for true dental pulp regeneration (Hargreaves *et al.*, 2013). The growth of new vital tissue capable of depositing dentine-like mineralised matrix on the existing dentinal walls of the root canal is a prerequisite for gaining a quantitative increase in root wall thickness. In the current clinical form of RET, stem cells are delivered to the root canal space by the provoked apical bleeding (Lovelace *et al.*, 2011); the scaffold is then established via a blood clot; and the signalling molecules are derived from the root dentinal walls (Chmilewsky *et al.*, 2014, Smith *et al.*, 2016) and are released from platelets during the clotting pathway (Arora *et al.*, 2009). However, the composition of the blood clot and the concentration of the cells and signalling molecules are not controlled and are likely to vary from cases to case depending on the tooth condition and the particular RET protocol resulting in unpredictable outcomes (Murray *et al.*, 2007). Additionally, an emerging body of evidence has indicated that the irrigants and the intra-canal medicaments that are used during the process of root canal disinfection might adversely affect the survival and

differentiation of the stem cells (Galler *et al.*, 2011b, Ruparel *et al.*, 2012, Althumairy *et al.*, 2014, Alghilan *et al.*, 2017, Widbiller *et al.*, 2019), as well as interfering with the release of dentine-derived signalling molecules (Galler *et al.*, 2015). Therefore, the current clinical form of RET does not fully enact the requirements of tissue engineering that are necessary for successful dental pulp regeneration. Further research and development are needed to reach a form of RET capable of regenerating the structure and restoring the functions of the damaged pulps in immature permanent teeth in a controlled and predictable manner. Meanwhile, the use of RET in managing immature permanent teeth with pulpal necrosis has been suggested for consideration only in cases where the root development is very incomplete that the use of MTA apical plug technique is unlikely to improve the prognosis (Duggal *et al.*, 2017).

Table 2-1: A summary of the studies comparing the outcomes of current clinical interventions for treating non-vital immature permanent teeth.

Study	Clinical intervention	Age (years)	Follow-up (months)	Clinical and radiographic outcomes
El Meligy and Avery (2006)	Group 1: Ca(OH) ₂ apexification (n = 15 teeth) Group 2: MTA apical plug technique (n = 15 teeth)	6 -12	12	Clinical and radiographic success rates: Ca(OH) ₂ apexification = 87% MTA apical plug technique = 100%
Pradhan <i>et al.</i> (2006)	Group 1: Ca(OH) ₂ apexification (n = 10 teeth) Group 2: MTA apical plug technique (n = 10 teeth)	8 - 15	No follow up	Clinical and radiographic success rates: 100% for both groups.
Bose <i>et al.</i> (2009)	Group 1: RET using a blood clot (n = 48 cases) Controls: MTA apical plug technique (20 cases) and non-surgical root canal treatment (20 cases)	-	Up to 36	Significant increase in the root dimensions (root length and thickness) was observed in RET-treated cases as compared to the controls.

Study	Clinical intervention	Age (years)	Follow-up (months)	Clinical and radiographic outcomes
Damle <i>et al.</i> (2012)	Group 1: Ca(OH) ₂ apexification (n = 15 teeth) Group 2: MTA apical plug technique (n = 15 teeth)	8 - 12	12	Clinical and radiographic success rates: Ca(OH) ₂ apexification = 93.3% MTA apical plug technique = 100%
Jadhav <i>et al.</i> (2012)	Group 1: RET using a blood clot with a platelet-rich plasma (n = 10 teeth) Group 2: RET using a blood clot without a platelet-rich plasma (n = 10 teeth)	15 - 28	12	Resolution of clinical signs and symptoms of pathology was achieved in both groups. Apical healing, dentinal wall thickening and apical closure were superior in the RET using a blood clot with a platelet-rich plasma group. Root lengthening was comparable in both groups.
Jeeruphan <i>et al.</i> (2012)	Group 1: Ca(OH) ₂ apexification (n = 22 cases)	8 - 20	Up to 57	RET promoted a significant increase in root width (28.2%) compared to the MTA apical plug (0.0%) and Ca(OH) ₂ apexification (1.5%).

Study	Clinical intervention	Age (years)	Follow-up (months)	Clinical and radiographic outcomes
	Group 2: MTA apical plug technique (n = 19 cases) Group 3: RET using a blood clot (n = 20 cases)			RET promoted a significant increase in root length (14.9%) compared to the MTA apical plug (6.1%) and Ca(OH) ₂ apexification (0.4%). Survival rates: 1 st group = 77.2%, 2 nd group 95%, 3 rd group = 100%
Alobaid <i>et al.</i> (2014)	Group 1: RET using a blood clot (n = 19 teeth) Group 2: MTA apical plug technique (n = 12 teeth)	-	Up to 33	Clinical success rates: RET-treated teeth = 78%, MTA-treated teeth = 100% Survival rates: RET-treated teeth = 95%, MTA-treated teeth = 100% RET-treated teeth showed an increase in the radiographic root width.
Nagata <i>et al.</i> (2014)	Group 1: RET using a triple antibiotic paste and a blood clot (n = 12)	7 -17	19	Significant pain reduction in both groups. Crown discoloration in the 1st group.

Study	Clinical intervention	Age (years)	Follow-up (months)	Clinical and radiographic outcomes
	Group 2: RET using combination of Ca(OH) ₂ and 2% chlorhexidine gel (n = 11)			<p>Periapical healing rates: 1st group = 100%, 2nd group = 80%</p> <p>Percentages of root length increase: 1st group = 41.7%, 2nd group = 27.3%</p> <p>Percentages of dentinal walls thickening: 1st group = 41.7%, 2nd group = 45.4%</p> <p>Apical closure: 1st group = 66.7%, 2nd group = 54.5%</p>
Nagy <i>et al.</i> (2014)	<p>Group 1: MTA apical plug technique (n = 12 teeth)</p> <p>Group 2: RET using a blood clot (n = 12 teeth)</p> <p>Group 3: RET using a blood clot and an injectable scaffold containing basic fibroblast growth factor (n = 12 teeth)</p>	9 -13	Up to 18	<p>Periapical healing rates: 1st group = 80%, 2nd group = 100%, 3rd group = 90%</p> <p>RET groups showed a comparable increase in root width and length with no apparent advantages of using the injectable scaffold in the 3rd group compared to the 2nd group.</p>

Study	Clinical intervention	Age (years)	Follow-up (months)	Clinical and radiographic outcomes
				Apical closure: 1 st group = 80%, 2 nd group = 100%, 3 rd group = 90%
Bezgin <i>et al.</i> (2015)	Group 1: RET using a blood clot (n = 10 teeth) Group 2: RET using a platelet-rich plasma (n = 10 teeth)	7 -13	Up to 18	Resolution of clinical signs and symptoms of pathology was achieved in both groups. Periapical healing rates: 1 st group = 88.9%, 2 nd group = 100% Both groups exhibited comparable increase in root dentinal walls thickness Apical closure: 1 st group = 60%, 2 nd group = 70%
Narang <i>et al.</i> (2015)	Group 1: MTA apical plug technique (n = 5 teeth) Group 2: RET using a blood clot (n = 5 teeth)	< 20	Up to 18	Resolution of clinical signs and symptoms of pathology was achieved in all groups.

Study	Clinical intervention	Age (years)	Follow-up (months)	Clinical and radiographic outcomes
	<p>Group 3: RET using a platelet-rich fibrin (n = 5 teeth)</p> <p>Group 4: RET using a platelet-rich plasma (n = 5 teeth)</p>			<p>Periapical healing rates: 1st group = 60%, 2nd group = 60%, 3rd group = 98%, 4th group = 80%</p> <p>Percentages of root length increase: 1st group = 0%, 2nd group = 40%, 3rd group = 99%, 4th group 40%</p> <p>Percentages of root width increase: 1st group = 0%, 2nd group = 50%, 3rd group = 60%, 4th group 50%</p>
Bonte <i>et al.</i> (2015)	<p>Group 1: Ca(OH)₂ apexification (n = 15 teeth)</p> <p>Group 2: MTA apical plug technique (n = 15 teeth)</p>	6 - 18	Up to 12	<p>Apical healing: 1st group = 80%, 2nd group = 93.3%</p> <p>Survival rates: 1st group = 73.3%, 2nd group = 100%</p>

Study	Clinical intervention	Age (years)	Follow-up (months)	Clinical and radiographic outcomes
Silujjai and Linsuwanont (2017)	<p>Group 1: MTA apical plug technique (n = 29 teeth)</p> <p>Group 2: RET using a blood clot (n = 17 teeth)</p>	8 - 46	≥ 12	<p>Clinical success rates: MTA-treated teeth = 80.77%, RET-treated teeth = 76.47%</p> <p>Functional retention rates: MTA-treated teeth = 82.76%, RET-treated teeth = 88.24%</p> <p>RET resulted in a greater percentage increase in root width (13.75%) compared to the MTA apical plug (-3.30%)</p> <p>RET showed various increases in root length ranging from -4% to 58%</p> <p>Tooth fracture was the main cause of failure in the 1st group, whilst persistent infection was the main failure cause in the 2nd group.</p>

2.3 Dental pulp tissue engineering

In 1993, tissue engineering emerged as an exciting interdisciplinary field integrating the biology and engineering sciences into a discipline focused on tissue regeneration (Langer and Vacanti, 1993). Tissue regeneration is defined as the development of a biological tissue substitute that restores, maintains or improves the function of the damaged body tissue (Vacanti and Langer, 1999). This is usually achieved by the meticulous and combined application of three key elements, namely stem cells, growth factors and a scaffold in a sterile environment suitable for cellular growth and tissue regeneration.

Dental pulp tissue engineering aims to regenerate the damaged dental pulp and restore its functions through the application of tissue engineering principles. Since the isolation and characterisation of dental pulp stem cells from primary and permanent teeth (Gronthos *et al.*, 2000, Gronthos *et al.*, 2002, Miura *et al.*, 2003), they have been recognised as promising cell sources for dental pulp regeneration. Early proof of concept studies on the transplantation of this cell types with a scaffold, such as biphasic hydroxyapatite/tricalcium phosphate, ectopically in an immunodeficient mouse model have demonstrated their potential to regenerate dental pulp-like tissue (Gronthos *et al.*, 2002, Miura *et al.*, 2003). Subsequent studies applied different strategies by either seeding dental stem cells in a scaffold and implanting the construct in an immunodeficient mouse model using a root slice (Cordeiro *et al.*, 2008, Sakai *et al.*, 2010) or a whole root (Huang *et al.*, 2010, Rosa *et al.*, 2013, Kuang *et al.*, 2016), or through using a cell-free scaffold integrated with growth factors to induce the homing of endogenous stem cells into the root canal (Eramo *et al.*, 2018, Widbiller *et al.*, 2018). However, to date, only stem cell transplantation based approaches have

shown *in situ* pulp-like tissue regeneration in preclinical (Iohara *et al.*, 2013) and clinical studies (Nakashima *et al.*, 2017, Xuan *et al.*, 2018, Sui *et al.*, 2019).

Studies have evaluated the dental pulp regeneration potential of stem cell transplantation approach through two strategies, namely a scaffold-free strategy and a scaffold-based strategy (Dissanayaka and Zhang, 2020). The scaffold-free strategy relies on the self-assembly of monodispersed cells into a three-dimensional tissue through the secretion of their own matrix (Dissanayaka and Zhang, 2020). This approach involves the use of cell sheets (Na *et al.*, 2016, Syed-Picard *et al.*, 2014), spheroids (Dissanayaka *et al.*, 2014) and tissue strands (Itoh *et al.*, 2018) as a building blocks for tissue regeneration. The main advantage of this approach is that it permits direct cellular interaction with no interference from a scaffold material.

On the contrary, the scaffold-based strategy relies on the use of a biomaterial to support the cells during the regenerative process (Dissanayaka and Zhang, 2020). The scaffold could be a porous three-dimensional matrix, a hydrogel or a combination of both. In choosing the scaffold biomaterial, several aspects including cell-matrix interaction, biocompatibility, biodegradability, growth factors incorporation possibility, vascularisation enhancement, contamination control, mineralisation induction and ease of modification have to be considered (Galler *et al.*, 2010, Galler *et al.*, 2011a, O'brien, 2011). An overview of the various classes of biomaterials investigated for use as scaffolds in dental pulp regeneration is presented in Table 2-2.

Table 2-2: Biomaterials used as scaffolds in dental pulp regeneration.

Biomaterials	Favourable characteristics	Limitations
<p>Synthetic polymers, such as:</p> <ul style="list-style-type: none"> - Polyglycolic acid (PGA) - Polylactic acid (PLA) - Copolymer of PGA and PLA (PLGA) 	<ul style="list-style-type: none"> • Cost effective. • Reproducible production. • Easy to modify into any shape. • Porosity, mechanical properties, degradation rate and wettability can be tailored according to the need. • Functional groups can be added to bind cells or growth factors 	<ul style="list-style-type: none"> • Poor resemblance to the natural ECM. • Release acidic cytotoxic products upon degradation. • Provokes inflammatory host responses
<p>Natural polymers, such as:</p> <ul style="list-style-type: none"> - Collagen - Chitosan - Hyaluronic acid - Alginate 	<ul style="list-style-type: none"> • Biocompatible and biodegradable. • Naturally-occurring biomaterials with unique structural characteristics. • Tailorable composition and chemistry. • Possible processing into many forms. 	<ul style="list-style-type: none"> • Poor mechanical properties. • Properties may differ from batch to batch.
<p>Synthetic hydrogels, such as:</p> <ul style="list-style-type: none"> - Self-assembling peptides - Polyethylene glycol 	<ul style="list-style-type: none"> • Injectable with in situ gelation. • Possible incorporation of functional molecules and growth factors. • Possible transformation into smart hydrogels. • Uniform encapsulation of the cells. 	<ul style="list-style-type: none"> • Slow gelation. • Requires ultraviolet light which can be cytotoxic. • Poor mechanical properties.

Biomaterials	Favourable characteristics	Limitations
<p>Natural hydrogels, such as:</p> <ul style="list-style-type: none"> - Collagen - Fibrin - Chitosan - Proteoglycans - Gelatin 	<ul style="list-style-type: none"> • Injectable. • Excellent biocompatibility. • Viscoelastic properties comparable to that of soft connective tissue. • Uniform cell encapsulation. • Transport of nutrients and wastes is efficient. • Allows cell-cell interaction. 	<ul style="list-style-type: none"> • Poor mechanical properties. • Rapid degradation rate. • Contraction.
<p>Host-derived scaffolds, such as:</p> <ul style="list-style-type: none"> - Platelet-rich plasma - Platelet-rich fibrin 	<ul style="list-style-type: none"> • Natural environment for cell growth and tissue formation. • Controlled release of growth factors. 	<ul style="list-style-type: none"> • Requires special equipment and reagents.

2.3.1 Challenges facing dental pulp tissue engineering

Despite the progress achieved in dental pulp tissue engineering and regeneration over the past decades, several challenges still exist (Huang *et al.*, 2020). These challenges include, but are not limited to, post-implantation vascularisation and cell survival in addition to the absence of adequate stimulation to promote lineage-specific cell differentiation (Dissanayaka and Zhang, 2020, Huang *et al.*, 2020). Stem cell survival tends to be compromised once transplanted to the root canal due to the lack of oxygen and nutrients (Novosel *et al.*, 2011, Dissanayaka and Zhang, 2017). A drop to less than 5% post-implantation cell survival was shown to occur within the first 10 days (Guest *et al.*, 2010). This is because the cells, following implantation, rely solely on the oxygen and nutrients provided through diffusion from the nearby microvessels. Since the diffusion of nutrients and oxygen only serves up to a distance of 200 μm (Carmeliet and Jain, 2000), cells beyond this diffusional distance undergo apoptosis rapidly post-implantation (Muschler *et al.*, 2004). Therefore, rapid formation of a capillary network is critical to ensure post-implantation cell survival.

In order to facilitate vascularisation following cell transplantation, several strategies have been investigated (Dissanayaka and Zhang, 2017). These include co-transplantation of dental stem cells with microvascular endothelial cells with or without a biodegradable scaffold (Dissanayaka *et al.*, 2014, 2015), incorporation of angiogenic growth factors into the transplanted construct (Richardson *et al.*, 2001, Mullane *et al.*, 2008, Yadlapati *et al.*, 2017) and the use of a scaffold with prefabricated microvessels (Athirasala *et al.*, 2017). Unfortunately, these strategies present many limitations including the poor control over growth factor delivery, challenging manipulation of endothelial cells

and the translational hurdle of a scaffold with prefabricated microvessels (Dissanayaka and Zhang, 2017).

In addition to post-implantation cell survival, stem cell differentiation into odontoblast-like cells following cell homing or transplantation to the root canal is impossible without the presence of proper and adequate signalling cues (Dissanayaka and Zhang, 2020). Current attention has focused on the delivery of a single or multiple growth factors to induce cell differentiation into dental pulp-specific lineage (Vo *et al.*, 2012). However, growth factors dosage, time of delivery and long-term stability have posed a challenge for the clinical translation (Ravindran and George, 2015).

Therefore, based on the challenges discussed above, there is an unmet need for a clinically translatable strategy capable of enhancing vascularisation and providing adequate stimulation to promote lineage-specific cell differentiation during dental pulp regeneration.

2.4 Decellularised biological scaffolds

Decellularised biological scaffolds composed of ECM and prepared through tissue decellularisation have shown a great potential in facilitating the vascularisation of the engineered construct (Menon *et al.*, 2003, Silverman *et al.*, 2004, Liu *et al.*, 2011) and in providing an instructive environment for stem cell differentiation (French *et al.*, 2012, Cheung *et al.*, 2014, Ning *et al.*, 2015, Zhang and Dong, 2015, Agmon and Christman, 2016, Swinehart and Badylak, 2016, Robb *et al.*, 2017) in many regenerative medicine applications. When a tissue is decellularised, the cellular components are eliminated leaving behind a relatively conserved ECM with retained vascular network and with several structural and functional components and biological cues that interact naturally with the cells of that particular tissue (Hoshiba *et al.*, 2010). This makes decellularised scaffolds promising platforms to facilitate vascularisation and provide stem cells with structural frameworks and biological signalling required to promote tissue-specific cell differentiation (Brown and Badylak, 2014, Robb *et al.*, 2017).

2.4.1 Methods of tissue decellularisation

The decellularisation process aims to remove cells and cell remnants from the tissue while retaining the native ECM structure and composition intact to the best extent possible (Crapo *et al.*, 2011). Several physical methods as well as chemical and enzymatic agents are employed in combination to decellularise a tissue or an organ (Keane *et al.*, 2015). The decellularisation methods, including their mode of action and effects on the ECM structure and composition, are discussed below and summarised in Table 2-3.

Table 2-3: Methods of tissue decellularisation.

Methods	Mode of action	Effects on the ECM
Physical decellularisation methods		
Immersion and agitation in a solution	Facilitate cell exposure to chemicals and cell removal	Aggressive agitation can disrupt the ECM structure
Vascular perfusion		High perfusion pressure can disturb the ECM structure and rupture the vessels leading to incomplete decellularisation
Thermal shock	Disrupt the cell membrane through the formation of ice crystals	Uncontrolled temperature change can disrupt the ECM structure
Mechanical disruption	Remove the undesirable cell-rich layer of a tissue	Aggressive application of mechanical force can disrupt the ECM
Chemical decellularisation agents		
High and low molarity ionic solutions	Lyse the cells through osmotic shock induction	-
Non-ionic detergents (e.g., Triton X100)	Solubilise cytoplasmic and nuclear membrane through disrupting lipid-lipid and lipid-protein interactions	Remove glycosaminoglycans from ECM
Ionic detergents (e.g., Sodium dodecyl sulfate)	Solubilise cytoplasmic and nuclear membrane by disturbing protein-protein interactions	Remove glycosaminoglycans and destroy collagen

Methods	Mode of action	Effects on the ECM
Zwitterionic detergents (e.g., CHAPS)	Solubilise cytoplasmic and nuclear membrane	Remove glycosaminoglycans from ECM
Acids (e.g., Peracetic acid)	Solubilise cytoplasmic and nuclear components, and oxidise microbial enzymes	Dissociate glycosaminoglycans from ECM
Solvents (e.g., Tri(n-butyl)-phosphate)	Denature proteins and nucleic acids through disruption of hydrogen bonds	Loss of collagen from ECM
Chelating agents (e.g., EDTA)	Binds metallic ions such as Ca^{+2} and Mg^{+2} , thus disrupting cell attachment to ECM	-
Protease inhibitors (e.g., aprotinin)	Protect the ECM from proteases released following cell rupture	-
Enzymatic decellularisation agents		
Nucleases (e.g., DNase, RNase)	Catalyse the hydrolysis of ribonucleotides and deoxyribonucleotides bonds leading to RNA and DNA degradation	If retained within the ECM can lead to unfavourable cellular response
α -galactosidase	Solubilise the galactose- α -(1,3)-galactose (Gal epitope)	-

2.4.1.1 Physical decellularisation methods

Physical decellularisation methods include thermal shock, sonication, mechanical/manual disruption, immersion and agitation in a solution and vascular perfusion (Gilbert *et al.*, 2006, Crapo *et al.*, 2011, Keane *et al.*, 2015). Thermal shock, which involves a single or multiple freeze-thaw cycles, and sonication are used to disrupt or rupture the cell membrane and facilitate their subsequent removal from the tissue. Mechanical/manual disruption, on the other hand, is utilised to enhance the decellularisation efficacy by removing the undesirable cell-rich area from the tissue manually. In general, thermal shock, sonication and mechanical disruption are usually used at the beginning of the decellularisation process to enhance the cell removal efficacy (Gilbert, 2012).

Immersion and agitation in a solution and vascular perfusion are commonly used throughout the decellularisation process to facilitate the transport of decellularisation agents to the cells and to enhance the removal of cellular debris and residual chemicals from the tissue (Gilbert *et al.*, 2006). The decision of which approach to choose depends highly on the tissue characteristics. Immersion and agitation in a solution is used often in the decellularisation of thin tissues such as amniotic membrane (Wilshaw *et al.*, 2006), blood vessels (Wilshaw *et al.*, 2012) and dermis (Reing *et al.*, 2010). In contrast, vascular perfusion is usually used for the decellularisation of complex organs with intact vascular networks such as the kidney (Ross *et al.*, 2009), lung (Ott *et al.*, 2010) and liver (Uygun *et al.*, 2010).

2.4.1.2 Chemical decellularisation agents

Several classes of chemical agents are used in tissue decellularisation including high osmolarity and low osmolarity ionic solutions, detergents, acids and alkaline solutions, solvents, chelating agents and protease inhibitors (Gilbert *et al.*, 2006,

Crapo *et al.*, 2011, Keane *et al.*, 2015). A combination of these chemicals is usually used in tissue decellularisation through a series of short washes in cycles, aiming to increase the cell removal efficiency and decrease the overall exposure time to the chemicals.

High and low osmolarity ionic solutions are used in succession to rupture the cells through osmotic shock induction (Gilbert, 2012). These solutions are usually employed during the initial steps of the decellularisation process to release the cell contents and facilitate their subsequent solubilisation and clearance out of the tissue. A potential of ECM disruption due to the ionic strength of high and low osmolarity solutions exists. Therefore, the overall tissue exposure time to these solutions must be kept as short as possible (Crapo *et al.*, 2011).

Detergents are the most commonly used chemicals for tissue decellularisation due to their ability to solubilise the cellular and nuclear membranes (Gilbert *et al.*, 2006, Crapo *et al.*, 2011). Detergents are classified into three categories, namely non-ionic detergents, ionic detergents and zwitterionic detergent. Non-ionic detergents, such as Triton X100, have the least impact on ECM protein as compared to other detergents because they lack the ionic charge. However, the cell removal efficiency of non-ionic detergents is inferior to that of ionic detergents (Nakayama *et al.*, 2010). Therefore, non-ionic detergents are usually used in combination with other categories of detergents to enhance the cell removal efficiency (Traphagen *et al.*, 2012, Chen *et al.*, 2015). Ionic detergents, such as sodium dodecyl sulfate and sodium deoxycholate, are very efficient for the solubilisation and removal of cellular and nuclear membranes and cytoplasmic proteins (Gilbert *et al.*, 2006, Crapo *et al.*, 2011). However, the ionic detergents are harsh on ECM components because of their ionic charge (Seddon *et al.*, 2004). Therefore, the concentration and duration of application of ionic

detergents have to be determined cautiously to minimise the risk of ECM components loss. Zwitterionic detergents have features of non-ionic and ionic detergents (Gilbert, 2012). These detergents have an increased tendency to denature proteins as compared to non-ionic detergents. Examples of zwitterionic detergents include 3-[(3-cholamidopropyl)dimethylammonio]-1-propanesulfonate (CHAPS) which have been used for blood vessel decellularisation (Dahl *et al.*, 2003) and sulfobetaine-10 and -16 which have been studied for nerve decellularisation (Hudson *et al.*, 2004).

Acids and alkaline solutions are used in the decellularisation protocols to solubilise the cytoplasmic components, eliminate nucleic acids and disinfect the final decellularisation product (Gilbert *et al.*, 2006; Crapo *et al.*, 2011). However, these chemicals can dissociate important ECM molecules such as glycosaminoglycans. Peracetic acid (PAA) at a percentage of approximately 0.1% (w/v) was shown efficient for decellularisation and simultaneous disinfection of thin tissues such as small intestinal submucosa and urinary bladder submucosa (Hodde and Hiles, 2002).

Solvents, such as Tri (n-butyl) phosphate, has been used as a chaotropic agents in the decellularisation of tendon and anterior cruciate ligaments (Gilbert *et al.*, 2006). Moreover, chelating agents, such as ethylenediaminetetraacetic acid (EDTA), are used in the decellularisation process to firmly bind and isolate metal ions necessary for cell attachment to collagen and fibronectin at Arg-Gly-Asp receptors (Gilbert *et al.*, 2006, Crapo *et al.*, 2011). Therefore, chelating agents are used to facilitate the subsequent cell removal from the tissue.

Protease inhibitors are used during tissue decellularisation to protect the ECM from damage due to the release of proteases from disrupted cells. Examples of

the most commonly used protease inhibitors include aprotinin and leupeptin (Gilbert *et al.*, 2006, Crapo *et al.*, 2011).

2.4.1.3 Enzymatic decellularisation agents

Enzymes are used commonly during the process of tissue decellularisation either to disrupt the interaction between the cells and ECM or to target and lyse a specific cellular protein (Gilbert *et al.*, 2006; Crapo *et al.*, 2011). Nucleases, such as DNase and RNase, are used to break the sequence of nucleic acids within the tissue, thus facilitating their removal or eliminating their function (Gilbert, 2012). Concerns about retention of nucleases in the final product, which could affect the cellular response, have been obviated by a study that showed no functional nucleases within the decellularised tissues following rinsing (Daly *et al.*, 2012).

The other enzyme which is frequently used in tissue decellularisation is α -galactosidase (Gilbert, 2012). This enzyme is used to target and remove the galactose- α -(1,3)-galactose (Gal epitope), a cellular antigen that is known to cause xeno-rejection in humans (Xu *et al.*, 2009, Galili, 2001). Tissue treatment with α -galactosidase is usually needed in complex tissues or organs decellularisation but is not necessary for thin tissues (Badylak and Gilbert, 2008).

2.4.2 Evaluation of tissue decellularisation

Criteria for assessing the efficacy of decellularisation process have been suggested by Crapo *et al.* (2011). The criteria include: (1) absence of visible cell nuclei in decellularised tissue sections stained with haematoxylin and eosin and DAPI, (2) the DNA content remaining in the tissue should not exceeds 50 ng/mg of dry tissue weight, and (3) the fragment size of remaining DNA should not exceed 200 base pairs (Crapo *et al.*, 2011). These criteria were defined based

on studies that showed a favourable host response to the decellularised scaffolds when they meet the criteria (Crapo *et al.*, 2011, Keane *et al.*, 2012).

2.4.3 Effects of decellularised scaffolds on stem cell behaviours

Decellularised scaffolds have been shown to produce chemoattractant peptides following chemical degradation *in vitro* (Brennan *et al.*, 2008) and to attract stem cells following implantation *in vivo* (Beattie *et al.*, 2009). Dziki *et al.* (2016) reported the mobilisation and recruitment of CD149⁺ perivascular stem cells to the margin and centre of the decellularised small intestinal submucosa following *in vivo* implantation in mice. A similar observation was demonstrated by Perniconi *et al.* (2011) showing detection of PW1⁺ muscle interstitial stem cells in a decellularised skeletal muscle scaffold following two weeks of *in vivo* implantation. This is consistent with the findings reported by Zantop *et al.* (2006) showing repopulation of decellularised small intestinal submucosa by bone marrow-derived progenitor cells following implantation in tendon defect in mice.

In addition to the chemoattraction effect, the decellularised scaffolds have shown a potential to induce site-appropriate tissue-specific differentiation of stem cells (Agmon and Christman, 2016, Swinehart and Badylak, 2016, Cramer and Badylak, 2019). A study by Iop *et al.* (2009) showed a decellularised heart valve scaffold capable of inducing the differentiation of human mesenchymal stem cells toward valve interstitial cell lineage. Another study by Cheung *et al.* (2014) demonstrated an increase in glycerol-3-phosphate dehydrogenase activity and adipogenesis on human adipose-derived stem cells when seeded on a composite hydrogel containing decellularised adipose tissues as compared to the hydrogel only. Furthermore, Zhang and Dong (2015) showed hepatic differentiation of mouse adipose-derived stem cells following seeding on decellularised liver

coating. Collectively, the findings of these studies demonstrated the potential of decellularised scaffolds to promote tissue-specific differentiation of stem cells.

The decellularised scaffolds showed a potential to promote vascularisation, in several regenerative medicine applications, probably due to the preservation of vasculature together with several angiogenic growth factors (Conconi *et al.*, 2004, Pellegata *et al.*, 2018, Alvarèz Fallas *et al.*, 2018). The use of a decellularised dermal scaffold as a graft for ventral hernia repair in the rabbit model revealed integration and revascularisation of the graft after 30 days following implantation (Menon *et al.*, 2003). Furthermore, Liu *et al.* (2011) reported greater vascularisation capacity of the decellularised intestinal submucosa and decellularised dermal matrix following subcutaneous implantation in mice as compared to a composite scaffold (collagen-chondroitin sulfate-hyaluronic acid). The same study showed that seeding the decellularised scaffolds with adipose-derived stem cells resulted in a greater amount of vascular endothelial growth factor secreted by the cells with enhanced vascularisation capacity of the decellularised scaffolds *in vivo* (Liu *et al.*, 2011). Additionally, seeding of the decellularised skin/adipose tissue flap with adipose-derived stem cells and umbilical vein endothelial cells was shown to result in vessel-like structures *in vitro* with neovascularisation *in vivo* (Zhang *et al.*, 2016).

2.4.4 Decellularised scaffolds of dental origin

An overview of the studies on dental tissues-derived decellularised scaffolds is presented in Table 2-4, with most of the studies published during the course of the present research. Tooth buds and dental pulps are the tissues that have attracted most attention for decellularised scaffolds development due to their potential use in dental pulp and whole tooth bioengineering. Traphagen *et al.*

(2012) reported decellularisation of porcine molar tooth buds using a high concentration of dual detergents (SDS/Triton X100). Significant production of organised enamel-like and dentine-like tissues was observed in the resultant scaffolds following seeding with human dental pulp stem cells (hDPSCs), porcine epithelial cells and human umbilical vein endothelial cells and implantation in the extraction sockets of pig mandibular teeth for six months (Zhang *et al.*, 2017).

The first attempt to decellularise dental pulp was reported by Chen *et al.* (2015) who used a combination of decellularised miniature swine dental pulp, treated dentine matrix and PLGA/gelatine electrospun sheet as a strategy for tooth root regeneration. Their work showed decellularised dental pulps supporting the cellular invasion of human dental follicle stem cells *in vitro*. These findings were further supported by Alqahtani *et al.* (2018) who showed the host cells infiltrating the decellularised pulps after eight weeks following implantation in dogs' teeth root canals containing provoked apical blood.

Several studies reported the odontogenic differentiation of human stem cells of the apical papilla, hDPSCs and human bone marrow-derived stem cells following *in vitro* culture on decellularised human dentine-pulp disks (Song *et al.*, 2017), coatings of hydrogels derived from decellularised human pulps (Li *et al.*, 2020) and freeze-dried hydrogels derived from decellularised bovine pulps (Bakhtiar *et al.*, 2020), respectively. However, it is still not clear if the decellularized pulps can promote stem cell differentiation into dental pulp-specific lineage in the absence of exogenous growth or differentiation factors.

Table 2-4: A summary of the studies on dental tissues-derived decellularised scaffolds.

Dental tissues	studies	Decellularisation methods	Characteristics of the decellularised scaffolds	Performance of the decellularised scaffolds
Porcine molar tooth buds	(Traphagen <i>et al.</i> , 2012)	One cycle of dual detergents (5% w/v sodium dodecyl sulfate (SDS) for 24 h / 1% w/v Triton X100 for 24 h) >>	- Intact decellularised tooth buds retaining collagen I and IV, fibronectin and laminin.	No evaluation was reported.
	(Zhang <i>et al.</i> , 2017)	four cycles of dual detergents (1% w/v SDS for 24 h / 1% w/v Triton X100 for 24 h) >> nuclease treatment	- Intact decellularised tooth buds retaining the matrix collagen networks.	<p><u><i>In vitro:</i></u></p> <p>- The scaffolds supported the growth of human dental pulp stem cells (hDPSCs), porcine epithelial cells (pECs) and human umbilical vein endothelial cells (HUVECs).</p> <p><u><i>In vivo</i> implantation in the extraction sockets of pigs' mandibular teeth showed:</u></p> <p>- Organised enamel-like, dentine-like and pulp-like tissues in the scaffolds seeded with hDPSCs, pECs and HUVECs.</p>

Dental tissues	studies	Decellularisation methods	Characteristics of the decellularised scaffolds	Performance of the decellularised scaffolds
Human pulp-dentine disks	(Song <i>et al.</i> , 2017)	Three cycles of dual detergents (1% w/v SDS for 24 h / 1% w/v Triton X100 for 24 h) >> nuclease treatment	- Retention of collagen I and fibronectin as well as the structure of the pulpal matrix, with elimination of major histocompatibility protein class I (HLA-A).	<u><i>In vitro:</i></u> - The decellularised pulp-dentine disks supported the growth of human stem cells of the apical papilla and promoted their differentiation into odontoblasts-like cells.
Human dental pulps	(Matoug-Elwerfelli <i>et al.</i> , 2018)	One cycle of single detergent (0.03% w/v SDS for 24 h) >> nuclease treatment.	- Intact biocompatible decellularised pulps retaining collagen I & III, fibronectin and laminin, with elimination of HLA-A.	<u><i>In vitro:</i></u> - The scaffolds supported the adhesion and growth of human dental pulp stem cells.

Dental tissues	studies	Decellularisation methods	Characteristics of the decellularised scaffolds	Performance of the decellularised scaffolds
Human dental pulps	(Li <i>et al.</i> , 2020)	Three cycles of dual detergents (1% w/v SDS for 24 h / 1% w/v Triton X100 for 24 h) >> nuclease treatment >> digestion and hydrogel formation	- Injectable hydrogels containing around 1213 protein species in known to be involved in the regulation of several biological activities and cellular behaviours.	<u><i>In vitro:</i></u> - A coating of the decellularised pulps hydrogel supported the growth of human dental pulp stem cells, and promoted their differentiation into odontoblasts-like, neural-like and endothelial-like cells, in the presence of specialised induction media.
Miniature swine dental pulps	(Chen <i>et al.</i> , 2015)	One cycle of dual detergents (1% w/v SDS for 12 h / 1% w/v Triton X100 for 30 min)	- Biocompatible. - Intact decellularised pulps retaining fibronectin, collagen I & III and laminin.	<u><i>In vitro:</i></u> - The scaffolds supported proliferation of human dental follicle stem cells. <u><i>In vivo</i> ectopic implantation in nude mice for 6 weeks showed:</u> - Host cells recruitment to the scaffolds with evidence of revascularisation.

Dental tissues	studies	Decellularisation methods	Characteristics of the decellularised scaffolds	Performance of the decellularised scaffolds
Swine dental pulps	(Alqahtani <i>et al.</i> , 2018)	0.02% Trypsin / 0.05% EDTA for 1 h >> 3% w/v Triton X100 for 30 min >> 4% deoxycholic acid for 30 min	<ul style="list-style-type: none"> - Biocompatible. - Intact decellularised pulpal matrices retaining collagen I, DMP-1, DSP, vWF, VEGF and TGF-β. 	<p><u><i>In vivo</i> implantation in dogs root canals for 8 weeks showed:</u></p> <ul style="list-style-type: none"> - Host cell infiltration into the scaffolds with positive expression of odontogenic and angiogenic markers (DSP and CD31).
Bovine dental pulps	(Bakhtiar <i>et al.</i> , 2020)	0.02% Trypsin/0.05% EDTA for 1 h >> four cycles of 0.1% (w/v) SDS for 12 h >> nuclease treatment >> digestion and transformation into a hydrogel.	<ul style="list-style-type: none"> - Injectable hydrogel. - Biocompatible. - Biodegradable. - More than 97% porosity. 	<p><u><i>In vitro:</i></u></p> <ul style="list-style-type: none"> - The scaffolds supported proliferation of human bone marrow-derived stem cells and promoted their odontogenic differentiation. <p><u><i>In vivo</i> subcutaneous implantation in rats for 2 weeks revealed:</u></p> <ul style="list-style-type: none"> - Low immunological response with evidence of angiogenesis.

2.5 Summary

There is an unmet need for regenerating functional dental pulp, particularly in non-vital immature permanent teeth where pulpal necrosis arrests further radicular maturation, putting young patients at risk of permanent tooth loss. Despite the advancements achieved over recent decades, dental pulp regeneration still faces challenges in promoting post-implantation vascularisation and inducing odontoblast-like cell differentiation.

Decellularised biological scaffolds have shown great potential to facilitate vascularisation and promote tissue-specific stem cell differentiation in many regenerative medicine applications. Therefore, it can be hypothesised that a decellularised dental pulp matrix with retained native histoarchitecture, composition and vasculature might facilitate vascularisation during the process of dental pulp regeneration and might also provide an instructive environment for stem cell differentiation into odontoblast-like cells.

Although allogeneic decellularised scaffolds are the preferred option, their use faces supply limitation, presenting a barrier to research progress and subsequent clinical translation. Therefore, the use of xenogeneic decellularised scaffolds may provide a readily available alternative.

2.6 Aim and objectives

Aim:

The overall aim of the research presented in this thesis was to investigate the potential of a decellularised dental pulp matrix of bovine origin to facilitate vascularisation and support dental pulp regeneration.

Objectives:

- To develop a decellularised bovine dental pulp matrix and characterise its structural and compositional characteristics.
- To recellularise the developed decellularised bovine dental pulp matrix using hDPSCs and to investigate its vascularisation capacity as well as its potential to promote odontoblast-like cell differentiation *in vitro*.
- To investigate the vascularisation capacity of a decellularised bovine dental pulp matrix seeded with hDPSCs *in vivo* and to evaluate the regenerative potential of seeded and unseeded decellularised dental pulps.

Chapter 3

Materials and Methods

3.1 Materials

3.1.1 Equipment

Details of the equipment that were used throughout the present research project are listed in Table 3-1.

Table 3-1: Details of the laboratory equipment used in the present study.

Items	Catalogue numbers	Suppliers
Accutom [®] -5 water-cooled cutting machine	-	Struers Inc.
Attune [®] NxT Acoustic Focusing Flowcytometer	-	Invitrogen via ThermoFisher scientific
Automatic tissue processor	TP1020	Leica Biosystems
Class II safety cabinet	N4-437-400E	NUAIRE
Confocal scanning laser microscopy	Leica TCS SP8	Leica microsystems
Extraction forceps	DFO600	Dental directory
Fluorescence microscope	Axio imager Z1 with Epitome	Zeiss
Freeze-dryer	Alpha 2-4 LD plus	CHIST
Haemocytometer	Z359629	Sigma Aldrich

Items	Catalogue numbers	Suppliers
Histology water bath	MH8515	Barnstead Electrothermal
Hot plate	E18.1 hotplate	Raymond A lamb
Humidity chamber with lid	H6644	Sigma-Aldrich
Inverted microscope	IX71	Olympus
Light cycler	Roche LC480	Roche LifeScience
Metal wax block moulds	GBC-3614-05A	Cellpath
Microtome	RM2125	Leica Biosystems
Mr. Frosty™ freezing container	11315674	ThermoFisher scientific Ltd.
NanoDrop™ 2000 spectrophotometer	Nc/2000	ThermoFisher scientific Ltd.
Pressure cooker	-	Menapath
Scalpel blade handles	5334	ThermoFisher scientific
Scanning electron microscope	S-3400N	Hitachi
Sterile Kerr endodontic files	EKK002, EKK506, EKK094	Dental Directory
Thermal cycler	PTC-100 (Version 9)	Bio-Rad
TopCount™ plate reader	Multiskan Spectrum 1500	ThermoFisher scientific
Upright bright-field microscope	Axioplan	Zeiss

3.1.2 Consumables

Details of the laboratory consumables that were used throughout the present research project are listed in Table 3-2.

Table 3-2: Details of the laboratory consumables used in the present study.

Items	Catalogue numbers	Suppliers
Adhesive PCR Plate Seals	AB0558	ThermoFisher scientific
Cell culture flasks (T75, T175)	430641U, 431079	Corning incorporated
Clear flat bottom well plates (6 well, 24 well and 96 well)	3506, 3527, 3988	Corning incorporated
Cryotubes (2 mL, 4 mL)	BR114832, BR114834	Sigma-Aldrich
Disposable sterile syringes (10 mL)	S75101	Scientific laboratory supplies
DNase/RNase-free microcentrifuge tubes (1.5 mL)	AM12400	ThermoFisher scientific
Eppendorf® microcentrifuge tubes (0.5 mL, 1.5 mL, 2 mL)	T8911, T9661, T2795	Sigma-Aldrich
ETHILON® Nylon suture	1668G	Johnson & Johnson Medical Devices Companies
FACS tubes	38007	STEMCELL™ Technologies

Items	Catalogue numbers	Suppliers
Falcon tubes (15 mL, 50 mL)	339650, 339652	ThermoFisher Scientific
Glass coverslips	COV12440S	Solmedia
Histology tissue bags	3801085	Leica Biosystems
Microscopic glass slides	x-tra® superfrost (3800050)	Leica Biosystems
OPSITE Flexigrid adhesive membrane	4629	Smith and nephew
PCR plates (96 well; Light cycler type)	1402-9909	Starlab
PCR tubes (0.2 mL)	TF10201	Bio-Rad
Plastic histology cassettes	M490-3	Simport™ scientific
Scalpel blades (Size 22)	53223	ThermoFisher Scientific
Silicon embedding moulds	E4390	Sigma-Aldrich
Specimen pots	IR1381	Alpha Laboratories
Steri-Strip™ Reinforced Adhesive	70200711060	3M™
SteriWare™ disposable tweezers	15849421	ThermoFisher scientific
Syringe filters (0.2 µm)	725-2520	ThermoFisher Scientific
White 96 well Optiplate	6005290	PerkinElmer

3.1.3 Chemical reagents and kits

Details of the chemical reagents and kits that were used throughout the present research project are listed in Table 3-3.

Table 3-3: Details of the chemical reagents and kits used in the present study.

Chemical reagents/kits	Catalogue numbers	Suppliers
Agar	A-9915	Sigma-Aldrich
Alcian blue solution	B8438	Sigma-Aldrich
Alexa-Fluor [®] 488 Phalloidin	A12379	ThermoFisher scientific
Alizarin red solution	TMS-008	Sigma-Aldrich
Alpha modified eagle's medium	BE12-169F	Lonza [™]
Antibody diluent solution	00-3218	ThermoFisher scientific
Aprotinin	A6279	Sigma-Aldrich
ATPlite [™] Luminescence Assay	6016943	PerkinElmer
Bovine serum albumin solution	A7979	Sigma-Aldrich
Boxall	SP-6000	Vector-Laboratories
Casein	SP-5020	Vector-Laboratories
Cell trace [™] Calcien violet viability stain	L34958	ThermoFisher scientific
Citric acid-based antigen unmasking solution	H-3301	Vector-Laboratories

Chemical reagents/kits	Catalogue numbers	Suppliers
Cyanoacrylate contact adhesive	-	Viking
DAPI	D1306	ThermoFisher scientific
Decal III	RRDC3-E	Atom Scientific
Deoxyribonuclease I	AMPD1	Sigma-Aldrich
Dimethyl sulfoxide	D2650	Sigma-Aldrich
DPX mounting medium	D/5319	ThermoFisher scientific
Dulbecco's modified Eagle's media	D6546	Sigma-Aldrich
EDTA Solution (Pulpdent)	EDTA-120	Dental Directory
Eosin solution	RRSP35-D	Atom Scientific
Ethanol	51976	Sigma-Aldrich
Ethylenediaminetetraacetic acid solution	03690	Sigma-Aldrich
FcR blocking reagent (Human)	130-059-901	Miltenyi biotec
Foetal bovine serum	F7524	Sigma-Aldrich
Giemsa solution	12-0440	Sigma-Aldrich
Harris's haematoxylin	HHS32	Sigma-Aldrich
High-Capacity RNA-to-cDNA™ Kit	4387406	ThermoFisher scientific
HistoReveal	Ab103720	Abcam

Chemical reagents/kits	Catalogue numbers	Suppliers
Hydrochloric acid (6 M)	H/1200/PB17	ThermoFisher Scientific
ImmPACT™ DAP Peroxidase Substrate Kit	SK-4105	Vector laboratories
ImmPRESS Excel HRP Polymer detection Kit (anti-mouse)	MP-7602	Vector laboratories
ImmPRESS HRP polymer detection kit (anti-rabbit)	MP-7451	Vector laboratories
L-Glutamine solution	G7513	Sigma-Aldrich
Live/Dead Assay Kit	30002-T	Biotium
Magnesium chloride solution	M1028	Sigma-Aldrich
Mayer's haematoxylin	RRSP60-D	Atom Scientific
Mouse on Mouse Polymer IHC Kit	Ab269452	Abcam
Neutral buffered formalin	BAF-6000-08A	Cellpath
Nuclear Fast Red	N3020	Sigma-Aldrich
Nuclease free water	10336503	ThermoFisher scientific
Oil red O solution	O1391	Sigma-Aldrich
Paraffin wax	8335	ThermoFisher scientific
Penicillin-Streptomycin solution	P4333	Sigma-Aldrich
Peracetic acid solution	77240	Sigma-Aldrich

Chemical reagents/kits	Catalogue numbers	Suppliers
Phosphate buffered saline	10010023	ThermoFisher scientific
Phosphate buffered saline without Calcium or Magnesium	17-512F	Lonza
Picrosirius Red Stain Kit	24901-500	Polysciences, Inc.
Qiagen DNeasy Blood and Tissue kit	69504	Qiagen
Quant-iT PicoGreen dsDNA assay kit	P7589	ThermoFisher scientific
Ribonuclease A	R4642	Sigma-Aldrich
RNeasy [®] fibrous tissue Kit	74704	Qiagen
Scott's tap water	EGW-0200-25A	Cellpath
Sodium azide solution	S8032	Sigma-Aldrich
Sodium dodecyl sulphate	71736	Sigma-Aldrich
Sodium hydroxide (6 M)	S8045	ThermoFisher Scientific
StemMACS AdipoDiff Media (Human)	130-091-677	Miltenyi biotec
StemMACS ChondroDiff Media (Human)	130-091-679	Miltenyi biotec
StemMACS OsteoDiff Media (Human)	130-091-678	Miltenyi biotec
TaqMan [™] Fast Advanced Master Mix	4444557	ThermoFisher scientific Ltd.

Chemical reagents/kits	Catalogue numbers	Suppliers
Tris hydrochloride solution	T3038	Sigma-Aldrich
Tris-buffered saline	T5912	Sigma-Aldrich
Tris-buffered saline with 0.1% Tween [®] 20	T9039	Sigma-Aldrich
Tris-EDTA-based antigen unmasking solution	H-3301	Vector-Laboratories
Triton X-100	HFH10	ThermoFisher scientific
Trypan Blue solution	T8154	Sigma-Aldrich
Trypsin-EDTA solution	T4049	Sigma-Aldrich
Vectashield Antifade Mounting Medium with DAPI	H-1500	Vector-Laboratories
Vetergesic [®] solution	-	Ceva animal health Ltd
Weigert's Haematoxylin (solution A, solution B)	RRSP72-C (A), RRSP73-C (B)	Atom Scientific

3.1.4 Antibodies

3.1.4.1 Antibodies used in the immunohistochemical staining

Details of the primary and isotype antibodies that were used in the immunohistochemical staining are listed in Table 3-4.

Table 3-4: Details of the primary and control isotype antibodies used in the immunohistochemical staining.

Antibodies	Catalogue numbers	Suppliers
Primary antibodies		
Mouse monoclonal anti-alpha gal epitope (anti-bovine)	M86, ALX-801-090	Enzo Life Sciences
Mouse monoclonal anti-collagen I (anti-bovine)	Ab90395	Abcam
Mouse monoclonal anti-dentin sialophosphoprotein (anti-human)	sc-73632	Santa Cruz
Mouse monoclonal anti-Fibronectin (anti-bovine)	Ab6328	Abcam
Mouse monoclonal anti-transforming growth factor β 1 (anti-bovine)	MCA797	Bio-Rad
Rabbit polyclonal anti-fibroblast growth factor 2 (anti-bovine)	NB600-1536	NovusBio
Rabbit polyclonal anti-bone morphogenic protein 2 (anti-bovine)	MBS2028438	MyBioSource

Antibodies	Catalogue numbers	Suppliers
Primary antibodies		
Rabbit polyclonal anti-CD 31 (anti-human)	ab28364	Abcam
Rabbit polyclonal anti-collagen III (anti-bovine)	Ab7778	Abcam
Rabbit polyclonal anti-Laminin (anti-bovine)	Ab140482	Abcam
Rabbit polyclonal anti-vascular endothelial growth factor A (anti-bovine)	AHP2382	Bio-Rad
Mouse monoclonal anti-human nuclei (clone 3E1.3)	MAB4383	Merck Millipore
Control Isotypes		
Mouse monoclonal IgG1	Ab91353	Abcam
Mouse monoclonal IgG2b Kappa	X0944	DAKO
Mouse monoclonal IgM	14-4752-82	ThermoFisher scientific
Rabbit polyclonal IgG	Ab37415	Abcam

3.1.4.2 Antibodies used in the flowcytometric analysis of the cell surface markers

Details of the fluorochrome-conjugated primary and isotype antibodies that were used in the flowcytometric analysis of the cell surface markers are listed in Table 3-5.

Table 3-5: Details of the fluorochrome-conjugated primary and isotype antibodies used in the flowcytometric analysis of the cell surface markers.

Antibodies-Conjugates	Catalogue numbers	Suppliers
Primary antibodies		
CD105 antibody-FITC	130-098-774	Miltenyi biotec
CD146 antibody-PE	130-092-853	Miltenyi biotec
CD90 antibody- PerCP-Vio700	130-114-864	Miltenyi biotec
CD45 antibody- VioGreen	130-113-183	Miltenyi biotec
Control Isotypes		
Mouse IgG1-FITC	130-092-213	Miltenyi biotec
Mouse IgG1-PE	130-092-212	Miltenyi biotec
Mouse IgG1-PerCP-Vio700	130-097-561	Miltenyi biotec
Mouse IgG1-VioGreen	130-096-919	Miltenyi biotec

3.1.5 TaqMan gene expression assays

Details of TaqMan gene expression assays that were used in the reverse transcription quantitative polymerase chain reaction (RT-qPCR) experiment are listed in Table 3-6. All TaqMan gene expression assays were purchased from Applied Biosystems at ThermoFisher Scientific (General catalogue number = 4331182).

Table 3-6: Details of TaqMan gene expression assays used in the RT-qPCR.

Gene name/symbol	Description	TaqMan [®] gene expression assay
Dentin matrix acidic phosphoprotein-1 (DMP-1)	Odontogenesis marker (Gene of interest)	Hs01009391_g1
Dentin sialophosphoprotein (DSPP)	Odontogenesis marker (Gene of interest)	Hs00171962_m1
Glyceraldehyde-3-phosphate dehydrogenase (GAPDH)	House-keeping gene (Endogenous control)	Hs99999905_m1
Kinase insert domain receptor (KDR)	Angiogenesis marker (Gene of interest)	Hs00911700_m1
Matrix extracellular phosphoglycoprotein (MEPE)	Odontogenesis marker (Gene of interest)	Hs00220237_m1
Platelet & endothelial cell adhesion molecule (PECAM-1)	Angiogenesis marker (Gene of interest)	Hs01065279_m1

3.2 Methods

3.2.1 Acquisition of bovine dental pulps

Bovine tissues procurement

Dissected bovine upper jaws were obtained from a local abattoir (John Penny & Sons, Leeds, UK) within six hours of animal slaughter for food production. The age range of the cattle was between 18 - 20 months. The abattoir routinely processes both British Blue and Limousin cattle and so the breed of the cattle used in this research was one of these two breeds.

Bovine teeth extraction and dental pulps harvesting

Teeth were extracted from bovine jaws using forceps and subsequently cleaned from adherent soft tissues using a scalpel blade (no. 22) in a Class II safety cabinet (Figure 3-1. A). The external surfaces of the teeth were then disinfected using 70% (v/v) Ethanol to minimise the risk of dental pulp tissues contamination upon retrieval. Teeth were then placed inside disinfected gloves and cracked-open using a screw vice clamp (Figure 3-1. B). Dental pulp tissues were then aseptically retrieved (n = 6 dental pulp tissues per cow) using sterile tweezers in a Class II safety cabinet and then examined carefully for any adherent dentine chips under magnification and illumination (Figure 3-1. C). The harvested dental pulps were stored individually in 2 mL cryotubes containing phosphate buffered saline (PBS) supplemented with 10% dimethyl sulfoxide (DMSO) at - 80°C until used. DMSO was used to minimise tissue disruption due to ice crystal formation.



Figure 3-1: Bovine dental pulp harvesting. Representative images of (A) bovine tooth, (B) bovine tooth cracked-opened using a screw vice clamp and (C) harvested bovine dental pulp.

3.2.2 Basic techniques for the histological and immunohistochemical staining methods

3.2.2.1 Tissue fixation

Principle: Tissue fixation is the process of preserving the tissue in a state as close to natural as possible. This process protects the tissue from potential damage due to autolysis and/or microbial decomposition (Eltoum *et al.*, 2001). The fixative reagents inhibit the tissue intrinsic proteolytic enzymes and make the tissue less favourable to microorganism colonisation. Tissue fixation is the first step in preparing the biological samples for histological and immunohistochemical staining. The most commonly used technique for tissue fixation is the immersion in 10% (v/v) neutral buffered formalin (NBF, 4% formaldehyde in PBS). This technique fixes the tissue through the formation of inter-molecular and intra-molecular cross-linking (Eltoum *et al.*, 2001).

Method: In this research, tissue samples were fixed by complete immersion in prefilled pots containing 10% (v/v) NBF (4% formaldehyde in PBS) at a ratio of 1:20 sample volume to fixative volume for 48 hours at room temperature.

3.2.2.2 Tissue processing, paraffin wax embedding and sectioning

Principle: Tissue processing is a procedure used to prepare the fixed samples for paraffin wax embedding and sectioning. In tissue processing, the water content of the tissue is replaced with molten paraffin wax that subsequently solidifies, making the tissue well supported for consistent thin sections cutting. This step is critical since paraffin wax is hydrophobic and cannot infiltrate the tissue successfully unless water is removed. Tissue processing involves tissue dehydration, tissue clearing and paraffin wax infiltration. Tissue dehydration is performed initially to replace the water content of the tissue with alcohol (ethanol). The concentration of alcohol is progressively increased to avoid tissue distortion. Following tissue dehydration, alcohol is cleared from the tissue using solvent (Xylene) that is fully miscible with both alcohol and paraffin. The solvent serves another important function which is the removal of a substantial amount of lipid from the tissue, rendering the tissue fully amenable to paraffin infiltration. The tissue is then infiltrated with a molten paraffin wax and subsequently embedded to create a wax block that can easily be clamped during sections cutting.

Method: In this research, fixed tissues were placed inside a tissue bag and enclosed in pencil-labelled plastic histology cassettes. Tissue samples were then processed using an automatic tissue processor (Leica TP1020) according to the programme described in Table 3-7. In brief, tissue samples were dehydrated in a series of ascending ethanol concentrations, cleared in three successive changes of 100% (v/v) xylene and then infused with molten paraffin wax.

Table 3-7: Details of Leica TP1020's overnight tissue processing program.

Station	Solution	Temperature	Duration
1	10% (v/v) neutral buffered formalin	21°C	30 minutes
2	70% (v/v) Ethanol	37°C	30 minutes
3	80% (v/v) Ethanol	37°C	30 minutes
4	90% (v/v) Ethanol	37°C	30 minutes
5	100% (v/v) Ethanol	37°C	60 minutes
6	100% (v/v) Ethanol	37°C	60 minutes
7	100% (v/v) Ethanol	37°C	60 minutes
8	Xylene	37°C	60 minutes
9	Xylene	37°C	60 minutes
10	Xylene	37°C	60 minutes
11	Paraffin wax	65°C	60 minutes
12	Paraffin wax	65°C	60 minutes

Following tissue processing, samples were embedded in molten paraffin wax using metal wax block moulds. The moulds were initially filled with molten wax. Samples were then transferred into the moulds, oriented and embedded in the paraffin wax. The bases of the histology cassettes were then placed on the top of the moulds and filled further with paraffin wax. Samples were allowed to set and solidify at room temperature. Once set, the wax blocks were removed from the metal moulds and the excess wax was trimmed away. The wax blocks were then stored at 4°C until sectioning.

Before sectioning, samples were initially cooled in a container filled with ice flakes and then serially sectioned at 5 µm thickness using a microtome (Leica RM2125) set at an angle of zero. Subsequently, tissue sections were floated in a histology water bath set at 45°C and then picked up using microscopic glass slides (x-tra® superfrost). Slides were left to dry overnight at 37°C and then stored at 4°C until used. Prior to use, slides were prepared by heating at 60°C for 20 minutes using a hotplate to enhance tissue adherence to the slides.

3.2.2.3 Tissue sections dewaxing and rehydration prior to the histological and immunohistochemical staining

Principle: The first two steps of histological and immunohistochemical staining of paraffin embedded tissue sections are dewaxing and rehydration. During the process of dewaxing, the paraffin wax is removed from the tissue sections using a hydrocarbon solvent (xylene) to allow staining solutions to penetrate tissue elements. This is followed by rehydration to bring tissue sections back to their normal status.

Method: In this research, tissue sections were dewaxed by immersion in four consecutive changes of 100% (v/v) xylene for three minutes each. Following this, tissue sections were rehydrated through complete immersion in a series of descending ethanol concentrations (100% (v/v), 100% (v/v), 90% (v/v), and 75% (v/v)) for two minutes each. Lastly, tissue sections were placed under running tap water for one minute to allow complete rehydration.

3.2.2.4 Tissue sections dehydration, clearing and mounting following the histological and immunohistochemical staining

Principle: The last steps of histological and immunohistochemical staining of paraffin embedded tissue sections are dehydration, clearing and mounting.

During the process of dehydration, the water is removed from the tissue sections using alcohol. Inadequate dehydration of the tissue sections renders them hazy or milky. The dehydration is followed with a clearing step using solvent to remove alcohol from the tissue sections and ensure the penetration of the mounting medium. Lastly, tissue sections are mounted to keep them stable for many years.

Method: In this research, tissue sections were dehydrated through complete immersion in 75% (v/v) ethanol for two minutes followed by three consecutive changes of 100% (v/v) ethanol for two minutes each. Following this, tissue sections were cleared through immersion in four successive changes of 100% (v/v) xylene for one minute each. Lastly, tissue sections were mounted using glass cover slips and a synthetic resin mounting medium (DPX mountant).

3.2.3 Histological staining methods

3.2.3.1 Haematoxylin and Eosin staining

Principle: Haematoxylin and Eosin (H&E) staining is a widely used histological staining method that was first described by A. Wissowzsky in 1876 (Wittekind, 2003). This staining method is based on the combined use of two main dyes. The first one is haematoxylin which is a colourless natural compound extracted from log-wood trees. This compound produces haematien upon oxidation, a compound which forms an active colourant basic cationic dye when linked to metal ions (mordant) such as aluminium salt. Hem-alum (Haematien-Aluminium complex) reacts with the acidic tissue components such as nucleic acids in the nuclei, rough endoplasmic reticulum, ribosomes, acidic mucine, collagen and elastic fibres and stains them with a blue/purple colour. The second dye in the H&E staining method is Eosin Y. This dye is an acidic anionic dye which interacts with the basic tissue components such as cytoplasm, extracellular matrix and red

blood cells and stains them with a pink/red colour. H&E staining method is used to examine the general tissue morphology (histoarchitecture) including cells layout and distribution (Wittekind, 2003).

Method: In this research, tissue sections were initially dewaxed and rehydrated as described in Section 3.2.2.3, then immersed in Mayer's haematoxylin solution for three minutes. Subsequently, tissue sections were rinsed gently under running tap water for one minute, immersed in Scott's tap water for one minute and then rinsed under running tap water for additional one minute (Scott's tap water and regular tap water are alkaline bluing agents used to enhance the blue/purple colour of haematoxylin). Tissue sections were then immersed in 1% (v/v) Eosin Y solution for seven minutes followed by washing under running tap water for one minute to remove the excess stain. Sections were then dehydrated, cleared and mounted as described in Section 3.2.2.4, allowed to air-dry overnight in a fume hood and then examined using an Axioplan upright microscope (Zeiss) with normal Köhler illumination. Digital images were captured using an AxioCam coloured camera (Zeiss) and AxioVision Rel. 4.8 software.

3.2.3.2 DAPI staining

Principle: DAPI (4',6-diamidino-2-phenylindole) is a membrane impermeant blue fluorescent nuclear dye with high affinity to double stranded DNA molecules (Kapuscinski, 1995). This dye exhibits around 20-fold enhancement of fluorescence upon binding to adenine-thymine (AT) regions of DNA double helix. DAPI stain is excited with a violet laser (405 nm) and is suitable for use with green and red fluorophores. DAPI is commonly used to visualise cell nuclei under fluorescent microscopy.

Method: In this research, DAPI staining was carried out using Vectashield Antifade Mounting Medium with DAPI according to the manufacturer's instructions. In brief, tissue sections were dewaxed and rehydrated as described in Section 3.2.2.3, then organised in a staining tray (StainTray™). Each tissue section was then stained with one drop of Vectashield Antifade Mounting Medium with DAPI and mounted with a cover slip. Stained tissue sections were allowed to cure in the dark for 24 hours at room temperature and then viewed using an Axio imager Z1 fluorescent microscope (Zeiss) equipped with apotome and with DAPI filter set at 365/450 nm emission and excitation wavelengths. Digital images were captured using an AxioCam camera and AxioVision Rel.4.7 software.

3.2.3.3 PicroSirius Red staining

Principle: PicroSirius Red staining is considered a specific staining method for collagen fibres staining in tissue sections (Junqueira *et al.*, 1979). This staining method is based on the combined use of two dyes: Picric acid dye and Sirius Red. Sirius Red is a hydrophilic acidic anionic dye with a sulfonic acid group. The sulfonic acid group in Sirius Red molecules interacts with the basic groups in collagen molecules, forming a bond and a red colour staining. The dye molecules bind to the collagen molecules in a parallel way leading to enhanced birefringence which is specific for the collagen (Junqueira *et al.*, 1979). Picric acid dye is an anionic hydrophobic dye used usually in combination with Sirius red to stain the cytoplasm yellow.

Method: In this research, PicroSirius Red staining was carried out using a PicroSirius Red staining kit according to the manufacturer's instructions. In brief, tissue sections were initially dewaxed and rehydrated as described in Section 3.2.2.3, then stained with Wiegert's haematoxylin solution (prepared by mixing

equal quantities of alcoholic haematoxylin solution and acidic iron-salt solution) for eight minutes. Wiegert's haematoxylin was used as a nuclear staining since it is more stable and more resistant to the acidic dyes. Following this, tissue sections were washed under running tap water, then immersed in PicroSirius Red solution for 60 minutes followed by immersion in hydrochloric acid solution (0.1 N) for two minutes to remove excess staining. Lastly, tissue sections were dehydrated, cleared and mounted as described in Section 3.2.2.4, allowed to dry overnight and then evaluated using an Axioplan upright microscope (Zeiss) with normal Köhler illumination. Digital images were captured using an AxioCam coloured camera (Zeiss) and AxioVision Rel. 4.8 software.

3.2.3.4 Alcian Blue staining

Principle: Alcian Blue is a basic cationic stain containing copper molecules, which gives the stain a blue colour (Scott, 1996). Alcian Blue, at pH 2.5, interacts with the negatively charged acidic glycosaminoglycans, forming a salt linkage with the acidic group. Alcian Blue is used commonly for the detection of sulphated and carboxylated glycosaminoglycans (Hayat, 1993).

Method: In this research, tissue sections were dewaxed and rehydrated as described in Section 3.2.2.3, then immersed in Alcian Blue solution (1% (w/v) Alcian Blue 8GX in 3% (v/v) acetic acid aqueous solution, pH 2.5) for 1 hour at room temperature. Subsequently, tissue sections were washed with four changes of distilled water and then counterstained using Nuclear Fast Red solution (0.1% (w/v) nuclear fast red in distilled water) for 10 minutes at room temperature to visualise cell nuclei. Tissue sections were then rinsed thrice using distilled water to remove excess staining and then dehydrated, cleared and mounted as described in Section 3.2.2.4. Stained sections were allowed to dry overnight in a

fume hood and then viewed using an Axioplan upright microscope (Zeiss) with normal Köhler illumination. Digital images were captured using an AxioCam coloured camera (Zeiss) and AxioVision Rel. 4.8 software.

3.2.4 Immunohistochemical staining technique

Principle: The immunohistochemical (IHC) staining is a highly sensitive and specific technique for the detection of antigens in tissue/cell sections by the means of immunological and chemical reactions. In IHC staining, an antibody with a specific binding characteristic to a target antigen is used to identify the presence and the location of a target antigen in the sample (Ramos-Vara, 2005). The antibody can be monoclonal (interact with a single antigenic epitope) or polyclonal (interact with several antigenic epitopes), and can also be primary or secondary (Pohanka, 2009). Antigen-unmasking is required sometimes prior to IHC staining to break the protein cross-linking caused by tissue fixation and make the antigen available for antibody binding. Additionally, endogenous proteins and enzymes blocking is important to prevent non-specific antibody binding and eliminate the background staining which would otherwise mask the detection of the target antigen (Ramos-Vara and Miller, 2014).

Method: In this research, IHC staining was performed on formalin-fixed paraffin-embedded tissue sections. Tissue sections were initially dewaxed and rehydrated as described in Sections 3.2.2.3 and then subjected to a specific antigen-unmasking technique (**Table 3-8**). Following antigen-unmasking, tissue sections were subjected to endogenous peroxidase blocking using dual enzyme blocking reagent (Boxall) for 20 minutes at room temperature followed by five minutes washing with TBS containing 0.1% (v/v) Tween-20 (TBS-T; pH 7.6). Tissue

sections were then subjected to protein blocking using Casein (10-fold dilution in antibody diluent solution) for 20 minutes at room temperature.

Subsequently, tissue sections were incubated with diluted primary or isotype antibodies according to the conditions described in Table 3-9, then washed twice in TBS-T for five minutes each. Tissue sections were then labelled with secondary antibodies using either ImmPRESS® HRP anti-mouse polymer detection Kit or ImmPRESS® HRP anti-rabbit polymer detection kit following the manufacturer's instructions at room temperature for 30 minutes. Next, tissue sections were washed twice with TBS and stained with ImmPACT™ DAB peroxidase chromogen substrate for five minutes at room temperature. Tissue sections were then washed under running tap water and counterstained with Mayer's haematoxylin for 30 seconds. Following IHC staining, tissue sections were dehydrated, cleared and mounted as described in Section 3.2.2.4. Sections were allowed to dry overnight and then examined using an Axioplan upright microscope (Zeiss) with normal Köhler illumination. Digital images were captured using an AxioCam coloured camera (Zeiss) and AxioVision Rel. 4.8 software.

For each antigen of interest, an optimisation was carried out for the antigen-unmasking technique, primary antibody concentration and incubation condition (duration and temperature). The final unmasking-technique for each antigen alongside the working concentration and incubation condition of the corresponding primary and isotype antibodies are summarised in Table 3-9. Unsuccessful attempts were rejected due to the lack of staining in the positive control tissue sections or the presence of staining in the negative control tissue sections.

Table 3-8: A summary of the antigen-unmasking techniques used in the immunohistochemical staining.

Antigen-unmasking technique	Description
Tris-EDTA buffer and high temperature	<ul style="list-style-type: none"> • Tissue sections were immersed in a pot containing a buffer (pH 9.0) composed of a commercially available Tris-EDTA based antigen-unmasking solution diluted in distilled water at 1:100 (v/v). • The pot was then transferred into a pressure cooker and heat was applied at 125°C for two minutes under full pressure.
Citric acid buffer and high temperature	<ul style="list-style-type: none"> • Tissue sections were immersed in a pot containing a buffer (pH 6.0) composed of a commercially available citric acid-based antigen-unmasking solution diluted in distilled water at 1:100 (v/v). • The pot was then transferred into a pressure cooker and heat was applied for two minutes at 125°C under full pressure.
Proteolytic enzyme	<ul style="list-style-type: none"> • Tissue sections were covered with two drops (100 µL) of a proteolytic enzyme (HistoReveal) and incubated in a humidity chamber for five minutes at room temperature. • Tissue sections were then washed twice with Tris-buffered saline (TBS) to deactivate the enzyme.

Table 3-9: A summary of the Immunohistochemical staining process of formalin-fixed paraffin-embedded tissue sections. Details of the antigen-unmasking technique used for each antigen alongside the working concentrations and the incubation conditions of the primary and isotype antibodies.

Antigen	Antigen unmasking technique	Primary antibody/Stock concentration	Dilution/working concentration/ Incubation condition	Isotype/stock concentration	Isotype dilution/working concentration	Secondary antibody
Collagen I	Tris-EDTA buffer under high temperature	Mouse monoclonal anti-collagen I (5 mg.mL ⁻¹)	1:50 100 µg.mL ⁻¹ (1 hour, at 25°C)	Mouse IgG1 (0.1 mg.mL ⁻¹)	1:1 100 µg.mL ⁻¹	ImmPRESS Excel HRP polymer kit (anti-mouse)
Collagen III	Citric acid buffer under high temperature	Rabbit polyclonal anti-collagen III (1 mg.mL ⁻¹)	1:100 10 µg.mL ⁻¹ (Overnight, at 4°C)	Rabbit IgG (5 mg.mL ⁻¹)	1:500 10 µg.mL ⁻¹	ImmPRESS HRP polymer kit (anti-rabbit)
Fibronectin	Proteolytic enzymatic	Mouse monoclonal anti-fibronectin (1.140 mg.mL ⁻¹)	1:50 22.8 µg.mL ⁻¹ (1 hour, at 25°C)	Mouse IgG1 (0.1 mg.mL ⁻¹)	1:4 22.8 µg.mL ⁻¹	ImmPRESS Excel HRP polymer kit (anti-mouse)

Antigen	Antigen unmasking technique	Primary antibody/Stock concentration	Dilution/working concentration/ Incubation condition	Isotype/stock concentration	Isotype dilution/working concentration	Secondary antibody
Laminin	Proteolytic enzymatic	Rabbit polyclonal anti-laminin (1 mg.mL ⁻¹)	1:200 5 µg.mL ⁻¹ (1 hour, at 25°C)	Rabbit IgG (5 mg.mL ⁻¹)	1:1000 5 µg.mL ⁻¹	ImmPRESS HRP polymer kit (anti-rabbit)
Alpha gal epitope	Tris-EDTA buffer under high temperature	Mouse monoclonal anti-alpha gal epitope (10 mg.mL ⁻¹)	1:50 200 µg.mL ⁻¹ (1 hour, at 25°C)	Mouse IgM (0.5 mg.mL ⁻¹)	1:2.5 200 µg.mL ⁻¹	ImmPRESS Excel HRP polymer kit (anti-mouse)
Bone morphogenic protein 2 (BMP-2)	Tris-EDTA buffer under high temperature	Rabbit polyclonal anti-BMP-2 (200 µg.mL ⁻¹)	1:25 8 µg.mL ⁻¹ (Overnight, at 4°C)	Rabbit IgG (5 mg.mL ⁻¹)	1:625 8 µg.mL ⁻¹	ImmPRESS HRP polymer kit (anti-rabbit)

Antigen	Antigen unmasking technique	Primary antibody/Stock concentration	Dilution/working concentration/ Incubation condition	Isotype/stock concentration	Isotype dilution/working concentration	Secondary antibody
Fibroblast growth factor 2 (FGF-2)	Citric acid buffer under high temperature	Rabbit polyclonal anti-FGF-2 (1 mg.mL ⁻¹)	1:100 10 µg.mL ⁻¹ (1 hour, at 25°C)	Rabbit IgG (5 mg.mL ⁻¹)	1:500 10 µg.mL ⁻¹	ImmPRESS HRP polymer kit (anti-rabbit)
Vascular endothelial growth factor A (VEGF-A)	Tris-EDTA buffer under high temperature	Rabbit polyclonal anti-VEGF-A (0.9 mg.mL ⁻¹)	1:200 4.5 µg.mL ⁻¹ (Overnight, at 4°C)	Rabbit IgG (5 mg.mL ⁻¹)	1:1111 4.5 µg.mL ⁻¹	ImmPRESS HRP polymer kit (anti-rabbit)
Transforming growth factor β1 (TGF-β1)	Citric acid buffer under high temperature	Mouse monoclonal anti-TGF-β1 (1 mg.mL ⁻¹)	1:500 2 µg.mL ⁻¹ (1 hour, at 25°C)	Mouse IgG1 (0.1 mg.mL ⁻¹)	1:50 2 µg.mL ⁻¹	ImmPRESS HRP polymer kit (anti-rabbit)

Antigen	Antigen unmasking technique	Primary antibody/Stock concentration	Dilution/working concentration/ Incubation condition	Isotype/stock concentration	Isotype dilution/working concentration	Secondary antibody
Dentin sialophosphoprotein-protein (DSPP)	Citric acid buffer under high temperature	Mouse monoclonal anti-DSPP (200 $\mu\text{g.mL}^{-1}$)	1:1000 0.2 $\mu\text{g.mL}^{-1}$ (1 hour, at 25°C)	Mouse IgG2b, Kappa (0.1 mg.mL^{-1})	1:500 0.2 $\mu\text{g.mL}^{-1}$	ImmPRESS Excel HRP polymer kit (anti-mouse)
CD 31	Citric acid buffer under high temperature	Rabbit polyclonal anti-CD31 (1 mg.mL^{-1})	1:100 10 $\mu\text{g.mL}^{-1}$ (1 hour, at 25°C)	Rabbit IgG (5 mg.mL^{-1})	1:500 10 $\mu\text{g.mL}^{-1}$	ImmPRESS HRP polymer kit (anti-rabbit)
Nuclei of all human cell types	Citric acid buffer under high temperature	Mouse monoclonal anti-human nuclei clone 3E1.3 (1 mg.mL^{-1})	1:250 4 $\mu\text{g.mL}^{-1}$ (1 hour, at 25°C)	Mouse IgG1 (0.1 mg.mL^{-1})	1:25 4 $\mu\text{g.mL}^{-1}$	Mouse on Mouse Polymer IHC Kit

3.2.5 Scanning electron microscopy

Principle: The scanning electron microscope (SEM) is used to scan the surface of a sample with a focused beam of electrons. The electron beam interacts with the electrons in the atoms of the sample, producing signals of various types including secondary electrons (SE), back scattered electrons (BSE), photons and light. These signals are collected by specific detectors to produce an image that contains information about the sample's surface (Stokes, 2008). The most commonly used electron detectors are SE and BSE. The former provides information about sample's topography whilst the latter demonstrates contrast between the surface's components of a multiphasic sample (Akhtar *et al.*, 2018).

Method: In this research, samples were prepared for SEM by fixing in 2.5% (v/v) glutaraldehyde solution at 4°C overnight. Subsequently, samples were washed in three successive changes of distilled water and then subjected to dehydration in ascending concentrations of ethanol 50% (v/v), 70% (v/v), 80% (v/v), 90% (v/v) and 100 % (v/v) for 10 minutes each. Samples were then exposed to 50% (v/v) hexamethyldisilazane (in ethanol) for 10 minutes followed by two changes of 100% (v/v) hexamethyldisilazane for 15 minutes each and then left to dry overnight in 100% (v/v) hexamethyldisilazane inside a fume hood. Finally, samples were attached to 1.2 mm aluminium stubs using an adhesive carbon tape, then subjected to gold sputter coating for 80 seconds in an argon gas chamber and viewed using SEM.

3.2.6 DNA extraction

Principle: DNA (Deoxyribonucleic acid) extraction is a process in which the DNA is isolated from the rest of the cellular components using a combination of chemical and physical methods (Elkins, 2012). This process involves three basic

steps: (1) sample disruption and lysis to break the cell membrane and expose the DNA, (2) DNA separation from other cellular components and (3) DNA isolation (Elkins, 2012).

Method: In this research, DNA extraction was carried out using a DNeasy Blood and Tissue kit according to the manufacturer's instructions. In brief, tissue samples were finely macerated using a sterile scalpel blade and then transferred individually into DNase/RNase-free microcentrifuge tubes, then lyophilised using a freeze-dryer at - 50°C (0.15 - 0.2 mbar) for 48 hours. The wet weight of the samples was recorded before the lyophilisation and the dry weight was determined after. Following lyophilisation, samples were digested and homogenised using 180 µL of buffer ATL supplemented with 20 µL of 600 mAU.mL⁻¹ proteinase K for three hours at 56°C. Subsequently, 200 µL of Buffer AL and 200 µL of absolute ethanol were added to each sample lysate and the mixture was transferred to DNeasy mini spin column and centrifuged at 6000 xg for one minute at room temperature. The flow-through of each sample was then discarded and the mini spin columns were loaded with 500 µL of buffer AW1 and centrifuged at 6000 xg for one minute at room temperature. The flow-through of each sample was then discarded and the mini spin columns were loaded with 500 µL of buffer AW2 and centrifuged at 6000 xg for 3 minutes at room temperature. Subsequently, the mini spin columns were placed in 1.5 mL DNase/RNase-free microcentrifuge tube, then 100 µL of AE buffer was added followed by tubes incubation for one minute at room temperature and centrifugation at 6000 xg for additional one minute to elute the DNA molecules. The extracted DNA molecules were then subjected to a quantification.

3.2.7 DNA quantification

3.2.7.1 Absorbance-based spectrophotometric quantification

Principle: absorbance-based spectrophotometric quantification depends on the principle that DNA molecules absorb ultraviolet light (UV) at a wavelength of 260 nm (Heptinstall and Rapley, 2000). According to the Beer-Lambert law, the amount of the absorbed light is considered proportional to the concentration of DNA molecules in the sample. In the spectrophotometer, a photodetector is used to collect the light that passes through the sample without being absorbed and the optical density (OD) value is then determined and used to calculate the DNA concentration (A_{260} of 1 = 50 $\mu\text{g}\cdot\text{mL}^{-1}$ DNA). The ratio between the absorbance at 260 nm and 280 nm is used to determine the purity of the DNA sample (i.e., presence/absence of protein contamination), since proteins absorb UV light at 280 nm. Samples with $A_{260/280}$ ratio between 1.7 - 1.9 are considered pure. The main limitation of this method is the overestimation of DNA content in the sample because all the molecules that absorb light at 260 nm including dsDNA, ssDNA and RNA contribute to the resultant value (Heptinstall and Rapley, 2000).

Method: the NanoDrop™ 2000 spectrophotometer was used to determine the concentration of the DNA in the samples at an absorbance wavelength of 260 nm. Buffer AE (2 μL , the buffer supplied in Qiagen DNeasy Blood and Tissue Kit) was used as a blank. DNA samples (2 μL) were then loaded on the sensor of the spectrophotometer and the absorbance was recorded at 260 nm and 280 nm. The concentration of the DNA in the sample ($\text{ng}\cdot\mu\text{L}^{-1}$) was automatically determined by the software of the spectrophotometer. For each sample, three readings were obtained, and the mean was calculated and considered the concentration of the DNA in the sample. The ratio between the absorbance at

260 nm and 280 nm was used to assess the purity of the DNA samples. Samples with ratio between 1.7 - 1.9 were considered pure. The DNA content per sample dry weight ($\text{ng}\cdot\text{mg}^{-1}$) was then determined by normalising for the total dilution volume and the dry weight of the sample.

3.2.7.2 Florescence-based dye tagging quantification

Principle: a florescent dye with selective bind to dsDNA molecules is used in the florescence-based dye tagging quantification. This method of DNA quantification is more sensitive than the absorbance-based method particularly for impure or low-concentration DNA samples (Nicklas and Buel, 2003). Furthermore, this method allows more specific quantification of the dsDNA concentration. A florescent dye is added to the test samples and to standard DNA samples of known concentration. The fluorecence of each test and standard sample is then measured and a standard curve is created to interpolate the dsDNA concentration of the test samples.

Method: The Quant-iT™ PicoGreen® kit was used to determine the dsDNA concentration of the samples according to the manufacturer's instructions. In brief, standards of known DNA concentration (0.2, 2.5, 10, 100 $\text{ng}\cdot\text{mL}^{-1}$) were initially prepared by diluting Lambda DNA (2 $\mu\text{g}\cdot\text{mL}^{-1}$) in 1X TE buffer (Supplied in the kit as 20X TE buffer). An aliquot of 100 μL DNA standards, DNA test samples (30 μL of each DNA test sample in 70 μL 1X TE buffer) and a blank (1X TE buffer alone) were then added to a clear flat bottom 96 well plate in triplicates. Subsequently, 100 μL of PicoGreen working solution (1: 200 dilution in 1X TE buffer) was added to each well and the plate was incubated in the dark for five minutes at room temperature. The fluorecence of each well was then measured using a TopCount™ plate reader at an excitation wavelength of 480 nm and an

emission wavelength of 520 nm. A standard curve was then created using Lambda DNA values. The unknown dsDNA concentrations of the test samples were then interpolated using the standard curve. The dsDNA content per milligram of test sample ($\text{ng}\cdot\text{mg}^{-1}$) was then determined by normalising for the total dilution volume and the dry weight of the test sample.

3.2.8 Cell culture techniques

3.2.8.1 Cell types used

The cell types that were used in the present research are listed in Table 3-10. For each cell type, a specific culture medium was used as described in Table 3-10. Cell culture media were prepared under aseptic conditions in a Class II laminar flow-hood. Cell culture media and all additive reagents were equilibrated at 37°C before use and stored at 4°C after preparation for up to two weeks.

Human dental pulp stem cells (hDPSCs) were kindly provided by Dr Hasanain Al-Khafaji (Oral Biology, University of Leeds) according to an ethical approval obtained from the Dental Research Ethics Committee at the University of Leeds (School of Dentistry Research Tissue Bank; Reference Number 060516/HA/204; Appendix A) and with patients informed consents to donate the extracted teeth. hDPSCs were isolated from the dental pulps of extracted healthy human teeth using an enzymatic digestion method described by Tomlinson *et al.* (2015). In brief, teeth were initially cleaned of adherent soft tissues, disinfected using 70% (v/v) ethanol and cracked-opened. The dental pulps were then aseptically retrieved, mechanically disrupted, digested in $3 \text{ mg}\cdot\text{mL}^{-1}$ collagenase type I and $4 \text{ mg}\cdot\text{mL}^{-1}$ dispase and incubated for 30 minutes at 37°C with gentle agitation. The resulting suspensions were passed through a 70 μm cell strainer and centrifuged at 200 xg for five minutes. Cell pellets were then resuspended in

Alpha modified eagle's medium supplemented with 10% (v/v) FBS, 1% (v/v) 200 mM L-Glutamine and 100 U.mL⁻¹ Penicillin and 100 µg.mL⁻¹ Streptomycin. hDPSCs were obtained at passage number 2 and expanded for use at passage number 4.

Table 3-10: A summary of cell types and cell specific culture media used in the study.

Cell types	Suppliers	Cell culture media
Murine L929 fibroblast cell line	Dental Research Tissue Bank School of Dentistry, University of Leeds	Dulbecco's modified eagle's medium (DMEM) supplemented with: <ul style="list-style-type: none"> - 10% (v/v) Foetal bovine serum (FBS) - 1% (v/v) 200 mM L-Glutamine - 100 U.mL⁻¹ Penicillin and 100 µg.mL⁻¹ Streptomycin
Human dental pulp stem cells	Dr Hasanain Al-Khafaji School of Dentistry, University of Leeds	Alpha modified eagle's medium (Alpha MEM) supplemented with: <ul style="list-style-type: none"> - 10% (v/v) FBS - 1% (v/v) 200 mM L-Glutamine - 100 U.mL⁻¹ Penicillin and 100 µg.mL⁻¹ Streptomycin

3.2.8.2 Cell resurrection and maintenance

Principle: The process of cell resurrection and maintenance involves defrosting cryopreserved cells and growing them *in vitro* under controlled culture conditions. The culture conditions varied according to cell types but generally consist of a substrate suitable for cell attachment (e.g., culture flask) and a medium capable of regulating the acidity/alkalinity of the environment and providing the cells with

the essential nutrients (amino acids, carbohydrates, minerals, vitamins, hormones, growth factors) and adhering proteins. Additionally, an incubator is used to maintain the gas (CO₂, O₂), temperature and humidity of the environment at a level appropriate for cell growth (Davis, 1994).

Method: In this research, cryopreserved cell suspension was defrosted in a bath set at 37°C, then transferred into a falcon tube containing 4 mL of cell culture medium. Cell suspension was then subjected to a centrifugation at 150 xg for five minutes at room temperature. Subsequently, the supernatant solution was carefully aspirated, and the cell pellet was resuspended in 5 mL of cell culture medium. The cell suspension was then transferred into a culture flask containing an appropriate volume of cell culture medium (15 mL for T75 and 30 mL for T175 size flasks) and incubated in a humidified atmosphere incubator containing 5 % (v/v) CO₂ at 37°C and 95% relative humidity. Cell attachment and growth were monitored regularly using an inverted microscope (Olympus) with phase-contrast illumination. The cell culture medium was changed every three days.

3.2.8.3 Cell harvesting using trypsin and cell passaging

Principle: The process of cell passaging involves splitting the cells and sub-culturing them into new culture flasks. This process is carried out usually when the cells reach approximately 80% growth confluence in order to avoid the abrupt arrest in cellular proliferation as a result of cells coming in contact with each other (Davis, 1994). In cell passaging, trypsin (a proteolytic enzyme) is used to detach the adherent cells from the walls of the culture flask by breaking the peptide bonds that link the cells to the flask. EDTA (a chelating agent) is usually used in combination with trypsin to enhance trypsin activity by neutralising calcium and magnesium ions.

Method: In this research, the cells were passaged at approximately 80% growth confluency as determined by visualising under an inverted microscope with phase-contrast illumination. The cell culture medium was carefully aspirated from the flask to avoid disrupting the cell monolayer. The cells were then washed twice with an appropriate volume of PBS without calcium and magnesium (10 mL for T75 and 20 mL for T175 size flasks) for five minutes. Subsequently, the cells were harvested using an appropriate volume of 0.25% trypsin / 0.02% EDTA solution (5 mL for T75 and 10 mL for T175 size flasks) for 5 minutes at 37°C. The flask was then tapped gently to dislodge the cells and then checked microscopically to confirm cell detachment. An appropriate volume of cell culture medium was then added to the flask (10 mL for T75 and 20 mL for T175 size flasks) to deactivate the Trypsin/EDTA solution. The contents of the flask were then transferred to a falcon tube and centrifuged at 150 xg for five minutes at room temperature. The supernatant solution was then gently aspirated, and the cell pellet was resuspended in 5 mL of cell culture medium. Viable cell counting was then performed as described below (Section 3.2.8.4) and the cell suspension was split, reseeded into new culture flasks and incubated in a humidified atmosphere containing 5% (v/v) CO₂ at 37°C and 95% relative humidity.

3.2.8.4 Viable cell counting using Trypan Blue dye and a haemocytometer

Principle: Trypan Blue dye and a haemocytometer are used routinely for viable cell counting. Trypan Blue is a membrane-impermeant dye which stains dead cells blue and leaves the viable cells without staining, thus facilitating ease of distinguishing between dead and viable cells. The haemocytometer is a device used for cell counting. It is composed of a thick microscopic slide with two chambers. Each chamber is made up of nine major squares, the volume of each equals 0.1 mm³ (10⁻⁴ mL)(Davis, 1994).

Method: In this research, viable cell counting was performed using Trypan Blue dye and a haemocytometer. An aliquot of cell suspension was mixed with Trypan Blue dye solution at a ratio of 1:1 (v/v) and a coverslip was placed on the face of a haemocytometer. Subsequently, 20 μL of Trypan Blue stained-cell suspension was dispensed carefully into the haemocytometer chambers. The haemocytometer was then observed using the 10X objective lens of an inverted microscope with phase-contrast illumination. Viable cells (appeared as bright white dots) were then counted in five major squares (corner and centre) of each haemocytometer chamber. The cells that were overlapping squares borders were included. The numbers of cells counted in all ten squares were then combined to give the number of cells per cubic millimetre (mm^3). This number was then multiplied by one thousand (10^3) to give the number of cells per millilitre (mL). The result was then multiplied by the dilution factor of Trypan Blue dye (equal to 2) and then by the total volume of original cell suspension to give the total viable cell number.

3.2.8.5 Cell cryopreservation and storage

Principle: Cryopreservation is a process by which viable cells are preserved by freezing at a very low temperature ($- 80^\circ\text{C}$ or $- 196^\circ\text{C}$). During the freezing process, cells are indeed at risk of damage due to ice crystals formation or dehydration. For this reason, a cryoprotectant, such as DMSO, is used in the medium and a well-controlled slow freezing is applied (Meryman, 2007).

Method: In this research, the cells were prepared for cryopreservation through suspending in a cell culture medium supplemented with 30% (v/v) FBS and 10% (v/v) sterile-filtered DMSO. Subsequently, aliquots of 1 mL cell suspension were transferred to cryotubes labelled with cell type, date and passage number. The

cryotubes were then placed in a cryo-freezing pot containing isopropanol (Mr. Frosty™ freezing container) and stored at - 80°C overnight for gradual temperature reduction (1°C per minute rate). The next day, cryotubes were transferred to a storage box and stored at - 80°C for short term storage (up to two weeks) or -196°C (liquid nitrogen) for long term storage.

3.2.9 Cell characterisation of human dental pulp stem cells

3.2.9.1 Flowcytometric analysis of cell surface markers

Principle: Flowcytometry is a technique used to analyse the physical and chemical characteristics of the cells as they pass individually through a light and multiple laser beams (Givan, 2011). The cells are initially suspended in a fluid, labelled with fluorescent markers and then injected into a flowcytometer. The flowcytometer focuses the cells to the core of the fluid, forcing the cells to pass uniformly through the centre of the light and laser beams. The light scattered by the cells is then collected to determine the size (Forward scattered light) and granularity (Side scattered light) of the cells. Additionally, the light emitted by the cells, upon binding to fluorescent markers is gathered by the flowcytometer to determine the cell phenotypic profile (Givan, 2011).

Method: In this research, an attune® NxT acoustic focusing flowcytometer was used to analyse the cell surface markers. The cells were prepared and labelled with a multicolour panel of fluorochrome-conjugated antibodies as following:

In a 5 mL FACS tube, 1×10^4 cells were suspended in 1 mL of a staining buffer (pH 7.2) consisting of PBS without calcium and magnesium supplemented with 0.5% (v/v) bovine serum albumin (BSA) and 0.1% (v/v) sodium azide. An appropriate volume of Cell trace™ Calcein violet viability stain (1 µL of stain per 1×10^4 cells suspended in 1 mL of staining buffer) was then added to cell

suspension and incubated at 4°C in the dark for 30 minutes. Subsequently, the cell suspension was centrifuged at 300 xg for 5 minutes and the supernatant was discarded. The cells were then resuspended in 100 µL of staining buffer and subjected to FcR (fragment crystallisable receptors) blocking using human FcR blocking reagent (10 µL per 1X10⁴ cells) for 10 minutes at 4°C. Following FcR blocking, the cells were incubated with diluted volume of fluorochrome-conjugated primary and control isotype antibodies as described in Table 3-11 in 100 µL of a staining buffer for 20 minutes at 4°C in the dark. Finally, the cells were washed twice, resuspended in 500 µL of staining buffer and analysed using the Attune[®] NxT Acoustic Focusing Flow Cytometer and Attune[®] Cytometric software version 2.1. Single-colour stained cells were used for flowcytometer compensation. Unstained cells and cells labelled with appropriate fluorochrome-conjugated isotype antibodies were used as a negative control for each stain. Flowcytometer compensation was done using single-colour stained samples for the viability stain and fluorochrome-conjugated antibodies. Compensation settings were adjusted in the flowcytometer until only a single colour was detected by each channel and no spectral overlap was observed.

Table 3-11: Dilutions of the fluorochrome-conjugated primary and isotype antibodies used in the flowcytometric analysis of the cell surface markers.

Test antibody	Dilution	Control isotype	Dilution
R-Phycoerythrin (PE) - Mouse anti-human CD146	1:11	PE - Mouse IgG1	1:11
Peridinin Chlorophyll protein (PerCP) -Vio700 - Mouse anti-human CD90	1:50	PerCP-Vio700 – Mouse IgG1	1:11
Fluorescein Isothiocyanate (FITC) - Mouse anti-human CD105	1:11	FITC – Mouse IgG1	1:11
VioGreen - Mouse anti-human CD45	1:50	VioGreen - Mouse IgG1	1:11

3.2.9.2 Assessment of multilineage cell differentiation

The cells were seeded in a 24 well plate (1×10^4 cells per well) and cultured under basal culture condition. At approximately 80% growth confluency, the cells were cultured in triplicates under basal, osteogenic, adipogenic and chondrogenic culture conditions using basal cell culture medium, commercially available osteogenic cell culture medium (StemMACS OsteoDiff media), adipogenic cell culture medium (StemMACS AdipoDiff media) and chondrogenic cell culture medium (StemMACS ChondroDiff Media), respectively. All cell culture media were subjected to change every three days. Cultures were terminated after three weeks and cell differentiation was evaluated using specific histological staining methods as described below.

Detection of osteogenic cell differentiation using Alizarin Red stain

Principle: Alizarin red stain is used frequently to detect the calcium reach deposits in a culture of stem cells exposed to osteogenic culture condition. The stain binds to calcium molecules in a chelation process, forming a bright-red

coloured complex (Puchtler *et al.*, 1969). The cells are usually fixed with alcohol prior to the staining process to avoid significant loss of calcium molecules if a calcium-solubilising fixative such as NBF is used (Puchtler *et al.*, 1969).

Method: In this research, cells were prepared for Alizarin red staining through fixing in cold 70% (v/v) Ethanol for 30 minutes at room temperature. Following this, the cells were washed once with distilled water, then stained using a commercially available Alizarin Red staining solution (pH 4.1) for ten minutes at room temperature. The cells were then washed well with distilled water and examined under inverted bright field microscopy.

Detection of adipogenic cell differentiation using Oil Red O stain

Principle: Oil Red O stain is a common dye used to visualise fat droplets in a culture of stem cells subjected to adipogenic culture condition. The stain dissolves in fat resulting in a red-orange coloured powder-like droplets (Kraus *et al.*, 2016).

Method: In this research, the cells were prepared for Oil Red O stain through fixing in 10% (v/v) NBF for 10 minutes at room temperature. Following fixation, the cells were washed twice in PBS without calcium and magnesium, then stained with Oil Red O staining solution (0.5% (w/v) in isopropanol) for 10 minutes at room temperature. Subsequently, the cells were washed well in PBS and counterstained with Harris's Haematoxylin solution for 45 seconds at room temperature. The cells were then washed well in distilled water and visualised using inverted bright field microscopy.

Detection of chondrogenic cell differentiation using Alcian Blue stain

Principle: Alcian Blue stain is frequently used to detect glycosaminoglycans deposition in a culture of stem cells subjected to chondrogenic culture condition

(Dominici *et al.*, 2006). Detailed information about Alcian Blue stain has been described in Section 3.2.3.3.

Method: In this research, the cells were prepared for Alcian Blue staining by fixing in 10% NBF for 10 minutes at room temperature. Following fixation, the cells were washed twice in distilled water, then stained using Alcian Blue solution (1% (w/v) in acetic acid; pH 2.5) for 45 minutes at room temperature. Subsequently, the cells were washed well in distilled water and visualised using inverted bright field microscopy.

3.2.10 Cell seeding onto the scaffolds using a dynamic technique

Principle: Dynamic cell seeding is a technique used to enhance the efficiency and uniformity of the cell seeding particularly when a three-dimensional scaffold is used (Nasseri *et al.*, 2003, Villalona *et al.*, 2010). In this research, a dynamic seeding technique was applied utilising a rotary apparatus developed in-house and optimised by Dr El Mostafa Raïf for three-dimensional scaffolds seeding (Figure 3-2).

Method: Scaffolds were placed in 500 μ L microcentrifuge tubes (1 scaffold per tube) supplemented with cell suspension at the required cell concentration. A hole was made in the lid of each tube, then sealed with sterile OPSITE Flexigrid adhesive polyurethane membrane to allow for gaseous exchange while protecting the tubes contents from leakage and contamination. The tubes were then mounted on a rotary dynamic seeding apparatus (Figure 3-2) set at 10 rotations per minute and incubated for 24 hours at 37°C in 5% (v/v) CO₂ and 98% relative humidity. After 24 hours, tubes were de-mounted and their contents were transferred to 12 well plates and maintained in culture for the required experimental time, with the cell culture medium changed every three days.

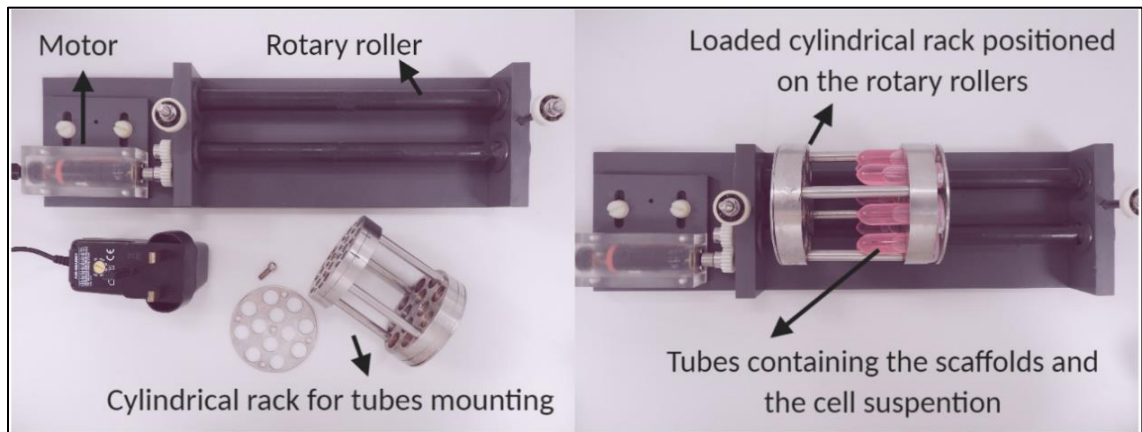


Figure 3-2: Representative image of the rotary dynamic seeding apparatus used in the scaffolds seeding process. The scaffolds were placed individually in microtubes containing the cell suspension and then mounted on a rotary dynamic seeding apparatus set at 10 rotations per minute.

3.2.11 Cell viability analysis

3.2.11.1 Cell viability analysis using ATPLite-M assay

Principle: Adenosine triphosphate (ATP) constitutes the primary source of energy in all metabolically active cells. The level of ATP decreases rapidly when cells undergo apoptosis or necrosis. For this reason, ATP is frequently used as a marker for cell viability (Cree and Andreotti, 1997). Several assays have been developed to detect the ATP including a calorimetric-based and a luminescence-based assays (Crouch *et al.*, 1993). ATPLite-M is a commercially available luminescence-based assay. In this assay, cellular ATP interacts with an added solution of Luciferase and D -Luciferin leading to the emission of light signals. The emitted signals are directly proportional to the cellular ATP content.

Method: In this research, ATPLite-M assay was used according to the manufacturer's instructions. In brief, the cell culture medium was initially aspirated, then 50 μ L of mammalian cell lysis solution and 50 μ L of fresh cell culture medium were added to the cells and incubated for five minutes at room temperature with gentle agitation. Subsequently, the contents of experimental wells were transferred into white 96 well Optiplate™ and 50 μ L of ATPLite lyophilised substrate solution (prepared by adding 5 mL ATPLite substrate buffer solution into a bottle of lyophilised substrate solution) was added to the wells and incubated for five minutes at room temperature with gentle agitation. The Optiplate was left to adapt to the dark for ten minutes at room temperature, then the luminescence was measured using a TopCount™ plate reader to determine the relative ATP contents of the samples (luminescence counts per second).

3.2.11.2 Cell viability analysis using Live/Dead® cells assay

Principle: Live/Dead® cells assay is a fluorescence-based assay utilises two dyes, namely Calcein AM and Ethidium homodimer III, for simultaneous differentiation between viable and dead cells. Calcein AM is a non-fluorescent membrane-permeable compound which upon interacting with the intracellular esterase enzyme, in the cytoplasm of the viable cells, forms a fluorescent membrane-impermeant compound. This compound becomes retained within the cytoplasm of the viable cells and emits fluorescent signals (Green colour) upon excitation. On the other hand, Ethidium homodimer III is a membrane-impermeant fluorescent dye with high affinity to DNA molecules. This dye passes through the compromised plasma membrane of the dead cells, binds to the DNA molecules and emits fluorescent signals (Red colour) upon excitation.

Method: In this research, a Live/Dead[®] cells assay was carried out according to the manufacturer's instructions. In brief, a staining solution composed of 2 μ M Calcién AM and 4 μ M Ethidium homodimer III was prepared by adding 5 μ L of 4 mM Calcién AM and 20 μ L of 2 mM Ethidium homodimer III to 10 mL of serum free alpha MEM. The staining solution was then added to the samples and incubated for 45 minutes in the dark at 37°C and 98% relative humidity in an incubator containing 5% (v/v) CO₂. Subsequently, samples were washed three times in PBS for 10 minutes and visualised using a confocal scanning laser microscope (Leica TCS SP8) with the following specifications: Calcién AM (Excitation/Emission = 494/517 nm) and Ethidium homodimer III (Excitation /Emission = 530/620 nm). Images were captured digitally using Leica LAS X software.

3.2.12 Gene expression analysis using RT-qPCR

Principle: Polymerase chain reaction (PCR) is a technique used to amplify a specific sequence of DNA or gene through repeated cycles of heating and cooling (Garibyan and Avashia, 2013). The amplification process is carried out in a buffer containing the DNA sample, DNA building blocks (Deoxynucleotide triphosphates; Adenine, Thiamine, Cytosine and Guanine), a heat-resistant DNA polymerase enzyme and two primers (forward and reverse sequence primers) that are specific for the targeted gene or DNA sequence and complementary to the three-prime end of the DNA strands. Each PCR cycle comprises of three stages of temperature change including temperature increase up to 95°C to allow the separation of the double-stranded DNA through denaturation of the hydrogen bonds, temperature decrease down to 65°C to allow the annealing (i.e., binding) of the primers to DNA strands and DNA synthesis and elongation, and

temperature decrease down to 4°C. This process results in the formation of two separated copies of the original DNA sequence or gene referred to as amplicons. In RT-qPCR, the generated amplicons are quantified continuously during each cycle of PCR process through the use of either a sensitive fluorescent dye such as Cyber Green dye or a highly-specific fluorescent probes such as TaqMan probes. The starting material in RT-qPCR is RNA molecules. These RNA molecules are extracted from the samples and then subjected to reverse transcription using reverse transcriptase enzyme to synthesise complementary DNA (cDNA) samples which can then be used as templates for PCR reaction.

Method:

RNA extraction

The extraction of RNA from the samples was carried out using a RNeasy® fibrous tissue Kit according to the manufacturer's instructions. In brief, samples were finely minced using a sterile blade, then transferred individually into 1.5 mL RNase-free microcentrifuge tubes containing 300 µL of buffer RLT solution (prepared by adding 10 µL β-mercaptoethanol to 1 mL of buffer RLT) and mixed thoroughly by pipetting. β-mercaptoethanol was added to buffer RLT to protect RNA from being digested during the extraction process through inhibiting RNase enzyme. Subsequently, 590 µL of RNase-free water and 10 µL of proteinase K were added to the lysate and incubated at 55°C for 10 minutes. Tubes were then centrifuged at 10000 xg for 3 minutes and the supernatants were collected and transferred into fresh 2 mL RNase-free microcentrifuge tubes.

Following samples lysis and homogenisation, 450 µL of 100% (v/v) ethanol was added to each sample lysate, mixed by pipetting and then 700 µL was transferred to RNeasy mini column placed in 2 mL collection tube and centrifuged at 8000 xg

for 15 seconds at room temperature. The flow-through was discarded and the step was repeated until all lysate, for each sample, was used. Subsequently, 350 μL of buffer RW1 was added to each sample, centrifuged at 8000 $\times g$ for 15 seconds at room temperature and the flow-through was then discarded.

Next, on column DNA digestion was performed by incubating the samples with a mixture of 10 μL of DNase I solution (prepared by dissolving lyophilised DNase I in 550 μL of RNase-free water, following the manufacturer's instructions) and 70 μL of buffer RDD for 15 minutes at room temperature. Following DNA digestion, 350 μL of buffer RW1 was added to each sample, centrifuged at 8000 $\times g$ for 15 seconds at room temperature and the flow-through was discarded. Subsequently, 500 μL of buffer RPE was then added, centrifuged at 8000 $\times g$ for 2 minutes at room temperature and the flow-through was discarded. RNeasy columns were then placed in new 1.5 mL RNase-free tubes, then 30 μL of RNase-free water was added and they were centrifuged at 8000 $\times g$ for one minute to elute RNA.

RNA quantification

A NanoDrop™ 2000 spectrophotometer was used to quantify the yield of RNA and assess its purity. For each sample, 2 μL of eluted RNA was loaded on the sensor. The absorbance was then measured at 260 nm and the quantity was determined in $\text{ng}\cdot\mu\text{L}^{-1}$. The ratio between the absorbance at 260 nm and 280 nm was used to assess the purity of RNA samples. Samples with ratio between 1.8 - 2.0 were considered pure.

RNA reverse transcription

RNA reverse transcription was carried out using a high-capacity RNA-to-cDNA™ kit according to the manufacturer's instructions. In brief, for each sample, a reaction volume of 20 μL was prepared in a 0.2 mL PCR tube by adding 10 μL of

2X RT buffer, 1 μ L of 20X RT enzyme and 9 μ L containing 60 ng of RNA diluted in RNase-free water. All samples were then transferred into a thermal cycler (PTC -100) and incubated for 60 minutes at 37°C followed by 5 minutes at 95°C and 20 minutes at 4°C. Negative controls for the experiment were created during this step by excluding the RNA sample from one reaction and the reverse transcriptase enzyme mix from another one. Samples were stored frozen at -20°C until the day of the RT-qPCR reaction.

RT-qPCR reaction

RT-qPCR was performed using TaqMan[®] gene expression assays for the following genes: GAPDH, DSPP, DMP-1, MEPE, KDR and PECAM-1 (Table 3-6) and the reaction was carried out in a light cycler (Roche LC480) according to the recommendations of Applied Biosystems. In brief, a reaction volume of 20 μ L was prepared for each cDNA sample by adding 10 μ L of TaqMan[®] fast advanced master mix, 1 μ L of TaqMan[®] gene expression assay and 9 μ L of diluted cDNA sample. Samples were then loaded in a 96 well PCR reaction plate in triplicates. Triplicates of reverse transcription negative controls and a none-template PCR negative control were also added to the plate. The plate was then sealed securely using an adhesive PCR plate sealer and subjected to centrifugation for 10 seconds using PCR plate centrifuge (Labnet MPS 1000 compact). Subsequently, the plate was transferred to a light cycler (Roche LC480) and the amplification process was carried out as follows: samples were subjected to a pre-incubation cycle at 95°C for 5 minutes, followed by 45 amplification cycles comprising of incubation at 95°C for 5 seconds and then at 65°C for 1 minute. Lastly, samples were subjected to cooling at 4°C for 30 seconds. Threshold cycle (Ct) values were automatically determined by the light cycler. These values were used in the data analysis process as described below in Section 3.2.12.1.

3.2.12.1 Analysis of RT-qPCR data

RT-qPCR data was analysed using the comparative Ct method described by Schmittgen and Livak (2008). In brief, the Δct values were initially calculated by normalising the average Ct values of the target genes to that of the house-keeping gene (GAPDH). Following this, the $\Delta\Delta\text{ct}$ values were calculated by normalising the Δct values of the test samples to that of the control samples. The relative changes in the expression of the target genes in the test samples as compared to the control samples were then determined using $2^{-\Delta\Delta\text{ct}}$ equation. Data were statistically analysed as described below in Section 3.2.13.

3.2.13 Statistical analysis

Numerical data are presented as means, standard deviations and 95% confidence intervals. Statistical analyses were performed using GraphPad Prism software (Version 9). Normality tests including D'Agostino & Pearson test and Shapiro-Wilk test were used to assess the distribution of the data. For normally distributed data, independent student's *t*-test and one-way or two-way analysis of variance (ANOVA) with Bonferroni correction were used to compare the means of two groups or more than two groups, respectively. A Kruskal-Wallis test with post hoc analysis was used to compare the mean rank of more than two groups of data not following normal distribution. The difference between the groups was considered significant when the *P*-value was less than 0.05.

Chapter 4

Development of a decellularised bovine dental pulp matrix

4.1 Introduction

The extracellular matrix (ECM) represents a natural scaffold for tissue development and repair, and could possibly be the ideal scaffold for tissue engineering and regeneration (Badylak, 2002, Badylak, 2004, Badylak, 2007, Robb *et al.*, 2017). As dental pulp regeneration faces challenges in promoting post-implantation vascularisation and inducing odontoblast-like cell differentiation, a decellularised dental pulp matrix with retained native histoarchitecture, composition and vasculature may help in overcoming these challenges.

Tissue decellularisation is achieved by means of several washes in detergents and enzymes coupled with physical methods (Gilbert *et al.*, 2006). Many decellularisation protocols have been developed, and vary widely in terms of the chemicals used, their concentrations and duration of application (Crapo *et al.*, 2011, Keane *et al.*, 2015). As the preservation of ECM structure and composition is of primary importance for the future performance of the resultant scaffold, the goal is to use a low concentration of chemicals for short duration of application in order to minimise ECM disruption to the best extent possible (Gilbert, 2012).

Detergents, such as sodium dodecyl sulfate (SDS) and Triton X100, are the most commonly used chemicals in decellularisation protocols since they are potent in solubilising the cellular and nuclear components. However, tissue exposure to SDS at a concentration of 1% (w/v) was reported to be associated with a high risk of ECM disruption, growth factors elimination and potential cytotoxicity of the

resultant scaffolds (Bodnar *et al.*, 1986, Reing *et al.*, 2010, Cebotari *et al.*, 2010). Reducing SDS concentration to 0.1% (w/v) was shown effective in decellularising human pericardium (Mirsadraee *et al.*, 2006), porcine urinary bladder (Rosario *et al.*, 2008) and human femoral artery (Wilshaw *et al.*, 2012) with retention of ECM histoarchitecture and composition. In addition, the use of a single cycle of very low SDS concentration (0.03% w/v) was reported effective in decellularising human amniotic membrane with retention of native ECM (Wilshaw *et al.*, 2006). Previous studies on dental pulp decellularisation used multiple cycles of concentrated dual detergents (SDS/Triton X100) (Chen *et al.*, 2015, Song *et al.*, 2017). Despite the complete cell removal achieved, it is well-known that the dual detergents used increases ECM disruption and protein loss (Crapo *et al.*, 2011). Therefore, attempting to decellularise dental pulp using a low concentration of a single detergent might be advantageous for the performance of the resultant scaffolds.

Although human dental pulps are the preferred option for decellularised dental pulp matrices development, they are limited by availability. Therefore, bovine dental pulps' use may provide a readily available alternative. In this chapter, the process of bovine dental pulp decellularisation using a gentle protocol involving a single cycle of low SDS concentration (0.03% w/v) in combination with protease inhibitor, enzymatic agents and mild physical decellularisation methods is described.

4.2 Aim and objectives

Aim

The aim of the research work presented in this chapter was to develop acellular dental pulp matrix with retained native histoarchitecture and vasculature through bovine dental pulp decellularisation.

Objectives

- To investigate the efficiency of the decellularisation protocol described by Wilshaw *et al.* (2006) in producing effectively decellularised scaffolds from bovine dental pulps with retention of the general native histoarchitecture and vasculature.
- To evaluate the efficiency of an optimised iteration of Wilshaw and colleagues' decellularisation protocol described by Matoug-Elwerfelli *et al.* (2018) in achieving effective decellularisation of bovine dental pulp with retention of the general native histoarchitecture and vasculature.

4.3 Experimental approach

This chapter describes the process of developing decellularised bovine dental pulp matrix with retained general histoarchitecture and vasculature. The process involved investigation of two published decellularisation protocols in two separate experiments as following:

Experiment I: Bovine dental pulps were subjected to a decellularisation protocol described by Wilshaw *et al.* (2006), named decellularisation protocol I and detailed in section 4.4.1.1. Following decellularisation, the efficacy of the protocol in achieving sufficient removal of the cells and nuclear materials was assessed based on the standard criteria of sufficiently decellularised tissues described by Crapo *et al.* (2011). The assessment includes evaluation of cells and nuclear materials removal qualitatively using haematoxylin and eosin (H&E) and 4', 6-diamidino-2-phenylindole (DAPI) staining methods, and quantitatively using absorbance-based spectrophotometric DNA quantification technique.

Experiment II: Bovine dental pulps were subjected to an optimised iteration of Wilshaw *et al.*'s decellularisation protocol (Matoug-Elwerfelli *et al.*, 2018), named decellularisation protocol II and detailed in section 4.4.1.2. The decellularisation efficacy of the protocol was assessed using histological staining methods (H&E and DAPI) and spectrophotometric DNA quantification.

4.4 Methods

4.4.1 Decellularisation protocols

4.4.1.1 Decellularisation protocol I

Twenty bovine dental pulps harvested from different cattle, as described in Chapter 3, Section 3.2.1, were used. The pulpal tissues were divided equally into a control group (n = 10) and a study group (n = 10). Study tissues were subjected to decellularisation as described below and summarised in Figure 4-1.

Tissue decellularisation was carried out in 7 mL sterile bijoux tubes, each containing a single bovine dental pulp tissue fully immersed in 4 mL of decellularisation solutions. Decellularisation solutions were freshly prepared prior to use as described in Table 4-1. All solutions were made up under sterile conditions in a Class II laminar flow hood. Non-sterile solutions were sterile filtered using 0.2 µm pore size filters.

Tissue samples were initially incubated in a hypotonic buffer supplemented with ethylenediaminetetraacetic acid (EDTA) and aprotinin (10 mM Tris, 0.1% w/v EDTA and 10 Kallikrein Inhibitor Unit/mL (KIU.mL⁻¹) aprotinin) at 4°C for 16 hours. The samples were then rinsed in three changes of phosphate buffered saline (PBS) washing buffer supplemented with aprotinin (10 KIU.mL⁻¹ aprotinin in PBS) at room temperature for 30 minutes each. Subsequently, the samples were incubated in hypotonic buffer supplemented with sodium dodecyl sulphate (SDS), EDTA and aprotinin (10 mM Tris, 0.03% w/v SDS, 0.1% w/v EDTA and 10 KIU.mL⁻¹ aprotinin) at room temperature for 24 hours with agitation at 150 revolutions per minute (rpm). Following this, the samples were washed in three changes of PBS washing buffer supplemented with aprotinin for 30 minutes each,

then incubated in Nuclease solution buffer (50 mM Tris hydrochloride, 50 U.mL⁻¹ DNase I, 1 U.mL⁻¹ RNase A, 10 mM magnesium chloride and 50 µg.mL⁻¹ bovine serum albumin) at 37°C for 3 hours with agitation at 80 rpm. The samples were then washed three times in PBS washing buffer supplemented with Aprotinin for 30 minutes each, then disinfected in peracetic acid solution buffer (0.1% v/v Peracetic acid in PBS) at room temperature for 3 hours with agitation at 150 rpm. Finally, samples were rinsed in three changes of PBS for 30 minutes each with gentle agitation. The samples were then stored frozen in 4 mL cryotubes containing sterile PBS at - 20°C until used.

4.4.1.2 Decellularisation protocol II

Fifteen bovine dental pulps harvested from different cattle, as described in Chapter 3, Section 3.2.1, were used in this experiment. Five were left untreated for use as a control in the process of DNA quantification and ten were subjected to decellularisation as described below and summarised in Figure 4-2.

Bovine dental pulps were initially placed individually in 2 mL cryotubes containing sterile PBS and subjected to a single freeze-thaw cycle. The cycle involved tissue freezing for 60 minutes at - 80°C followed by tissue thawing at 37°C. After tissue thawing, the decellularisation process was carried out following the same steps described in decellularisation protocol I (Section 4.4.1.1).

Table 4-1: Decellularisation solutions.

Decellularisation solutions	Preparation (100 mL)
<p>Hypotonic buffer supplemented with ethylenediaminetetraacetic acid (EDTA) and aprotinin.</p> <p>(10 mM Tris, 0.1% w/v EDTA and 10 Kallikrein Inhibitor Unit/mL (KIU.mL⁻¹) aprotinin)</p> <p>pH 8.0 – 8.2</p>	<ul style="list-style-type: none"> - 1 mL of 1 M Tris hydrochloride solution. - 680 µL of 500 mM EDTA solution. - 96.2 µL of 10,400 KIU.mL⁻¹ aprotinin. - 196.4 mL of distilled water.
<p>Hypotonic buffer supplemented with sodium dodecyl sulfate (SDS), EDTA and aprotinin.</p> <p>(10 mM Tris, 0.03% w/v SDS, 0.1% w/v EDTA and 10 KIU.mL⁻¹ aprotinin)</p> <p>pH 8.0 – 8.2</p>	<ul style="list-style-type: none"> - 300 µL of 10% w/v SDS solution. - 99.70 mL of hypotonic buffer with EDTA and Aprotinin solution described above.
<p>Phosphate buffered saline (PBS) washing buffer supplemented with aprotinin.</p> <p>(10 KIU.mL⁻¹ aprotinin in PBS)</p> <p>pH 7.2 – 7.5</p>	<ul style="list-style-type: none"> - 480 µL of 10,400 KIU.mL⁻¹ aprotinin - 499.52 mL PBS without magnesium and calcium.

Decellularisation solutions	Preparation (100 mL)
<p>Nuclease solution buffer. (50 mM Tris hydrochloride, 50 U.mL⁻¹ DNase I, 1 U.mL⁻¹ RNase A, 10 mM magnesium chloride and 50 µg.mL⁻¹ bovine serum albumin) pH 7.2 - 7.5</p>	<ul style="list-style-type: none"> - 5 mL of 1 M Tris hydrochloride. - 1 mL of 1 M magnesium chloride. - 14.28 mL of bovine serum albumin. - 5 mL of 1000 U.mL⁻¹ DNase I solution. - 40 µL of 2523 U.mL⁻¹ RNase A solution. - 149.4 mL of distilled water.
<p>Peracetic acid solution buffer. (0.1% v/v peracetic acid in PBS) pH 7.2 – 7.5</p>	<ul style="list-style-type: none"> - 225 µL of 44.5% v/v Peracetic acid solution. - 99.8 mL of PBS without magnesium and calcium.

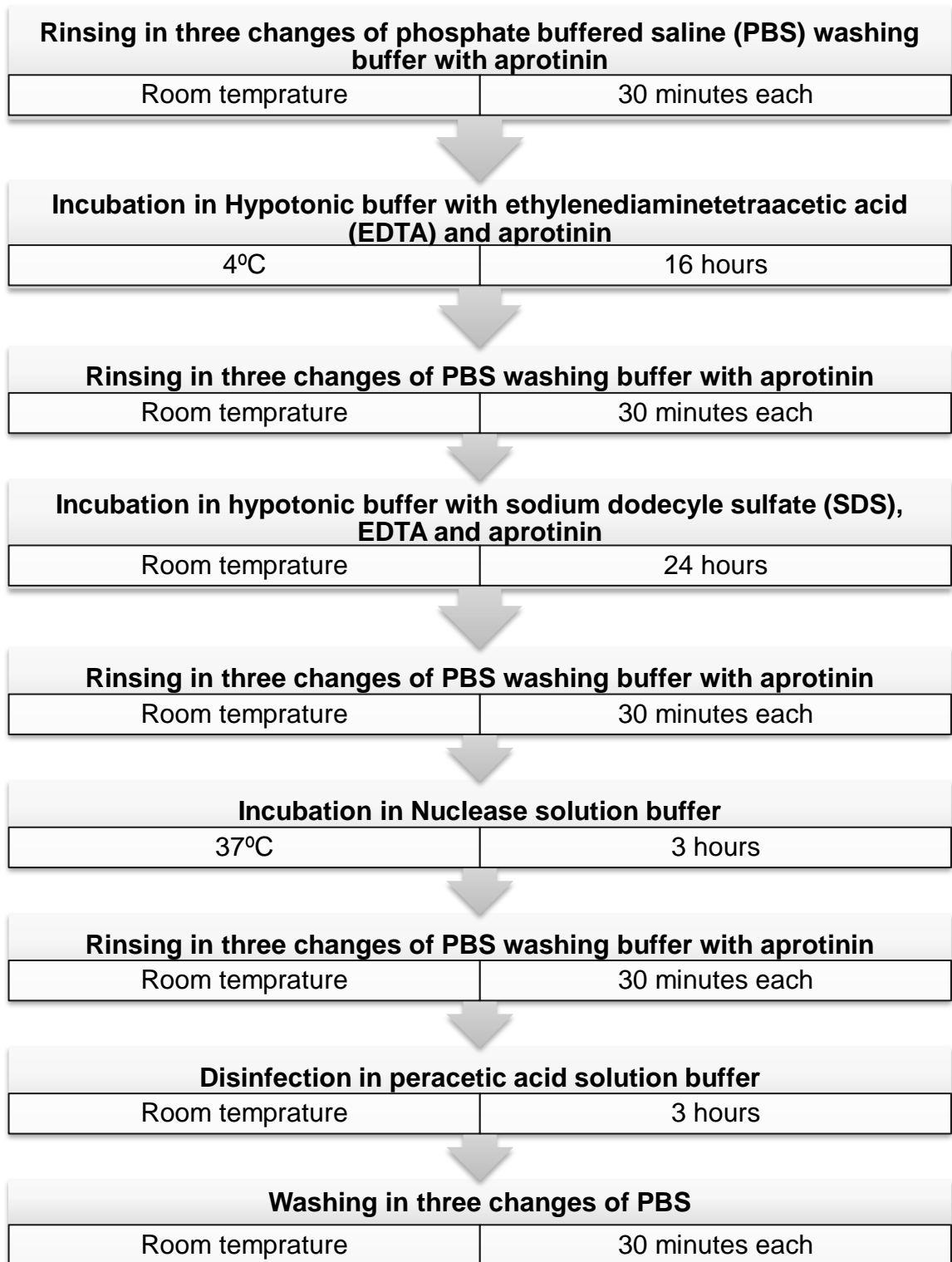


Figure 4-1: Flowchart demonstrates decellularisation protocol I.

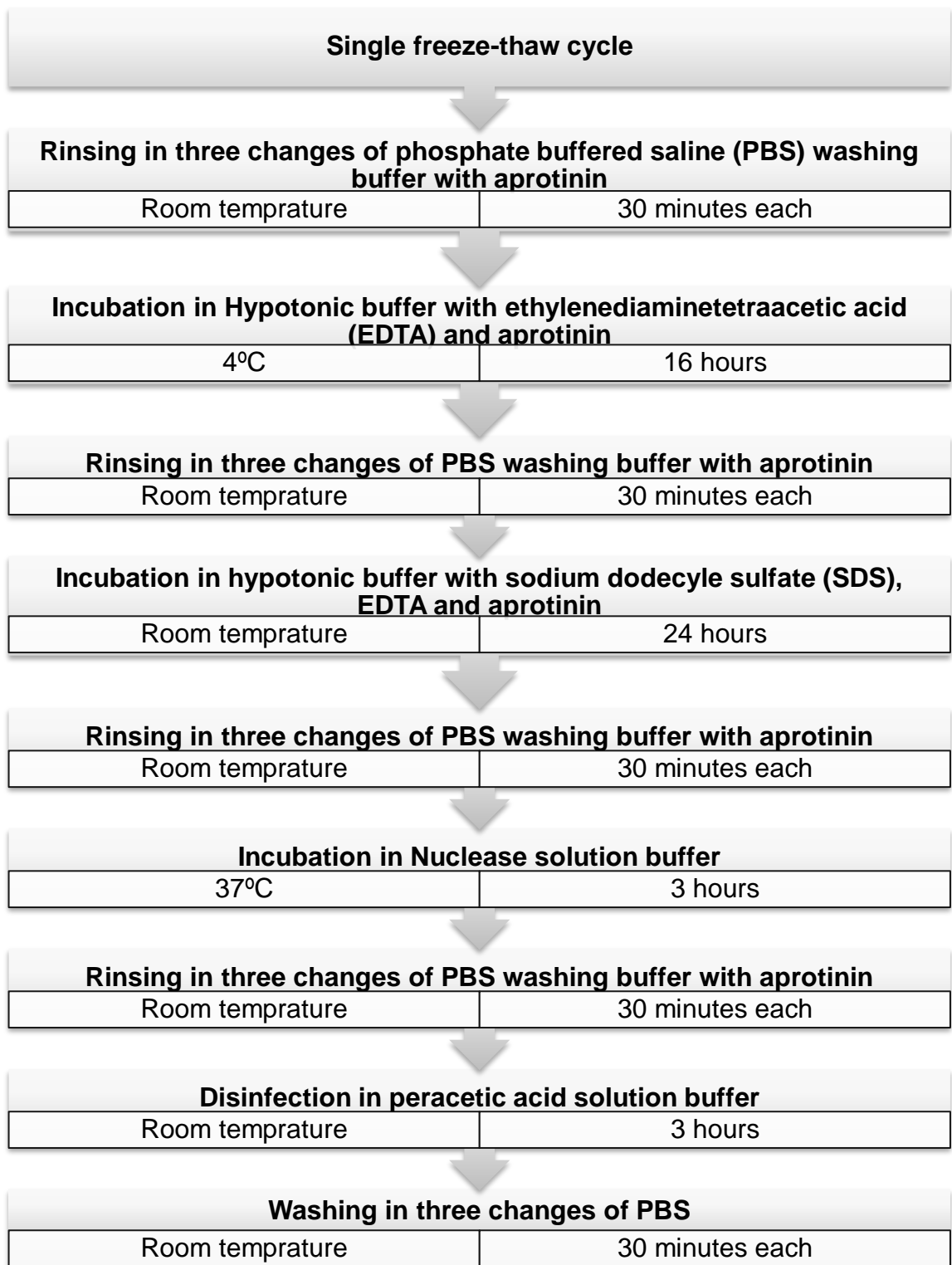


Figure 4-2: Flowchart demonstrates decellularisation protocol II.

4.4.2 Evaluation of decellularisation protocols efficiency

Following bovine dental pulps decellularisation, the efficiency of the protocols on achieving sufficient removal of the cells and nuclear materials from the tissues was evaluated using histological analysis and spectrophotometric DNA quantification.

4.4.2.1 Histological analysis

Study and control tissues (n = 5 per group) were prepared for the histological staining as described in Chapter 3, Section 3.2.2. Serial sections of 5 μm thickness were subjected to staining using H&E and DAPI as described in Chapter 3, Section 3.2.3.1 and Section 3.2.3.2, respectively. H&E stained sections were viewed using bright-field microscopy with normal Köhler illumination and DAPI stained sections were visualised using a florescent microscope equipped with a DAPI filter. All images were captured digitally.

4.4.2.2 Spectrophotometric DNA quantification

Study and control tissues (n = 5 per group) were subjected to DNA extraction using a DNeasy Blood and Tissue kit as described in Chapter 3, Section 3.2.6. DNA samples were then subjected to a quantification using the NanoDrop™ 2000 spectrophotometer at an absorbance wavelength of 260 nm (Chapter 3, Section 3.2.7.3.2.7.1). DNA content per sample dry weight ($\text{ng}\cdot\text{mg}^{-1}$) was then determined for each sample by normalising the concentration of DNA obtained from the spectrophotometer to the total volume of eluted DNA and the sample dry weight. Statistical analysis was carried out as described in Chapter 3, section 3.2.13. The average DNA contents of the study and control samples were compared using independent student's *t*-test. The *P*-value was considered significant if fall below 0.05. The data were plotted as mean DNA content \pm standard deviation.

4.5 Results

4.5.1 Cell nuclei and DNA removal efficiency following bovine dental pulp decellularisation using protocol I

Cell nuclei removal and general histoarchitecture preservation

Serial sections of native and decellularised bovine dental pulps were stained with H&E and DAPI to assess cell nuclei removal and general histoarchitecture preservation following decellularisation protocol I.

Representative image of H&E stained tissue sections of native bovine dental pulps visualised using bright-field microscope are shown in Figure 4-3A. Native bovine dental pulp appeared as a soft connective tissue rich with cells. The cell nuclei (stained blue with haematoxylin) exhibited different morphological appearances including elongated spindles and polygonal and spherical shapes. The connective tissue stroma of the native bovine dental pulp (stained pink with eosin) displayed different morphological regions based on cell organisation including the odontoblast layer at the periphery of the pulpal tissue, cell-rich zone subjacent to the odontoblast layer and the pulp core. However, the cell-free zone (zone of Weil) was not distinguishable. Multiple capillaries and vascular channels appeared dispersed in the sub-odontoblastic zone and the pulp core.

Representative image of DAPI stained tissue sections of native bovine dental pulps is shown in Figure 4-4A. Native bovine dental pulp showed high nuclear density. The cell nuclei were observed as a bright blue spherical and elongated structures organised in a black background.

Representative images of H&E and DAPI stained tissue sections of bovine dental pulps subjected to decellularisation protocol I are shown in Figure 4-3B and

Figure 4-4B, respectively. Following decellularisation protocol I, bovine dental pulps showed reduced cellular density as compared to the native pulps. However, complete removal of cell nuclei was not achieved. The cell nuclei were detected throughout the treated tissues as light-purple coloured dots. The extracellular matrix of the treated tissues stained light pink and retained its structure as compared to the control tissues. The general histoarchitecture including the vasculature seem to be preserved following decellularisation. DAPI staining of bovine dental pulps subjected to decellularisation protocol I revealed blue nuclear florescent staining in several areas of the tissues. However, the density of the nuclear DNA was markedly reduced as compared to the native tissues.

DNA content removal

Results of the spectrophotometric DNA quantification of the native and decellularised samples following decellularisation protocol I are shown in Figure 4-5. The mean DNA content of native bovine dental pulps was 1410 ± 60.24 ng.mg⁻¹ compared to 642 ± 43.50 ng.mg⁻¹ in the dental pulp tissues subjected to decellularisation protocol I. Data analysis using the independent student *t*-test revealed a significant difference ($P < 0.0001$) between the mean DNA content of the native and decellularised tissues. The percentage of DNA reduction was around 54.5%.

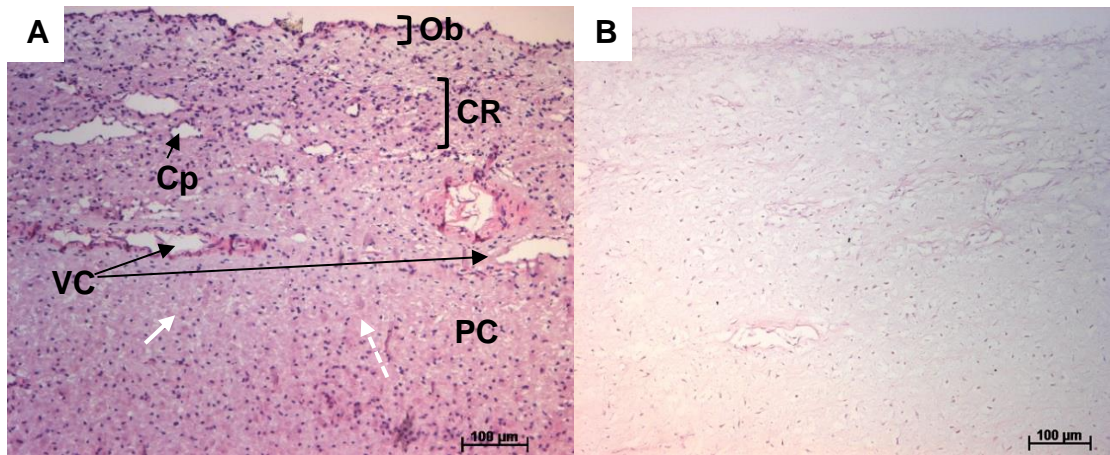


Figure 4-3: Bright-field microscopic images of native and decellularised bovine dental pulps stained with H&E. Representative images of (A) native bovine dental pulp shows soft connective tissue rich with cells and (B) bovine dental pulp subjected to decellularisation protocol I shows reduction in cell density with preservation of general histoarchitecture. Cell nuclei stained blue (solid white arrow) and the connective tissue stroma (extracellular matrix) stained pink (dashed white arrow). (Ob) odontoblasts layer, (CR) cell-rich zone, (PC) pulp core, (Cp) capillaries, (VC) vascular channels.

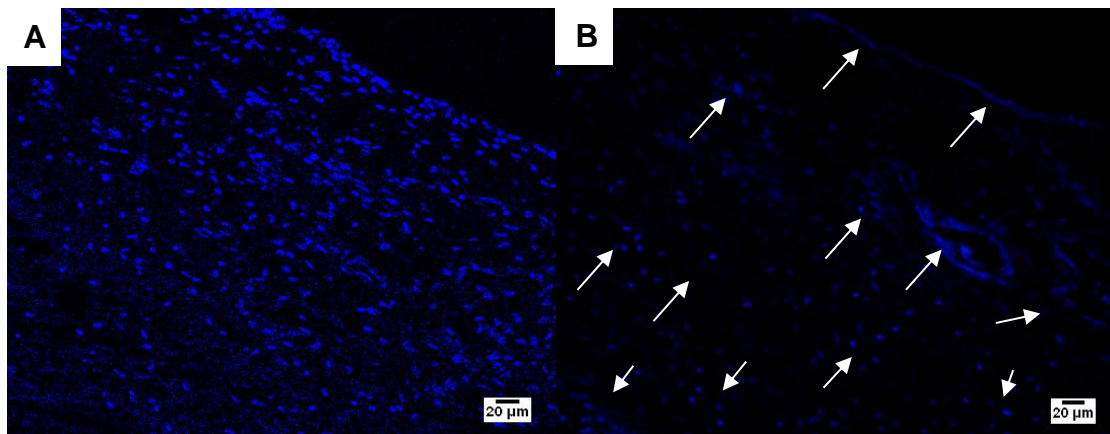


Figure 4-4: Florescent microscopic images of native and decellularised bovine dental pulps stained with DAPI. Representative images of (A) native bovine dental pulp shows rich nuclear contents and (B) bovine dental pulp subjected to decellularisation protocol I shows reduced nuclear contents. Nuclear DNA stained blue (white arrows).

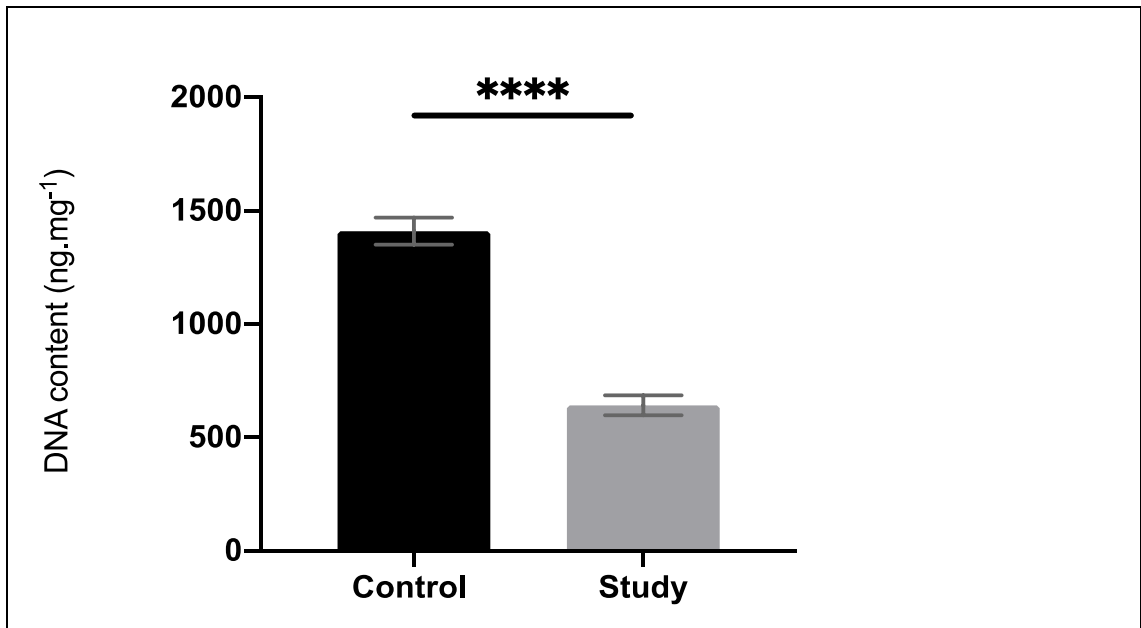


Figure 4-5: Bar graph demonstrates the DNA content of native and decellularised bovine dental pulps as determined by the NanoDrop spectrophotometer. Data represent the mean values (n = 5 samples per group) \pm standard deviation. The mean DNA content of native bovine dental pulps (control) was 1410 ± 60.24 ng.mg⁻¹ compared to 642 ± 43.50 ng.mg⁻¹ in the pulpal tissues subjected to decellularisation protocol I (study). Data analysis revealed significant difference between the mean DNA content of the control and study group (independent student's t-test, **** $P < 0.0001$).

4.5.2 Cell nuclei and DNA removal efficiency following bovine dental pulp decellularisation using protocol II

Cell nuclei removal and general histoarchitecture preservation

Representative images of H&E and DAPI stained sections of native bovine dental pulps are shown in Figure 4-6A and Figure 4-7A, respectively. H&E staining of the native bovine dental pulps showed soft connective tissues rich with cells organised in different morphological zones (odontoblast layer, cell-rich zone and pulp core). On the other hand, DAPI staining of native bovine dental pulps showed high density of blue-stained nuclear DNA (Figure 4-7A).

Following tissue decellularisation, H&E staining of the decellularised bovine dental pulps showed soft connective tissues stained pink and devoid of cell nuclei (Figure 4-6B). The general histoarchitecture of the decellularised pulps including the vascular channels appeared to be preserved. The findings of H&E staining were further confirmed by DAPI staining which showed no visible blue nuclear fluorescent staining in the decellularised pulps as compared to the native pulps (Figure 4-7B).

DNA content removal

Results of the spectrophotometric DNA quantification of the native and decellularised samples subjected to decellularisation using protocol II are shown in Figure 4-8. The mean DNA content of the native pulps was 1640.1 ± 105.20 ng.mg⁻¹ compared to 14.86 ± 2.24 ng.mg⁻¹ in the decellularised pulps. Data analysis using independent student's *t*-test revealed significant difference ($P < 0.0001$) between the mean DNA content of the native and decellularised pulps. The percentage of DNA reduction was more than 99%.

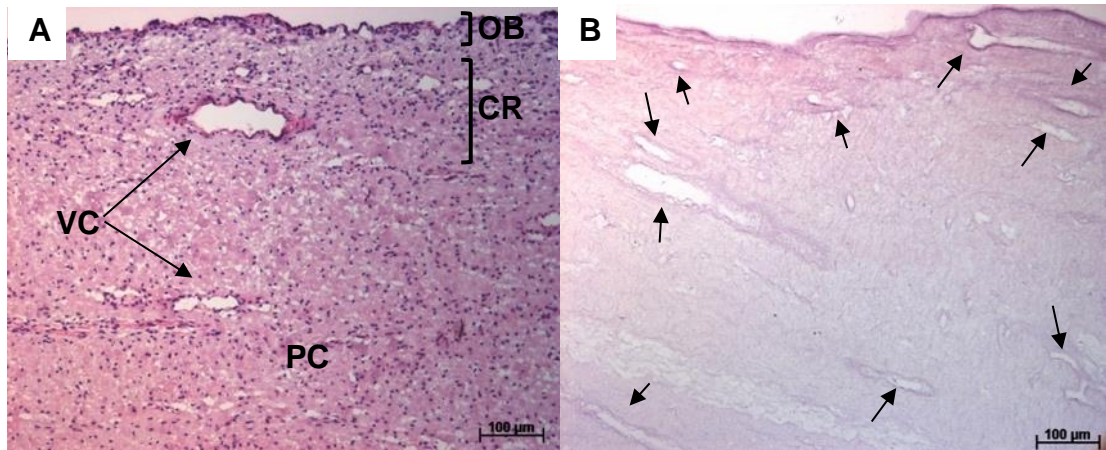


Figure 4-6: Bright-field microscopic images of native and decellularised bovine dental pulps stained with H&E. Representative images of (A) native bovine dental pulp shows high density of cell nuclei within connective tissue stroma and (B) decellularised bovine dental pulp subjected to decellularisation protocol II shows acellular matrix with highly preserved histoarchitecture and vascular channels integrity (Solid black arrows). Cell nuclei stained blue and the connective tissue stroma (extracellular matrix) stained pink. (OB) odontoblasts layer, (CR) cell-rich zone, (PC) pulp core, (VS) vascular channels.

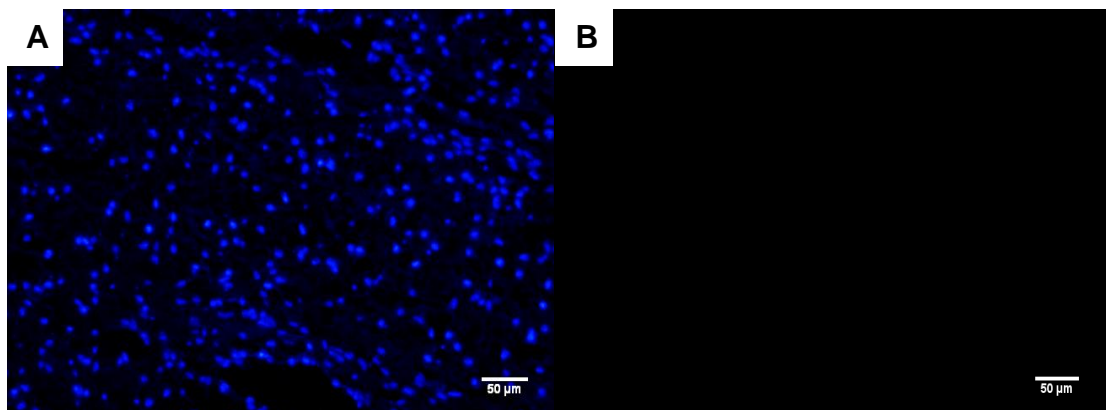


Figure 4-7: Florescent microscopic images of native and decellularised bovine dental pulps stained with DAPI. Representative image of (A) native bovine dental pulp shows high density of nuclear DNA and (B) decellularised bovine dental pulp subjected to decellularisation protocol II shows no visible nuclear DNA. Nuclear DNA stained blue.

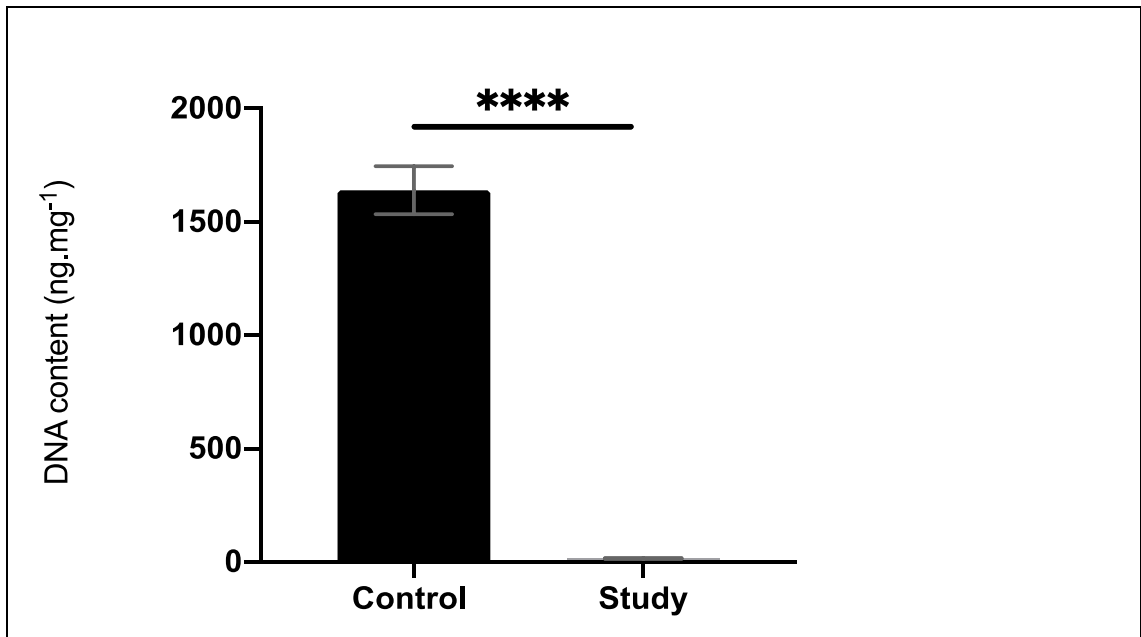


Figure 4-8: Bar graph demonstrates the DNA content of native and decellularised bovine dental pulps as determined by the NanoDrop spectrophotometer. Data represent the mean value (n = 5 samples per group) \pm standard deviation. The mean DNA content of native bovine dental pulps (control) was 1640.1 ± 105.20 ng/mg in comparison to 14.86 ± 2.24 ng/mg in the decellularised pulps (study) subjected to decellularisation protocol II. Data analysis revealed significant difference between the mean DNA content of the native and decellularised pulps (Independent student *t*-test, **** $P < 0.0001$).

4.6 Discussion

In the present research, decellularised bovine dental pulps were developed. The main advantages of utilising xenogeneic sources such as bovine dental pulps for the preparation of decellularised scaffolds are the wide availability, ease of obtaining tissues in abundant quantities as by-products of food supply chain and clinical practicality. However, concerns regarding the risk of disease transmission from the donor tissues as well as the risk of adverse immune-mediated response by the host need to be addressed before attempting clinical translation. Effective sterilisation of the decellularised tissues has shown a potential to eliminate endotoxins and intact viral and bacterial DNA (Hodde and Hiles, 2002, Qiu *et al.*, 2009). In addition, thorough decellularisation of the source tissues with adequate removal of the donor cells, DNA and Gal epitope may minimise the likelihood of adverse immune-mediate response by the host (Keane and Badylak, 2015).

Selecting an appropriate decellularisation protocol is thus important for the future performance of the developed scaffolds (Gilbert, 2012). The goal is to use a mild decellularisation protocol capable of achieving thorough removal of the cells and cell remnants from the tissue while retaining the native structure, composition and vasculature intact to the best extent possible (Keane *et al.*, 2015). Retention of ECM structure and composition following decellularisation has been directly linked to the use of low concentrations of chemicals, particularly detergents (Knight *et al.*, 2008). It has been shown that the use of highly concentrated detergents for a prolonged duration leads to extracellular matrix disruption and growth factors elimination (Reing *et al.*, 2010), and often results in a cytotoxic scaffolds (Cebotari *et al.*, 2010).

Therefore, in the present chapter, a mild protocol described by Wilshaw *et al.* (2006) for amniotic membrane decellularisation was selected for bovine dental pulp decellularisation. The protocol involved cell membrane lysis using hypotonic tris buffer with disruption of cell components binding to ECM using EDTA (chelating agent). This was followed by solubilisation of cellular and nuclear components using a single cycle of low SDS concentration (0.03% w/v) and ending with the degradation of nucleic acids using nuclease treatment. A protease inhibitor, aprotinin, was utilised to prevent extracellular matrix digestion due to the release of endogenous proteases during cell lysis. Multiple washing cycles with gentle physical agitation were also included in the protocol to facilitate the removal of cellular debris and chemical residues from the tissues.

Unfortunately, effective decellularisation of bovine dental pulp was not possible using decellularisation protocol I. This is most likely due to the higher density of dental pulp tissue as compared to the amniotic membrane (the tissue used by Wilshaw and colleagues to develop protocol I), which may hampered cell exposure to decellularisation chemicals and subsequent cell removal. Therefore, an optimised iteration of decellularisation protocol I described by Matoug-Elwerfelli *et al.* (2018) was employed next in an attempt to achieve effective decellularisation of bovine dental pulp. The protocol involved a single freeze-thaw cycle at the beginning of the decellularisation process. This temperature change aims to open up the dense structure of the pulpal ECM through ice crystal formation. It has been shown that freeze-thaw cycles incorporation in the decellularisation protocols can help in disrupting the cellular membrane and minimising the amount of chemicals required to achieve sufficient decellularisation (Burk *et al.*, 2014, Fu *et al.*, 2014, Keane *et al.*, 2015). Successful decellularisation following incorporation of freeze-thaw cycles in

decellularisation protocols has been reported for many tissues including medial meniscus (Stapleton *et al.*, 2008), femoral artery (Wilshaw *et al.*, 2012) and pulmonary valves (Luo *et al.*, 2014).

The use of decellularisation protocol II resulted in acellular scaffolds with retained general native histoarchitecture and with more than 99% reduction in the DNA content of the dental pulp tissue. The trace amount of DNA that remained in the scaffolds following decellularisation fell below the threshold (50 ng.mg⁻¹ dry tissue weight) indicated in the standard criteria of sufficiently decellularised tissues (Crapo *et al.*, 2011). Furthermore, the protocol resulted in the preservation of the native vascular channels. This finding is in accordance with previous studies which demonstrated that the decellularisation of several tissues and organs resulted in retained vascular networks (Ott *et al.*, 2008, Totonelli *et al.*, 2012, Maghsoudlou *et al.*, 2013, Bonandrini *et al.*, 2014).

The combined use of qualitative and quantitative methods to assess the decellularisation efficacy is essential to ensure sufficient removal of the cellular and nuclear materials from the tissue. Indeed, residual cellular and nuclear materials can impact the host response as well as the remodelling outcomes of the resultant scaffolds (Brown *et al.*, 2009, Keane *et al.*, 2012, Keane *et al.*, 2015). Objective criteria for assessing the decellularisation efficacy has been proposed by Crapo and colleagues (2011). The criteria include the absence of visible cell nuclei on tissue sections stained using H&E and DAPI with reduction of DNA content below 50 ng.mg⁻¹ (dry tissue weight) (Crapo *et al.*, 2011). In the present research, H&E (shows the general tissue histoarchitecture and cellular content) and DAPI (shows nuclear materials) staining were used in combination as qualitative methods to assess the decellularisation efficacy of the used protocols. Additionally, the spectrophotometric DNA quantification was used as a

quantitative assessment method enabling the detection of double and single stranded DNA molecules.

Collectively, the research work presented in this chapter shows the successful development of a decellularised bovine dental pulp matrix using a gentle protocol involving low SDS concentration in combination with protease inhibitor, enzymatic agents and mild physical stress. Bovine dental pulps represent an abundant source for decellularised scaffolds development, which could help overcome the supply limitation of human dental pulps. The developed decellularised dental pulp matrix retained the general native histoarchitecture and the vasculature, a characteristic that could be beneficial for dental pulp regeneration. Further characterisation of the developed decellularised dental pulp matrix was performed and is described in the next chapter.

Chapter 5

Characterisation of the developed decellularised dental pulp matrix

5.1 Introduction

The previous chapter demonstrated the successful development of a decellularised bovine dental pulp matrix using a gentle protocol involving low concentrations of decellularisation chemicals. Retention of the native ECM constituents (i.e. biochemical components and their three-dimensional ultrastructure) following decellularisation is considered crucial for the future performance of the generated scaffolds (Hoshiba *et al.*, 2010). The ECM constituents provide structural support and attachment sites for the cells and act as sources of biophysical and biochemical cues which could promote tissue-specific cell differentiation (Agmon and Christman, 2016, Swinehart and Badylak, 2016, Robb *et al.*, 2017).

Several previous studies demonstrated the tissue-specific effects of the decellularised scaffolds on stem cell differentiation. In a study by Iop *et al.* (2009), human mesenchymal stem cells showed evidence of differentiation towards valve interstitial cell lineage following seeding onto a decellularised heart valve scaffold. Likewise, Cheung *et al.* (2014) reported an increase in glycerol-3-phosphate dehydrogenase activity and adipogenesis on human adipose-derived stem cells, when seeded on a decellularised adipose tissue hydrogel. Furthermore, Zhang and Dong (2015) showed hepatic differentiation of mouse adipose-derived stem cells following seeding on a decellularised liver coating. Collectively, the tissue-specific effect observed in these studies is most likely due to the unique biological

cues presented to the cells by the decellularised scaffolds, a characteristic that distinguishes these scaffolds from other scaffold types. Therefore, preservation of this unique characteristic of the decellularised scaffolds, through ensuring retention of ECM constituents following tissue decellularisation, is important.

Collagen, fibronectin, laminin and glycosaminoglycans constitute essential components of the dental pulp ECM (Sloan, 2015). They provide structural support for the cells and attachment sites for several cell surface receptors and growth factors (Novoseletskaia *et al.*, 2019). Many growth factors, such as vascular endothelial growth factor (VEGF), fibroblast growth factor 2 (FGF-2), transforming growth factor β 1 (TGF- β 1) and bone morphogenic proteins (BMPs) have been identified in the ECM of dental pulp (Gu *et al.*, 1996, Toyono *et al.*, 1997, Chen *et al.*, 2003, Wang *et al.*, 2007). It is noteworthy that the use of purified forms of these growth factors has been investigated as an approach to enhance angiogenesis and promote odontoblast-like cell differentiation during dental pulp regeneration (Melin *et al.*, 2000, Saito *et al.*, 2004, Mullane *et al.*, 2008). However, difficulties in determining the optimal dose, delivery method and long-term stability of these growth factors limit the translational potential severely. Therefore, retention of these growth factors in the developed decellularised dental pulp matrix might be advantageous for its future performance in dental pulp regeneration.

In the research work presented in this chapter, the developed decellularised dental pulp matrix was characterised for the retention of essential ECM components (collagen, fibronectin, laminin and glycosaminoglycans), growth factors (VEGF-A, FGF-2, TGF- β 1 and BMP-2) and surface topography of the native dental pulp.

5.2 Aim and objectives

Aim

The aim of the research work presented in this chapter was to characterise the structural and compositional characteristics of the developed decellularised dental pulp matrix.

Objectives

- To characterise the histoarchitecture of the developed decellularised dental pulp using histological staining methods in comparison to native bovine dental pulp.
- To assess the retention of essential extracellular matrix proteins and growth factors in the developed decellularised dental pulp using immunohistochemical staining in comparison to native bovine dental pulp.
- To evaluate alpha gal epitope elimination from bovine dental pulp following tissue decellularisation using immunohistochemical staining.
- To characterise the surface topography of the developed decellularised dental pulp using scanning electron microscopy in comparison to native bovine dental pulp.

5.3 Experimental approach

The histoarchitecture of the generated decellularised dental pulps was initially characterised for the retention of collagen and glycosaminoglycans using PicroSirius Red staining and Alcian Blue staining, respectively, in comparison to native bovine dental pulps. The decellularised dental pulps were then further characterised for the retention of essential ECM components (collagen I, collagen III, fibronectin and laminin) and growth factors (VEGF-A, FGF-2, TGF- β 1 and BMP-2) using immunohistochemical staining. The decellularised dental pulps were also assessed for the elimination of alpha-gal epitope using immunohistochemical staining. The surface topography of the developed decellularised dental pulps was characterised in comparison to native bovine dental pulps using scanning electron microscopy.

5.4 Methods

5.4.1 Histological staining

Tissue sections of native and decellularised bovine dental pulps (n = 5 samples per group) were stained using PicroSirius Red and Alcian Blue as described in Chapter 3, Section 3.2.3.3 and Section 3.2.3.4, respectively. Stained sections were viewed under a bright-field microscope with normal Köhler illumination and Images were captured digitally.

5.4.2 Immunohistochemical staining

Tissue sections of native and decellularised bovine dental pulps (n = 5 samples per group) were subjected to immunohistochemical staining as described in Chapter 3, Section 3.2.4. Briefly, tissue sections were initially exposed to an appropriate antigen unmasking technique, and then labelled with primary and

secondary antibodies. The primary antibodies used in this chapter include monoclonal antibodies against collagen I, fibronectin, alpha-gel epitope and TGF- β 1, and polyclonal antibodies against collagen III, laminin, VEGF-A, FGF-2 and BMP-2. The isotype control antibodies were used as negative controls at the same concentrations and under the same conditions but with omission of the primary antibodies. Stained sections were viewed under a bright-field microscope with normal Köhler illumination and Images were captured digitally.

5.4.3 Scanning electron microscopy

Samples of native and decellularised bovine dental pulps (n = 5 samples per group) were prepared for scanning electron microscopy as described in Chapter 3, Section 3.2.5. The prepared samples were then attached to aluminium stubs and coated with a very thin layer of gold using E5000 sputter coater. Samples visualisation was subsequently achieved using a conventional high vacuum scanning electron microscope with back scattered electron mode and beam energy equal 15 keV. The aperture was set at 600 μ m, the emission current was set at 70 μ A and the condenser lens was set between 0.18 - 0.22 mA. All images were captured digitally using a slow speed scanning mode.

5.5 Results

5.5.1 Retention of native pulpal histoarchitecture in the developed decellularised dental pulps

PicroSirius Red stained tissue sections of native and decellularised bovine dental pulps observed using the bright-field microscope are shown in Figure 5-1. Native bovine dental pulp appeared as a highly cellular matrix composed of an entangled porous network of collagen fibres and fibrils (Figure 5-1 A). Following decellularisation, the porous collagenous architecture of the dental pulp matrix was clearly visible (Figure 5-1 B). Abundant collagen fibres and fibrils were observed throughout the matrix of the decellularised dental pulps and around the vascular structures. However, the matrix of the decellularised dental pulps appeared slightly denser than that of the native bovine dental pulps.

Representative images of native and decellularised bovine dental pulps stained with Alcian Blue and viewed under the bright-field microscope are shown in Figure 5-2. Native bovine dental pulp appeared as a cellular matrix with a uniform distribution of glycosaminoglycans (Figure 5-2 A). Following decellularisation, the glycosaminoglycans of the matrix appears to be highly retained with no major differences in the staining pattern between the decellularised and native bovine dental pulps could be seen (Figure 5-2 B).

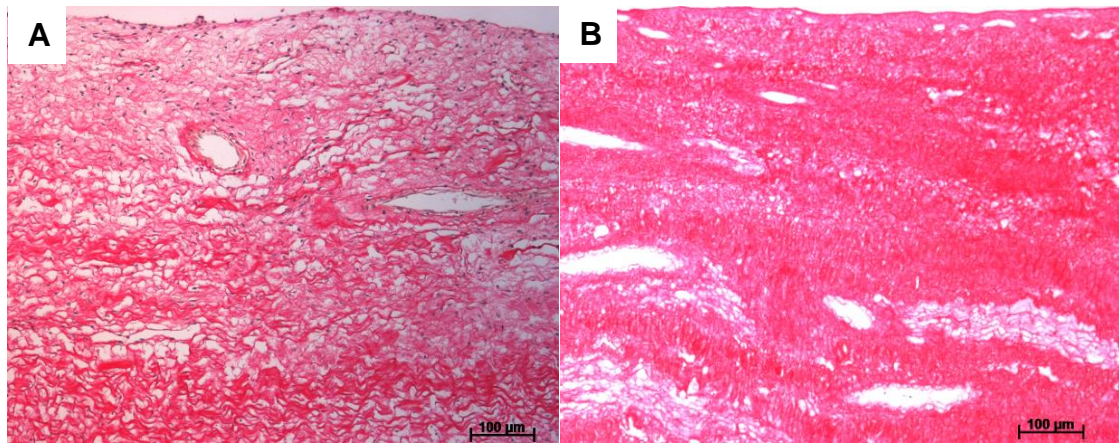


Figure 5-1: Bright-field microscopic images of PicroSirius Red-stained tissue sections of native and decellularised bovine dental pulps. (A) Representative image of native bovine dental pulp showing the cells organised within a porous network of collagen fibres and (B) Representative image of decellularised bovine dental pulp showing acellular porous matrix rich with collagen fibres. Collagen fibres stained red and cell nuclei stained dark brown/black.

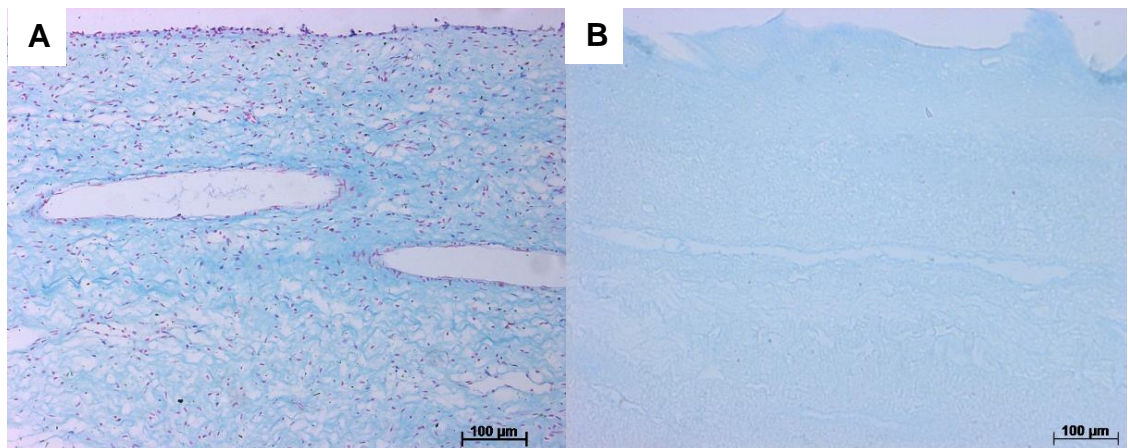


Figure 5-2: Bright-field microscopic images of Alcian Blue-stained tissue sections of native and decellularised bovine dental pulps. (A) Representative image of native bovine dental pulp showing the cells dispersed within a matrix containing abundance of glycosaminoglycans and (B) Representative image of decellularised bovine dental pulp scaffold showing acellular matrix with high retention of glycosaminoglycans content. Glycosaminoglycans stained blue and cell nuclei stained pink.

5.5.2 Retention of extracellular matrix components in the developed decellularised dental pulps

Collagen I

Representative images of native and decellularised bovine dental pulps labelled with a monoclonal antibody against collagen I are shown in Figure 5-3. Native bovine dental pulp showed a strong brown staining, indicating a positive immunoreactivity to collagen I antigen (Figure 5-3 A). The entire pulp depth extending from the odontoblasts layer to the pulp core appeared positively stained with increased staining intensity around the vascular structures. Following decellularisation, the peripheral zone of the pulp showed negative immunoreactivity to collagen I antigen (Figure 5-3 B). Despite this finding, the rest of the pulpal matrix showed a strong positive immunoreactivity indicating high retention of collagen I fibres following decellularisation. No brown staining was observed in the negative control sections (Figure 5-3 C and D).

Collagen III

Representative images of native and decellularised bovine dental pulps labelled with anti-collagen III and viewed under a bright-field microscope are shown in Figure 5-4. Native bovine dental pulp showed a positive immunoreactivity to collagen III antigen (Figure 5-4 A). The staining pattern resembled reticular fibres and was seen consistently in all examined tissue sections. The entire depth of the pulpal tissue extending from the odontoblasts layer to the pulp core stained brown. Following decellularisation, the staining pattern appeared highly retained; however, the staining intensity seemed slightly reduced (Figure 5-4 B). No brown staining occurs in the negative control tissue sections (Figure 5-4 C and D).

Fibronectin

Representative images of native and decellularised bovine dental pulps labelled with anti-fibronectin and viewed under the bright-field microscope are shown in Figure 5-5. Native bovine dental pulp showed a positive immunoreactivity to fibronectin antigen throughout the entire depth of the tissue with increased staining intensity at the cell-rich zone (Figure 5-5 A). Fibronectin appeared as a fibrous plexus scattered within the pulpal matrix. Following decellularisation, a positive immunoreactivity to fibronectin antigen with slight reduction in the staining intensity was evident (Figure 5-5 B). Retention of the staining pattern was clearly visible in all examined sections of the decellularised dental pulp. The negative control sections showed absence of brown staining (Figure 5-5 C and D).

Laminin

Representative images of native and decellularised bovine dental pulps labelled with anti-laminin and visualised using the bright-field microscope are shown in Figure 5-6. Native bovine dental pulp showed a positive immunoreactivity to laminin antigen mainly around the basement membrane of the vascular structures (Figure 5-6 A). The staining pattern of laminin antigen appeared as thin fibres accentuated mainly around the vascular channels. Following decellularisation, a positive immunoreactivity to laminin antigen was visible in the pulpal matrix (Figure 5-6 B). However, the staining intensity appeared highly reduced around the vascular structures as compared to the native bovine dental pulp. No brown staining occurs in the negative control tissue sections (Figure 5-6 C and D).

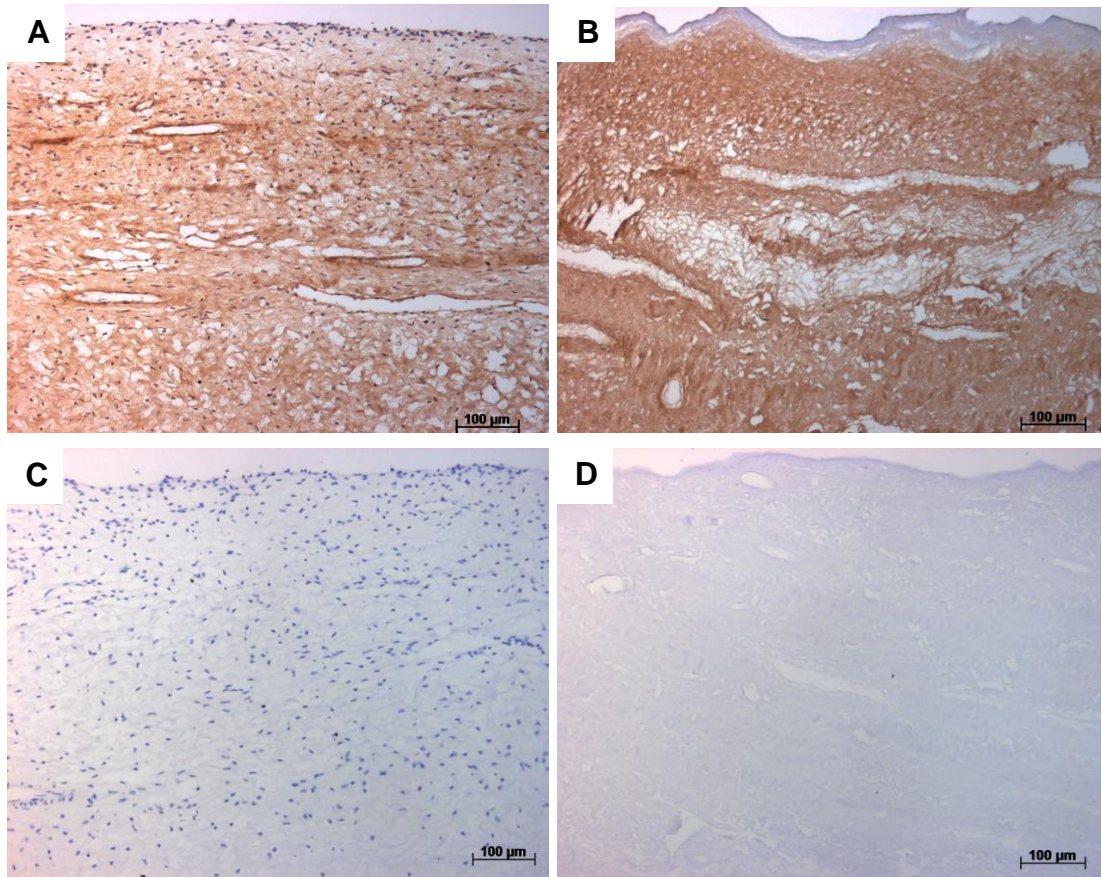


Figure 5-3: Bright-field microscopic images of native and decellularised bovine dental pulps labelled with anti-collagen I and the corresponding control isotype antibody. (A and B) Representative images of tissue sections of (A) native and (B) decellularised bovine dental pulps labelled with anti-collagen I. The images show a strong positive immunoreactivity to collagen I antigen. (C and D) Representative images of the negative controls of (C) native and (D) decellularised bovine dental pulps showing absence of brown staining. Areas of positive immunoreactivity stained brown and cell nuclei stained blue.

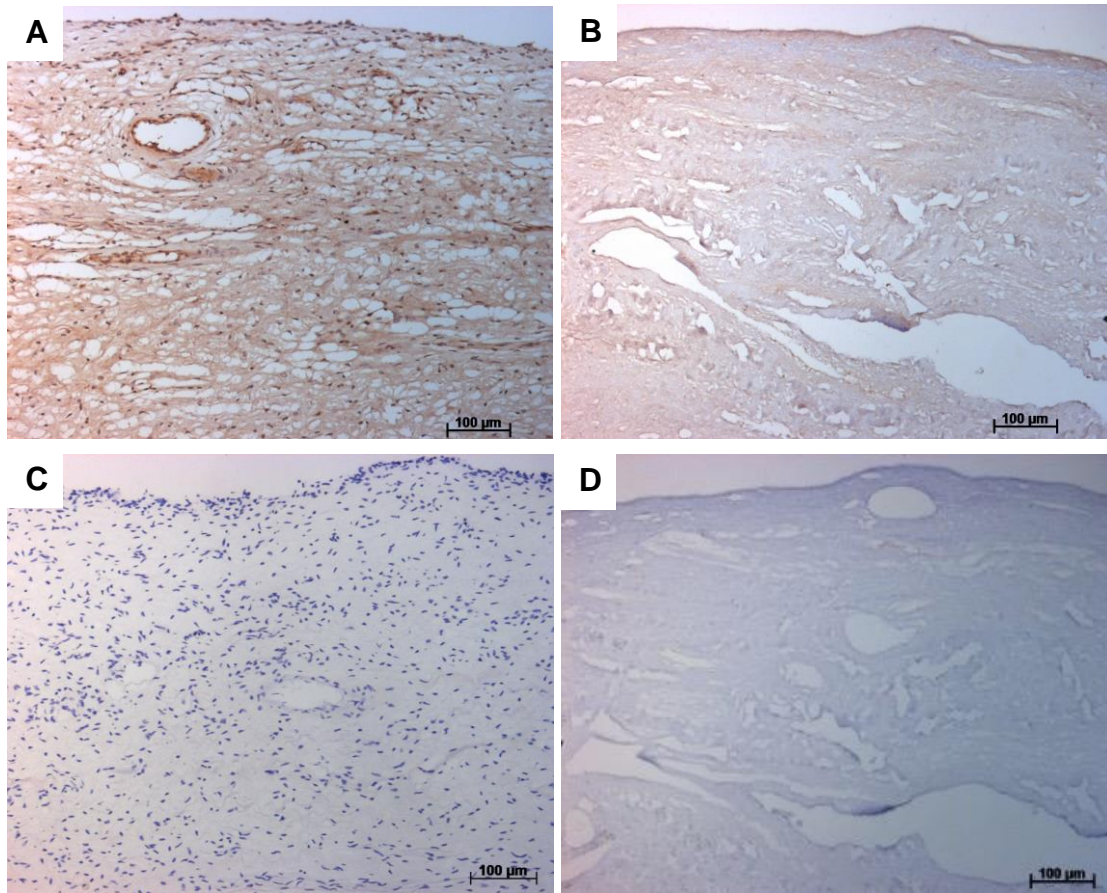


Figure 5-4: Bright-field microscopic images of native and decellularised bovine dental pulps labelled with anti-collagen III and the corresponding control isotype antibody. (A and B) Representative images of (A) native bovine dental pulp showing a positive immunoreactivity to collagen III antigen and (B) decellularised bovine dental pulp showing weak positive immunoreactivity to collagen type III antigen. (C and D) Representative images of the negative control tissue sections of (C) native and (D) decellularised bovine dental pulps showing no visible brown staining. Areas of positive immunoreactivity stained brown and cell nuclei stained blue.

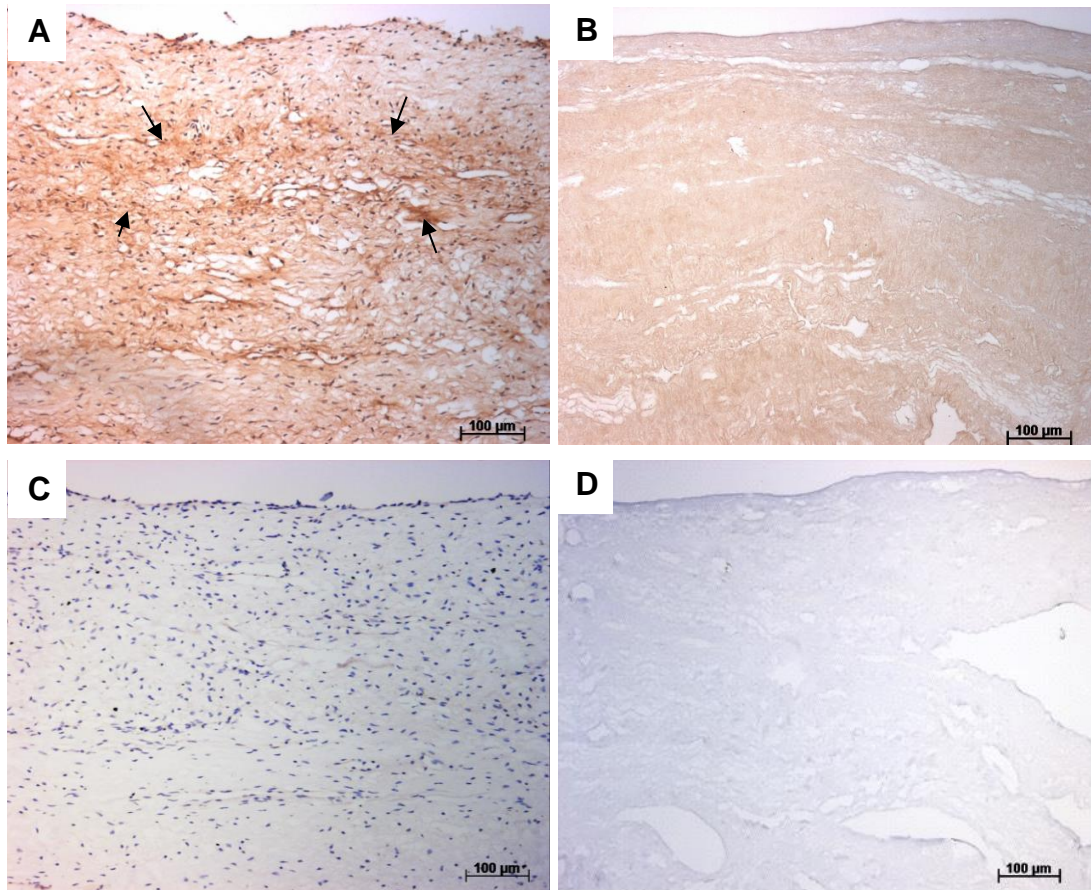


Figure 5-5: Bright-field microscopic images of native and decellularised bovine dental pulps labelled with anti-fibronectin and the corresponding control isotype antibody. (A and B) Representative images of (A) native bovine dental pulp showing a positive immunoreactivity to fibronectin antigen with increased staining intensity at the cell-rich zone (black arrows) and (B) decellularised bovine dental pulp showing retention of the positive immunoreactivity to fibronectin. (C and D) Representative images of the negative control tissue sections of (C) native and (D) decellularised bovine dental pulps showing no visible brown staining. Areas of positive immunoreactivity stained brown and cell nuclei stained blue.

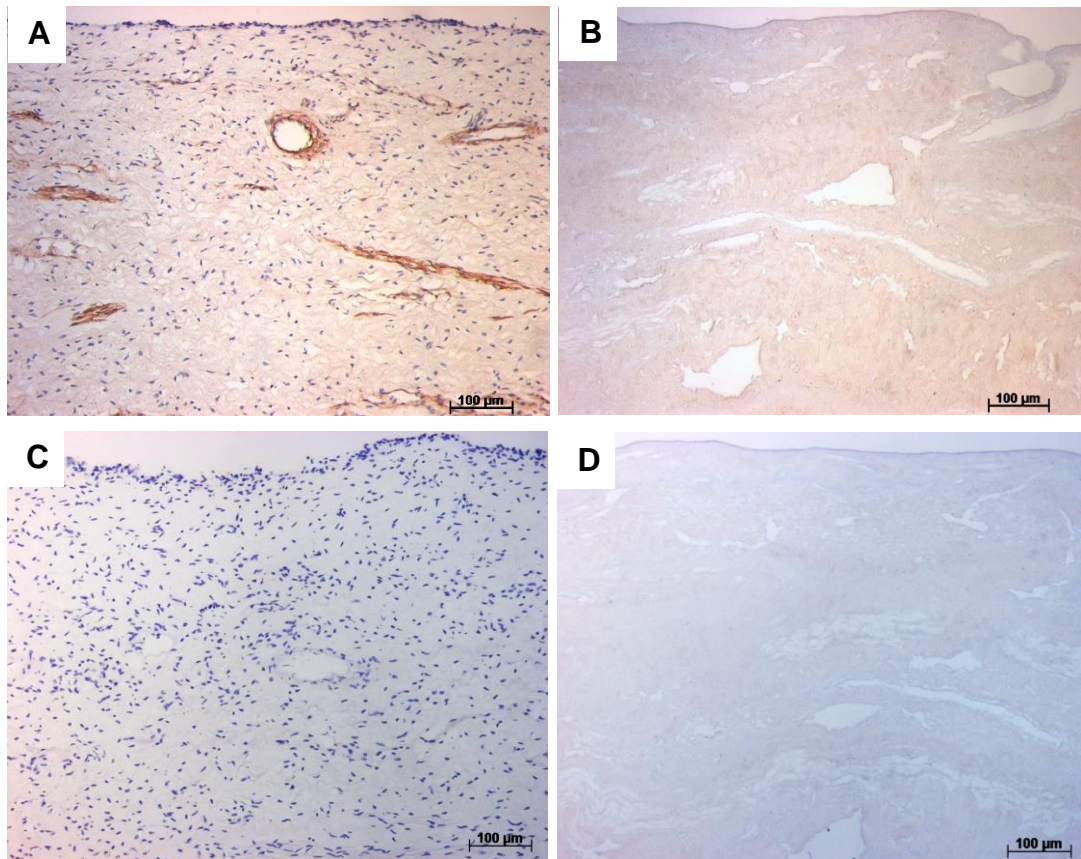


Figure 5-6: Bright-field microscopic images of native and decellularised bovine dental pulps labelled with anti-laminin and the corresponding control isotype antibody. (A and B) Representative images of (A) native bovine dental pulp showing positive immunoreactivity to laminin accentuated mainly around the vascular channels, and (B) decellularised bovine dental pulp scaffold showing weak positive immunoreactivity to laminin antigen. (C and D) Negative control sections of (C) native and (D) decellularised bovine dental pulps showing absence of brown staining. Areas of laminin antigen stained brown and cell nuclei stained blue.

5.5.3 Retention of growth factors in the developed decellularised dental pulps

VEGF-A

Tissue sections of native and decellularised bovine dental pulps labelled with antibody against VEGF-A and viewed under the bright-field microscope are shown in Figure 5-7. In the native dental pulp, a positive immunoreactivity (brown staining) to VEGF-A antigen was evident around the vascular structures (Figure 5-7 A). Following decellularisation, the positive immunoreactivity to VEGF-A antigen was still evident around the vessels; however, the staining intensity appeared reduced as compared to the native bovine dental pulp (Figure 5-7 B). No brown staining occurs in the negative control sections (Figure 5-7 C and D).

FGF-2

The results of immunohistochemical staining of native and decellularised bovine dental pulps with an antibody against FGF-2 are shown in Figure 5-8. Native dental pulp showed a positive immunoreactivity to FGF-2 antigen (Figure 5-8 A). The brown staining appeared in multiple areas of the matrix and became more accentuated around vascular channels. Following decellularisation, a positive immunoreactivity was still evident in the pulpal matrix (Figure 5-8 B). Brown staining with reduced intensity, as compared to native pulp, was visible around the vessels. No brown staining occurs in the negative control sections (Figure 5-8 C and D).

TGF- β 1

Representative images of native and decellularised bovine dental pulps labelled with antibody against TGF- β 1 and visualised under the bright-field microscope are shown in Figure 5-9. Native dental pulp showed a positive immunoreactivity

to TGF- β 1 antigen (Figure 5-9 A). The brown staining appeared in multiple areas within the stroma and around the vascular channels. In comparison, decellularised dental pulp showed a reduced, yet positive immunoreactivity to TGF- β 1 antigen (Figure 5-9 B). The weak brown staining was clearly visible around the vessels and within the matrix. No brown staining detected in the negative control (Figure 5-9 C and D).

BMP-2

Tissue sections of native and decellularised bovine dental pulps labelled with antibody against BMP-2 and viewed under the bright-field microscope are shown in Figure 5-10. In the native dental pulp, a positive immunoreactivity to BMP-2 antigen was observed in the pulpal matrix (Figure 5-10 A). The staining intensity appeared more accentuated around the vascular structures. In comparison, decellularised dental pulp showed a reduced, yet positive immunoreactivity to BMP-2 antigen (Figure 5-10 B). Similar to the native pulpal matrix, the brown staining was observed within the matrix of the decellularised pulp and around the vascular channels. No brown staining was detected in the negative control tissue sections (Figure 5-10 C and D).

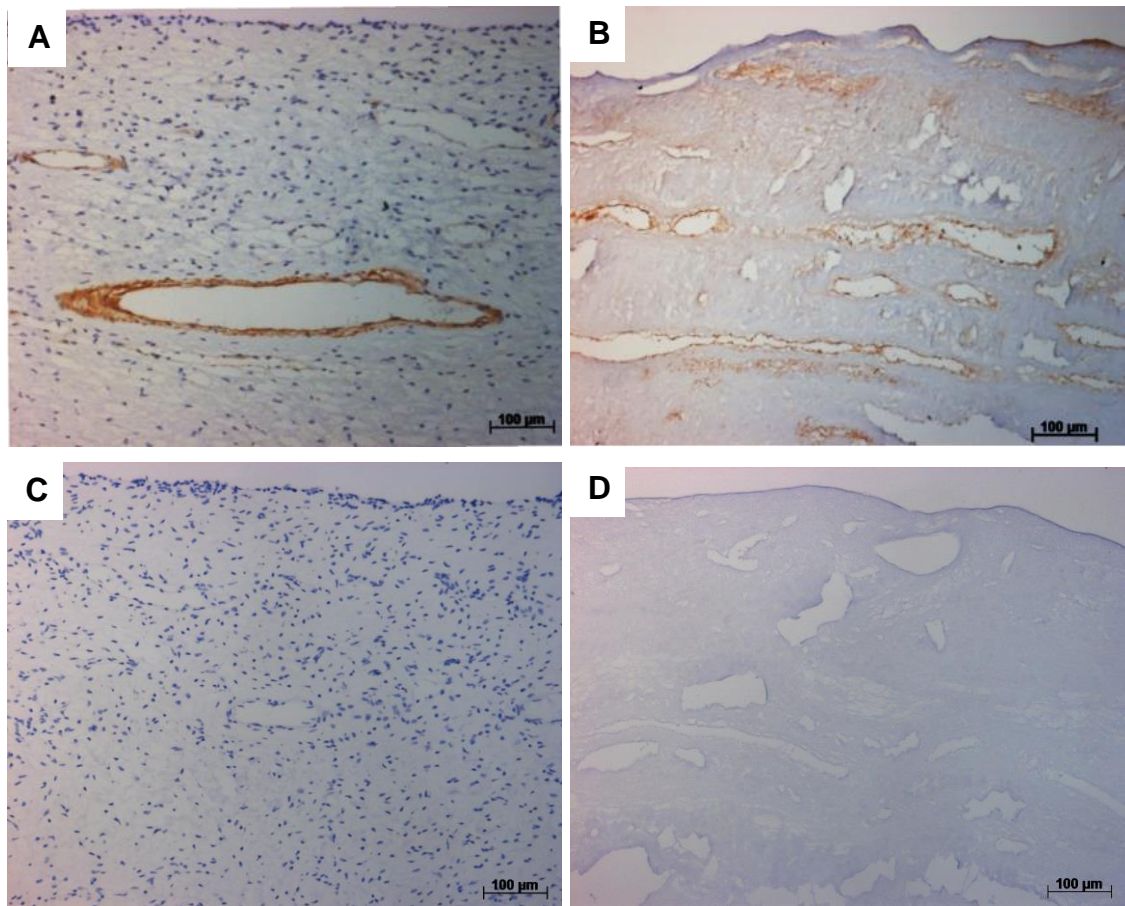


Figure 5-7: Bright-field microscopic images of native and decellularised bovine dental pulps labelled with an antibody against bovine VEGF-A and its corresponding control isotype. (A and B) Representative images of (A) native bovine dental pulp showing positive immunoreactivity to VEGF-A antigen around the vessels and (B) decellularised dental pulp scaffold showing weak positive immunoreactivity to VEGF-A antigen around the vascular channels. (C and D) Representative images of the negative control tissue sections of (C) native and (D) decellularised bovine dental pulps showing no visible brown staining. Areas of positive immunoreactivity to VEGF-A stained brown and cell nuclei stained blue.

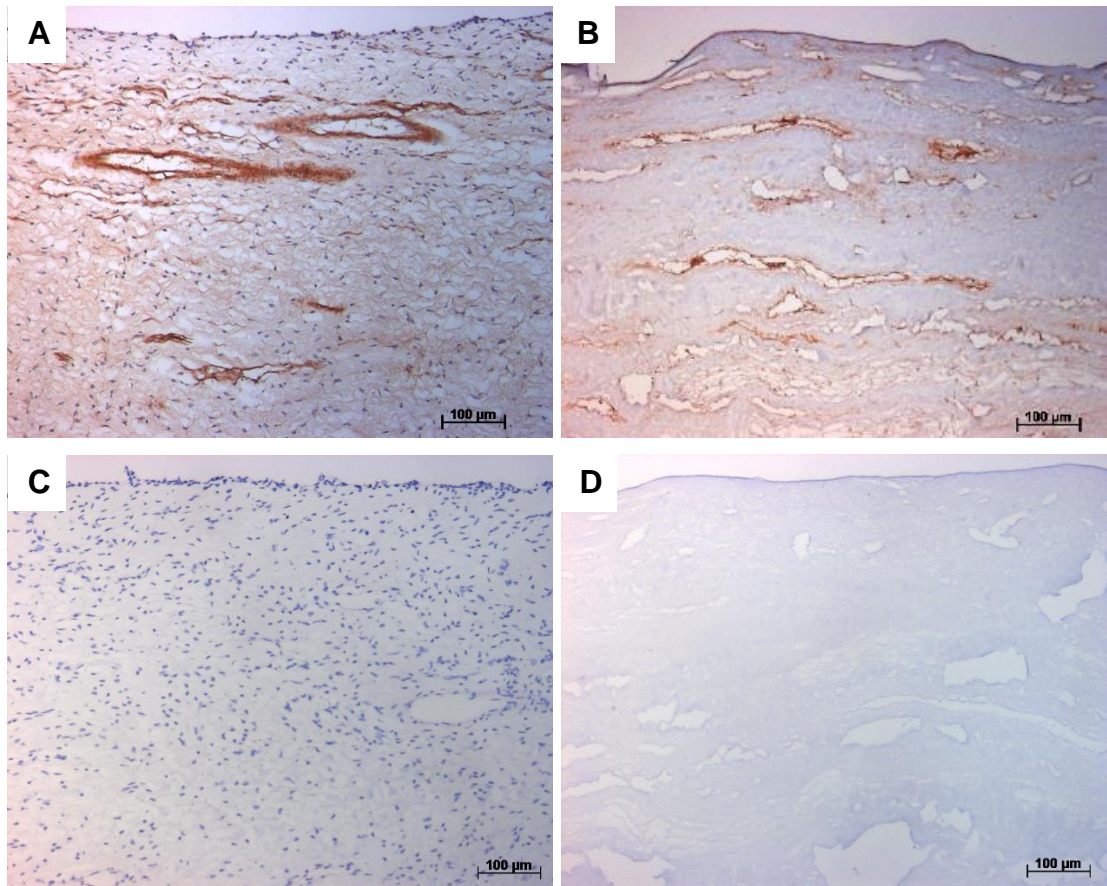


Figure 5-8: Bright-field microscopic images of native and decellularised bovine dental pulps labelled with an antibody against bovine FGF-2 and its corresponding control isotype. (A and B) Representative images of (A) native and (B) decellularised bovine dental pulps showing positive immunoreactivity to FGF-2 antigen. (C and D) Representative images of the negative control sections of (C) native and (D) decellularised bovine dental pulps showing no brown staining. Areas of positive immunoreactivity to FGF-2 antigen stained brown and the cell nuclei stained blue.

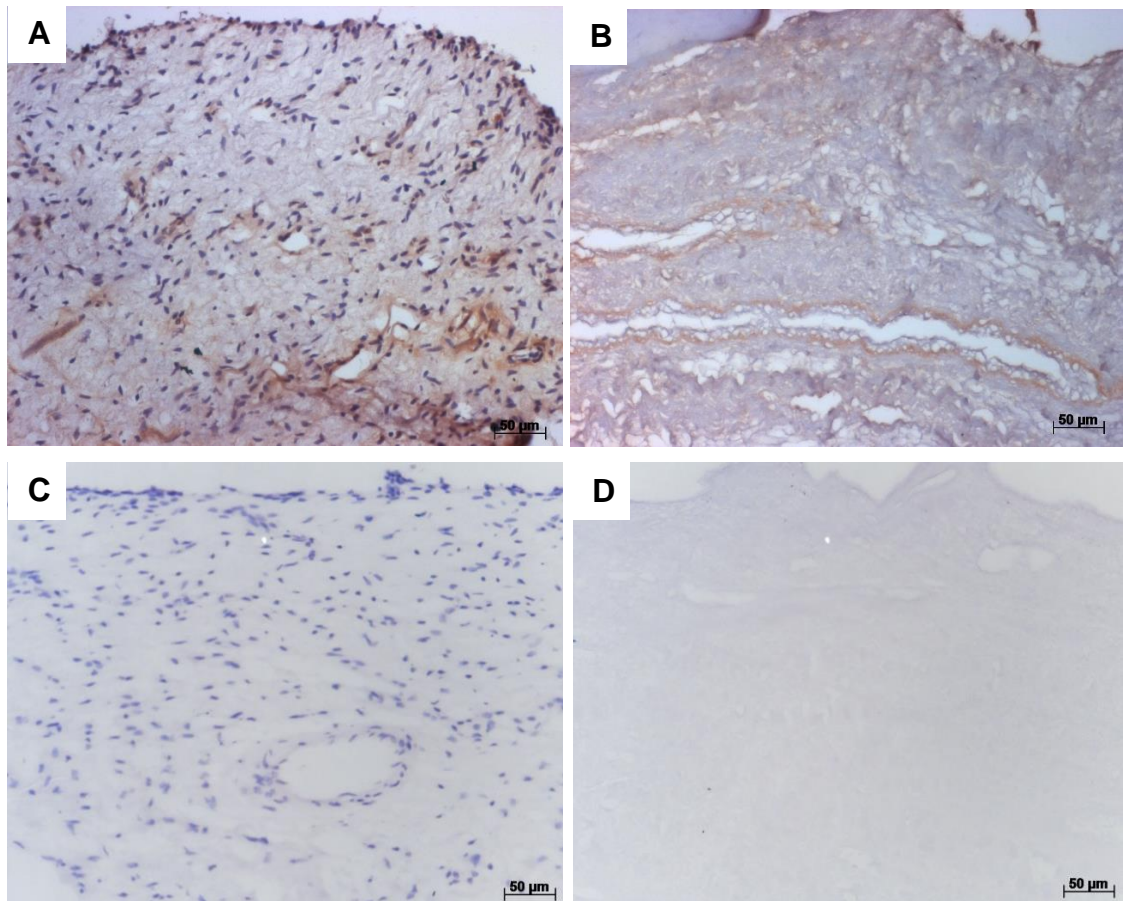


Figure 5-9: Bright-field microscopic images of native and decellularised bovine dental pulps labelled with an antibody against bovine TGF- β 1 and its corresponding isotype antibody. (A and B) Representative images of (A) native bovine dental pulp showing positive immunoreactivity to TGF- β 1 antigen and (B) decellularised bovine dental pulp scaffold showing weak positive immunoreactivity to TGF- β 1 antigen. (C and D) Representative images of the negative control tissue sections of (C) native and (D) decellularised bovine dental pulps demonstrating absence of brown staining. Areas with positive immunoreactivity to TGF- β 1 stained brown and cell nuclei stained blue.

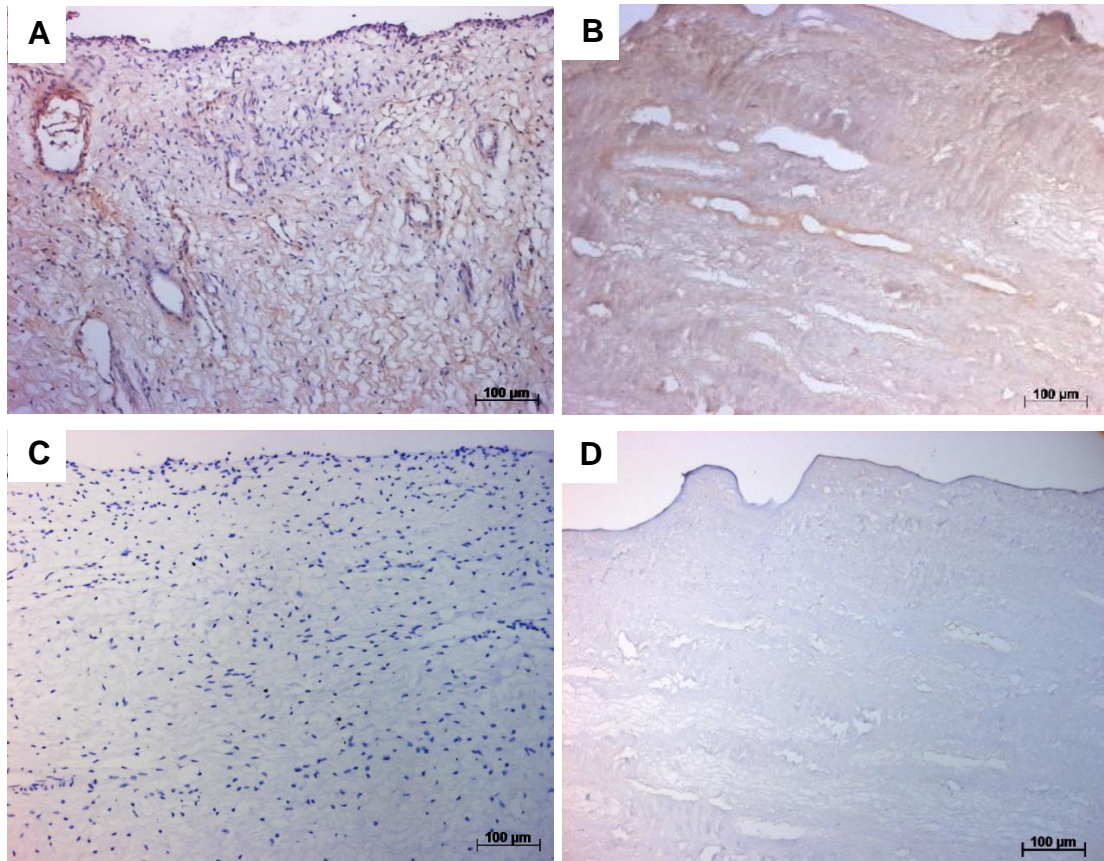


Figure 5-10: Bright-field microscopic images of native and decellularised bovine dental pulps labelled with an antibody against bovine BMP2 antigen and its corresponding control isotype. (A and B) Representative images of (A) native and (B) decellularised bovine dental pulps showing positive immunoreactivity to BMP-2 antigen. (C and D) Representative images of the negative control sections of (C) native and (D) decellularised bovine dental pulps demonstrating absence of brown staining. Areas of positive immunoreactivity to BMP-2 antigen stained brown and the cell nuclei stained blue.

Elimination of alpha-gal epitope from the developed decellularised dental pulps

Representative images of native and decellularised bovine dental pulps labelled with antibody against alpha-gal epitope are shown in Figure 5-11. Native dental pulp showed positive immunoreactivity to alpha-gal epitope throughout the matrix (Figure 5-11 A). On the contrary, no immunoreactivity to alpha-gal epitope was observed in the pulpal matrix following the decellularisation (Figure 5-11 B). No brown staining was detected in the negative control sections (Figure 5-11 C and D).

5.5.5 Surface topography of the developed decellularised dental pulps

Scanning electron microscope generated images of the native and decellularised bovine dental pulps are shown in Figure 5-12. The surface of the native dental pulp appeared as a meshwork of dense fibres covered with the other components of the dental pulp (Figure 5-12 A). Following decellularisation, the fibrous structure of the surface appeared loose and denuded of some components (most likely the cells and other non-fibrous components) (Figure 5-12 B). Despite this slight alteration of the surface, the retention of the entangled dense fibrous network was clearly visible after tissue decellularisation. This observation was consistently seen in all examined tissue sections of the decellularised dental pulps.

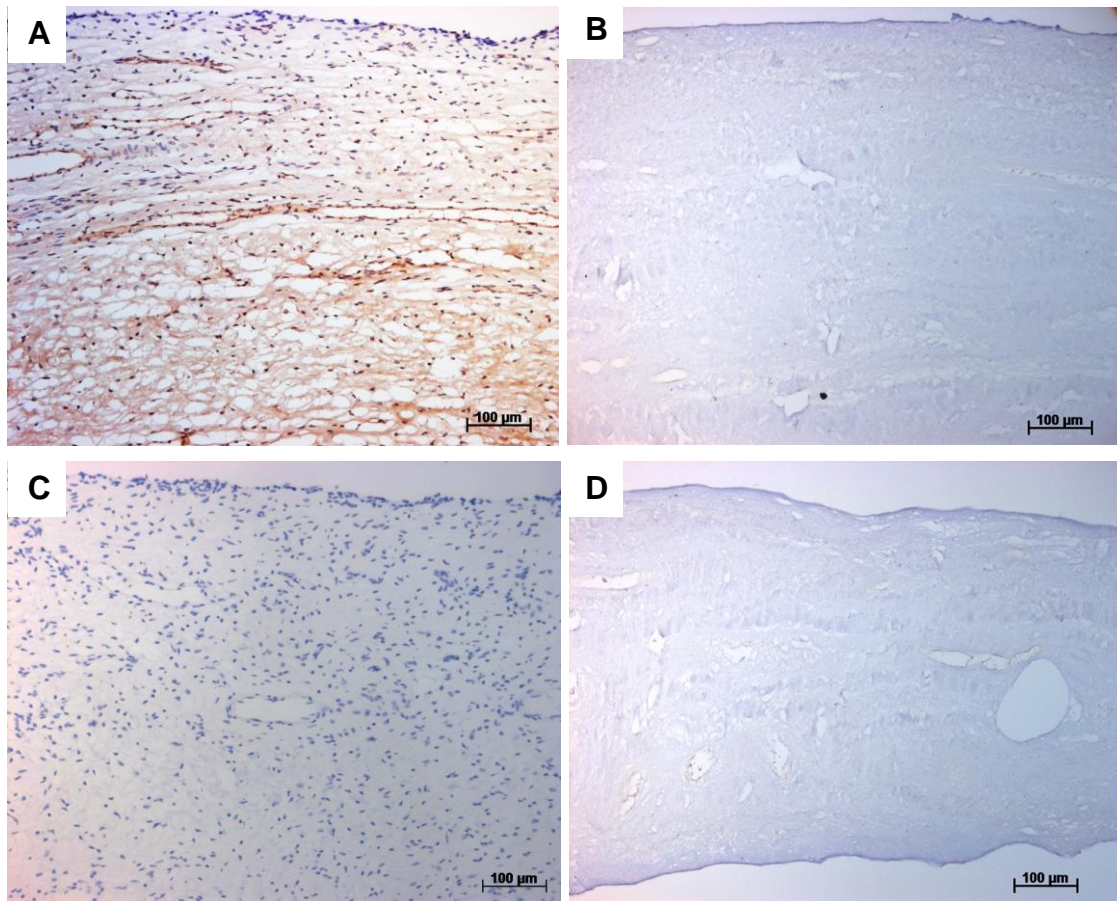


Figure 5-11: Bright-field microscopic images of native and decellularised bovine dental pulps labelled with antibody against bovine alpha-gal epitope and the corresponding isotype antibody. (A and B) Representative images of (A) native bovine dental pulp showing positive immunoreactivity to alpha-gal epitope compared to negative immunoreactivity in (B) decellularised dental pulp. (C and D) Representative images of negative control of (C) native and (D) decellularised bovine dental pulps showing no visible brown staining. Areas of positive immunoreactivity stained brown and the cell nuclei stained blue.

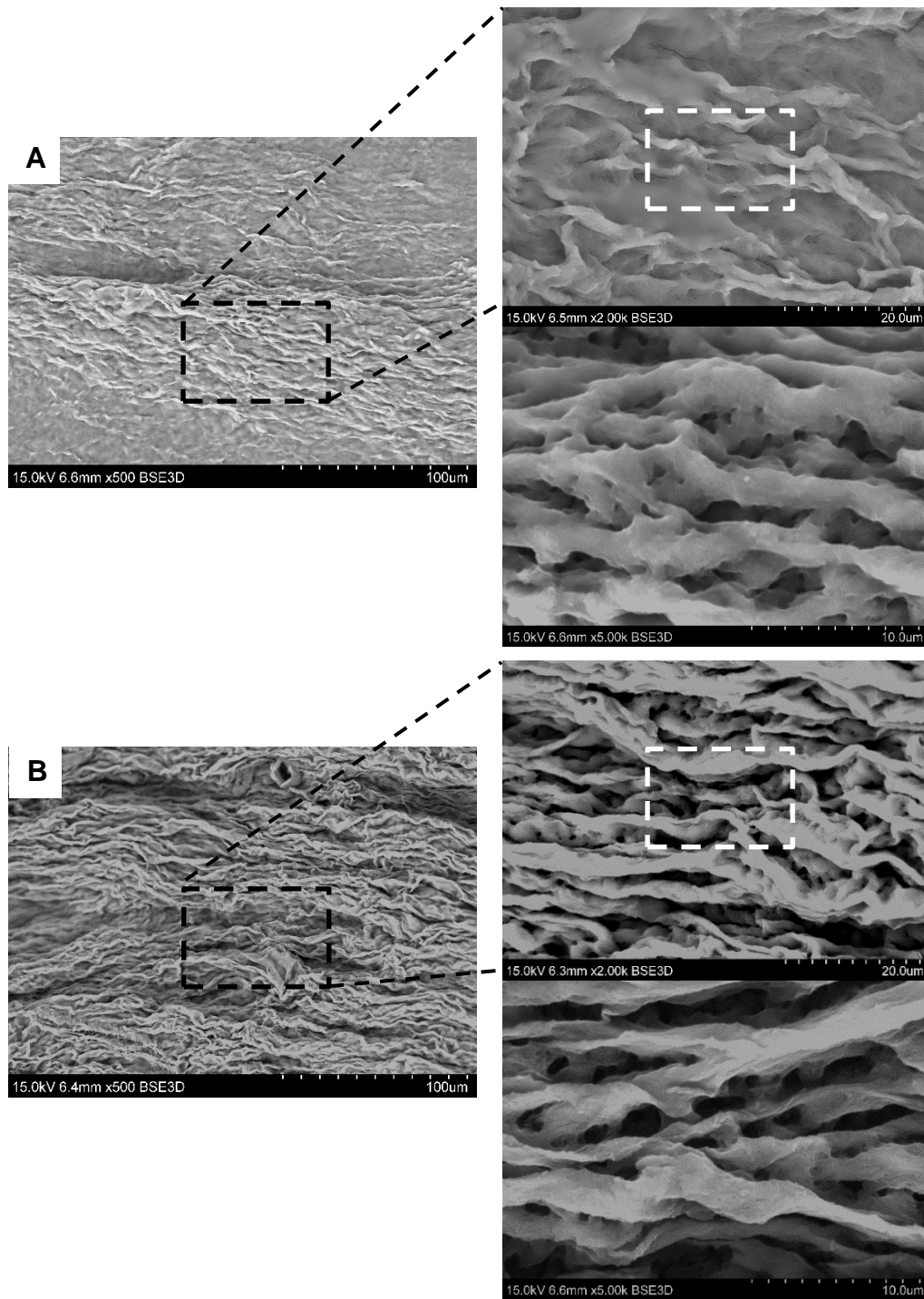


Figure 5-12: Scanning electron microscopic images of native and decellularised bovine dental pulps. (A and B) Representative images of (A) native bovine dental pulp showing the surface consisting of a network of dense fibres with the tissue components attached to the fibres and occupied the interfibrillar spaces compared to (B) decellularised bovine dental pulp scaffold showing retention of the porous fibrous network with removal of the other tissue components. Images on the right-hand side represent a magnification of the delineated areas in A and B.

5.6 Discussion

In the present research, the structural and compositional properties of the decellularised bovine dental pulp matrix, developed using the gentle protocol described in Chapter 4, Section 4.4.1.2, were characterised. Decellularised scaffolds are, by definition, composed of an extracellular matrix devoid of cells. The extracellular matrix represents a three-dimensional meshwork of fibrillar components embedded in a porous gel-like ground substance. These components provide structural support and attachment sites for the cells and act as reservoirs for signalling molecules that modulate different cellular activities in health and disease (Badylak, 2002). Retention of the extracellular matrix components and structure, following tissue decellularisation, could help in providing the cells with the biological cues necessary to promote their tissue-specific differentiation (Agmon and Christman, 2016, Robb *et al.*, 2017).

Collagen is the most prominent fibrillar protein in the extracellular matrix of the dental pulp (Lechner and Kalnitsky, 1981, Van Amerongen *et al.*, 1983). It provides structural support and adhesion motifs for the cells. Furthermore, collagen has (Gly-Pro-Hyp)₂-Gly-Phe-Hyp-Gly-Glu-Arg-(Gly-Pro-Hyp)₃ subunits, a peptide sequence, which upon interaction with specific cell surface receptors modulates several biological processes including cell adhesion, cell growth and cell differentiation (Emsley *et al.*, 2004). Collagen I and III are the most abundant types of collagen in the dental pulp matrix (Van Amerongen *et al.*, 1983). The former provides structural support for the resident cells, and the latter contributes to the elasticity of the pulpal matrix. Collagen, therefore, is an important constituent of the dental pulp extracellular matrix.

As detailed in section 5.5.1 of this chapter, initially collagen was detected in the decellularised dental pulps by means of histological staining using PicroSirius red, a specific staining method for collagen detection in tissue sections (Junqueira *et al.*, 1979). Further detection and localisation of collagen I and III fibres in the decellularised dental pulps was achieved using immunohistochemical staining. The findings agreed with the results reported by Matoug-Elwerfelli *et al.*, showing retention of collagen I and III following human dental pulp decellularisation using the same protocol employed in this research (Matoug-Elwerfelli *et al.*, 2018, 2020). In contrast, Chen *et al.* (2015) reported a significant reduction in collagen I and III contents following miniature swine dental pulp decellularisation. Since the decellularisation in their work was achieved through the use of dual detergents at an increased concentration (1% w/v SDS and 1% w/v Triton X100), this might be the reason behind their observation.

In addition to collagen, fibronectin and laminin are important adhesion glycoproteins of the dental pulp ECM (Yuasa *et al.*, 2004). Fibronectin is rich with the Arg-Gly-Asp (RGD) subunits, a tri-peptide that is critical for cell binding via $\alpha_5\beta_1$ integrin (Badylak, 2007), whereas Laminin represents an essential component of the basement membrane. The specific role of laminin in tissue regeneration, when a decellularised scaffold is used, is not clear. However, it has been suggested that this molecule might play a role in vascular structures' formation (Badylak, 2007). While fibronectin appeared to be highly retained in the decellularised dental pulps, the results revealed reduced staining intensity of laminin when compared to native bovine dental pulp. This finding is consistent with the results reported by several previous studies showing laminin reduction following tissue decellularisation using detergent-based protocols (Traphagen *et al.*, 2012, Chen *et al.*, 2015, Matoug-Elwerfelli *et al.*, 2018).

The ground substance of the dental pulp extracellular matrix has an abundance of glycosaminoglycans, including dermatan sulphate, heparin sulphate, chondroitin sulphate and hyaluronic acid (Linde, 1973b, 1970, 1972). These components give the matrix a gel-like property and play a role in water retention and growth factors in addition to cytokines binding (Linde, 1985). Since numerous cell surface receptors, growth factors and cytokines have heparin-binding characteristics, the retention of glycosaminoglycans, following bovine dental pulp decellularisation, was highly desirable. The findings were consistent with several previous studies showing marked retention of glycosaminoglycans following tissue decellularisation using a protocol involving a single cycle of either 0.1% (w/v) or 0.03% (w/v) SDS concentrations (Mirsadraee *et al.*, 2006, Wilshaw *et al.*, 2006, Wilshaw *et al.*, 2012, Matoug-Elwerfelli *et al.*, 2018). In contrast, studies that used more cycles of SDS at an increased concentration reported a significant reduction of glycosaminoglycans following decellularisation (Kheir *et al.*, 2011).

The presence of growth factors in their native three-dimensional ultrastructure is one of the advantages of the decellularised scaffolds (Badylak, 2007). Findings from the current research revealed detection of VEGF-A, FGF-2, TGF- β 1 and BMP-2 in the developed decellularised dental pulps. VEGF-A and FGF-2 are two powerful angiogenic growth factors known to be potent in promoting blood vessels formation. These growth factors are used frequently in tissue engineering to improve scaffold vascularisation by stimulating the angiogenic host tissue response at the implantation site (Kaigler *et al.*, 2006, Guan *et al.*, 2007, Zhao *et al.*, 2009, He *et al.*, 2011). VEGF, in particular, is known to play a role in inducing the angiogenic differentiation of dental pulp stem cells (Matsushita *et al.*, 2000), stimulating the proliferation of endothelial cells and promoting their adhesion, survival and migration (Byzova *et al.*, 2000). TGF- β 1 is known to be involved in

the regulation of a wide range of cellular activities, including cell migration, cell proliferation, cell differentiation and ECM synthesis (Kim *et al.*, 2012). This growth factor has a chemotactic effect on dental pulp stem cells (Howard *et al.*, 2010), and has been shown to promote their proliferation and odontoblastic differentiation *in vitro* (Melin *et al.*, 2000). BMP-2 has also been shown to induce mRNA expression of dentine sialophosphoprotein in dental pulp stem cells and stimulate their differentiation into odontoblast-like cells both *in vitro* and *in vivo* (Iohara *et al.*, 2004, Saito *et al.*, 2004). Observations from this present work are consistent with several previous studies, showing decellularised scaffolds of different tissues retaining various growth factors, including FGF-2, TGF- β 1 and VEGF (Voytik-Harbin *et al.*, 1997, Hodde *et al.*, 2001, McDevitt *et al.*, 2003, Hodde *et al.*, 2005).

The bovine dental pulp decellularisation carried out in this research resulted in high retention of the surface topography and the three-dimensional structure of the dental pulp extracellular matrix in the resultant scaffolds. This might have an impact on the cell response to the developed decellularised dental pulps. It has been suggested that preservation of the native surface topography and the three-dimensional structure may provide physical cues to guide stem cell differentiation into tissue-specific lineage (Agmon and Christman, 2016, Cramer and Badylak, 2019).

The porosity and pore interconnectivity directly impact scaffold's functionality in tissue engineering applications (Murphy *et al.*, 2010). The ultimate aim of tissue scaffolding strategies is to mimic the pore structure of the native extracellular matrix of the tissue to be regenerated (Causa *et al.*, 2007). Analysis of the developed decellularised dental pulp matrix using the scanning electron microscope showed retention of the porous entangled meshwork of the native

pulpal matrix. This could impact cellular response to the scaffold by facilitating nutrients and oxygen diffusion and wastes removal, enhancing angiogenesis and modulating cell-cell and cell-matrix interactions, which influence cell attachment, proliferation, migration, differentiation and new tissue formation (Loh and Choong, 2013, Prat-Vidal and Bayes-Genis, 2020).

One of the major barriers to using decellularised scaffolds of animal origin in humans is the presence of natural antibodies against alpha-gal epitope. Alpha-gal epitope ($\text{Gal}\alpha 1\text{-3Gal}\beta 1\text{-4GlcNAc-R}$), which is a cell surface antigen expressed on all mammals except humans and old world monkeys (Badylak, 2004). The interaction of human antibodies with this antigen could result in hyperacute or delayed rejection of the decellularised scaffolds (Galili, 2001). Therefore, elimination of alpha-gal epitope is a prerequisite for any xenogeneic decellularised scaffolds intended for human use. Incorporation of the alpha-galactosidase enzyme in the decellularisation protocol has been suggested for alpha-gal epitope elimination (Crapo *et al.*, 2011). However, in the present research work, the possibility of alpha-gal epitope elimination has been demonstrated through the use of a single detergent-based decellularisation protocol not involving the alpha-galactosidase enzyme.

Collectively, the research work presented in this chapter has demonstrated retention of several extracellular matrix components and growth factors in the developed decellularised dental pulp matrix. This is likely to be advantageous for the performance of the developed scaffolds with stem cells, since the extracellular matrix components are known to provide structural support, attachment sites and tissue-specific biological signalling. The performance of the developed decellularised dental pulp matrix with human dental pulp stem cells was investigated *in vitro* and is presented in the next chapter.

Chapter 6

***In vitro* performance of the developed decellularised dental pulp matrix**

6.1 Introduction

Selecting an appropriate scaffold is a critical step in dental pulp regeneration (Galler *et al.*, 2011a). Several aspects including cell-matrix interaction, biocompatibility, biodegradability, growth factors incorporation possibility, vascularisation enhancement, mineralisation induction and ease of modification have to be considered (Chan and Leong, 2008, Galler *et al.*, 2010, O'brien, 2011). The ideal scaffold should possess a structural framework and biological composition capable of supporting stem cell attachment, migration, proliferation and tissue-specific differentiation (Yang *et al.*, 2001). The scaffold should also be biocompatible to prevent adverse tissue reaction by the host, and biodegradable to facilitate cell infiltration, vascularisation and new tissue formation (Yuan *et al.*, 2011). From a clinical perspective, the scaffold should be sterilisable, easy to modify for application in the narrow root canal space, cost-effective and scalable for large batch production.

Several synthetic and natural scaffolds have been investigated for use in dental pulp regeneration with limited success (Dissanayaka and Zhang, 2020). A recent systematic review demonstrated lack of dental pulp-like tissue in the root canal of immature non-vital animal teeth, following regenerative endodontic therapy, using different scaffold types including blood clot, platelet rich plasma, collagen alone or in combination with blood clot, gelfoam in combination with blood clot and a hydrogel containing FGF-2 in combination with blood clot (Altai *et al.*,

2017). The poor resemblance to the complex nanostructure and composition of the dental pulp extracellular matrix, together with the poor control over newly formed tissue that resembles more of a periodontal-like tissue rather than a dental pulp-like tissue, were the main limitations of the currently available scaffold materials (Galler *et al.*, 2011a, Gathani and Raghavendra, 2016, Dissanayaka and Zhang, 2020).

As detailed in Chapter 4 and Chapter 5, a decellularised scaffold consisting of natural dental pulp extracellular matrix was developed and characterised in this present research. The developed decellularised dental pulp matrix may serve as a suitable scaffold for dental pulp regeneration due to two characteristics. First, the retained native histoarchitecture and composition might provide attachment sites for the cells and tissue-specific biological cues capable of promoting odontoblast-like cell differentiation. Second, the preservation of the vascular channels in the decellularised dental pulp matrix may facilitate vascularisation. It has been reported that among the many techniques used to achieve vascularisation of the engineered constructs, the most promising results have been obtained by seeding endothelial cells into decellularised scaffolds, thereby taking advantage of the retained native vasculature (Pellegata *et al.*, 2018). However, endothelial cells' use is highly limited due to several factors, including sensitive harvesting technique, impaired proliferative potential following expansion and functional modifications of the cells when kept in tissue culture (Novosel *et al.*, 2011).

Seeding mesenchymal stem cells, which have the potential to enhance angiogenesis, into decellularised scaffolds has been suggested as a promising strategy to address this problem (Zhao *et al.*, 2010, Liu *et al.*, 2011). Dental pulp stem cells (DPSCs) have been shown to differentiate into endothelial-like cells in

numerous studies (d'Aquino *et al.*, 2007, Marchionni *et al.*, 2009, Karbanová *et al.*, 2011, Aksel and Huang, 2017), suggesting the potential use of these cells in promoting vascularisation during the process of dental pulp regeneration. Therefore, it can be hypothesised that a combination of DPSCs and a decellularised dental pulp matrix might provide a suitable vascularisation promoting strategy for dental pulp regeneration.

In the research work presented in this chapter, the *in vitro* performance of the developed decellularised dental pulp matrix, including its potential to support the attachment and growth of DPSCs and its angiogenic and odontogenic potentials, when used in combination with DPSCs, were investigated.

6.2 Aim and objectives

Aim

The aim of the research work presented in this chapter was to investigate the *in vitro* performance of the developed decellularised dental pulp matrix when seeded with human dental pulp stem cells (hDPSCs).

Objectives

- To evaluate the cytocompatibility of the developed decellularised dental pulp matrix using *in vitro* cytotoxicity assays.
- To seed hDPSCs onto the surface of the decellularised dental pulp matrix using a dynamic cell seeding technique and to assess cell attachment, viability, proliferation and migration *in vitro*.
- To investigate the expression of the markers involved in angiogenesis and odontogenesis in hDPSCs colonising the decellularised dental pulp matrix *in vitro*.

6.3 Experimental approach

The cytocompatibility of the developed decellularised dental pulps was evaluated *in vitro* using contact and extract cytotoxicity assays and murine L929 fibroblast cell line according to the international standards for the biological evaluation of medical devices (BS EN ISO 10993-5, 2009). Following cytocompatibility confirmation, the decellularised dental pulps were seeded with hDPSCs using a dynamic cell seeding technique. Cell attachment, cell morphology, cell viability, cell proliferation and cell migration were then assessed using scanning electron microscopy, fluorescent staining, Live/Dead[®] cell viability assay, dsDNA quantification via a fluorescence-based dye tagging assay, and histological analysis, respectively. Subsequently, the decellularised dental pulps' effects on the gene expression of markers involved in angiogenesis and odontogenesis in hDPSCs were evaluated using RT-qPCR. Moreover, the expressions of CD31 (angiogenic marker) and DSPP (odontogenic marker) were assessed in hDPSCs-seeded decellularised dental pulps at protein level using immunohistochemical staining.

6.4 Methods

Bovine dental pulps were harvested and decellularised as described in Chapter 4, Section 4.4.1.2. The effectiveness of tissue decellularisation was then verified histologically by staining two randomly selected samples with H&E and DAPI as described in Chapter 3, Sections 3.2.3.1 and 3.2.3.2. The generated decellularised dental pulps were stored in PBS at 4°C until used in the experiments described below.

6.4.1 Cytocompatibility evaluation

The cytocompatibility assessment was carried out under aseptic condition in Class II laminar flow hood. Cell culture procedures including cell resurrection, passage and counting were performed as described in Chapter 3, Section 3.2.8.

6.4.1.1 Contact cytotoxicity assay

Contact cytotoxicity assay was carried out using Murine L929 fibroblast cell line. The cells were cultured in direct contact with the decellularised dental pulp scaffolds and the relevant controls. Controls include cyanoacrylate contact adhesive as a positive control and Steri-Strip™ reinforced adhesive as a negative control.

Decellularised dental pulps (n = 6 samples; one sample per well) were initially attached to the centre of an appropriate wells of 6 well plate using Steri-Strip™ reinforced adhesive. Similarly, the positive control (n = 6 drops; one drop per well) and the negative control (n = 6 pieces; one piece per well) were added to another 6 well plates. All well plates were then washed with three changes of sterile PBS. Murine L929 fibroblast cell line at cell density of 2×10^5 cells.cm² were seeded into the test and control wells and maintained under basal culture conditions using DMEM supplemented with 10% (v/v) FBS, 1% (v/v) 200 mM L-Glutamine, 100 U.mL⁻¹ Penicillin and 100 µg.mL⁻¹ Streptomycin for 48 hours at 37°C in a humidified atmosphere incubator containing 5% (v/v) CO₂ and with 95% relative humidity.

After two days of *in vitro* culture, the cell culture media were carefully aspirated from well plates. The cells were then washed once with PBS and fixed with 10% (v/v) NBF for 10 minutes. Following this, the cells were stained using 5% Giemsa solution (2 mL per well) for 5 minutes followed by gentle washing in distilled water

until running clear. Well plates were then left to dry overnight, then examined using an inverted bright-field microscope with normal Köhler illumination to assess changes in cell growth and morphology. Digital images were acquired using an AxioCam camera and AxioVision Rel.4.7 software.

6.4.1.2 Extract cytotoxicity assay

Extract cytotoxicity assay was carried out using Murine L929 fibroblast cell line. The cells were cultured in a medium containing an extract of the decellularised dental pulps or the relevant controls. Controls include 40% (v/v) DMSO in DMEM as a positive control and serum-free DMEM as a negative control.

To prepare the extract, decellularised dental pulps were finely macerated using a sterile blade and weighed aseptically. The macerated samples were then incubated in a serum-free DMEM (100 mg of the macerated samples per 1 mL of DMEM) at 37°C with gentle agitation. After 72 hours, the medium was subjected to centrifugation at 500 g for 15 minutes and the supernatant (extract) was then aseptically collected. The sterility of the extract was then checked by streaking into a fresh blood agar followed by incubation for 48 hours at 37°C to confirm the absence of microbial contamination. The extract was stored at - 20°C until used.

Murine fibroblast L929 cell line were seeded into appropriate wells of clear flat-bottom 96 well plates at a density of 1×10^4 cells per well and cultured under basal culture conditions using DMEM supplemented with 10% (v/v) FBS, 1% (v/v) 200 mM L-Glutamine, 100 U.mL⁻¹ Penicillin and 100 µg.mL⁻¹ Streptomycin at 37°C in a humidified atmosphere chamber containing 5% (v/v) CO₂ with 98% relative humidity. After 24 hours, the cell culture media were aspirated and replaced with 100 µL of double strength cell culture medium (DMEM supplemented with 20% (v/v) FBS, 2% (v/v) 2 mM L-glutamine, 200 U.mL⁻¹

penicillin and 200 µg.mL⁻¹ streptomycin). Subsequently, 100 µL of the extract and the controls were added to the appropriate wells in triplicates and incubated for 24 hours at 37°C and 98% relative humidity in an incubator containing 5% (v/v) CO₂.

Cell viability was then determined by measuring the relative content of Adenosine Triphosphate (ATP) in the cells using a luminescence-based ATP detection assay (ATPLite-M assay) as described in Chapter 3, Section 3.2.11.1. The relative ATP content of the study group, positive and negative controls were plotted as the mean ± standard deviation. Data analysis was performed using one-way ANOVA with Bonferroni correction ($P < 0.05$).

6.4.2 Characterisation of hDPSCs prior to seeding onto the surface of decellularised dental pulps

hDPSCs were harvested from the dental pulps of extracted healthy human teeth (n = 3 teeth from different donors) using an enzymatic digestion method, then expanded for experimentation at passage number 4 (Chapter 3, Section 3.2.8.1). Details of the teeth donors are described in Table 6-1. All cell culture procedures were performed as described in Chapter 3, Section 3.2.8. hDPSCs were characterised before use as described below.

Table 6-1: Details of the donors of human dental pulp stem cells.

Donor	Age	Gender	Tooth condition and type
1	14	Female	Healthy lower second premolar
2	19	Female	Healthy upper first premolar
3	15	Female	Healthy upper first premolar

6.4.2.1 Cell adherence to the surface of the culture flasks

hDPSCs from the three different donors were seeded at a density of 1×10^4 cell.cm² in tissue culture flasks (T175) containing 20 mL of alpha MEM supplemented with 10% (v/v) FBS, 1% (v/v) 2 mM L-Glutamine, 100 U.mL⁻¹ Penicillin and 100 µg.mL⁻¹ Streptomycin and incubate at 37°C in 5% (v/v) CO₂ and 95% relative humidity. Cell adherence to the surface of the culture flasks was monitored using an inverted phase-contrast microscope and images were captured digitally after 24 hours of culture.

6.4.2.2 Evaluation of mesenchymal stem cell surface markers expression in the harvested cell populations

hDPSCs from the three different donors were tested for the positive expression of mesenchymal stem cell surface markers (CD105; endoglin; cell adhesion molecule, CD90; Thy-1; cell adhesion molecule, CD146; melanoma cell adhesion molecule) and the negative expression of leukocyte marker (CD45; haematopoietic stem cell marker, leucocyte common antigen) at protein level by the means of flowcytometry as described in Chapter 3, Section 3.2.9.1.

6.4.2.3 Evaluation of multilineage differentiation potential of the harvested cell populations

hDPSCs from the three different donors were assessed for the multilineage differentiation potential as described in Chapter 3, Section 3.2.9.2. The osteogenic, adipogenic and chondrogenic cell differentiation potential were evaluated using Alizarin Red staining, Oil Red O staining and Alcian Blue staining, respectively, following 21 days of *in vitro* culture under basal, osteogenic, adipogenic and chondrogenic conditions. Stained cultures were

visualised using an inverted bright-field microscope and the images were captured digitally.

6.4.3 Seeding of hDPSCs onto the surface of the decellularised dental pulps using a dynamic cell seeding technique

Characterised populations of hDPSCs were dynamically seeded onto the surface of the decellularised dental pulps at a density of 1×10^5 cells per scaffold using in-house built rotary dynamic seeding apparatus (Chapter 3, Section 3.2.10) and incubated for 24 hours at 37°C in 5% (v/v) CO₂ and 95% relative humidity. Prior to cell seeding, the scaffolds were made at a consistent length of approximately 1 cm. The cell seeding density was determined based on the results of a preliminary experiment described below. Following 24 hours of cell seeding, recellularised scaffolds were transferred individually into 12 well-plates containing 2 mL of cell culture medium per well and maintained in culture for the required time points of the subsequent experiments.

Cell seeding density determination

A preliminary experiment was carried out to determine the most suitable density of hDPSCs for seeding onto the surface of the decellularised dental pulps. In brief, decellularised dental pulps of consistent length (approximately 1 cm in length) were dynamically seeded with hDPSCs (Chapter 3, Section 3.2.10) at a density of 1×10^4 cells per sample ($n = 2$ scaffolds) and 1×10^5 cells per sample ($n = 2$ scaffolds) and maintained in culture for 7 days. Recellularised scaffolds were then stained using Live/Dead[®] cells assay as described in Chapter 3, Section 3.2.11.2 and analysed using a confocal scanning laser microscope. The generated images are shown in Figure 6-1. Limited cells were visible in the scaffolds at the seeding density of 1×10^4 cells per scaffold. On the contrary, a

reasonable cell repopulation was observed in the scaffolds at the seeding density of 1×10^5 cells per sample. Based on these observations, the seeding density of 1×10^5 cells per sample was selected for use in decellularised dental pulps recellularisation.

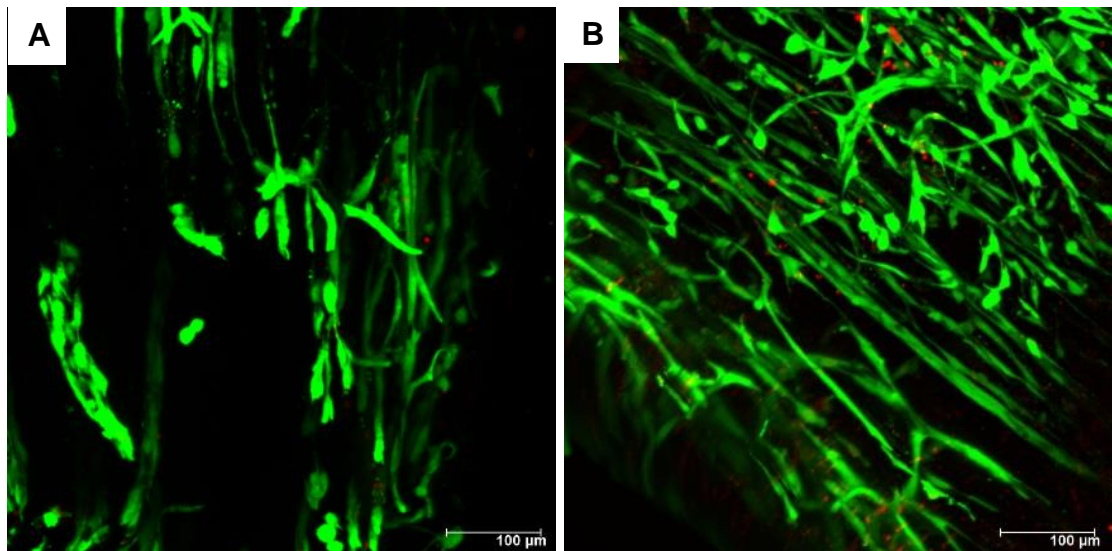


Figure 6-1: Cell seeding density determination. Representative images of hDPSCs seeded on the surface of decellularised dental pulps at a density of (A) 1×10^4 cells per sample and (B) 1×10^5 cells per sample and analysed using Live/Dead[®] cells assay and a confocal scanning laser microscope. The images show more cells repopulating the scaffolds at a cell seeding density of 1×10^5 cells per sample as compared to 1×10^4 cells per sample.

6.4.4 Scanning electron microscopy

Cell attachment of hDPSCs to the surface of the decellularised dental pulps was evaluated using scanning electron microscopy following three days of scaffolds recellularisation and *in vitro* culture under basal conditions. Samples of decellularised and recellularised scaffolds ($n = 3$ per group) were prepared as described in Chapter 3, Section 3.2.5 and visualised using a conventional high vacuum scanning electron microscope with back scattered electron mode and

beam energy equal to 15 keV. The aperture was set at 600 μm , the emission current was set at 70 μA and the condenser lens were set between 0.18 - 0.22 mA. Images were captured digitally using a slow speed scanning mode.

6.4.5 Fluorescent staining and confocal scanning laser microscopy

Cell morphology and three-dimensional organisation of hDPSCs following seeding onto the surface of decellularised dental pulps were evaluated using Alexa-Fluor[®] 488 Phalloidin and DAPI and a confocal scanning laser microscope. Samples of recellularised scaffolds following 7 days of *in vitro* culture under the basal conditions (n = 5) were fixed in 10% (v/v) NBF for 20 minutes at room temperature. Samples were then washed thrice in PBS for one minute each and permeabilised with 0.1% (v/v) Triton-X 100 in PBS for 15 minutes at room temperature before washing in PBS. Samples were subsequently incubated in Alexa-Fluor[®] 488 Phalloidin (1:20 in PBS; Thermo Fisher Scientific) for 2 hours at room temperature in the dark, then washed and incubated in DAPI (VectorLabs) for 15 minutes at room temperature in the dark. After a final wash in PBS, samples were washed and examined under confocal scanning laser microscope (Leica TCS SP8) with the following specifications: Alexa-Fluor[®] 488 Phalloidin (Excitation/Emission: 488/519 nm) and DAPI (Excitation/Emission: 358/461 nm). Images were acquired digitally using Leica LAS X software and are representing a composite of merged Z-series images.

6.4.6 Cell viability analysis

Cell viability of hDPSCs seeded onto the decellularised dental pulps was evaluated using Live/Dead[®] cells assay, as described in Chapter 3, Section 3.2.11.2, after 7 and 14 days (n = 3 samples per time point) of *in vitro* culture under basal conditions. The samples were visualised using a confocal scanning

laser microscope (Leica TCS SP8) with the following specifications: Calcein AM (Excitation/Emission = 494/517 nm) and Ethidium homodimer III (Excitation/Emission = 530/620 nm). Composite of merged Z-series images were captured digitally using Leica LAS X software.

6.4.7 Cell proliferation analysis

Cell proliferation of hDPSCs following seeding onto the surface of the decellularised dental pulps at a density of 1×10^5 cells per scaffold, as described previously in section 6.4.3, was evaluated using Quant-iT™ PicoGreen® dsDNA assay as described in Chapter 3, Section 3.2.7.2. In brief, recellularised scaffolds were subjected to DNA extraction following 1, 3, 5, 7 and 14 days of *in vitro* culture (n = 5 samples per time point) under basal conditions using DNeasy Blood and Tissue kit as described in Chapter 3, Section 3.2.6. DNA standards of known concentrations were made up at 0.2, 2.5, 10 and 100 ng.mL⁻¹ of Lambda DNA (2 µg.mL⁻¹) via dilution in an appropriate volume of 1X TE buffer. Subsequently, aliquots of 100 µL of the test samples (30 µL of DNA extracted from the recellularised scaffolds in 70 µL 1X TE buffer), standards and blank (1X TE buffer) were then added to 100 µL of PicoGreen® working solution in triplicates in 96 well plate. The fluorescence of the samples was then measured using a TopCount™ plate reader (Excitation/Emission = 480/520 nm). The fluorescence value of the blank was then subtracted from all samples and the standard curve was generated as shown in Figure 6-2.

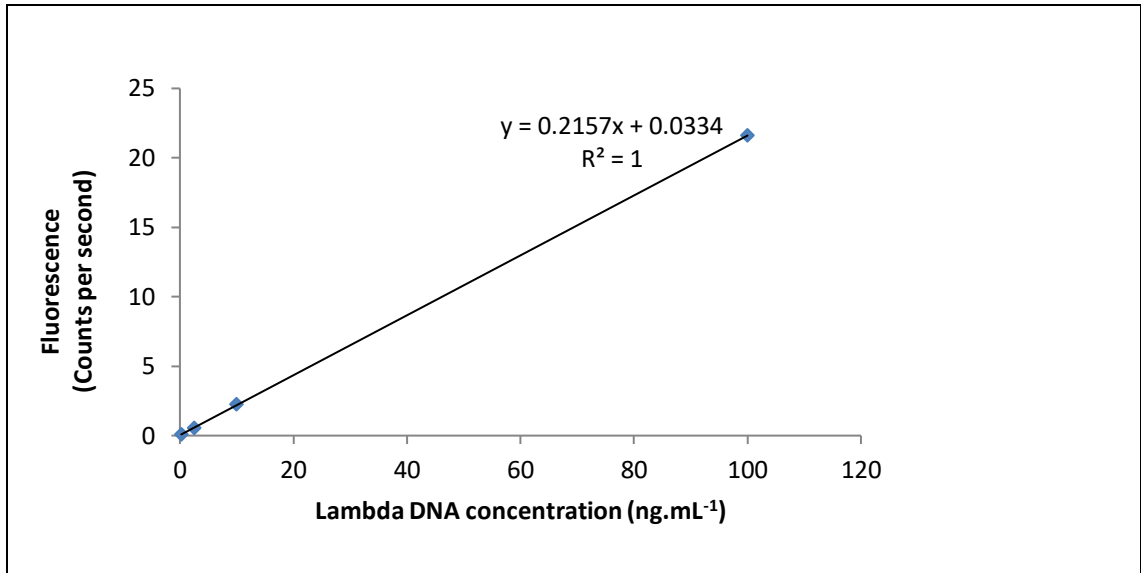


Figure 6-2: A curve of Lambda DNA standards. A representative standard curve showing the fluorescence values of Lambda DNA standards made up at different concentrations.

Calculation of the dsDNA content per sample dry weight

The fluorescence values of the test samples were used to determine the dsDNA concentrations in the samples using the standard curve (Figure 6-2) as following:

$$dsDNA \text{ concentration (ng/mL)} = \frac{\text{Fluorescence value} - 0.0334}{0.2157}$$

The dsDNA content per sample dry weight (ng.mg⁻¹) was then determined by normalising for the total volume of the sample's eluted DNA (100 µL) and the sample's dry weight as following:

dsDNA content per sample dry weight

$$= \frac{dsDNA \text{ concentration} \times \text{total volume of the DNA extracted from the sample}}{\text{Sample's dry weight}}$$

The dsDNA contents of the test samples at each time point were then plotted as the mean ± standard deviation. Data analysis was performed using one-way ANOVA with Bonferroni correction ($P < 0.05$).

6.4.8 Histological analysis

Cell migration and spreading of hDPSCs on the decellularised dental pulps was assessed following 7, 14 and 21 days of *in vitro* culture under basal conditions using H&E staining. Recellularised scaffolds (n = 3 samples per time point) were initially fixed in 10% NBF, then placed carefully in silicon moulds and embedded in 2% (w/v) agar (dissolved in PBS) and left to set for 30 minutes at 4°C. This step was performed to protect the samples from potential damage due to frequent handling. Agar embedded samples were then processed, embedded in paraffin wax and serial sectioned at 5 µm as described in Chapter 3, Section 3.2.2. Tissue sections were then stained using H&E (Chapter 3, Section 3.2.3.1) and visualised using a bright-field microscope with normal Köhler illumination. All images were captured digitally.

6.4.9 Gene expression analysis using RT-qPCR

hDPSCs from three different donors were dynamically seeded onto the surface of the decellularised dental pulps and control BioGide® collagen scaffolds (Geistlich, Manchester, UK) of consistent length (approximately 1 cm in length) at a density of 1×10^5 cells per sample, and also statically seeded in 24 well-plates (control monolayer culture) (n = 9 samples in all groups). Dynamically seeded samples were transferred into 24 well-plates after 24 hours. All samples were then cultured under the basal condition, and the culture media were changed twice a week.

Following 7, 14 and 21 days of culture, mRNA was extracted from the samples (n = 3 samples per group at each time point) using RNeasy® Fibrous Tissue kit (Qiagen) and quantified using the NanoDrop™ spectrophotometer at 260/280 nm, as described in Chapter 3, Section 03.2.12. Reverse transcription was then

performed using a high-capacity RNA-to-cDNA™ kit (Chapter 3, Section 03.2.120). Samples were then used as templates for the polymerase chain reaction using TaqMan® fast advanced master mix and TaqMan® gene expression assays including: glyceraldehyde-3-phosphate dehydrogenase (GAPDH: house-keeping gene), kinase insert domain receptor (KDR: angiogenesis marker), platelet and endothelial cell adhesion molecule-1 (PECAM-1: angiogenesis marker), dentine sialophosphoprotein (DSPP: odontogenesis marker), dentine matrix protein-1 (DMP-1: odontogenesis marker) and matrix extracellular phosphoglycoprotein (MEPE: odontogenesis marker), as described in Chapter 3, Section 03.2.12. The amplification process was carried out using Roche LC480 light cycler. The change in gene expression in the cells grown in the decellularised dental pulps as compared to the cells grown in two-dimensional (monolayers) and three-dimensional (BioGide® collagen scaffolds) models was calculated using the comparative delta-delta cycle threshold method (Chapter 3, Section 03.2.123.2.12.1).

Validation of GAPDH for use as a house keeping gene

The expression of GAPDH was assessed in hDPSCs seeded on monolayers, decellularised dental pulps and BioGide® collagen scaffolds and cultured *in vitro* under basal conditions for 7, 14 and 21 days. Threshold cycle (Ct) values of GAPDH expression were determined in all samples at each time point by the light cycler (Roche LC480). Data were then analysed using two-way ANOVA with Bonferroni correction ($P < 0.05$) and presented as the mean Ct value \pm standard deviation (Figure 6-3). Statistical analysis revealed no significant differences ($P > 0.05$) between the mean Ct values of GAPDH expression in all samples across the examined time points. This indicates that GAPDH was consistently expressed in all experimental samples regardless of the changes in the culture conditions

and duration. Based on these results, GAPDH was deemed suitable for use as a house-keeping gene in RT-qPCR experiment.

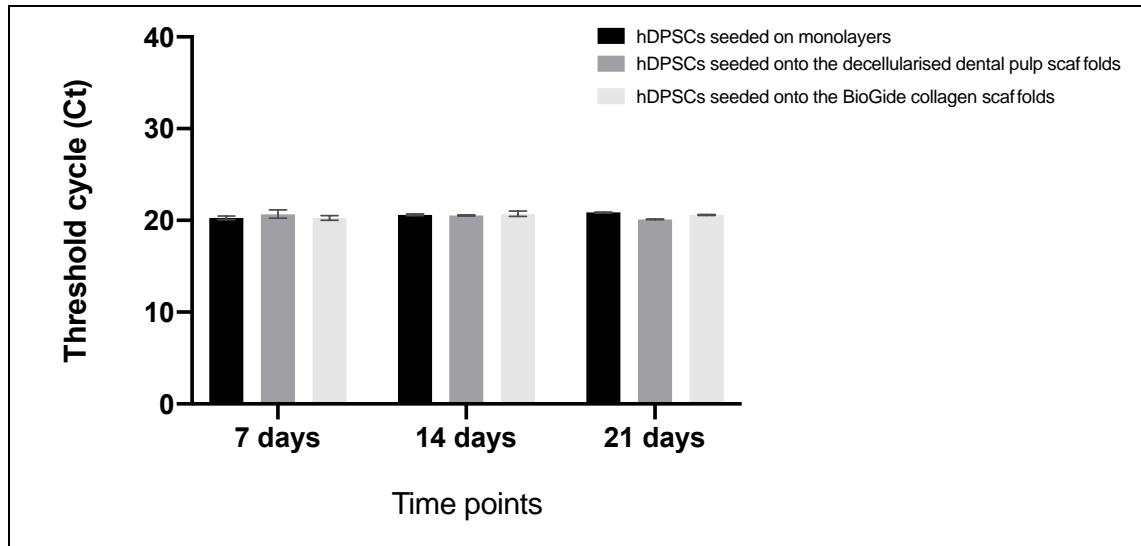


Figure 6-3: Validation of GAPDH as a house keeping gene. Bar graph demonstrates the Ct values of GAPDH expression in hDPSCs seeded on monolayers, decellularised dental pulps and BioGide® collagen scaffolds and cultured *in vitro* under basal conditions for a range of time points. Data represent the mean Ct value ($n = 3$ samples) \pm standard deviation. Data analysis revealed no significant difference between the mean Ct value of GAPDH expression in all samples across the examined time points.

6.4.10 Immunohistochemical staining

Tissue sections from recellularised scaffolds following 7, 14 and 21 days of seeding with hDPSCs and *in vitro* culture under basal conditions and from decellularised dental pulps were subjected to immunohistochemical staining as described in Chapter 3, Section 3.2.4. The used primary antibodies include a monoclonal antibody against human dentine sialophosphoprotein (DSPP) and a polyclonal antibody against human CD31. Isotype control antibodies corresponding to anti-DSPP and anti-CD31 were used as negative controls at the

same concentrations and under the same conditions but with omission of the primary antibodies. Stained sections were viewed under a bright-field microscope with normal Köhler illumination and Images were captured digitally.

6.5 Results

6.5.1 Cytocompatibility evaluation using contact cytotoxicity assay

Representative images of Giemsa stained L929 cell line cultured *in vitro* for 48 hours on monolayers alone or in direct contact with the decellularised dental pulps, the negative control (Steri-Strip reinforced adhesive) and the positive control (Cyanoacrylate contact adhesive) are shown in Figure 6-4. L929 cell line showed a confluent growth pattern and exhibited a fibroblastic spindle-shape morphology when cultured alone in a monolayer under the basal condition for 48 hours (Figure 6-4 A). The culture of L929 cell line in direct contact with the decellularised dental pulps showed the cells grew up to and in contact with the scaffolds and maintained the normal fibroblastic morphology (Figure 6-4 B). Similar results were observed following the culture of the L929 cell line in direct contact with the negative control (Figure 6-4 C). On the contrary, the culture of L929 cell line in direct contact with the cytotoxic positive control resulted in cell lysis and death as evidenced by the disappearance of almost all the cells from the well with a few only remained exhibiting round morphology (Figure 6-4 D). Overall, the results of the contact cytotoxicity assay indicated no apparent cytotoxicity of the developed decellularised dental pulps.

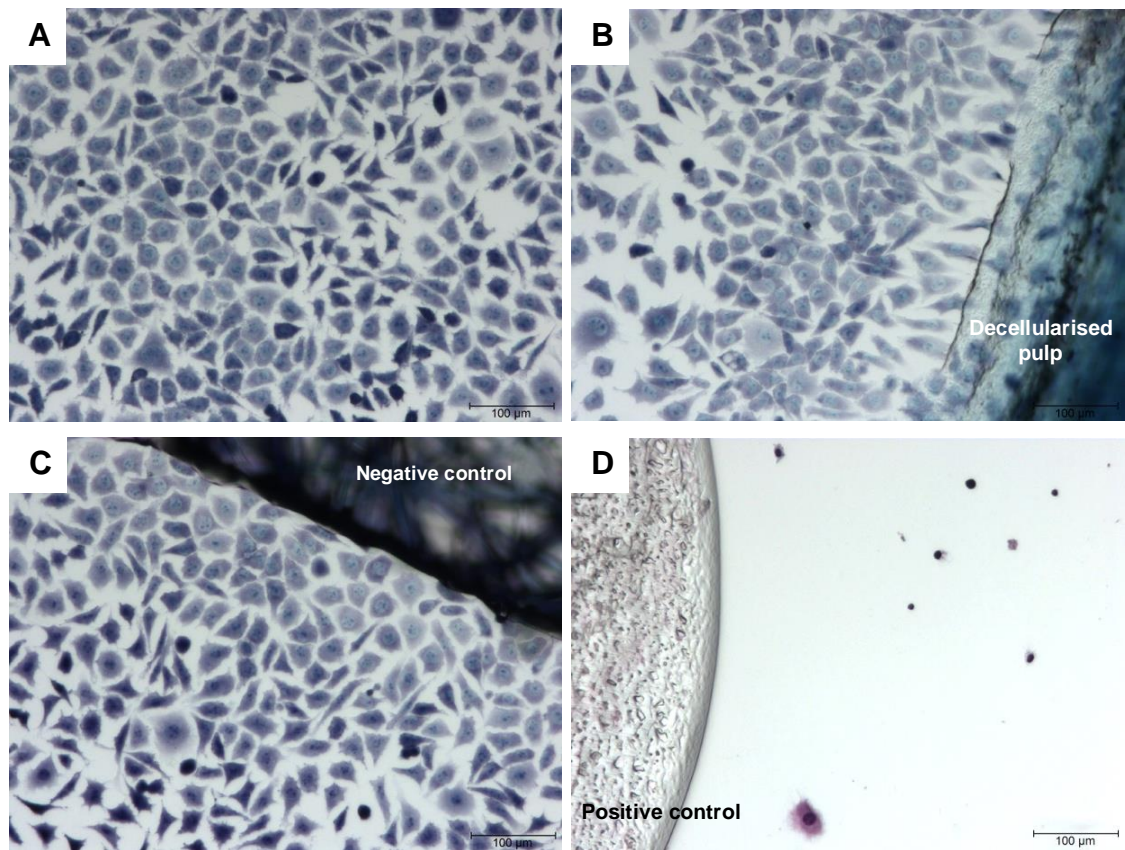


Figure 6-4: Contact cytotoxicity assay. Representative bright-field microscopic images of Giemsa stained L929 cell line cultured on monolayers (A) alone or in direct contact with (B) decellularised dental pulps, (C) Steri-Strip reinforced adhesive (negative control, NC) and (D) cyanoacrylate contact adhesive (positive control, PC) for 48 hours. The images indicates no apparent cytotoxicity of the decellularised dental pulp on the cultured cells as compared to the negative and positive controls.

6.5.2 Cytocompatibility evaluation using extract cytotoxicity assay

The viability of L929 cell line, as determined through measuring the relative ATP content using ATPlite™ assay, when culture in a medium containing an extract of the decellularised dental pulps, plain DMEM (negative control) or 40% (v/v) DMSO (positive control) is demonstrated in Figure 6-5. No significant difference was detected between the mean relative ATP content of the cells exposed to an extract of the decellularised dental pulps as compared to the cells exposed to the

negative control ($P = 0.39$). In contrast, cell exposure to the cytotoxic positive control resulted in a significant decrease in the relative ATP content of the cells as compared with the cells exposed to an extract of the decellularised dental pulps or to the negative control ($P < 0.0001$). Collectively, the findings of the extract cytotoxicity assay indicated lack of cytotoxic components in the developed decellularised dental pulps.

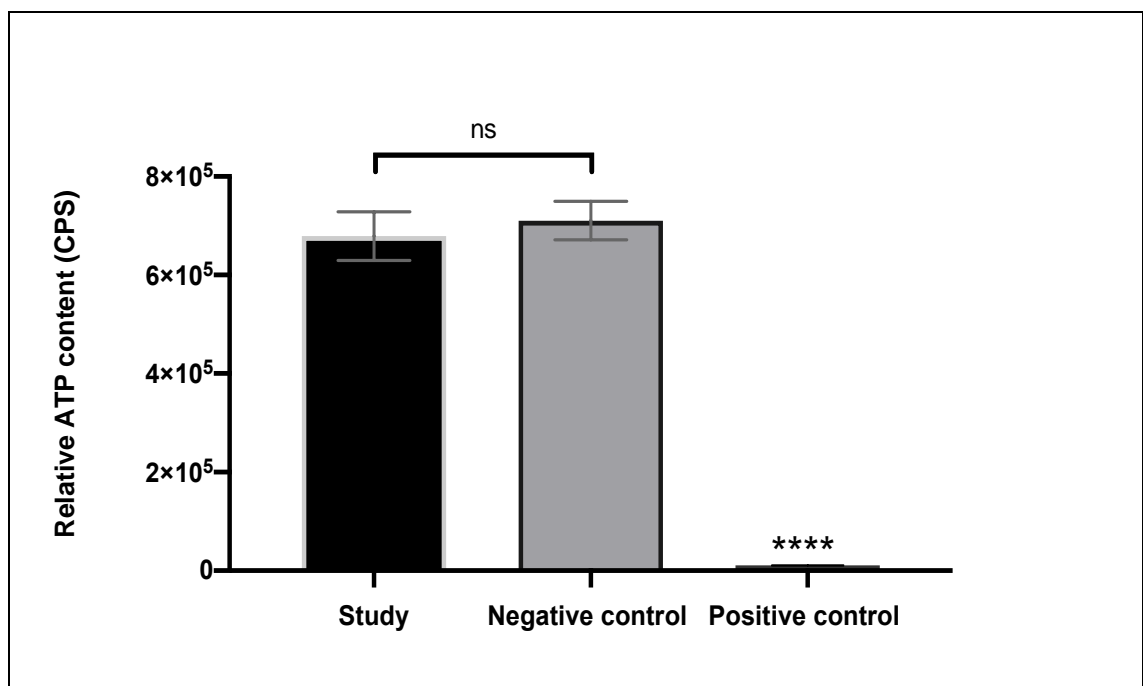


Figure 6-5: Extract cytotoxicity assay. Bar graph demonstrates the relative ATP content of L929 cell line when cultured for 24 hours in a medium containing an extract of the decellularised pulps or the relevant controls. Data represent mean ($n = 3$ replicates) \pm standard deviation. Data was analysed using one-way ANOVA with Bonferroni correction (**** $P < 0.0001$, ns = no significant difference). (CPS) counts per second.

6.5.3 The harvested populations of hDPSCs exhibited mesenchymal stem cell characteristics

6.5.3.1 The cells adhered to the surface of the tissue culture flasks

Images of hDPSCs from three different donors cultured in monolayers under basal culture conditions for 24 hours and visualised using an inverted phase-contrast microscope are shown in Figure 6-6. hDPSCs from all the three donors demonstrated adherence to the surface of the tissue culture flasks and exhibited the normal spindle-shape fibroblastic morphology.

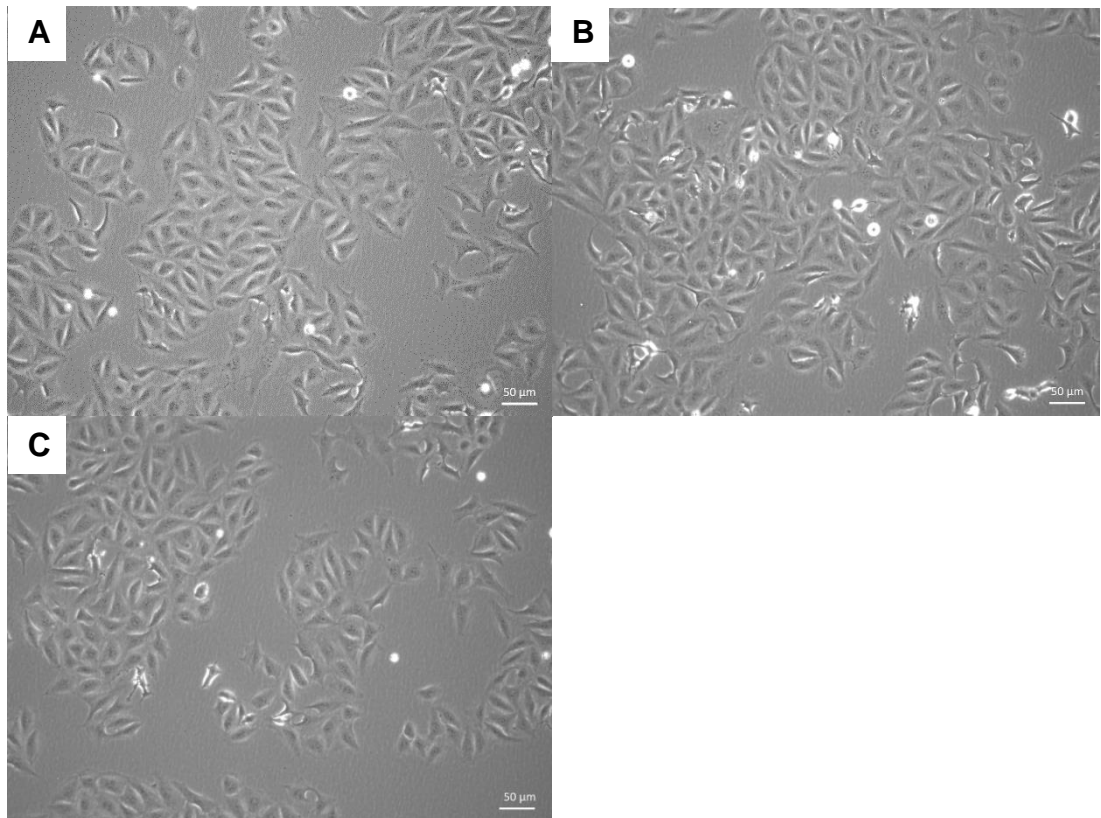


Figure 6-6: Images of hDPSCs cultured in monolayers and viewed using an inverted phase-contrast microscope. Representative images of hDPSCs obtained from (A) first donor, (B) second donor and (C) third donor following 24 hours of culture under basal conditions. The images show the cells adhered to the surface of the tissue culture flasks and exhibited spindle-shape morphology.

6.5.3.2 The cells expressed mesenchymal stem cell surface markers

The positive expression of mesenchymal stem cell surface markers (CD105, CD146 and CD90) and the negative expression of leukocyte marker (CD45) was investigated in hDPSCs harvested from the three different donors using flowcytometry. An example of the gating strategy used in the analysis of the collected data is shown in Figure 6-7. Cells labelled with fluorochrome-conjugated isotype antibodies were used as a negative control for each stain. The negative control gate was set where 98% of the population is included in the gate, making any movement of the positive stain beyond this point represents more than three standard deviations away from the mean of the negative control, which is considered a statistically relevant.

Flowcytometric analyses of CD105, CD146 and CD90 expression by the hDPSCs harvested from the three donors are shown in Figure 6-8. Cells from all the three donors showed positive expression of CD105, CD146 and CD90 with variable percentages. The expression of CD105 was higher in the cells obtained from the first donor (92.89%) as compared to the second (11.7%) and the third (20.90%) donors. The cell populations of all the three donors showed high expression of CD146. The first donor revealed 88.04% CD146 positive cell population whilst the second and third donors showed 90.70% and 89.34% CD146 positive cell populations, respectively. CD90 was highly expressed in hDPSCs obtained from the first (99.77%) and the third (99.63%) donors as compared to the second donor (21.14%). Very low expression of CD45 was detected in hDPSCs harvested from the three donors (Figure 6-9).

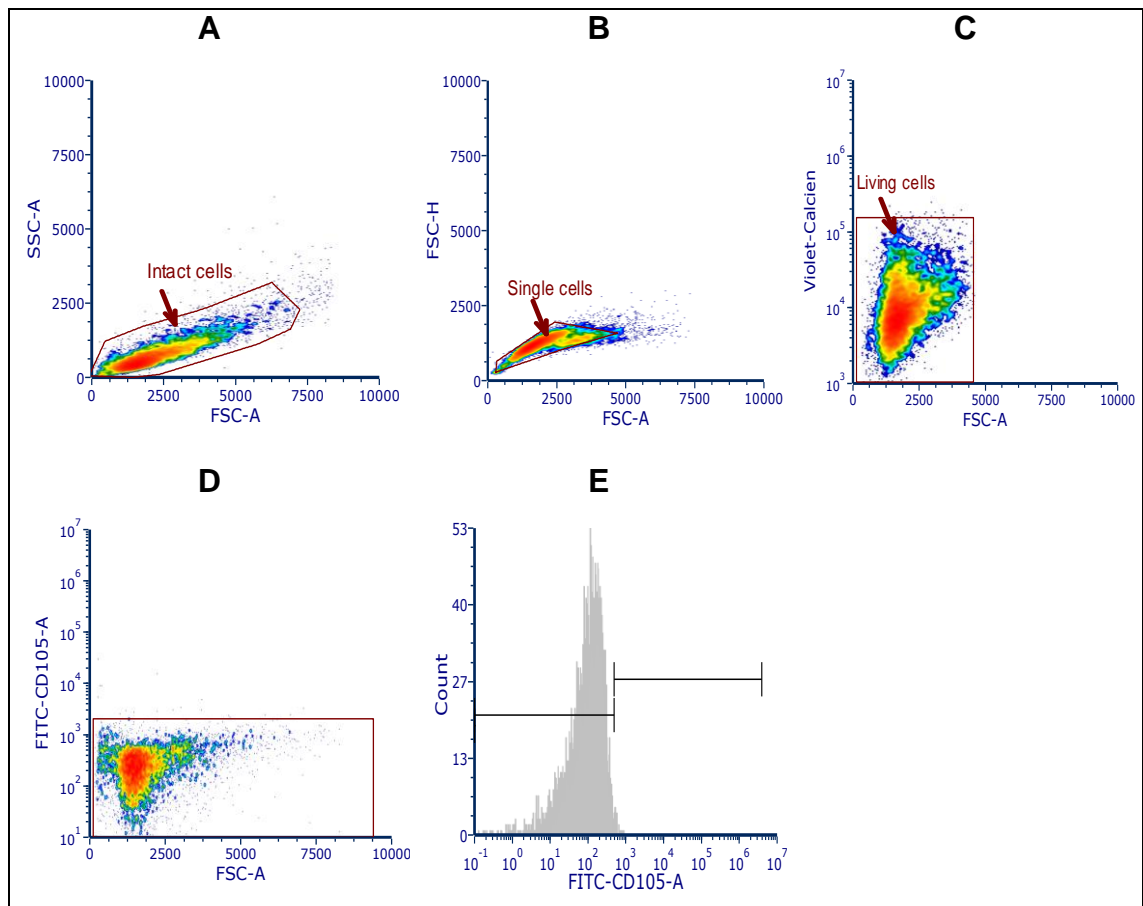


Figure 6-7: An example of the gating strategy used in analysing the expression of a single stem cell surface marker in hDPSCs. A flowcytometric analysis of mesenchymal stem cell surface markers expression in hDPSCs cultured under the basal condition and analysed using Attune[®] acoustic focusing flowcytometer and Attune[®] cytometric software version 2.1 (CD105 was used here as an example). (A, B, C and D) Representative density plots of (A) intact hDPSCs gating created by excluding scattered debris, (B) single cell gating created by excluding doublets, (C) viable cell (Calcein positive cell) gating and (D) negative control (isotype antibody) relevant to CD105 (FITC). (E) Representative single parameter histogram for the negative control relevant to CD105, where the gate is positioned at 98% of the negative control events and any events beyond this point in the CD105 stained samples was considered positive. (FSC-A) Forward scatter area, (SSC-A) Side scatter area, (FSC-H) Forward scatter pulse height.

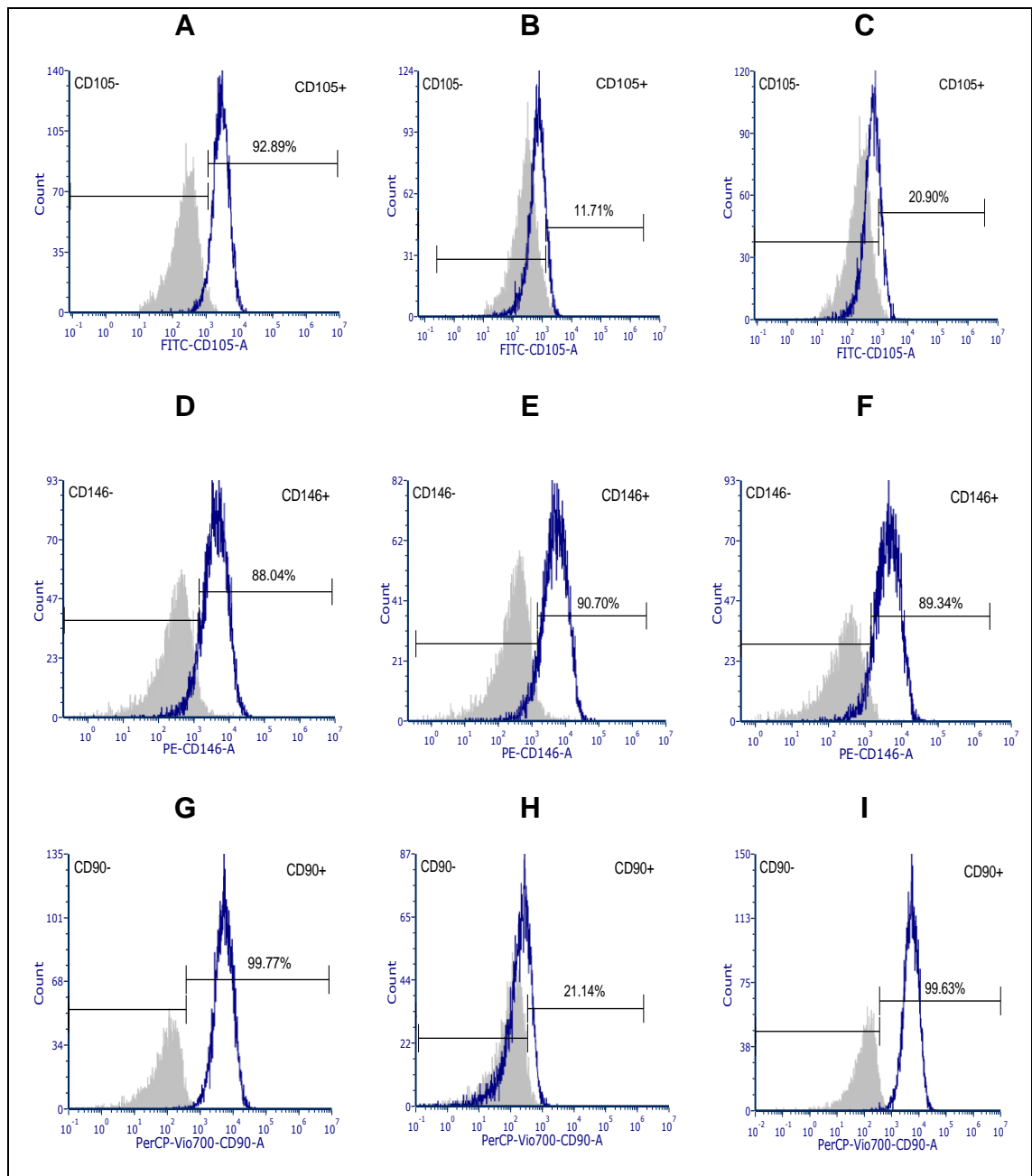


Figure 6-8: Expression of CD105, CD146 and CD90 in hDPSCs cultured under basal conditions and analysed using a flowcytometer. Representative single parameter histograms demonstrating the expression of (A, B and C) CD105, (D, E and F) CD146 and (G, H and I) CD90 in hDPSCs obtained from (A, D and G) first donor, (B, E and H) second donor and (C, F and I) third donor. The grey-coloured histograms represent the negative controls, where the gate is positioned at 98% of the negative control events and any events beyond this point in the stained samples was considered positive. The blue-coloured histograms represent the positive cell population. The gating strategy followed what was described in Figure 6-7.

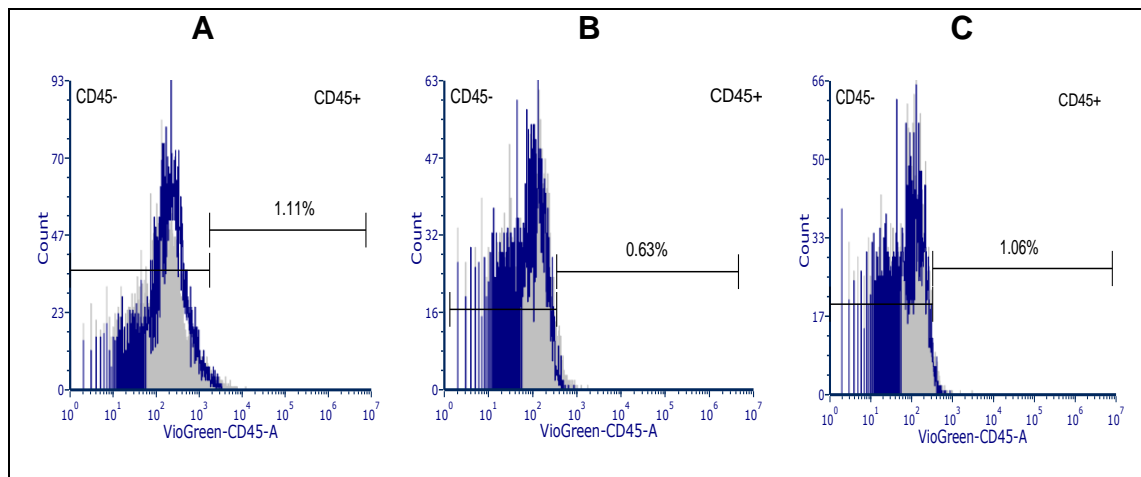


Figure 6-9: Expression of CD45 in hDPSCs cultured under basal conditions and analysed using a flowcytometer. Representative single parameter histograms showing the expression of CD45 in hDPSCs obtained from the (A) first donor, (B) second donor and (C) third donor. The grey-coloured histograms represent the negative control relevant to CD45, where the gate is positioned at 98% of the negative control events and any events beyond this point in the CD45 stained samples were considered positive. The blue-coloured histograms represent CD45 positive cell population. The gating strategy followed what was described in Figure 6-7.

6.5.3.3 The cells showed multilineage differentiation potential

The multilineage differentiation potential of hDPSCs obtained from the three donors was assessed by evaluating the ability of the cells to undergo osteogenic, adipogenic and chondrogenic differentiation when exposed to an appropriate culture condition.

Osteogenic differentiation potential

Images of hDPSCs obtained from the three donors and cultured under the basal or osteogenic conditions for three weeks before being analysed using Alizarin Red staining are shown in Figure 6-10. The results showed robust deposition of calcium-rich mineralised nodules in the extracellular matrix of the cells cultured

under osteogenic conditions (Figure 6-10 A, C and E) as compared to the cells cultured under basal conditions (Figure 6-10 B, D and F).

Adipogenic differentiation potential

Images of hDPSCs obtained from the three donors and cultured under the basal or adipogenic conditions for three weeks before being analysed using Oil Red staining are shown in Figure 6-11. No evidence of lipid droplets formation by the cells was observed under the basal conditions (Figure 6-11 A, C and E). On the contrary, red-colour stained lipid droplets were clearly visible in the cytoplasm of the cells exposed to the adipogenic culture conditions (Figure 6-11 B, D and F).

Chondrogenic differentiation potential

Images of hDPSCs obtained from the three donors and cultured under the basal or chondrogenic conditions for three weeks, then analysed using Alcian Blue staining are shown in Figure 6-12. The results revealed increased deposition of glycosaminoglycans by the cells cultured under the chondrogenic conditions (Figure 6-12 A, C and E) as compared to the cells cultured under the basal conditions (Figure 6-12 B, D and F).

Taken together, the findings described above confirm the potential of hDPSCs harvested from the three donors to undergo multilineage differentiation when exposed to an inductive environment.

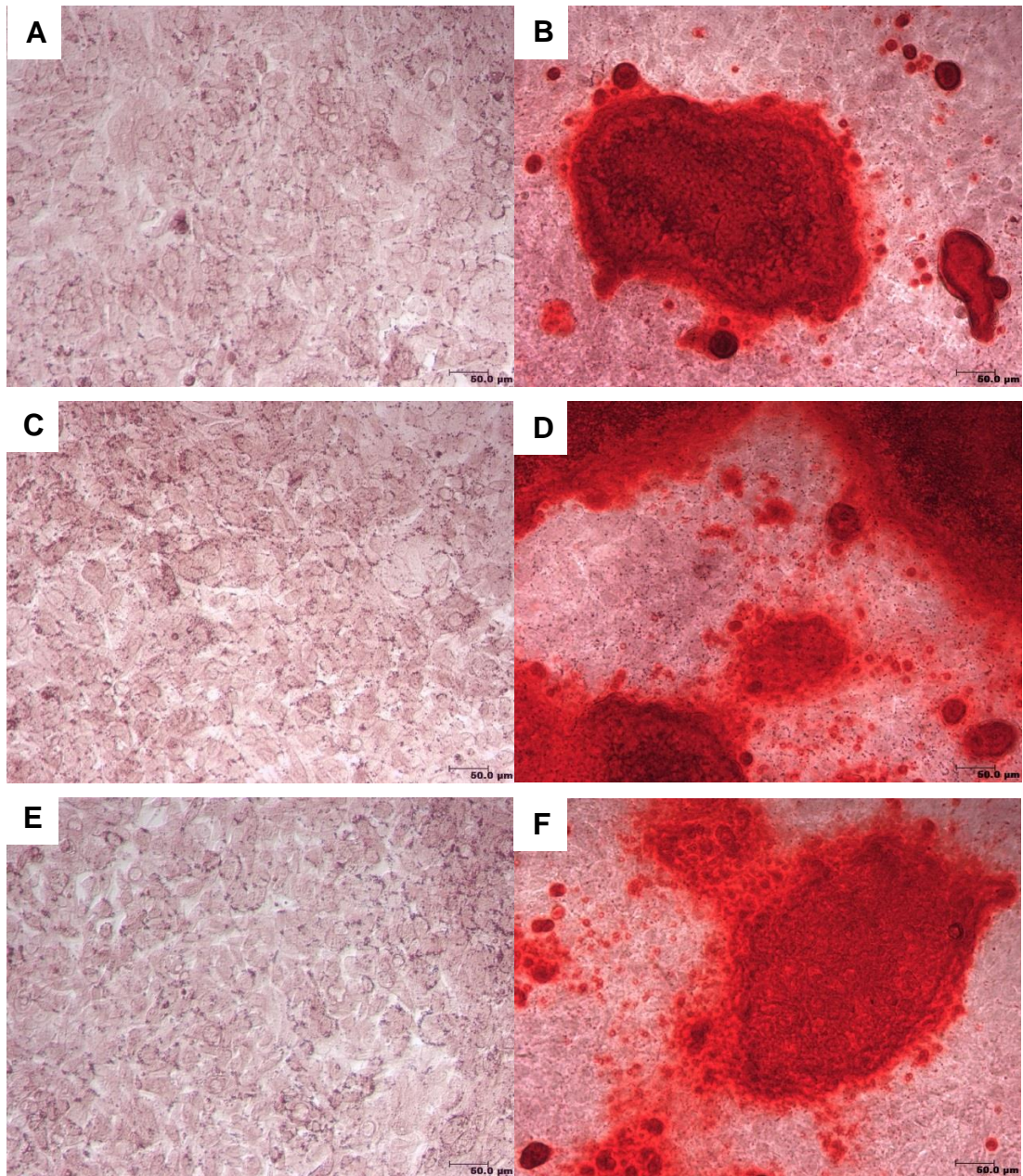


Figure 6-10: Bright-field microscopic images of hDPSCs stained with alizarin red after three weeks of culture under osteogenic conditions. Representative images of hDPSCs harvested from (A and B) first donor, (C and D) second donor and (E and F) third donor and cultured under (A, C and E) the basal or (C, D and F) osteogenic conditions for three weeks then stained with alizarin red dye. The images show deposition of calcium-rich mineralised nodules by the cells cultured under osteogenic conditions as compared to the cells cultured under the basal conditions. Calcium-rich mineralised nodules stained bright red. Scale bars represent 50 µm.

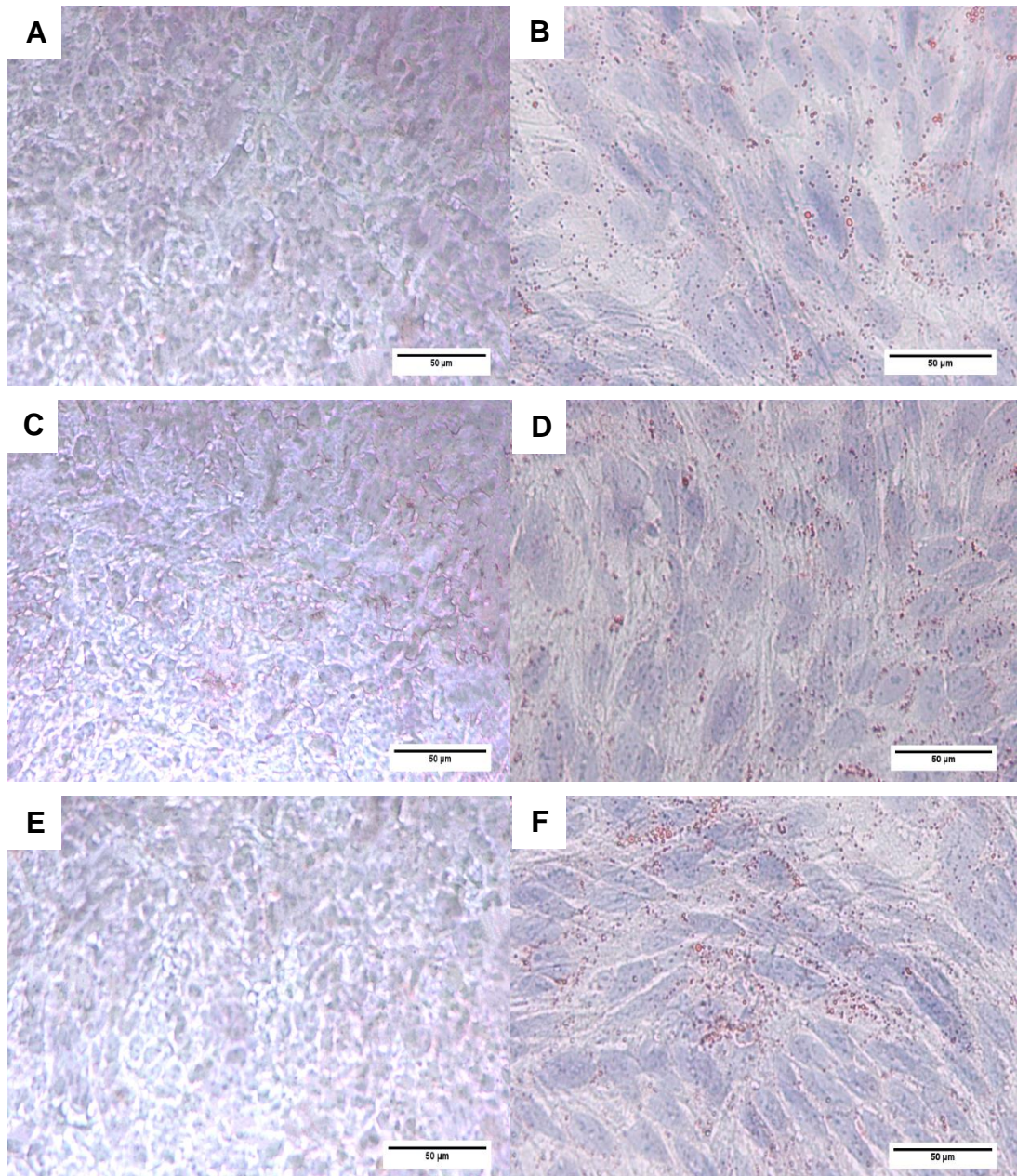


Figure 6-11: Bright-field microscopic images of hDPSCs stained with Oil red after three weeks of culture under adipogenic conditions. Representative images of hDPSCs harvested from (A and B) first donor, (C and D) second donor and (E and F) third donor and cultured under (A, C and E) the basal or (C, D and F) adipogenic conditions for three weeks then stained using Oil Red. The images show lipid droplets formation on the culture exposed to adipogenic condition. Lipid droplets stained red and the cell nuclei stained blue. Scale bars represent 50 μm .

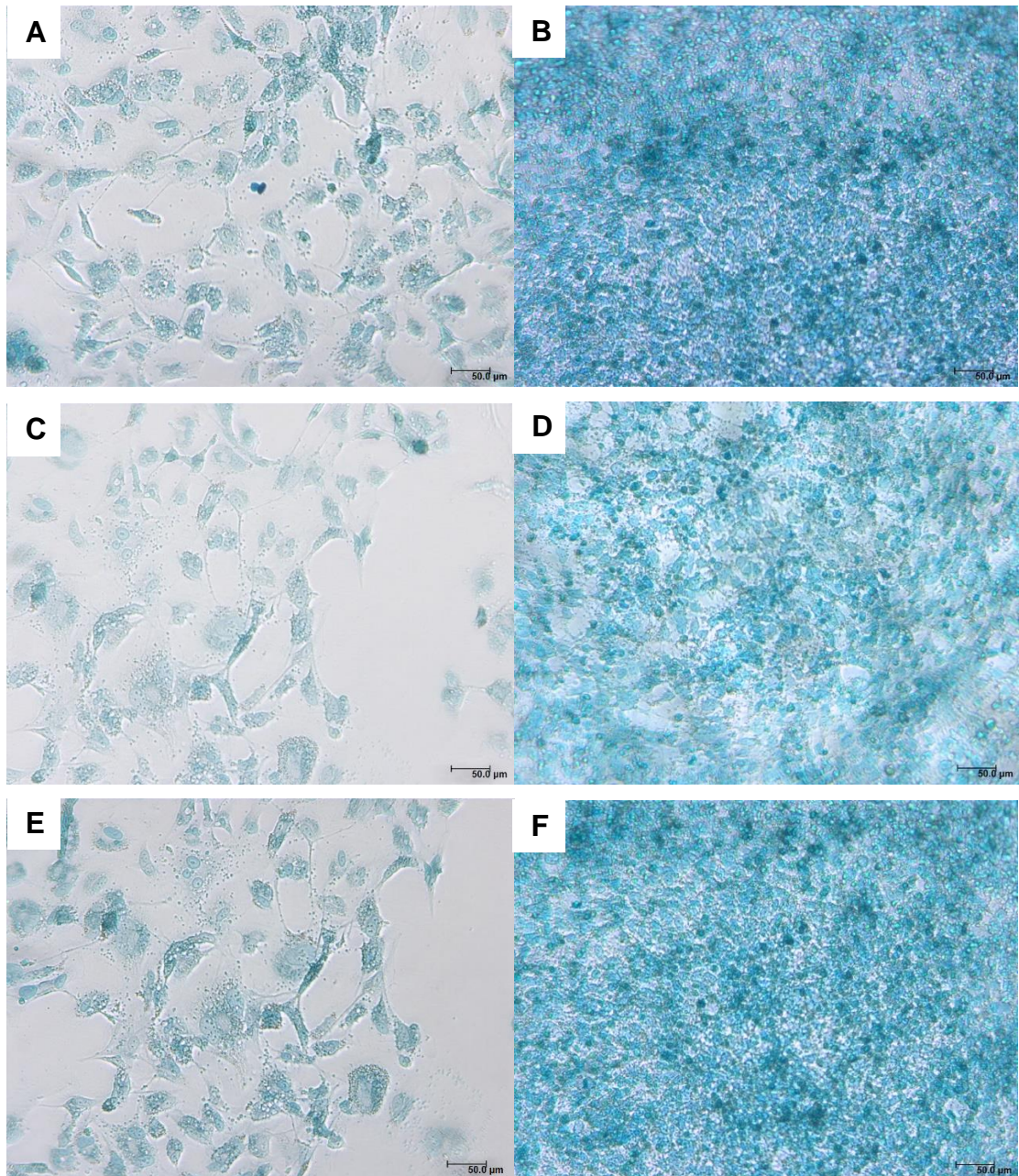


Figure 6-12: Bright-field microscopic images of hDPSCs stained with Alcian Blue after three weeks of culture under chondrogenic conditions. Representative images of hDPSCs harvested from (A and B) first donor, (C and D) second donor and (E and F) third donor cultured under (A, C and E) the basal or (C, D and F) chondrogenic conditions for three weeks then stained with Alcian Blue dye. The images show increased deposition of glycosaminoglycans (blue colour) by the cells exposed to a chondrogenic conditions as compared to the cells cultured under basal conditions. Scale bars represent 50 μm .

6.5.4 hDPSCs attached to the surface of the decellularised dental pulp matrix

Scanning electron microscopic images of hDPSCs following three days of seeding onto the surface of the decellularised dental pulps are shown in Figure 6-13. The images showed hDPSCs attached and spread across the surface of the decellularised dental pulps. The cells exhibited a spindle-shape morphology and extended to bridge the interfibrillar spaces of the scaffolds. Some structural features such as fenestrations and pseudopodia were clearly visible at the areas of cell attachment to the scaffolds.

6.5.5 hDPSCs organised in tube-like structures following seeding onto the surface of the decellularised dental pulp matrix

Confocal scanning laser microscopic images of hDPSCs following seven days of seeding onto the surface of the decellularised dental pulps are shown in Figure 6-14. The images show hDPSCs engrafted into the scaffolds and exhibited an elongated fibroblastic spindle-shape morphology. The cells showed three-dimensional orientation and appeared colonising tube-like structures (10 - 30 μm in diameter) resembling a capillary network.

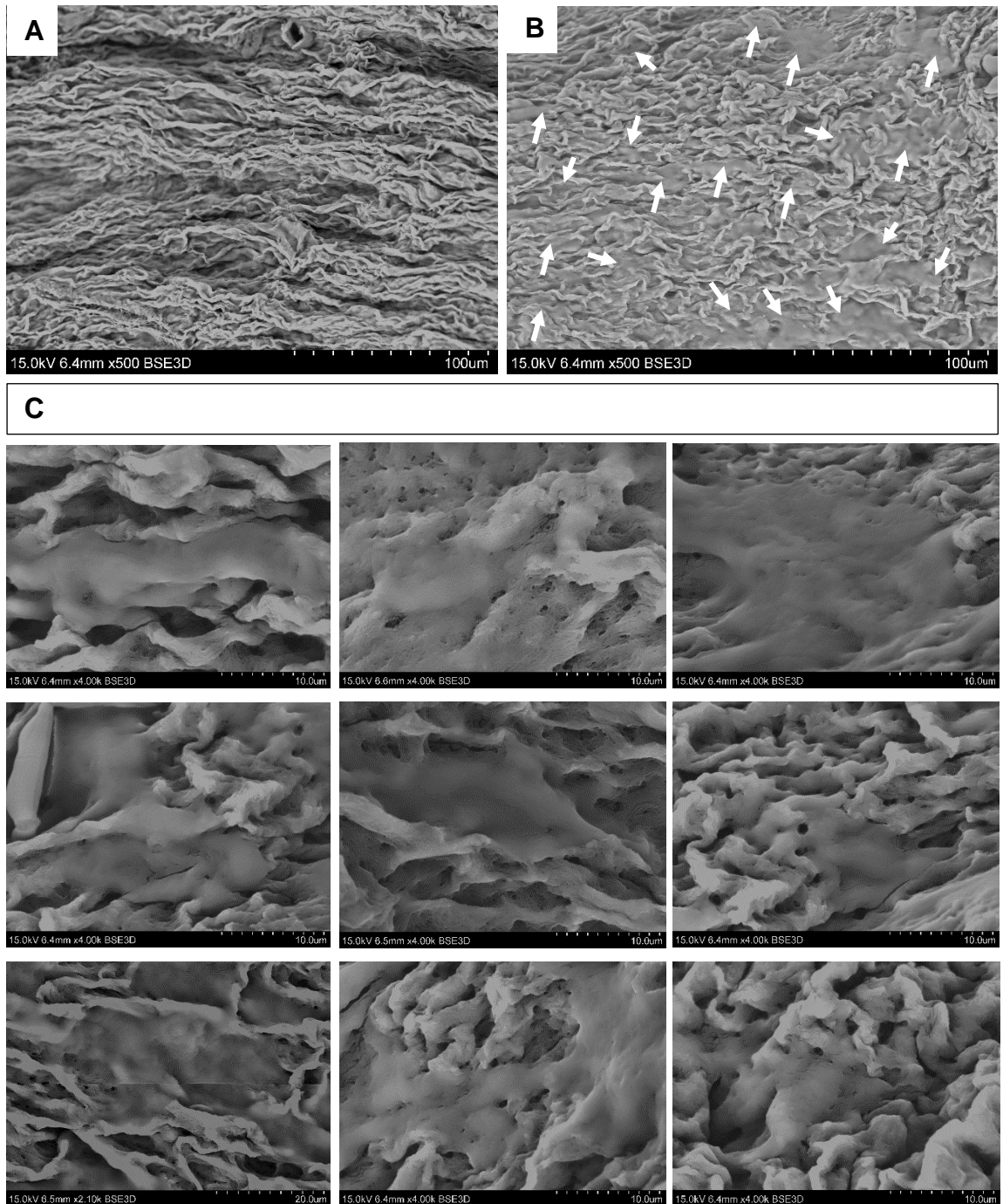


Figure 6-13: Images of hDPSCs after three days of seeding onto the surface of the decellularised dental pulps viewed using a conventional high vacuum SEM. Representative images of the decellularised dental pulps (A) before and (B) after seeding with hDPSCs. The images show the structural elements of the scaffold before the seeding and cell binding to the surface of the scaffolds following the seeding (white arrows). (C) Representative high magnification images of the recellularised scaffolds demonstrating cellular attachment. Scale bars A and B at 100 μm and C at 10 μm .

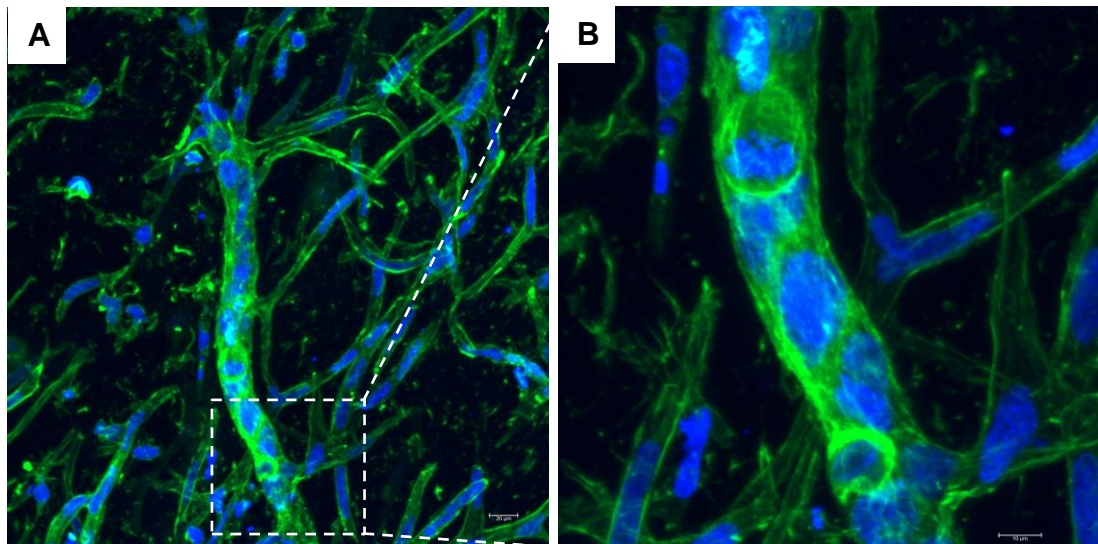


Figure 6-14: Images of hDPSCs after seven days of seeding onto the decellularised dental pulps stained using Alexa-Fluor[®] 488 Phalloidin and DAPI and visualised using a confocal scanning laser microscope. (A) Representative stack image of hDPSCs seeded onto the decellularised dental pulps showing the cells colonising tube-like structures (10 – 30 μm in diameter), and (B) is a high power magnification of the area delineated in (A). Cytoskeleton stained green and the cell nuclei stained blue. Scale bars set at 20 μm.

6.5.6 hDPSCs maintained viability following seeding onto the surface of the decellularised dental pulp matrix

The results of cell viability analysis of hDPSCs following 7 and 14 days of seeding onto the surface of the decellularised dental pulps using Live/dead[®] cell viability assay are shown in Figure 6-15. The results revealed excellent cell viability in all examined recellularised scaffolds following seven days of culture (Figure 6-15 A). Viable cells (stained green with Calcein-AM) appeared repopulating the scaffolds with only a few dead cells (stained red with Ethidium Homodimer). The viable cells appeared spreading through the surface of the scaffolds. The cell morphology, where possible to be distinguished, was a mixture of an elongated spindle-shaped and a cuboidal-shape. Following 14 days of culture, the density

of the viable cells repopulating the scaffolds showed marked increase whilst the dead cells remain a few (Figure 6-15 B).

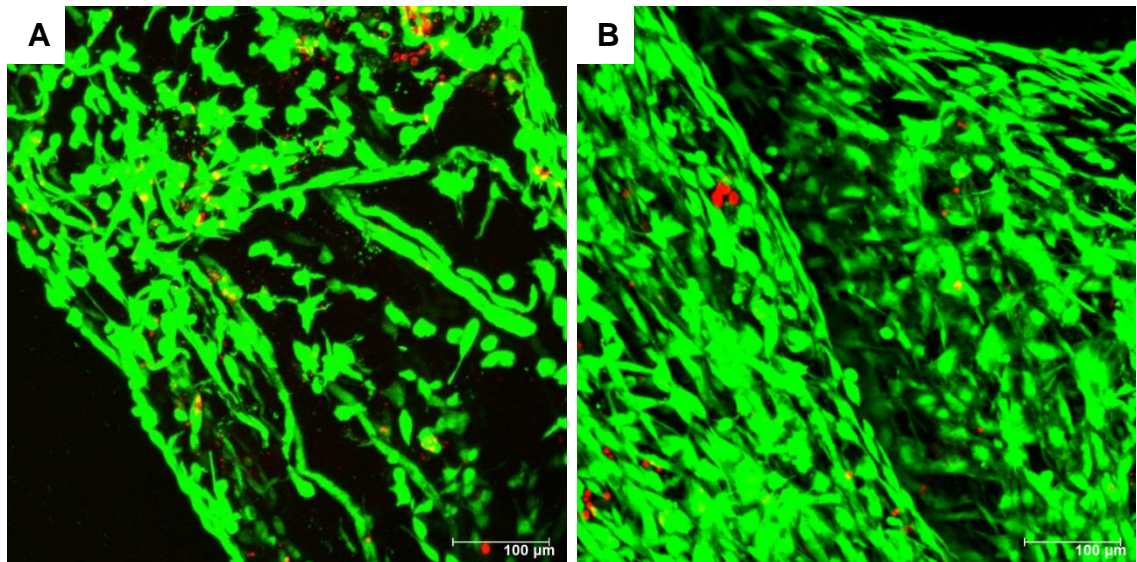


Figure 6-15: Images of hDPSCs seeded onto the decellularised dental pulps and analysed using Live/Dead[®] staining and a confocal scanning laser microscope. Representative confocal stack images of the recellularised scaffolds after (A) seven and (B) fourteen days of *in vitro* culture under the basal condition. The images show most of the cells repopulating the decellularised scaffolds at each time points viable with only a few dead cells. Viable cells stained green and dead cells stained red.

6.5.7 hDPSCs proliferated following seeding onto the surface of the decellularised dental pulp matrix

Proliferation hDPSCs following seeding onto the surface of the decellularised dental pulps was assessed following 1, 3, 5, 7 and 14 days of seeding through measuring the dsDNA contents of the recellularised scaffolds. The results are demonstrated in Figure 6-16. A progressive increase in the dsDNA content of the scaffolds was observed following seeding with hDPSCs (Day 1 = 58.63 ± 10.19 ng.mg⁻¹, Day 3 = 66.36 ± 12.49 ng.mg⁻¹, Day 5 = 104.27 ± 16.43 ng.mg⁻¹, Day 7 = 135.12 ± 14.47 ng.mg⁻¹ and Day 14 = 207.57 ± 24.31 ng.mg⁻¹). A significant

increase in the dsDNA content of the scaffolds was observed following one day of cell seeding ($P < 0.0001$) as compared to dsDNA content of the scaffolds before cell seeding ($2.13 \pm 1.16 \text{ ng.mg}^{-1}$). Although an apparent increase in the dsDNA content of the scaffolds was detected between day 1 and day 3, the increase was not statistically significant ($P = 0.96$). Following day 3 and up to day 14, the dsDNA content of the scaffolds increased significantly.

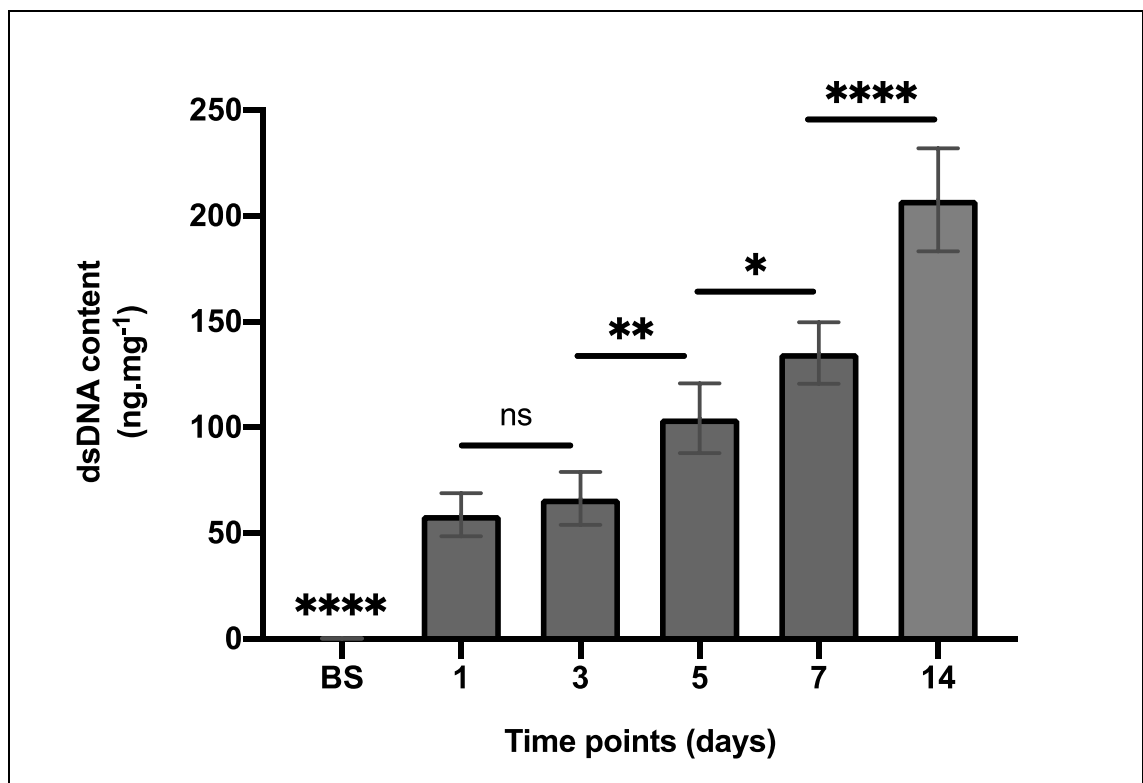


Figure 6-16: Bar graph demonstrates the dsDNA content of decellularised dental pulps after seeding with hDPSCs as determined using Quant-iT™ PicoGreen® dsDNA assay. Data represent mean ($n = 5$ samples per time point) \pm standard deviation. Data was analysed using one-way ANOVA with Bonferroni correction ($*P < 0.01$, $**P < 0.001$, $****P < 0.0001$, ns: no significant difference). (BS) Before cell seeding.

6.5.8 hDPSCs repopulated the matrix and vasculature of the decellularised dental pulp matrix

Microscopic images of H&E-stained tissue sections of decellularised dental pulps seeded with hDPSCs and cultured *in vitro* under basal conditions for 7, 14 and 21 days are shown in Figure 6-17, Figure 6-18 and Figure 6-19, respectively. The images showed engraftment and progressive repopulation of the decellularised dental pulps with hDPSCs over the 21 days studied. At day 7, the cells were uniformly lining the surface of the scaffolds and interestingly, the luminal surface of the vessels close to the surface (Figure 6-17). However, the medial area of the decellularised dental pulps remained acellular. After 14 days, hDPSCs were uniformly lining the surface of the scaffolds and the luminal surface of the vessels with many cells engrafted and scattered within the matrix (Figure 6-18). Following 21 days, the cells were still lining the surface of the decellularised dental pulps and the luminal surface of the vascular canals with many more cells dispersed within the stroma of the scaffolds (Figure 6-19).

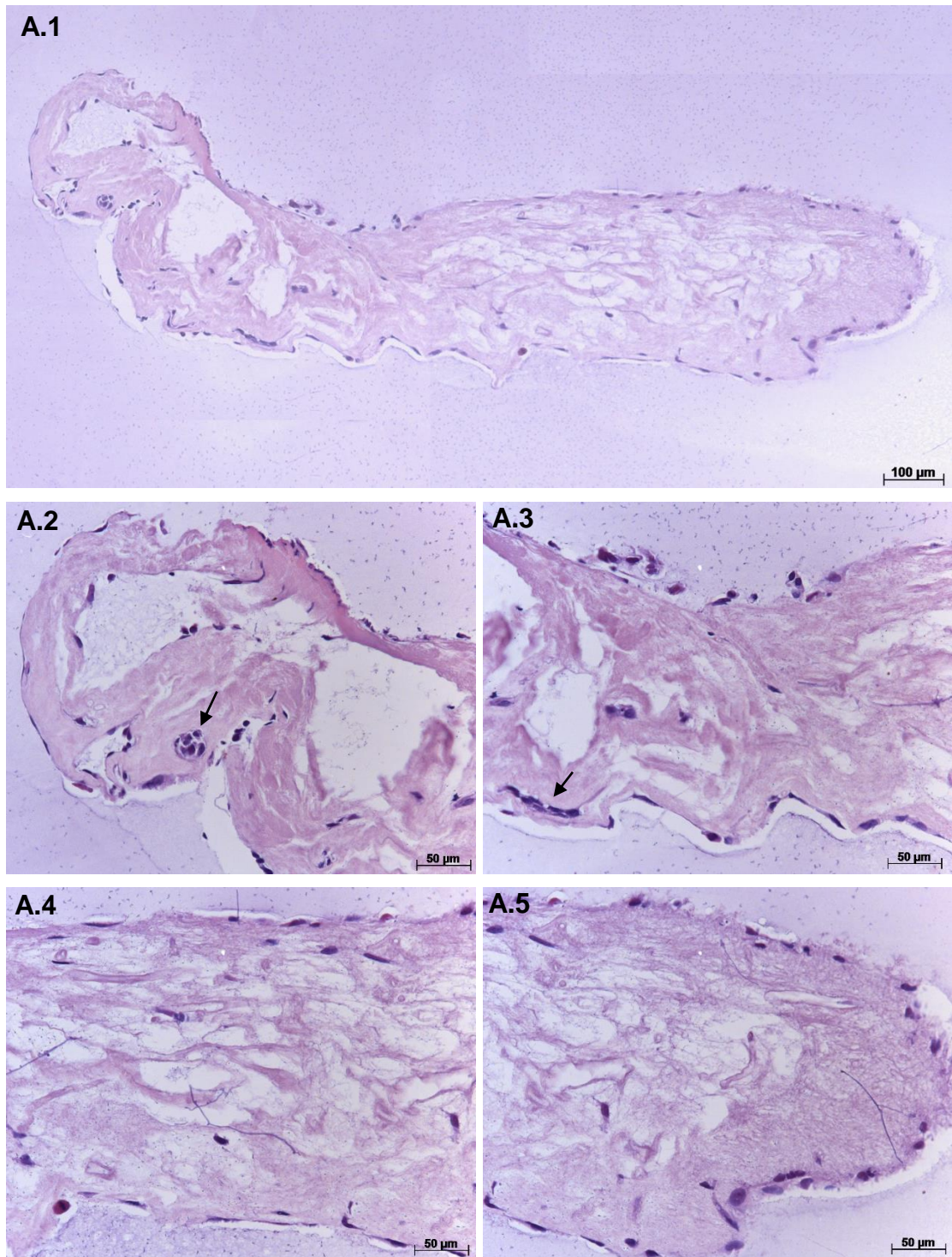


Figure 6-17: Bright-field microscopic images of H&E-stained sections of decellularised dental pulps seeded with hDPSCs and cultured *in vitro* for 7 days. (A.1) Representative image of a full-length recellularised scaffold shows apparent cell attachment. Images (A.2 - A.5) are a high magnification of (A.1) show the cells on the surface and lumina of the vessels (black arrows). Cell nuclei stained blue and the ECM stained pink.

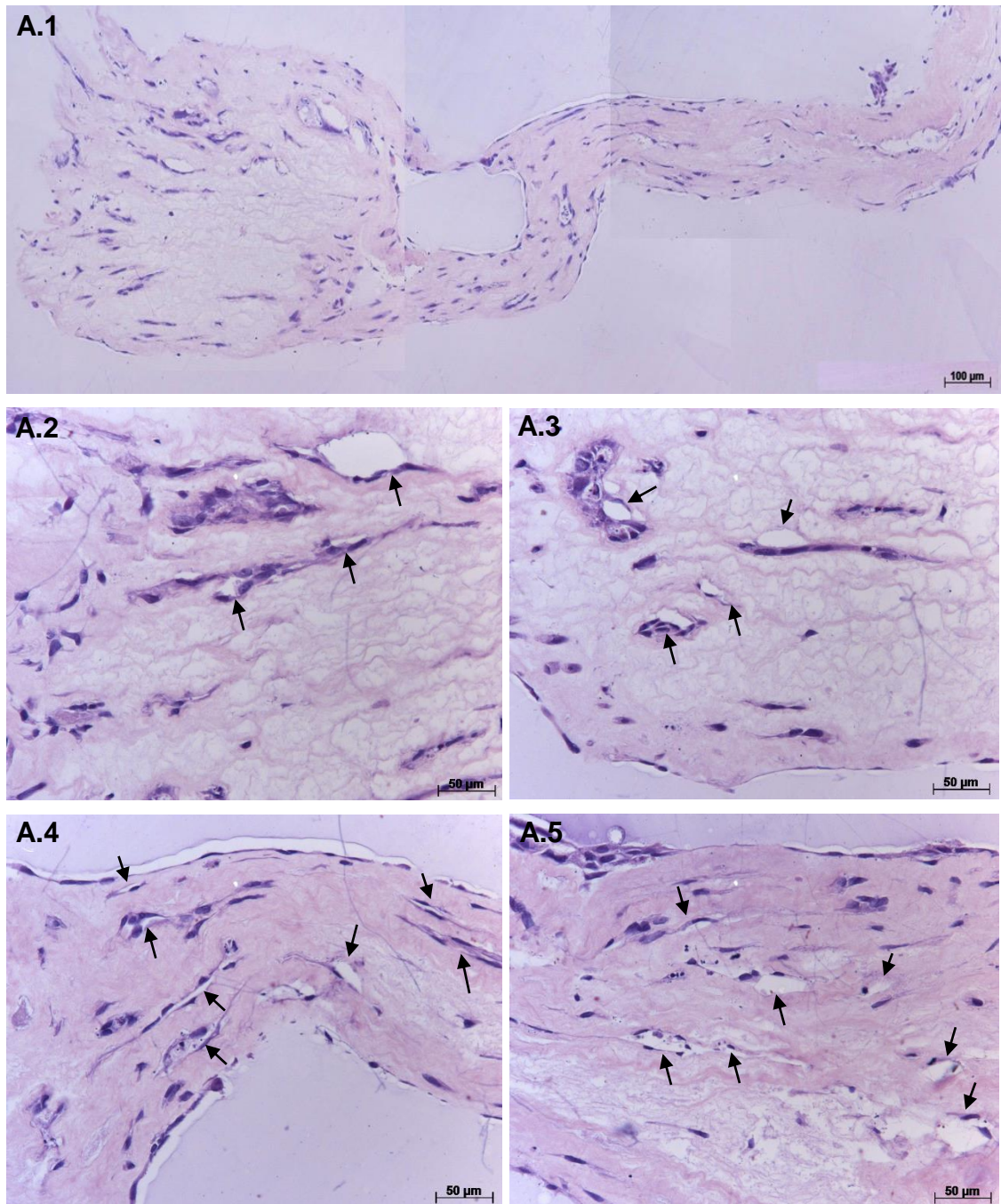


Figure 6-18: Bright-field microscopic images of H&E-stained sections of decellularised dental pulps seeded with hDPSCs and cultured *in vitro* for 14 days. (A) Representative image of a full-length recellularised scaffold shows clear cell attachment and infiltration. (A.2 - A.5) High magnifications images of (A.1) show hDPSCs attached to the surface, migrated within the matrix and aligned the lumina of the vessels (Black arrows). Cell nuclei stained blue and the ECM stained pink.

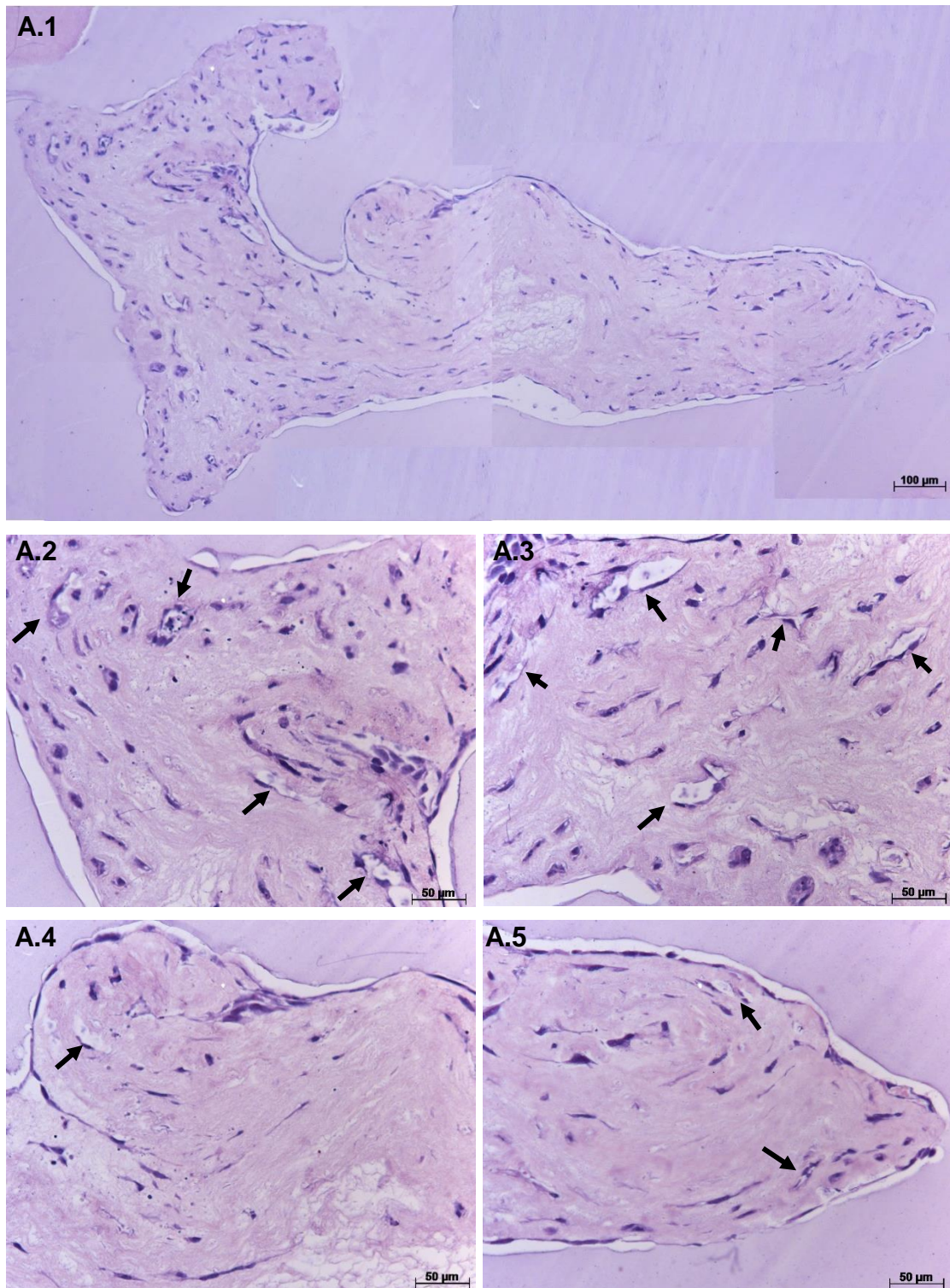


Figure 6-19: Bright-field microscopic images of H&E-stained sections of decellularised dental pulps seeded with hDPSCs and cultured *in vitro* for 21 days. (A) Representative image of a full-length recellularised scaffold shows apparent cell attachment and migration. (A.2 – A.5) High magnification images of (A.1) show the cells attached, spread and aligned the lumina of the vascular channels. Cell nuclei stained blue and the ECM stained pink.

6.5.9 The effects of decellularised dental pulp on gene expression of markers involved in angiogenesis and odontogenesis in hDPSCs

The expressions of the angiogenesis markers (KDR and PECAM-1) and odontogenesis markers (DSPP, DMP-1 and MEPE) at mRNA level in hDPSCs grown in the decellularised dental pulps were analysed *in vitro* and compared to the markers' expression in hDPSCs grown in two-dimensional (monolayers) and three-dimensional (BioGide® collagen scaffolds) models. The experiments were repeated three times, each with hDPSCs obtained from a different donor. The results from individual donor (individual analysis) as well as the average of all donors (global analysis) were plotted for all genes.

Gene expression analysis of the angiogenesis markers

KDR

The level of KDR gene expression in hDPSCs cultured in the decellularised dental pulps was higher compared to the expression in similar cells cultured in two-dimensional and three-dimensional models in all the three cell donors at all the examined time points (Figure 6-20).

When compared to two-dimensional model, the KDR gene expression level in hDPSCs colonising the decellularised dental pulps was higher by 8.08 ± 1.94 fold at day 7, 17.98 ± 5.01 fold at day 14 and 25.29 ± 3.37 fold at day 21 in the first donor (Figure 6-20 A), 6.06 ± 0.62 fold at day 7, 8.04 ± 3.35 fold at day 14 and 9.92 ± 3.50 fold at day 21 in the second donor (Figure 6-20 B), and 16.25 ± 1.54 fold at day 7, 18.60 ± 9.28 fold at day 14 and 20.24 ± 6.57 fold at day 21 in the third donor (Figure 6-20 C).

When compared to three-dimensional model, the KDR gene expression level in hDPSCs colonising the decellularised dental pulps was higher by 7.48 ± 1.80 fold at day 7, 18.57 ± 5.17 fold at day 14 and 15.36 ± 2.04 fold at day 21 in the first donor (Figure 6-20 A), 4.44 ± 0.45 fold at day 7, 7.43 ± 3.10 fold at day 14 and 7.14 ± 2.52 fold at day 21 in the second donor (Figure 6-20 B), and 15.24 ± 1.44 fold at day 7, 15.06 ± 7.51 fold at day 14 and 17.70 ± 5.75 fold at day 21 in the third donor (Figure 6-20 C).

The global analysis revealed that the expression of KDR gene was higher in hDPSCs colonising the decellularised pulp as compared to both two-dimensional and three-dimensional models at all the examined time points (Figure 6-20 D).

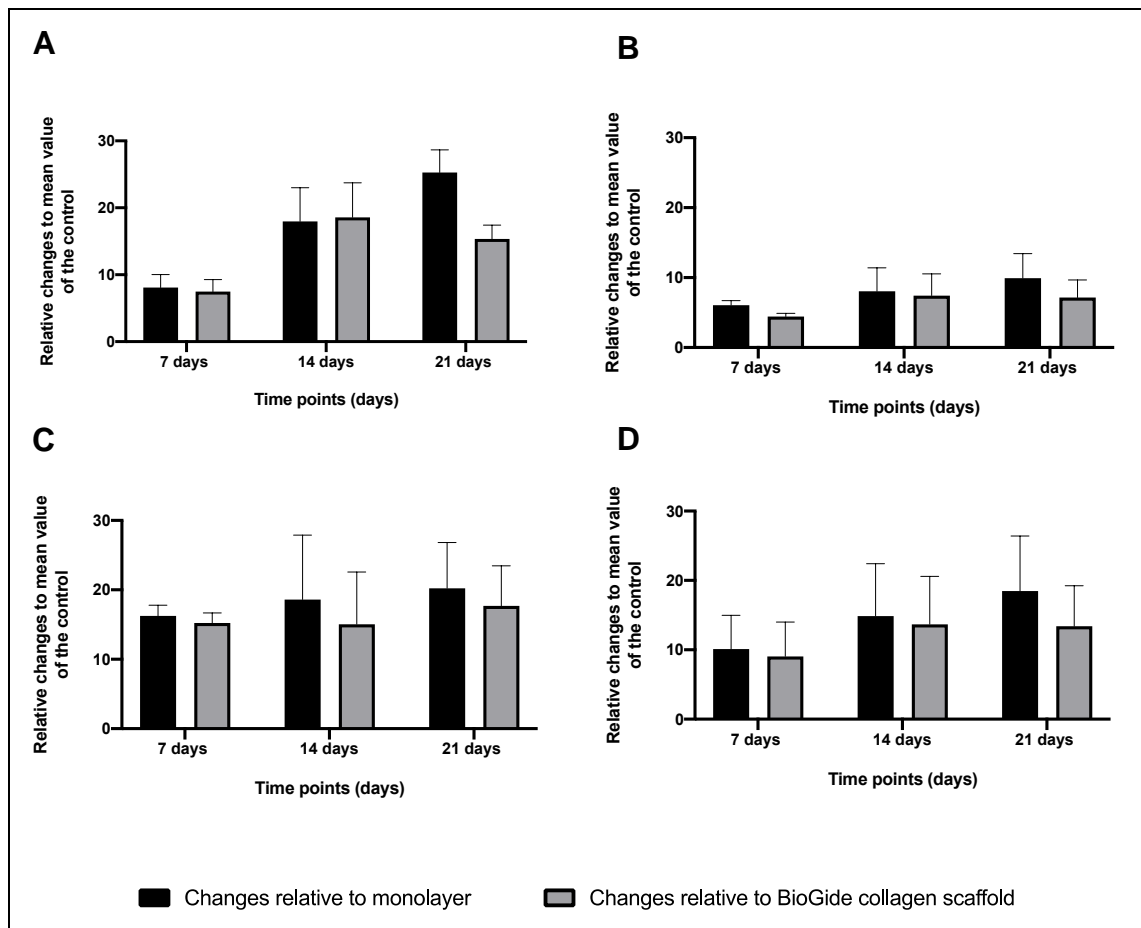


Figure 6-20: Bar graphs demonstrate the changes in KDR gene expression in hDPSCs grown on the decellularised dental pulps relative to similar cells grown on the controls. The expression of KDR gene in hDPSCs obtained from (A) 1st donor, (B) 2nd donor and (C) 3rd donor, then grown on the decellularised dental pulps *in vitro* under basal conditions for 7, 14 and 21 days was normalised to the gene expression in similar cells grown under the same conditions on monolayers or BioGide[®] collagen scaffolds. Data represents mean $2^{-\Delta\Delta Ct}$ (n = 3 samples) \pm standard deviation. (D) Global analysis show the average KDR gene expression of all donors at the examined time points.

PECAM-1

In all the three cell donors, the level of PECAM-1 gene expression in hDPSCs grown in the decellularised dental pulps was higher as compared to the expression level in similar cells grown in two-dimensional and three-dimensional models (Figure 6-21).

When compared to two-dimensional model, the expression level of PECAM-1 gene in hDPSCs seeded onto the decellularised dental pulps was higher by 7.89 ± 2.28 fold at day 7, 12.92 ± 4.90 fold at day 14 and 6.07 ± 2.23 fold at day 21 in the first donor (Figure 6-21 A), 2.67 ± 1.33 fold at day 7, 4.97 ± 1.05 fold at day 14 and 3.02 ± 0.25 fold at day 21 in the second donor (Figure 6-21 B), and 4.95 ± 0.49 fold at day 7, 4.21 ± 0.97 fold at day 14 and 5.33 ± 1.12 fold at day 21 in the third donor (Figure 6-21 C).

When compared to three-dimensional model, PECAM-1 gene expression level in hDPSCs colonising the decellularised pulps was higher by 6.44 ± 1.86 fold at day 7, 10.12 ± 3.83 fold at day 14 and 6.00 ± 2.20 fold at day 21 in the first donor (Figure 6-21 A), 2.40 ± 1.19 fold at day 7, 3.59 ± 0.76 fold at day 14 and 2.75 ± 0.23 fold at day 21 in the second donor (Figure 6-21 B), and 3.82 ± 0.38 fold at day 7, 4.15 ± 0.96 fold at day 14 and 4.86 ± 1.02 fold at day 21 in the third donor (Figure 6-21 C).

The global analysis showed the level of PECAM-1 gene expression in hDPSCs grown in the decellularised dental pulps higher as compared to both two-dimensional and three-dimensional models at all the examined time points (Figure 6-21 D).

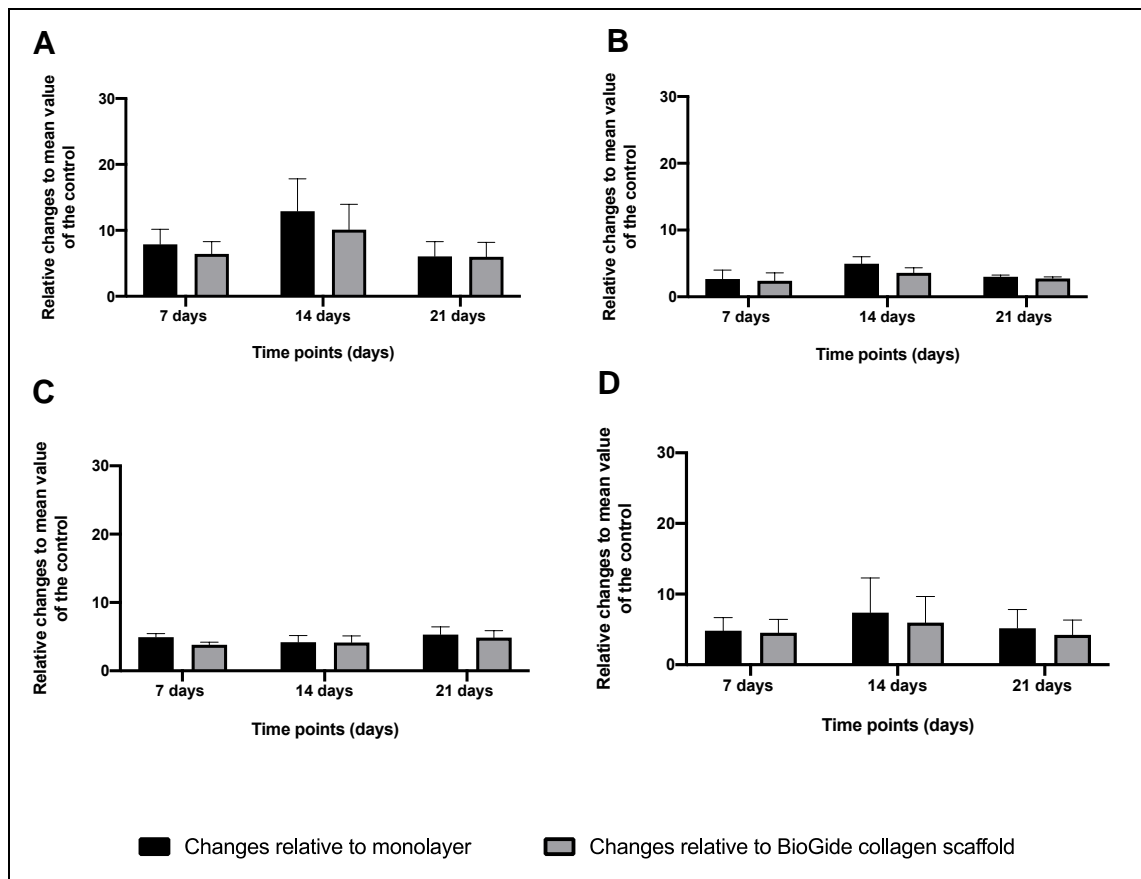


Figure 6-21: Bar graphs demonstrate the changes in PECAM-1 gene expression level in hDPSCs grown on the decellularised dental pulps compared to similar cells grown on the controls. The expression of PECAM-1 gene in hDPSCs obtained from (A) 1st donor, (B) 2nd donor and (C) 3rd donor and grown on the decellularised dental pulps *in vitro* under basal conditions for 7, 14 and 21 days was compared to the expression in similar cells grown under the basal conditions on monolayers or BioGide[®] collagen scaffolds. Data represents mean $2^{-\Delta\Delta Ct}$ ($n = 3$ samples) \pm standard deviation. (D) Global analysis show the average PECAM-1 gene expression of all donors at the examined time points.

Gene expression analysis of the odontogenesis markers

DSPP

The results of gene expression analysis of DSPP in hDPSCs grown in the decellularised dental pulps as compared to similar cells grown in two dimensional and three-dimensional models are shown in Figure 6-22.

Comparing to two-dimensional model, the expression level of DSPP gene in hDPSCs colonising the decellularised dental pulps was higher by 2.96 ± 1.09 fold at day 7, 3.21 ± 1.01 fold at day 14 and 5.42 ± 2.04 fold at day 21 in the first donor (Figure 6-22 A), 1.19 ± 0.15 fold at day 7, 1.34 ± 0.25 fold at day 14 and 7.27 ± 2.01 fold at day 21 in the second donor (Figure 6-22 B), and 3.67 ± 0.70 fold at day 7, 2.68 ± 0.36 fold at day 14 and 6.24 ± 1.68 fold at day 21 in the third donor (Figure 6-22 C).

Comparing to three-dimensional model, DSPP gene expression level in hDPSCs seeded onto the decellularised dental pulps was higher by 2.81 ± 1.03 fold at day 7, 1.95 ± 1.27 fold at day 14 and 2.90 ± 1.09 fold at day 21 in the first donor (Figure 6-22 A). In the second donor, no significant change was observed at day 7 (0.99 ± 0.12 fold) with upregulation at day 14 (1.30 ± 0.24 fold) and day 21 (5.55 ± 2.30 fold) (Figure 6-22 B). In the third donor, the expression level was higher by 2.47 ± 0.47 fold at day 7, 2.42 ± 0.32 fold at day 14 and 3.90 ± 1.04 fold at day 21 (Figure 6-22 C).

The global analysis showed the expression level of DSPP gene in hDPSCs colonising the decellularised pulps higher than both the two dimensional and three-dimensional models at all the examined time points (Figure 6-22 D).

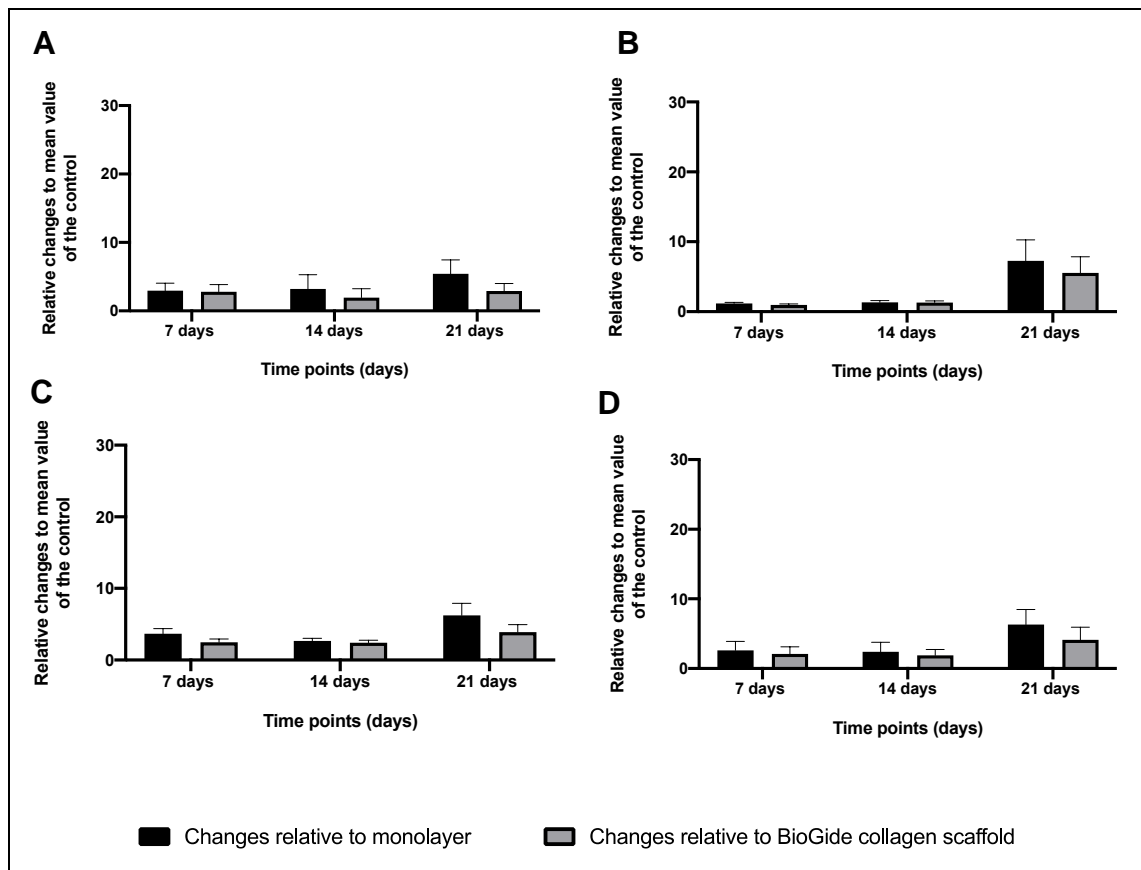


Figure 6-22: Bar graphs demonstrate the changes in DSSP gene expression in hDPSCs grown on the decellularised dental pulps relative to similar cells grown on the controls. DSSP gene expression in hDPSCs obtained from (A) 1st donor, (B) 2nd donor and (C) 3rd donor, then grown on the decellularised dental pulps *in vitro* under basal conditions for 7, 14 and 21 days was normalised to gene expression in similar cells grown under basal conditions on monolayers or BioGide[®] collagen scaffolds. Data represents mean $2^{-\Delta\Delta Ct}$ (n = 3 samples) \pm standard deviation. (D) Global analysis show the average DSSP expression of all donors at the examined time points.

DMP-1

The results of gene expression analysis of DMP-1 in hDPSCs grown on the decellularised dental pulps compared to similar cells grown on two-dimensional and three-dimensional models are shown in Figure 6-23.

When compared to two-dimensional model, DMP-1 expression in hDPSCs colonising the decellularised dental pulps was higher by 2.75 ± 0.30 fold at day 7, 4.42 ± 0.45 fold at day 14 and 4.79 ± 1.90 fold at day 21 in the first donor (Figure 6-23 A), 1.52 ± 0.22 fold at day 7, 5.47 ± 0.83 fold at day 14 and 5.30 ± 0.67 fold at day 21 in the second donor (Figure 6-23 B), and 1.85 ± 0.10 fold at day 7, 5.03 ± 0.96 fold at day 14 and 4.15 ± 0.88 fold at day 21 in the third donor (Figure 6-23 C).

When compared to three-dimensional model, the expression level of DMP-1 in the decellularised dental pulps was higher by 2.76 ± 0.30 fold at day 7, 3.31 ± 0.34 fold at day 14 and 3.11 ± 1.23 fold at day 21 in the first donor (Figure 6-23 A), 1.34 ± 0.20 fold at day 7, 5.44 ± 0.83 fold at day 14 and 5.02 ± 0.64 fold at day 21 in the second donor (Figure 6-23 B), and 1.71 ± 0.09 fold at day 7, 4.46 ± 0.85 fold at day 14 and 5.06 ± 1.07 fold at day 21 in the third donor (Figure 6-23 C).

The global analysis showed DMP-1 expression level upregulated in hDPSCs colonising the decellularised pulps as compared to both two-dimensional and three-dimensional models at all the examined time points (Figure 6-23 D).

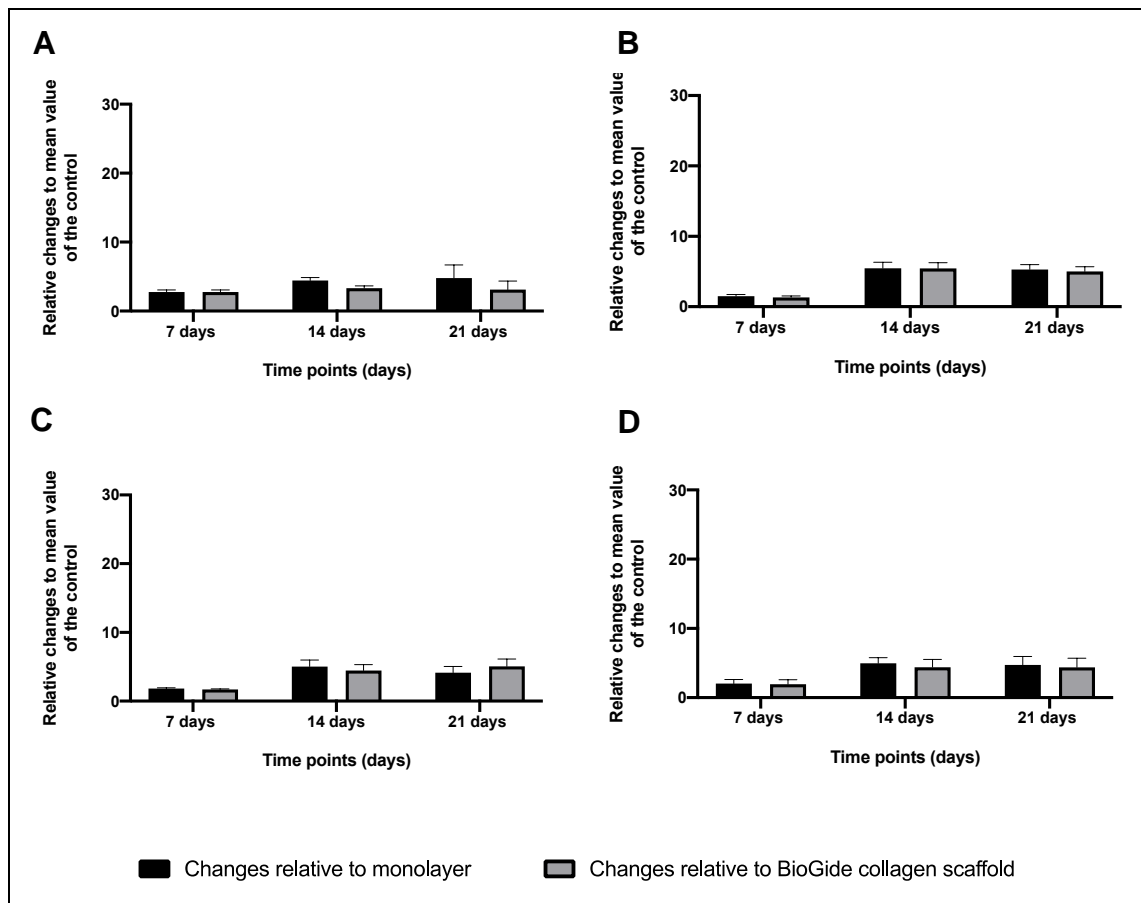


Figure 6-23: Bar graphs demonstrate the changes in DMP-1 gene expression in hDPSCs grown on the decellularised dental pulps compared to similar cells grown on the controls. The expression of DMP-1 gene in hDPSCs harvested from (A) 1st donor, (B) 2nd donor and (C) 3rd donor then grown on the decellularised dental pulps *in vitro* under basal conditions for 7, 14 and 21 days was normalised to gene expression in similar cells grown under the basal conditions on monolayers or BioGide[®] collagen scaffolds. Data represents mean $2^{-\Delta\Delta Ct}$ (n = 3) \pm standard deviation. (D) Global analysis show the average relative expression of DMP-1 gene of all donors at the examined time points.

MEPE

The results of gene expression analysis of MEPE in hDPSCs grown on the decellularised dental pulps compared to similar cells grown in two-dimensional and three-dimensional models are shown in Figure 6-24.

When compared to two-dimensional model, the fold change in MEPE gene expression in hDPSCs grown in the decellularised dental pulps was 1.08 ± 0.34 fold at day 7, 1.49 ± 0.03 fold at day 14 and 1.86 ± 0.87 fold at day 21 in the first donor (Figure 6-24 A), 1.05 ± 0.44 fold at day 7, 1.05 ± 0.18 fold at day 14 and 1.08 ± 0.41 fold at day 21 in the second donor (Figure 6-24 B), and 1.67 ± 0.12 fold at day 7, 1.67 ± 0.65 fold at day 14 and 1.85 ± 0.40 fold at day 21 in the third donor (Figure 6-24 C).

When compared to three-dimensional model, the changes in MEPE gene expression in hDPSCs grown on the decellularised dental pulps were 1.06 ± 0.34 fold at day 7, 1.07 ± 0.02 fold at day 14 and 1.19 ± 0.56 fold at day 21 in the first donor (Figure 6-24 A), 1.02 ± 0.43 fold at day 7, 1.01 ± 0.19 fold at day 14 and 1.08 ± 0.41 fold at day 21 in the second donor (Figure 6-24 B), and 1.06 ± 0.07 fold at day 7, 1.27 ± 0.49 fold at day 14 and 1.75 ± 0.38 fold at day 21 in the third donor (Figure 6-24 C).

The global analysis revealed no significant change in MEPE gene expression level in hDPSCs colonising the decellularised pulps as compared to similar cells cultured in two-dimensional and three-dimensional models at all the examined time points (Figure 6-24 D).

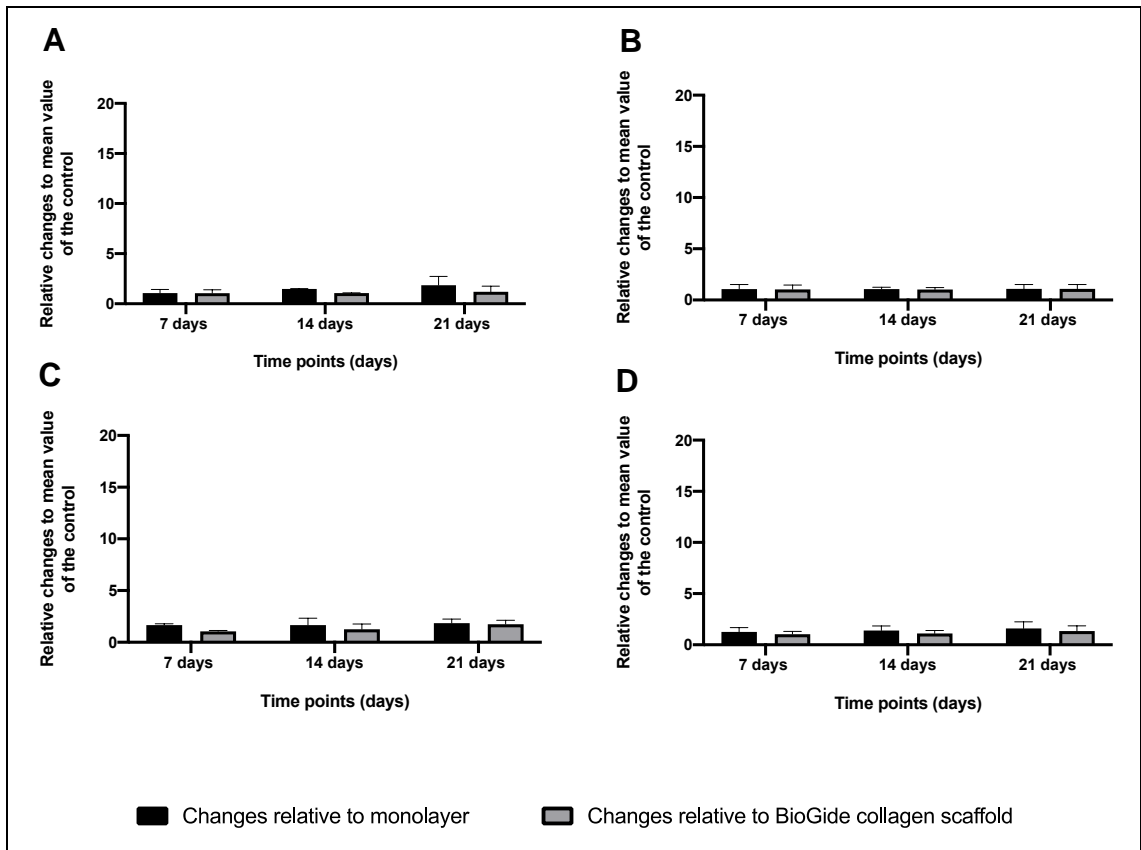


Figure 6-24: Bar graphs demonstrate the changes in MEPE gene expression in hDPSCs grown on the decellularised dental pulps compared to similar cells grown on the controls. The expression of MEPE gene in hDPSCs obtained from (A) 1st donor, (B) 2nd donor and (C) 3rd donor then grown on the decellularised dental pulps *in vitro* under basal conditions for 7, 14 and 21 days was normalised to gene expression in similar cells grown under basal conditions on monolayers or BioGide[®] collagen scaffolds. Data represents mean $2^{-\Delta\Delta Ct}$ ($n = 3$) \pm standard deviation. (D) Global analysis show the average relative expression of MEPE gene of all donors at the examined time points.

6.5.10 Detection and localisation of CD31-positive cells in hDPSCs-seeded decellularised dental pulp matrix *in vitro*

CD31-positive cells were detected and localised in hDPSCs-seeded decellularised dental pulps by means of immunohistochemical labelling following 7, 14 and 21 days of *in vitro* culture under basal conditions. The results showed positive immunoreactivity to human CD31 antigen by the cells colonising the decellularised dental pulps (Figure 6-25). At day 7, CD31-positive cells were observed mainly near the peripheral zone of the decellularised dental pulps, with only a few positive cells in the deeper zone of the scaffolds (Figure 6-25 A). At day 14, small clusters of CD31-positive cells were observed scattered in the decellularised dental pulps (Figure 6-25 B). At day 21, more positive cells were observed in the decellularised dental pulps lining the luminal surface of the vascular channels (Figure 6-25 C). No brown staining occurs in the negative control sections (Figure 6-25 D).

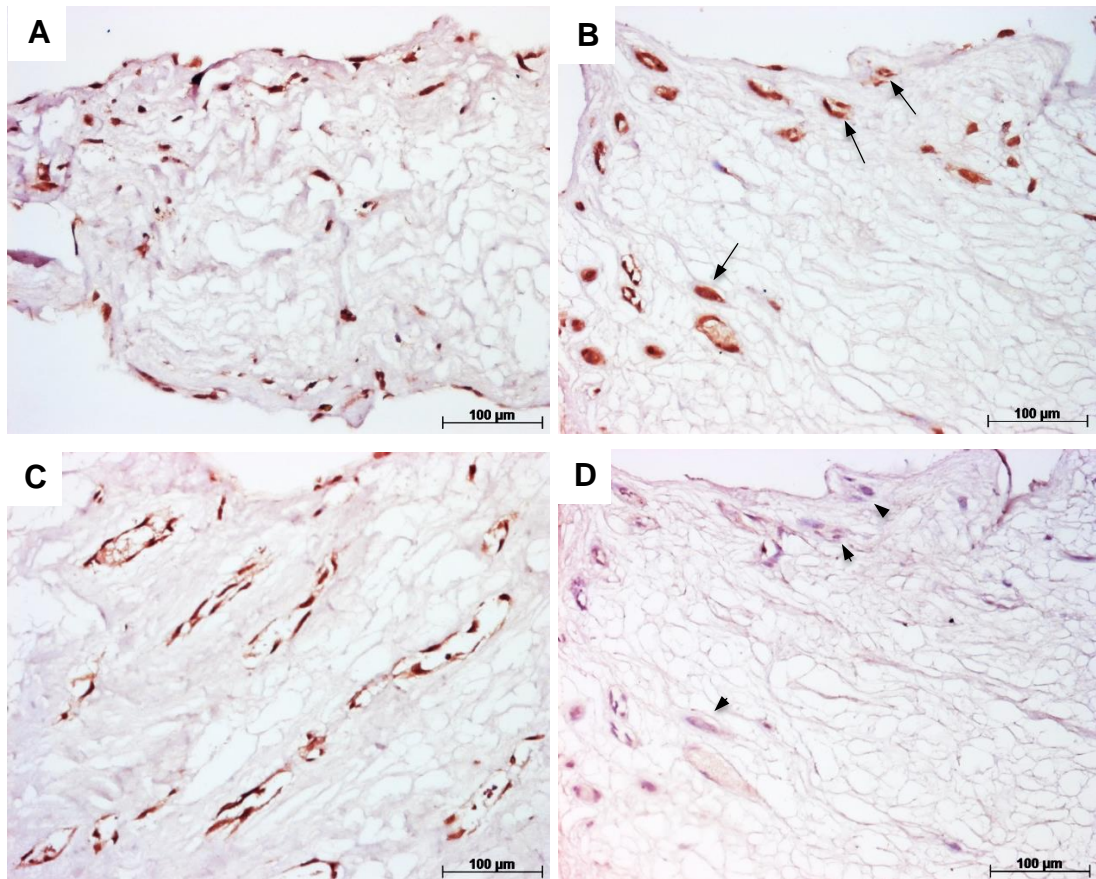


Figure 6-25: Detection and localisation of CD31-positive cells in hDPSCs-seeded decellularised dental pulps. (A, B and C) Representative bright-field microscopic images of hDPSCs-seeded decellularised dental pulps labelled with anti-human CD31 antibody following (A) 7 days, (B) 14 days and (C) 21 days of *in vitro* culture under basal conditions. The images show positive immunoreactivity to CD31 antigen (brown staining). (D) Representative negative control image of hDPSCs-seeded decellularised pulps labelled with the isotype antibody corresponding to anti-human CD31 following 14 days of *in vitro* culture. Black arrows indicate some of the positively stained cells following 14 days of culture and head arrows indicate the same cells negatively stained in the isotype control.

6.5.11 Detection and localisation of DSPP in hDPSCs-seeded decellularised dental pulp matrix *in vitro*

Images of decellularised dental pulps seeded with hDPSCs and cultured *in vitro* under basal conditions for 7, 14 and 21 days, then labelled with an antibody against human DSPP antigen are shown in Figure 6-26. A positive immunoreactivity to DSPP antigen was observed in the recellularised scaffolds at all the examined time points. At day 7, DSPP-positive staining was detected mainly at the surface of the scaffolds with a few positive areas within the stroma (Figure 6-26 A). An increase in DSPP-positive immunoreactivity was apparent following 14 and 21 days of seeding as compared to 7 days (Figure 6-26 B and C). No brown staining occurs on the negative control sections (Figure 6-26 D).

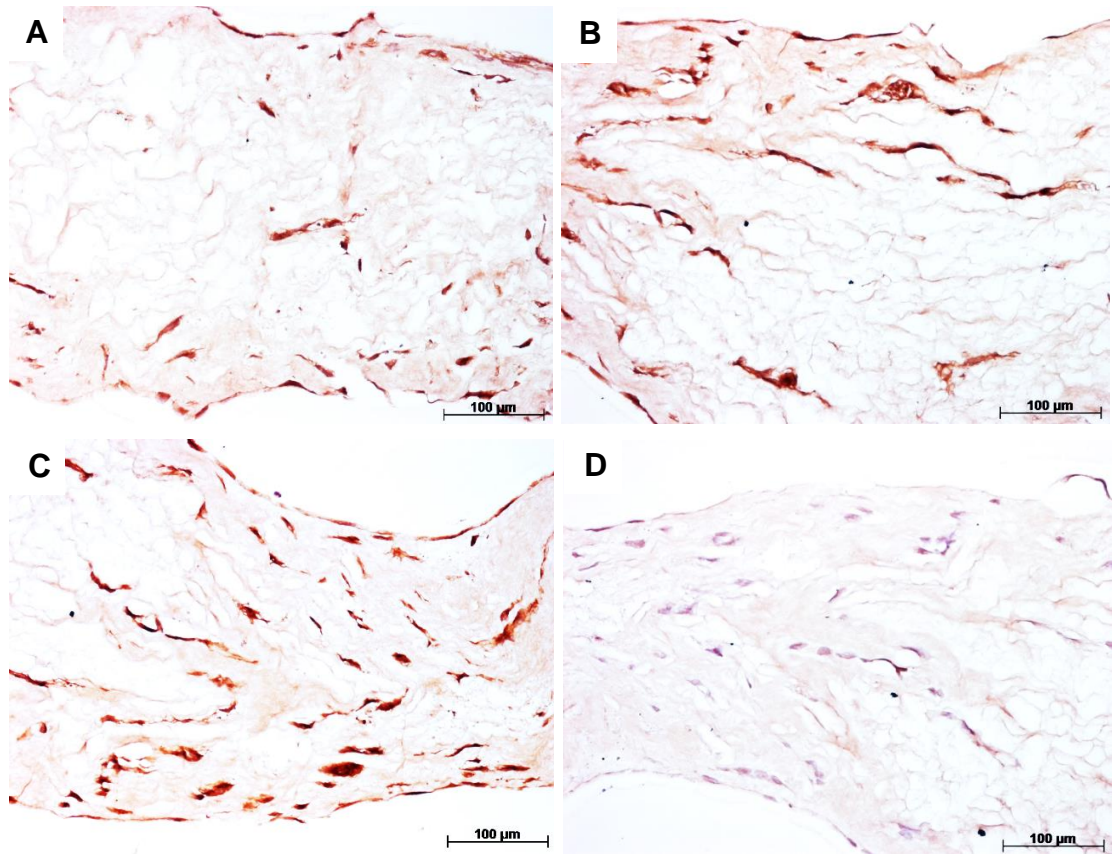


Figure 6-26: Detection and localisation of DSPP expression in hDPSCs-seeded decellularised dental pulps. (A, B and C) Representative bright-field microscopic images of hDPSCs-seeded decellularised dental pulps labelled with an antibody against human DSPP following (A) 7days, (B) 14 days, and (C) 21 days of *in vitro* culture under basal conditions. The images show positive immunoreactivity to DSPP antigen (brown staining). (D) Representative negative control image of hDPSCs-seeded decellularised pulps labelled with the isotype antibody corresponding to anti-human DSPP following 21 days of *in vitro* culture. The image show absence of brown staining.

6.6 Discussion

In the present research, the *in vitro* performance of the decellularised dental pulp matrix, developed using the gentle protocol described in Chapter 4, Section 4.4.1.2, with hDPSCs was investigated. The findings revealed pro-angiogenic and pro-odontogenic properties in the decellularised dental pulp, suggesting that the use of the developed scaffold in dental pulp regeneration could be advantageous. Dental pulp regeneration requires the availability of an appropriate scaffold with structural and compositional characteristics resembling those of the extracellular matrix. The desired scaffold should be capable of promoting cell attachment, migration, tissue-specific differentiation and angio/vasculogenesis (Galler *et al.*, 2010, Galler *et al.*, 2011a). Moreover, the scaffold should address several challenges including, but not limited to, vascularisation enhancement as well as growth factors' incorporation to promote odontoblast-like cell differentiation (Dissanayaka and Zhang, 2020).

As detailed in Chapter 4 and Chapter 5, the developed decellularised dental pulp matrix not only has retained extracellular matrix components and growth factors, but also has a retained native vasculature. The retained vascular channels in the decellularised dental pulp could have the potential to develop interconnections with the host microvessels following *in vivo* implantation, leading to blood flow in the new vessel connections. This process, which is referred to as inosculation (Laschke *et al.*, 2009), involves the growth of vascular sprouts from the host microvessels towards the connecting ends of the vascular channels retained in the decellularised dental pulp, or vice versa. This growth of vascular sprouts has been reported to be directed by the endothelial cells located at the tips of the sprouts, which extend multiple filopodia along the VEGF-A gradient (Gerhardt *et al.*, 2003, Gerhardt and Betsholtz, 2005). This process results in sprouts'

elongation and eventual connection with adjacent sprouts to form continuous lumina and establish blood flow.

Endothelial cells thus play an active role in orchestrating the process involved in the vascularisation. Seeding of the endothelial cells into a decellularised scaffold has been shown to achieve encouraging results in terms of the vascularisation enhancement (Pellegata *et al.*, 2018). However, endothelial cells' use is highly limited due to the difficulties in culture expansion techniques and the insufficient number of cells available for implantation (Novosel *et al.*, 2011). Given this limitation, the use of mesenchymal stem cells, which have the potential to enhance angiogenesis in the scaffold, has been suggested as a promising strategy (Egaña *et al.*, 2009). These cells could contribute to the vascularisation process, either through differentiating into endothelial-like cells or through releasing angiogenic growth factors (paracrine effect). In a study by Zhao *et al.* (2010), endothelial-like cell differentiation of bone marrow-derived mesenchymal stem cells was observed following seeding into a decellularised arterial scaffold. Furthermore, Liu *et al.* (2011) reported that seeding of adipose-derived mesenchymal stem cells, into two types of decellularised scaffolds, resulted in increased secretion of vascular endothelial growth factor by the cells and enhanced vascularisation capacity of the scaffolds.

Mesenchymal stem cells are a type of postnatal stem cell that are found throughout the body in many tissues and organs after birth (Egusa *et al.*, 2012). These stem cells can be identified in culture based on three standard criteria proposed by the mesenchymal and tissue stem cell committee of the international society for cellular therapy (Dominici *et al.*, 2006). The criteria are (i) cell adherence to tissue culture flasks under the basal culture condition, (ii) cell expression of specific cell surface markers, and (iii) cell differentiation into

osteoblasts, chondroblasts and adipocytes under specific culture conditions (Dominici *et al.*, 2006). Mesenchymal stem cells have been identified and isolated from a wide range of tissues in the oral and maxillofacial region (Sloan and Waddington, 2009, Lee *et al.*, 2014).

Dental pulp stem cells represent a population of mesenchymal stem cells identified in the dental pulp of permanent teeth (Gronthos *et al.*, 2000, Gronthos *et al.*, 2002). An important characteristic of dental pulp stem cells is their odontoblastic differentiation potential (Huang *et al.*, 2009). Human dental pulp stem cells (hDPSCs) can be induced *in vitro* to differentiate into odontoblast-like cells expressing several odontogenic markers such as DSPP and DMP-1 (Couple *et al.*, 2000). Furthermore, several studies have demonstrated the potential of hDPSCs to differentiate into endothelial-like cells and express several angiogenic markers when grown *in vitro* under specialised conditions (d'Aquino *et al.*, 2007, Marchionni *et al.*, 2009, Karbanová *et al.*, 2011, Aksel and Huang, 2017). Therefore, in the present research, hDPSCs were selected for use in evaluating the *in vitro* performance of the developed decellularised dental pulp matrix. The results from cell characterisation experiments indicated mesenchymal stem cell-like qualities in the used populations of hDPSCs, which were consistent with previous reports describing the properties of hDPSCs (Gronthos *et al.*, 2000, Gronthos *et al.*, 2002, Huang *et al.*, 2009).

Prior to seeding hDPSCs onto the developed decellularised dental pulp, the cytocompatibility of the scaffold was assessed. It has been shown that inadequate washing of residual chemicals, in particular detergents such as sodium dodecyl sulphate, from the decellularised scaffolds is often associated with cytotoxicity (Cebotari *et al.*, 2010). Cytotoxicity, which is possible even at low concentration of chemicals, could inhibit or completely negate the

recellularisation potential of the decellularised scaffolds (Rieder *et al.*, 2004). In the present research, the contact and extract cytotoxicity assays indicated no apparent cytotoxicity in the developed decellularised dental pulp, neither on the growth of cells cultured in direct contact with the scaffold nor on the viability of cells cultured on an extract of the decellularised dental pulp. The lack of cytotoxicity in the decellularised scaffolds has been linked to the use of multiple washing cycles in combination with mechanical agitation (Wilshaw *et al.*, 2012).

As the decellularised dental pulp showed good cytocompatibility, it was seeded with hDPSCs to assess its potential to support cell attachment, viability and growth. A dynamic cell seeding technique was used to enhance cell seeding efficiency and uniformity. Upon seeding of the hDPSCs onto the decellularised dental pulp, the cells were able to attach, proliferate and migrate through the scaffold, demonstrating its suitability for cell binding and growth. Cell attachment might have been mediated by the interaction of integrins, which are transmembrane cell surface adhesion receptors, with specific ligands in the extracellular matrix components of the decellularised dental pulp (Hynes, 1992). A high affinity to RGD subunits in fibronectin has been reported in progenitor stem cell populations expressing high levels of $\alpha 5$ and $\beta 1$ integrins (Dowthwaite *et al.*, 2004, Waddington *et al.*, 2009). Since fibronectin is among the extracellular matrix components recovered in the decellularised dental pulp matrix, as demonstrated in Chapter 5, it might have played a role in mediating cell attachment to the scaffold.

Excellent cell viability was observed on the decellularised dental pulp, confirming its cytocompatibility. Interestingly, the early migrated cells settled around the vascular channels before repopulating the entire scaffold. Histological and immunohistochemical analyses of *in vitro* engineered tissue showed hDPSCs

aligning the luminal surface of the decellularised dental pulp's vasculature and exhibiting positive immunoreactivity to CD31 antigen. Gene expression analysis of hDPSCs grown in the decellularised dental pulp, relative to similar cells grown in two-dimensional and three-dimensional models, showed an increase in the expression of two angiogenic markers, namely kinase insert domain receptor (KDR) and platelet and endothelial cell adhesion molecule (PECAM-1). Interestingly, this enhancement of angiogenic markers expression took place in the absence of specialised differentiation media. This suggests that the developed decellularised dental pulp, like many other reported decellularised scaffolds (Sun *et al.*, 2016, Rameshbabu *et al.*, 2018), is a pro-angiogenic scaffold characterised by the retention of the vasculature and several angiogenic growth factors in the matrix following decellularisation.

Among growth factors that have demonstrated retention in the developed decellularised dental pulp are VEGF-A and FGF-2, two powerful angiogenic growth factors known to be effective in promoting microvascular formation. These growth factors are used frequently in tissue engineering to improve scaffold vascularisation by stimulating angiogenic host tissue response at the implantation site (Kaigler *et al.*, 2006, Guan *et al.*, 2007, Zhao *et al.*, 2009, He *et al.*, 2011). VEGF, in particular, is known to play a role in inducing the angiogenic differentiation of hDPSCs (Matsushita *et al.*, 2000), stimulating the proliferation of endothelial cells and promoting their adhesion, survival and migration (Byzova *et al.*, 2000). In light of the described functions of VEGF-A and FGF-2 together with their detected localisation around the decellularised dental pulp's vasculature, these growth factors, at least in part, are responsible for the migration and enhancement of angiogenic markers expression in hDPSCs.

Another interesting finding, observed following seeding hDPSCs onto the decellularised dental pulp, was the gene expression upregulation of two odontogenic markers, namely dentine sialophosphoprotein (DSPP) and dentine matrix protein 1 (DMP-1). Changes in the expression profile of these two genes have been used as a marker of odontoblast-like cell differentiation (Casagrande *et al.*, 2010, Demarco *et al.*, 2010). DSPP and DMP-1 genes are known to be expressed in differentiating odontoblasts and are responsible for the coding of non-collagenous proteins that have roles in dentine mineralised matrix formation (Couple *et al.*, 2000, Butler *et al.*, 2002, Wei *et al.*, 2007). Matrix extracellular phosphoglycoprotein (MEPE) is another putative marker of odontoblast-like cell differentiation. This protein plays a role in regulating odontogenesis through mineralisation inhibition during advanced stages of odontogenesis (Liu *et al.*, 2005). The increase in DSPP and DMP-1 gene expression, together with immunohistochemical detection of DSPP protein on the *in vitro* engineered tissues, suggests that a fraction of hDPSCs, following seeding onto the decellularised dental pulps, have undergone differentiation into odontoblast-like cells and acquired the capacity to initiate dentine-like matrix secretion. This links well with the findings reported by Song *et al.* (2017), demonstrating odontoblast-like cell differentiation of apical papilla stem cells (SCAP) following seeding onto a decellularised dentine-pulp disk. However, in their study, they assume that the odontoblast-like cell differentiation of SCAP was due to the effect of growth and differentiation factors released from dentine walls of the decellularised disks. In contrast, the results of the present research showed the decellularised dental pulp tissue clearly contributing to the odontoblast-like cell differentiation, since no dentine matrix exists, neither were exogenous differentiation factors used.

Collectively, the present research has demonstrated the *in vitro* performance of the developed decellularised dental pulp with hDPSCs. The decellularised dental pulp exhibited pro-angiogenic and pro-odontogenic properties. Seeding of hDPSCs onto the decellularised dental pulp led to progressive cell repopulation of the matrix and vasculature and enhanced expression of the markers involved in angiogenesis and odontogenesis in hDPSCs. Overall, the decellularised dental pulp showed promising results in terms of providing the cells with the correct microenvironment to support dental pulp regeneration. *In vivo* performance of the decellularised dental pulp was investigated and is described in the next chapter.

Chapter 7

***In vivo* performance of the developed decellularised dental pulp matrix**

7.1 Introduction

There are two possible tissue engineering approaches for dental pulp regeneration, namely cell transplantation and cell homing. In the former, an *ex vivo* population of autologous stem cells is loaded onto a scaffold and transplanted into the host root canal to allow tissue regeneration (Conde *et al.*, 2016, Sui *et al.*, 2019). Conversely, the cell homing approach is based on recruiting the host endogenous stem cells to the root canal via chemotactic signalling (Kim *et al.*, 2010, Eramo *et al.*, 2018). Both approaches requires an appropriate scaffold to support cell growth and new tissue formation. The scaffold should address several challenges, specific to each approach, such as the capability of facilitating vascularisation to maintain post-implantation cell survival in the cell transplantation approach, and the incorporation of chemotactic signalling to promote cell recruitment in the cell homing approach (Piva *et al.*, 2014, Dissanayaka and Zhang, 2020). The presence of growth and differentiation factors relevant to odontoblast-like cell differentiation is also an essential candidate scaffold characteristic for both approaches (Dissanayaka and Zhang, 2020).

In Chapter 6, the potential of a decellularised dental pulp matrix to support the growth of hDPSCs and promote vascularisation and odontoblast-like cell differentiation was demonstrated *in vitro*. Decellularised scaffolds of different tissues have been shown to produce chemoattractant peptides following

enzymatic degradation *in vitro* (Brennan *et al.*, 2008) and to attract stem cells from the neighbouring tissues following implantation *in vivo* (Beattie *et al.*, 2009). Dziki *et al.* (2016) reported the mobilisation and recruitment of CD149⁺ perivascular stem cells to the margin and centre of a decellularised small intestinal submucosa scaffold, following *in vivo* implantation in mice. A similar observation was recorded by Perniconi *et al.* (2011) showing detection of PW1⁺ muscle interstitial stem cells in a decellularised skeletal muscle scaffold, following two weeks of *in vivo* implantation. As such, in this work it was hypothesised that the developed decellularised dental pulp matrix might serve as a suitable scaffold for dental pulp regeneration approaches. To begin testing this hypothesis, a preliminary study was conducted using an animal model.

Several animal models, including mice, ferrets, dogs and miniature swine, have been utilised when investigating the suitability of different scaffolds for use in dental pulp regeneration approaches (Nakashima *et al.*, 2019). These models are divided, based on the location where the dental pulp regeneration is tested, into ectopic, semi-orthotopic and orthotopic. In the research work presented in this chapter, a semi-orthotopic dental pulp regeneration model, consisting of human premolar root slices implanted subcutaneously into immunodeficient mice, was used in the preliminary testing of decellularised dental pulp potential to support dental pulp regeneration *in vivo* when used in an acellular or recellularised form.

7.2 Aim and objectives

Aim

The aim of the research work presented in this chapter was to evaluate the potential of the generated decellularised dental pulp matrix to support dental pulp regeneration *in vivo*.

Objectives

- To assess the possibility of inserting intact decellularised dental pulp in a debrided root canal of human root slices.
- To investigate the vascularisation capacity of a decellularised dental pulp matrix seeded with hDPSCs.
- To evaluate the potential of an unseeded decellularised dental pulp matrix to mobilise and recruit host cells from the neighbouring tissues following *in vivo* implantation.

7.3 Experimental approach

A semi-orthotopic dental pulp regeneration model, consisting of a debrided human premolar root slice and a severely combined immunodeficient (SCID) mouse, was used to evaluate the potential of the decellularised dental pulps to support dental pulp regeneration *in vivo*. Decellularised dental pulps, either seeded or unseeded with hDPSCs, were initially inserted in the debrided root canal of human premolar root slices. The constructs were then implanted subcutaneously into SCID mice. After 30 days, the samples were retrieved and analysed qualitatively, using histological (H&E) and immunohistochemical staining. Furthermore, the density of blood-perfused vascular channels in the tissues engineered using hDPSCs-seeded decellularised dental pulps was determined and compared to that of the unseeded decellularised dental pulps and the native dental pulps.

7.4 Methods

7.4.1 Preparation of the root slices

Freshly extracted healthy human premolars were collected in the department of oral surgery at Leeds Dental Institute (Leeds, UK) from young donors (14 - 18 year old patients) following written informed patients' consents and according to the ethical approval obtained from NHS Health Research Authority, East Midlands–Nottingham-2 Research Ethics Committee (reference number 17/EM/0040, Appendix A). The teeth were transported to the laboratory in specimen pots containing sterile PBS. The external surfaces of the teeth were then cleaned from residual soft tissues using a scalpel blade and disinfected using 70% (v/v) ethanol. Subsequently, annular root slices of approximately 3 mm thickness were prepared by cutting the roots horizontally at the cervical third

using a water-cooled cutting machine (Accutom[®]-5). Dental pulp tissues were then extirpated, and the canals were subjected to instrumentation using sterile Kerr endodontic files up to size 80 with frequent irrigation with sterile PBS. Following this, root slices were soaked in 70% ethanol for 30 minutes, followed by PBS supplemented with penicillin and streptomycin (100 units of each per mL) for 30 minutes. Subsequently, root slices were washed in sterile PBS followed by a final wash with 17% (w/v) EDTA to remove the smear layer. Root slices were then incubated in α -MEM supplemented with 10% FCS for 48 hours at 37°C to confirm the absence of microbial contamination. Root slices were then washed and maintained in sterile PBS at 4°C until used.

7.4.2 Preparation of the root slice/scaffold constructs

Root slices were randomly divided into three groups (n = 4 slices per group). The first group received decellularised dental pulps seeded with hDPSCs and cultured *in vitro* for 14 days, the second group received unseeded decellularised dental pulps, and the third group was left empty for use as a control. In the first and second group, the scaffolds were aseptically cut into 3 mm long samples before inserting into the root slices. Samples of the three groups were placed in 12-well plates containing 2 mL of alpha MEM supplemented with 10% (v/v) FBS, 1% (v/v) 2 mM L-Glutamine, 100 U.mL⁻¹ Penicillin and 100 μ g.mL⁻¹ Streptomycin and incubated overnight at 37°C in 5% (v/v) CO₂ and 95% relative humidity until the next morning. The samples were then implanted subcutaneously into SCID mice as described below in Section 7.4.3.

7.4.3 *In vivo* implantation

All animal procedures were carried out according to the guidelines laid down by the Animal (Scientific Procedures) Act 1986 and followed a protocol approved by

the Animal Welfare and Ethical Review Committee at the University of Leeds with a personal license granted from the Home Office (Reference number I2E7F18DE; Appendix A) and under the project license of Dr Xuebin Yang (Reference number 70/8549).

Severely combined immunodeficient mice (5 - 7 week old males, CB17 SCID, Charles River, Kent, UK) were used in this experiment (n = one mouse per group). The surgical procedure was conducted under general anaesthesia using 5% isoflurane as shown in Figure 7-1. Four incisions were initially made in the dorsal body surface of each mouse (two in the shoulder area and two in the lumbar area). Subcutaneous pockets were then created by blunt dissection. The experimental samples were then implanted in the pockets and the surgical wounds were closed using non-resorbable sutures (ETHILON® Nylon suture). Injectable Vetergesic® (Ceva animal health Ltd, Amersham, United Kingdom) was used post-operatively (0.05 mg.kg⁻¹) for pain control. All mice were housed in the animal facility at St. James Biomedical Services at the University of Leeds. The food and drink were provided under 12 hours day/night cycle and the surgical wounds were checked regularly.

After 30 days, all mice were euthanised according to the regulations of the Home Office for humane killing of animals (Schedule I: rising concentration of carbon dioxide followed by cervical dislocation). The experimental samples were then retrieved and analysed as described below.

7.4.4 Histological and immunohistochemical analyses

All samples were fixed in 10% (v/v) NBF and then decalcified by full immersion in pots containing a commercially available EDTA-based decalcification solution (Decal III). The decalcification solution was changed every three days until two

non-experimental root slices displayed no resistance for cutting with a scalpel blade (this was after 14 days). Following decalcification, the samples were processed, embedded in paraffin wax and serial sectioned at 5 µm as described in Chapter 3, Section 3.2.2. Non-implanted root slices with their native dental pulps not removed (n = 4) were used as an additional control.

For the histological analysis, tissue sections were stained using H&E, as described in Chapter 3, Section 3.2.3.1. The presence of hDPSCs in the root slices which received hDPSCs-seeded decellularised dental pulps was assessed using immunohistochemical staining. Tissue sections were labelled with a mouse monoclonal antibody against human nuclei as described in Chapter 3, Section 3.2.4. An isotype control antibody was used as a negative control at the same concentration and under the same condition but with omission of the primary antibody. All histological and immunohistochemical stained sections were viewed under a bright-field microscope with normal Köhler illumination and Images were captured digitally.

7.4.5 Quantification of the blood-perfused vessels in the experimental samples

The density of functional blood-perfused vessels (blood vessels infiltrated with erythrocytes) was determined in H&E-stained tissue sections obtained from hDPSCs-seeded and unseeded decellularised dental pulps groups as well as from the native dental pulps group (n = 27 sections per group). In each tissue section, four high power fields (X200) were randomly selected, and the number of blood vessels infiltrated with erythrocytes was recorded. The results were then statistically analysed using a Kruskal-Wallis test with post hoc comparisons ($P < 0.05$).

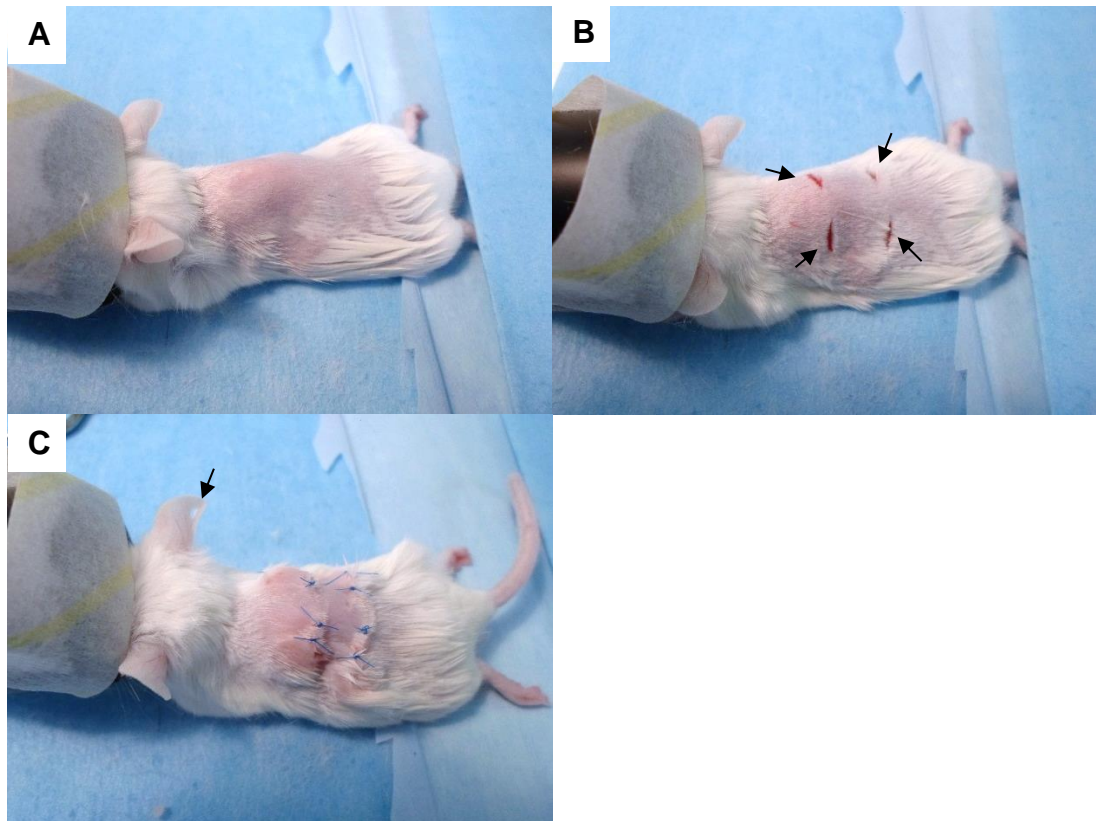


Figure 7-1: Surgical implantation of the root slice/scaffold constructs in the dorsal subcutaneous space of SCID mice. Representative images showing the steps involved in the surgical implantation of the root slice/scaffold constructs in the SCID mice. (A) Each mouse was anaesthetised using 5% isoflurane inhalation, then placed on a warming pad to control the body temperature and the dorsum hair was shaved. (B) Four incisions were made on the dorsal surface (black arrows) and subcutaneous pockets were created using blunt dissection. (C) The root slice/scaffold constructs were then implanted inside the pockets and the wounds were closed. All mice were transferred to the recovery chamber and then back to the husbandry cage after recovery.

7.5 Results

7.5.1 Macroscopic analysis of the tissues-engineered *in vivo* using hDPSCs-seeded and unseeded decellularised dental pulps

A representative image of a mouse at the samples' retrieval time is shown in Figure 7-2. All mice showed normal body activities and were healthy throughout the duration of the experiment. Healing of the surgical wounds was clearly visible at the retrieval time and regrowth of the hair in the surgical area was observed.

Macroscopic images of the root slice/scaffold constructs at the retrieval time are shown in Figure 7-3. All the constructs were encapsulated with fibrous membranes attached to the mouse subcutaneous tissues. The root slices which received hDPSCs-seeded or unseeded decellularised dental pulps showed vascularised soft tissues in the root canals with clear anastomoses to the host vasculature (Figure 7-3 A and B). The vascular network in the group which received hDPSCs-seeded decellularised dental pulps appeared more organised compared to the unseeded decellularised dental pulps' group. The empty root slices showed ingrowth of the mouse subcutaneous tissues (Figure 7-3 C).

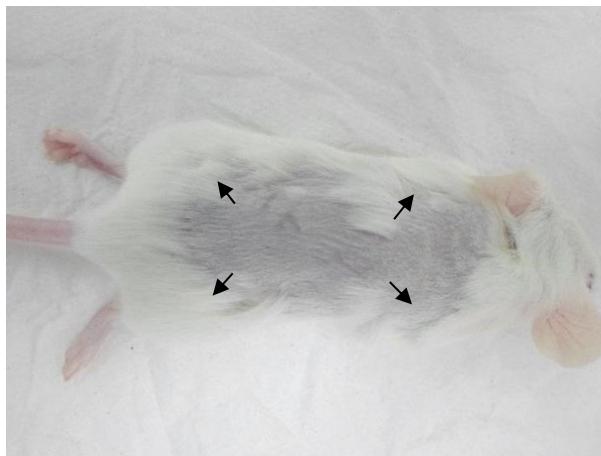


Figure 7-2: A representative image of a mouse at the samples' retrieval time. The image shows healing of the surgical wounds (black arrows) with hair regrowth over the mouse's dorsal body surface.

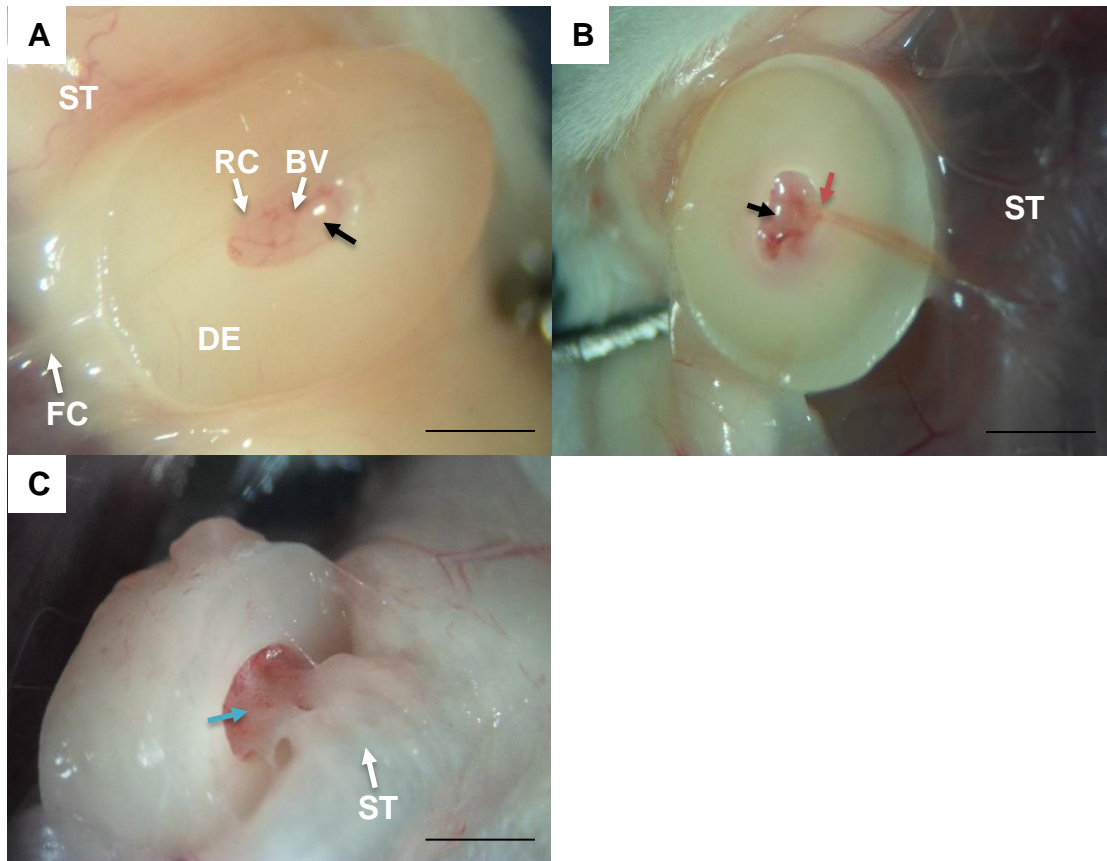


Figure 7-3: Macroscopic images of the root slice/scaffold constructs at the retrieval time. Representative images of the root slices with (A) hDPSCs-seeded decellularised dental pulps, (B) unseeded decellularised dental pulps show vascularised soft tissues in the root canals (black arrow) with anastomoses to the host vasculature (red arrow). (C) A representative image of an empty root slice shows ingrowth of the mouse subcutaneous tissue (blue arrow). (DE) Dentine, (RC) Root canal, (BV) Blood vessels, (FC) Fibrous capsule, (ST) Mouse subcutaneous tissue. Scale bars represent 2 mm.

Histological analysis of the tissues-engineered *in vivo* using hDPSCs-seeded and unseeded decellularised dental pulps

Images of H&E-stained sections of human premolar root slice with native dental pulp are shown in Figure 7-4. The native dental pulp appeared as a soft connective tissue occupying the root slice's pulp space and exhibiting intimate contact with the surrounding dentine walls (Figure 7-4 A). The tissue has a heterogeneous population of cells dispersed within an extracellular matrix consisting of fibres and ground substance. At the periphery of the dental pulp tissue, the odontoblasts layer was observed with the cells exhibiting a pseudostratified organisation pattern and showing cellular processes in the dentinal tubules (Figure 7-4 B, C, D and E). Multiple capillaries appeared in the sub-odontoblastic layer with large blood vessels in the pulp core. The cell-free zone was not visible, whilst the cell-rich zone and the pulp core were apparent.

Images of H&E-stained sections of the tissue-engineered *in vivo* in a human premolar root slice using unseeded decellularised dental pulp are shown in Figure 7-5. The engineered tissue presented the soft connective tissue's histological features and was populated with cells migrated from the host (Figure 7-5 A). The cells followed a random and non-uniform distribution pattern throughout the engineered tissue and exhibited, mainly, a spindle-shape morphology. Multiple blood-perfused vessels were visible within the tissue. At the dentin-tissue interface, two histological features were observed. Elongated spindle-shaped cells aligned the existing dentinal walls in some areas (Figure 7-5 B, C and D), whilst scaffold's degradation was apparent in other regions (Figure 7-5 E).

Images of H&E-stained sections of the tissue-engineered *in vivo* in a human premolar root slice using hDPSCs-seeded decellularised dental pulp are shown in Figure 7-6. The engineered tissue appeared as a soft connective tissue populated with cells and has multiple blood vessels with erythrocytes in their lumina indicating they were functional (Figure 7-6 A). At the periphery of the engineered tissue, multiple cells appeared aligning the existing dentinal walls (Figure 7-6 B, C, D and E). Some of the cells showed cytoplasmic processes extending in the dentinal tubules (Figure 7-6 B). Toward the core of the pulp space, a zone rich with a heterogeneous population of cells was visible. Round, cuboidal and elongated spindle-shaped cells were all seen in this zone.

Images of H&E-stained sections of the tissue grew in the empty root slice after 30 days of subcutaneous implantation in SCID mice are shown in Figure 7-7. The tissue presented the adipose tissue's histological features. Moreover, the tissue has cells exhibiting a signet ring appearance due to the accumulation of lipid droplets in the cytoplasm, causing the nuclei to move peripherally. The tissue's histological features were very distinct from the tissues engineered in the root slices using hDPSCs-seeded and unseeded decellularised dental pulps.

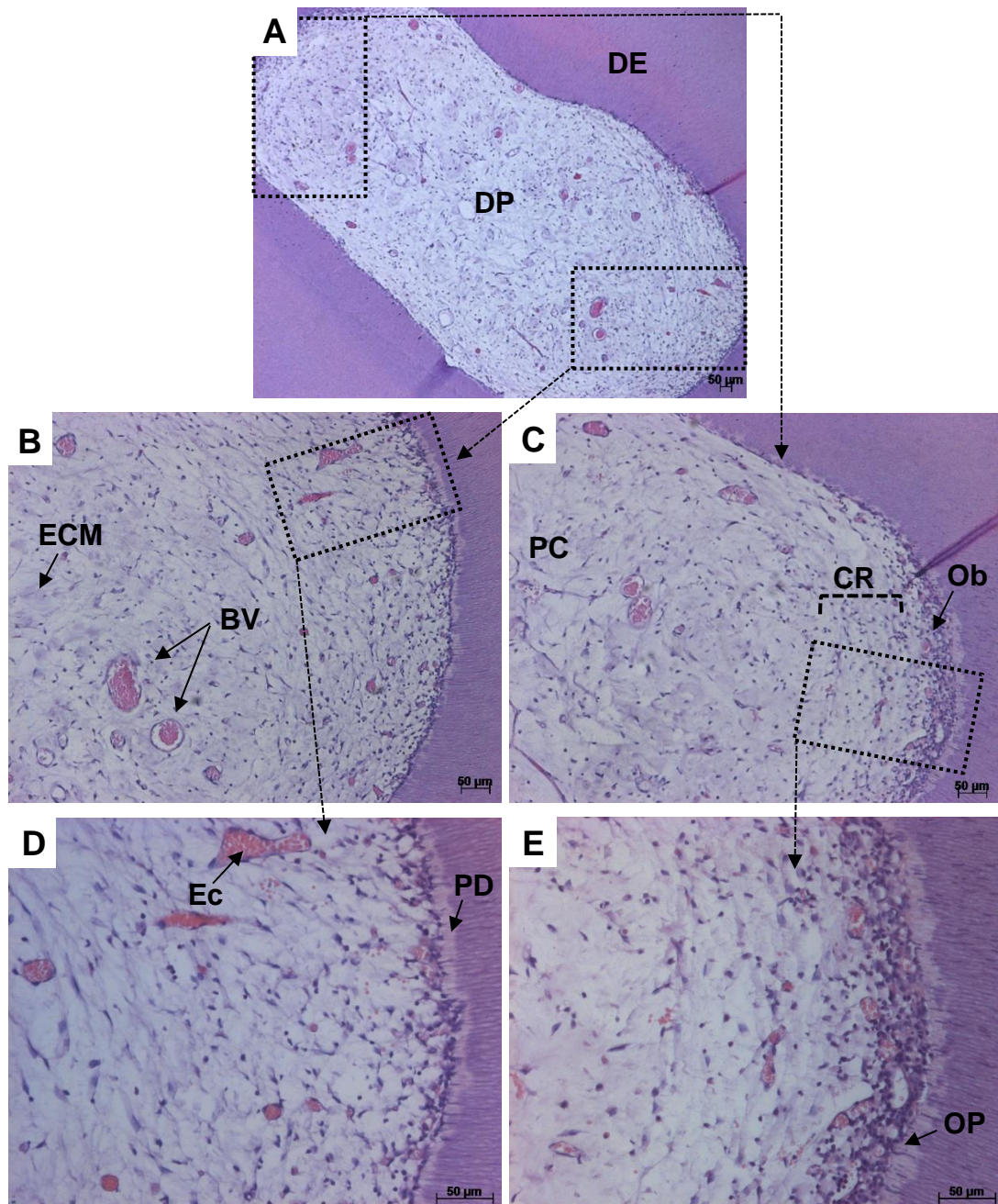


Figure 7-4: Bright-field microscopic images of H&E-stained sections of a root slice with native dental pulp. (A) Representative image of a human root slice with native dental pulp shows the normal histomorphological characteristics of the tissue. (B and C) High power magnification of the areas delineated in image A. (D and E) High power magnification of the areas delineated in images B and C. Cell nuclei stained blue. (DE) Dentine, (DP) Dental pulp, (ECM) Extracellular matrix, (BV) Blood vessel, (Ob) Odontoblasts layer, (CR) Cell-rich zone, (PC) Pulp core, (PD) Pre-dentine, (OP) Odontoblastic process, (Ec) Erythrocytes.

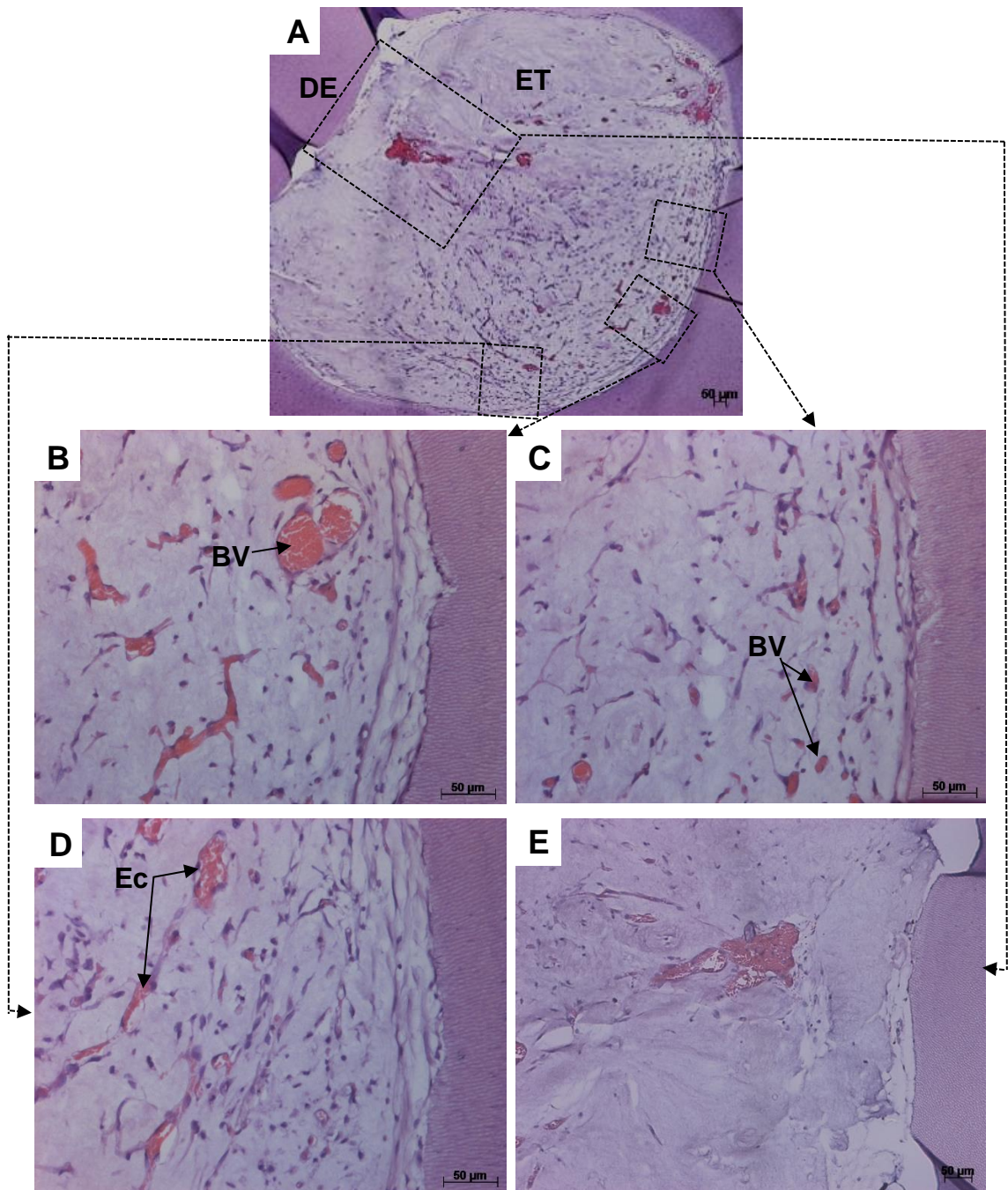


Figure 7-5: Bright-field microscopic images of H&E-stained sections of the tissue-engineered *in vivo* in a root slice using unseeded decellularised dental pulp. (A) Representative image of the engineered tissue shows a vascularised cellularised soft tissue in the root canal. (B, C, D and E) High magnification images of the areas delineated in image A. The images show the histomorphological characteristics of the engineered tissue. The cell nuclei are stained blue and the ECM is stained pink. (DE) Dentine, (ET) Engineered tissue, (BV) Blood vessel, (Ec) Erythrocytes.

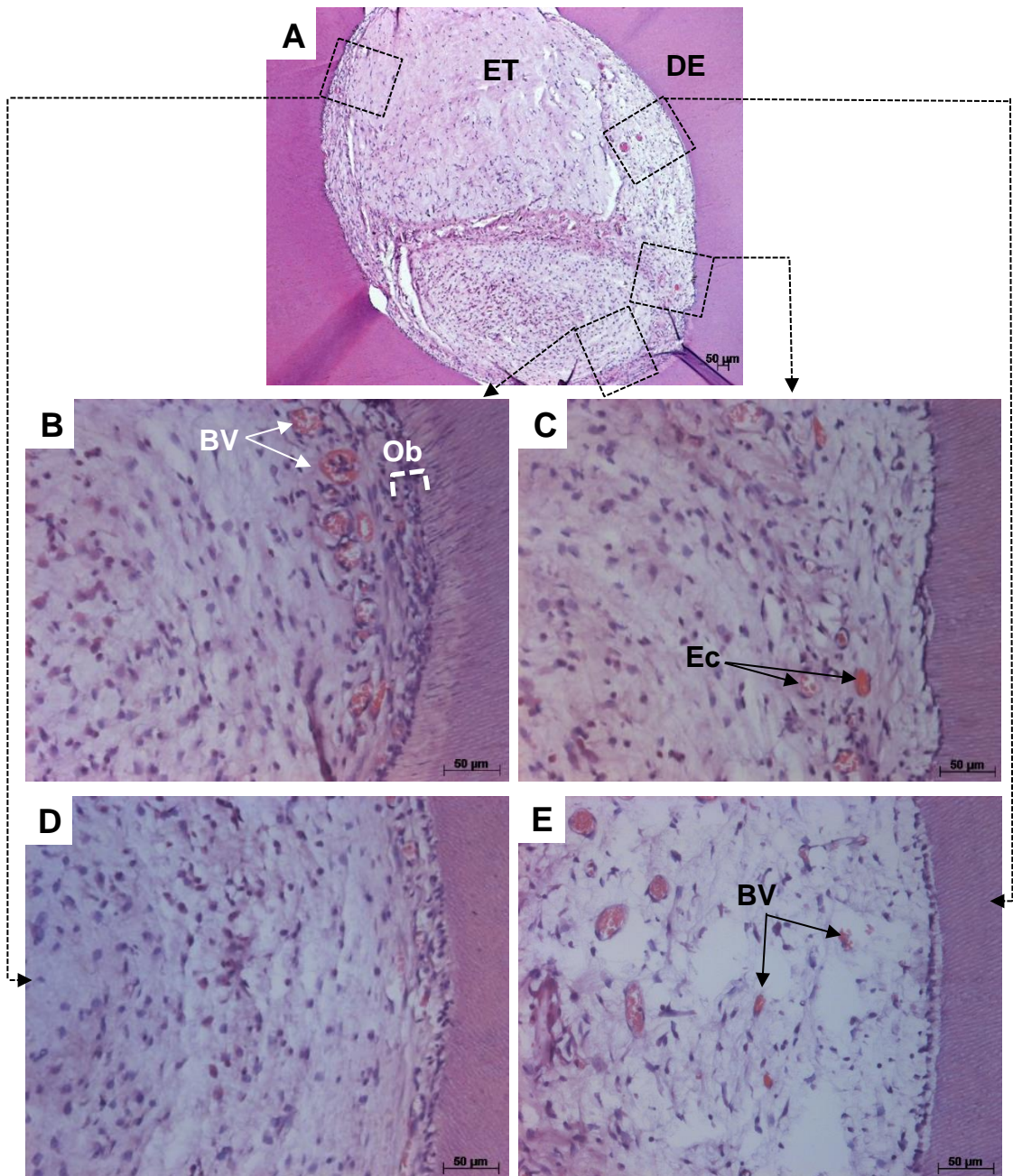


Figure 7-6: Bright-field microscopic images of H&E-stained sections of the tissue-engineered *in vivo* in a root slice using hDPSCs-seeded decellularised dental pulp. (A) Representative image of the engineered tissue shows a vascularised cellularised soft tissue in the root canal. (B, C, D and E) High magnification images of the areas delineated in image A. The images show the histomorphological characteristics of the engineered tissue. The cell nuclei are stained blue and the ECM is stained pink. (DE) Dentine, (ET) Engineered tissue, (Ob) Odontoblast-like cell layer, (BV) Blood vessel, (Ec) Erythrocytes.

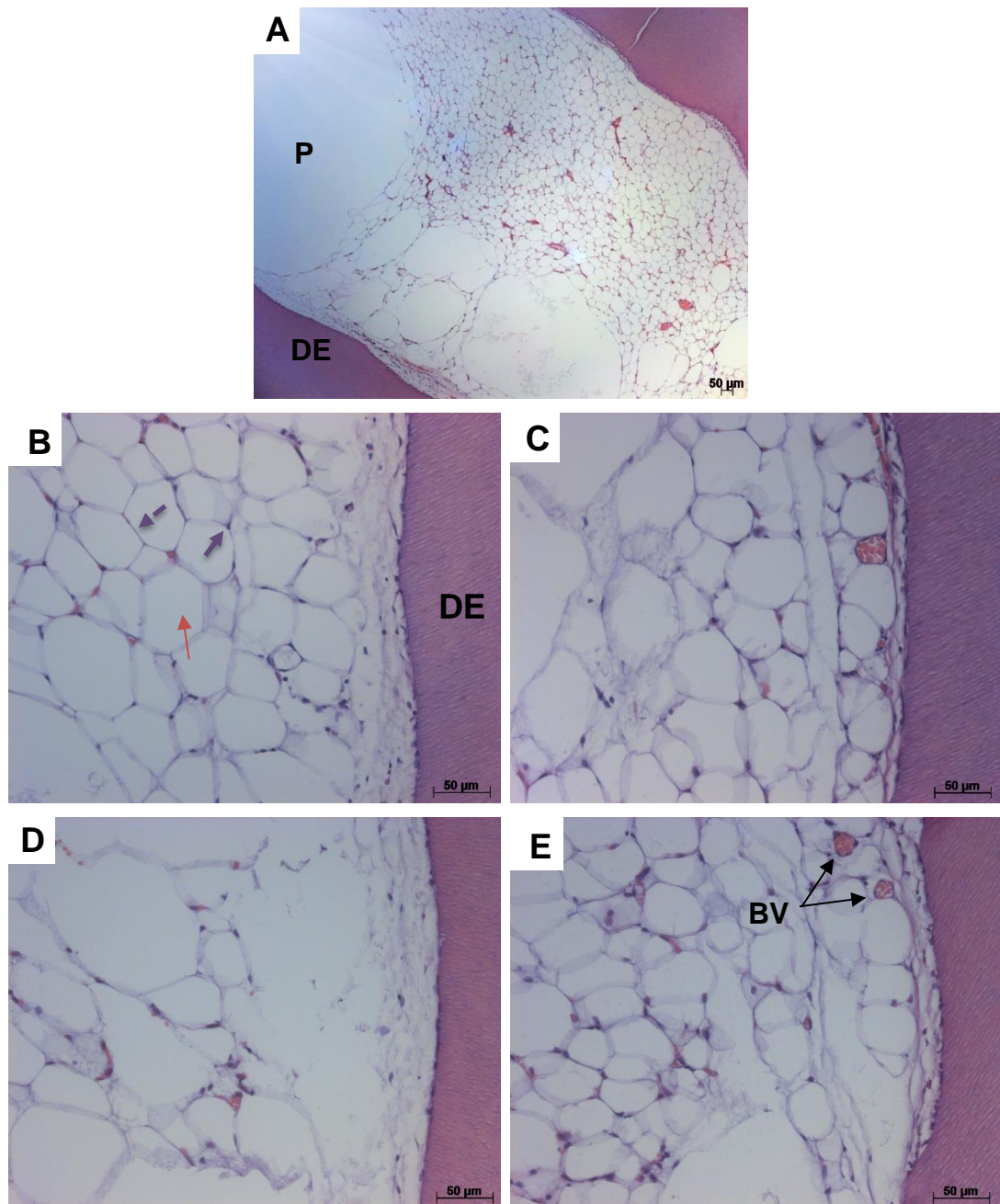


Figure 7-7: Bright-field microscopic images of H&E-stained sections of the tissue grew in an empty root slice following implantation into SCID mouse. (A) Representative image shows the histological features of the tissue. (B, C, D and E) High magnification images of the tissue show the cell nuclei as blue dots (solid purple arrow) surrounded with thin rims of cytoplasm (dashed purple arrow) containing large lipid vacuoles (red arrow). (DE) Dentine, (BV) Blood vessels.

7.5.3 Detection and localisation of hDPSCs in the tissues-engineered *in vivo* using hDPSCs-seeded decellularised dental pulps

To confirm the presence of hDPSCs in the tissues-engineered *in vivo* using hDPSCs-seeded decellularised dental pulps, tissue sections of the root slices which received hDPSCs-seeded and unseeded decellularised dental pulps were labelled with an antibody against human nuclei. The results revealed positive immunoreactivity in the group which received hDPSCs-seeded decellularised dental pulps (Figure 7-8 A) compared to negative immunoreactivity in the group which received unseeded decellularised dental pulps (Figure 7-8 B). The positively-stained cells were lining the existing dentinal walls of the root slice, dispersed within the engineered tissue and also aligning the luminal surface of the vascular channels. No brown staining occurs in the negative control (Figure 7-8 C).

7.5.4 Quantification of the blood-perfused vessels in the tissues-engineered *in vivo* using hDPSCs-seeded and unseeded decellularised dental pulps

The results of blood-perfused vessels quantification in the root slices with hDPSCs-seeded decellularised dental pulps, unseeded decellularised dental pulps and native dental pulps are demonstrated in Figure 7-9. Data analysis using a Kruskal-Wallis test with post hoc analysis revealed significant differences in the density of blood-perfused vessels in the hDPSCs-seeded decellularised dental pulps' group (mean rank = 192.3) and the native dental pulps' group (mean rank = 221.6) as compared to the unseeded decellularised dental pulps' group (mean rank = 73.56) ($H(2) = 161.8, P < 0.0001$). However, no significant difference was

found between the hDPSCs-seeded decellularised dental pulps' group and the native dental pulps' group ($P = 0.053$).

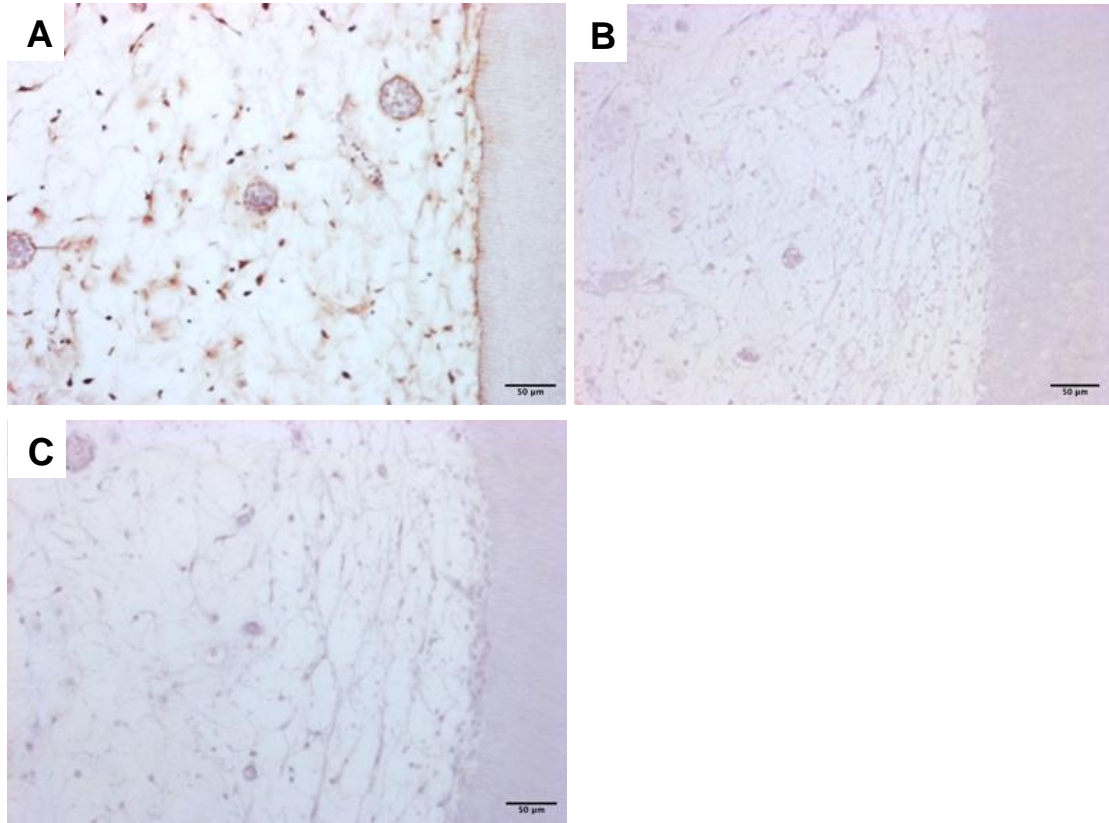


Figure 7-8: Bright-field microscopic images of the tissues-engineered *in vivo* using hDPSCs-seeded and unseeded decellularised dental pulps labelled with an antibody against human nuclei and the corresponding control isotype. (A and B) Representative images of the tissues labelled with anti-human nuclei antibody show (A) positive immunoreactivity (brown staining) in hDPSCs-seeded decellularised dental pulps' group compared to (B) negative immunoreactivity in unseeded decellularised dental pulps' group. (C) A representative image of the negative control tissue section from hDPSCs-seeded decellularised dental pulps' group shows absence of brown staining.

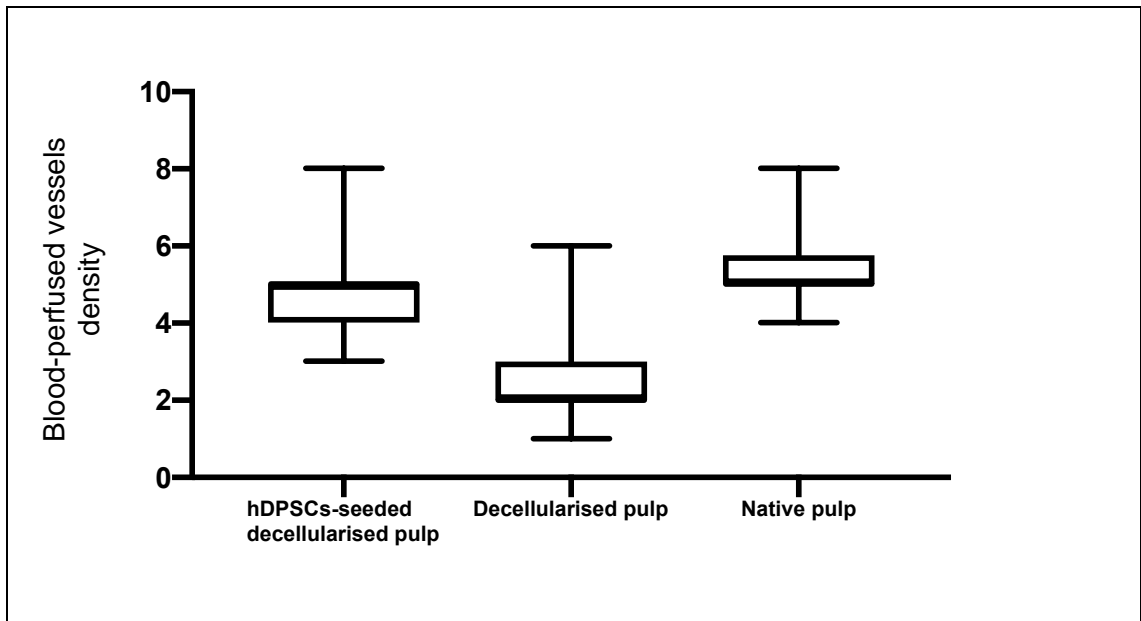


Figure 7-9: Box plot demonstrates the blood-perfused vessels density in the tissues-engineered *in vivo* using hDPSCs-seeded and unseeded decellularised dental pulps compared to native dental pulps. The density of blood vessels infiltrated with erythrocytes were counted in four random areas of H&E stained sections (n= 27 sections per group) under high power magnification (X200). The box plot shows the range of blood-perfused vessels in each group. The median of hDPSCs-seeded decellularised pulps' group (median = 5) was higher than that of the unseeded decellularised pulps' group (median = 2) and similar to that of the native pulps' group (median = 5).

7.6 Discussion

In the present research, the potential of the developed decellularised dental pulp matrix, to serve as a suitable scaffold for dental pulp regeneration via the cell transplantation or cell homing approach, was preliminarily tested *in vivo* using a semi-orthotopic dental pulp regeneration model. This model allows tissue regeneration to occur inside the root canal of a real human tooth, even though the tooth is implanted in an ectopic location (Nakashima *et al.*, 2019). Since the introduction of the semi-orthotopic dental pulp regeneration model by Gonçalves *et al.* (2007), it has been regarded as a simple, reliable and reproducible model useful for the initial *in vivo* evaluation of novel dental pulp therapeutic strategies (Sakai *et al.*, 2011). The model utilises a SCID murine host which allows the use of human cells due to the lack of mature B and T lymphocytes.

To investigate the *in vivo* vascularisation capacity of a decellularised dental pulp seeded with hDPSCs, decellularised dental pulps were initially seeded with hDPSCs and cultured *in vitro* for 14 days to allow sufficient cell repopulation of the matrix and vasculature, as demonstrated in this work's *in vitro* study (Chapter 6). Recellularised scaffolds were then implanted in human premolar root slices and transplanted into SCID mice, together with empty slices and slices containing unseeded decellularised dental pulps. All constructs were retrieved and histologically analysed following 30 days of *in vivo* implantation. This is the time point around which previous studies have demonstrated evidence of vascularised dental pulp-like tissue formation in root fragments implanted subcutaneously in mice (Rosa *et al.*, 2013, Widbiller *et al.*, 2018). Observation of blood-perfused vessels suggested that inosculation may have taken place, resulting in blood flow from the host to the tissues engineered using decellularised dental pulps. However, this does not exclude the possibility that some of the observed blood-

perfused vessels may be neovessels originating from the host. The immunohistochemical detection of human cell nuclei around the lumina of erythrocytes-containing vessels, together with the significant increase in blood-perfused vessel density in the group which received hDPSCs-seeded decellularised dental pulps as compared to the group which received unseeded decellularised dental pulps, indicated that hDPSCs had played a role in enhancing the vascularisation capacity of the decellularised dental pulp.

hDPSCs might have contributed to this advantageous vascularisation enhancement through two putative mechanisms. First, through their differentiation into endothelial-like cells and participation in the inosculation process (Singh *et al.*, 2011). Second, the contribution of hDPSCs to the vascularisation enhancement could be due to the so-called paracrine effect by stimulating blood vessels' formation through the secretion of angiogenic growth factors. Indeed, several angiogenic growth factors have previously shown to be expressed by hDPSCs, including VEGF, FGF-2 and platelet-derived growth factor (Tran-Hung *et al.*, 2006, Tran-Hung *et al.*, 2008, Bronckaers *et al.*, 2013). These growth factors could act as chemotactic signals to promote vascular ingrowth into the engineered tissues (Agarwal *et al.*, 2019). Further experiments are required to identify the origin of blood-perfused vessels and to gain more insight into the role of hDPSCs in enhancing the vascularisation capacity of the decellularised dental pulp *in vivo*.

The histomorphological organisation pattern of the tissues engineered using hDPSCs-seeded decellularised dental pulps suggested that cell differentiation might have taken place, resulting in the formation of dental pulp-like tissue. hDPSCs may have contributed to new tissue development directly through differentiation, or indirectly via the secretion of paracrine factors that promoted

the establishment of a more conducive milieu for tissue regeneration. This observation requires further investigation in the future.

Interestingly, in the group that received unseeded decellularised dental pulps, host cells' migration and infiltration were clearly observed. Several previous studies have shown that ECM components, such as collagen, when subjected to proteolytic degradation, release molecules that possess chemotactic activity enabling cell migration (Bellon *et al.*, 2004, Tran *et al.*, 2005). *In vitro* degradation of dental pulp matrix has been shown to result in products that possess chemotactic properties leading to cell migration (Smith *et al.*, 2012). Based on this, cell recruitment, which has been clearly observed in the unseeded decellularised dental pulps, is most likely due to chemotactic breakdown products generated as the scaffold degraded and was remodelled by the host. This is consistent with the findings reported by Gilbert *et al.* (2007) showing host cell infiltration as decellularised small intestinal submucosa degraded by the host. The decellularised dental pulp is composed of naturally occurring ECM and is therefore expected to be responsive to the same proteases as the natural ECM (Beattie *et al.*, 2009). Degradation products of collagen, fibronectin and laminin are known to participate in modulation of various cellular activities, including growth factors' signalling and matrix metalloproteases' synthesis (Li *et al.*, 2000). The observation herein suggested that the developed decellularised dental pulp might have the potential to recruit host cells from the periapical tissues during dental pulp regeneration via the cell homing approach. Further investigations of the decellularised dental pulp remodelling process and its correlation with host cell recruitment, infiltration and new tissue formation are required.

Collectively, the research work presented in this chapter shows the possibility of inserting intact decellularised dental pulp matrix in a debrided root canal of human

teeth slices. The findings suggest that decellularised dental pulp seeded with hDPSCs may provide a promising strategy to facilitate post-implantation vascularisation during dental pulp regeneration via cell transplantation. The findings also suggest the potential success of the decellularised dental pulp matrix in dental pulp regeneration via the cell homing approach, due to its inherent chemotactic property, which enables cell migration and recruitment.

Further experiments in orthotopic sites in larger animal models are required to verify the findings of the preliminary study presented in this chapter. Additionally, future work is required to investigate the potential of decellularised dental pulp seeded with hDPSCs to stimulate rapid vascularisation during dental pulp regeneration and to evaluate the potential of unseeded decellularised dental pulp to promote dental pulp regeneration via cell homing. To further understand if cell homing is occurring, *in vivo* method involving the use of a semi-orthotopic model consisting of a root fragment or a whole root implanted together with the unseeded decellularised pulp in a genetically-modified mouse model, in which host cells tracking in real-time is possible, can be utilised. In addition, the inclusion of a group in which the decellularised pulp is subjected to denaturation could help discriminate the host cell response. Furthermore, a modified *in vivo* model in which collagen, seeded with green fluorescence protein-expressing DPSCs, is placed at the tip of a root, containing the decellularised pulp, before implantation in a mouse model, as described by Widbiller *et al.* (2018), may provide a useful method to monitor stem cell recruitment into the scaffold. The green fluorescence protein-expressing DPSCs can also be utilised in an *in vitro* model as described by Colombo *et al.* (2015).

Chapter 8

General discussion, conclusions and future directions

8.1 General discussion

Dental pulp is a specialised and metabolically active soft connective tissue occupying the core of the tooth and playing an indispensable role in maintaining homeostasis of the tooth as a viable organ (Yang *et al.*, 2016). Necrosis of the dental pulp, secondary to trauma and/or infection, leads to functions loss and dentinogenesis interruption. This arrests the radicular maturation process in young permanent teeth, rendering the teeth weak and susceptible to fracture. Indeed, dental pulp necrosis in immature permanent teeth increases the probability of teeth loss and impacts the quality of life for growing children (Diogenes *et al.*, 2016).

The traditional management of non-vital immature permanent teeth uses the apical plug technique. This technique, although successful in certain cases, is incapable of restoring the competency of dental pulp functions and promoting the completion of radicular maturation (Duggal *et al.*, 2017). Therefore, its use in treating non-vital immature permanent teeth, with very short and thin roots, often has a poor prognosis. To address this limitation, regenerative endodontic therapy (RET), through apical bleeding induction into a disinfected root canal system, was introduced in an attempt to regenerate the structure and restore the functions of the damaged pulps in immature permanent teeth (Kim *et al.*, 2018). Unfortunately, early optimism regarding the use of RET in treating non-vital immature permanent teeth has faded due to the unpredictable capacity of the therapy to restore dentinogenesis and promote radicular maturation (Nazzal and

Duggal, 2017). For this reason, further research and development were deemed necessary to achieve a form of RET capable of regenerating the damaged pulps in immature permanent teeth in a controlled and predictable manner.

Dental pulp regeneration via a tissue engineering approach, such as cell transplantation or cell homing, is currently under active investigation for clinical translation in treating non-vital immature permanent teeth (Sui *et al.*, 2019, Galler and Widbiller, 2020, Dissanayaka and Zhang, 2020). Despite the progress achieved, several issues remain including, but not limited to, the difficulty of stimulating vascularisation to maintain post-implantation cell survival and the absence of adequate signalling to promote odontoblast-like cell differentiation (Dissanayaka and Zhang, 2020, Huang *et al.*, 2020). Therefore, the development of a strategy capable of facilitating vascularisation and promoting odontoblast-like cell differentiation is essential for the success of dental pulp regeneration.

Tissue decellularisation is a process by which a tissue-specific acellular scaffold could be prepared with a preserved extracellular matrix structure and composition, and, interestingly, a retained native vasculature (Crapo *et al.*, 2011). The use of decellularised scaffolds in regenerative medicine applications has been shown to promote vascularisation and provide an instructive environment for stem cell differentiation (Agmon and Christman, 2016, Robb *et al.*, 2017). The decellularised scaffolds not only have a retained native vasculature that could play a role in facilitating the vascularisation process, but also have a tissue-specific structure, composition and biological cues that could act in concert as an instructive platform to promote lineage-specific cell differentiation (Robb *et al.*, 2017). These scaffolds are composed of a natural extracellular matrix, which consists of numerous cell-secreted molecules that are essential to provide

structural support and biological signalling for the tissue resident cells (Kim *et al.*, 2011).

Broadly, the extracellular matrix comprises collagen, cell-adhesive glycoproteins, glycosaminoglycans, proteoglycans and a diverse array of growth factors which vary widely in their proportion and organisation from tissue to tissue (Frantz *et al.*, 2010). The tissue-specificity of the extracellular matrix imparts unique properties that help in regulating the cells' phenotype and functions within the tissue. The extracellular matrix could affect cell behaviours through direct binding of the cells to bioactive components. Another potential influence could involve the action of extracellular matrix degradation products, named matrikines (Ricard-Blum and Salza, 2014). These are known to modulate different cellular behaviours, including cell adhesion, migration and differentiation (Davis *et al.*, 2000, Mauney *et al.*, 2010). The molecular and three-dimensional architecture of the extracellular matrix is another factor that could influence stem cell behaviours. Structural features, such as the basement membrane, which could be retained following tissue decellularisation, have been shown to direct cell migration and growth pattern (Brown *et al.*, 2006). Additionally, the ultrastructural characteristics of the extracellular matrix may provide regional cues for cell attachment and differentiation (Robb *et al.*, 2017). Furthermore, the surface topography of the extracellular matrix has been postulated to mediate cell binding and influence their activities (Brown *et al.*, 2010). Other parameters, such as porosity, could impact cell response by facilitating nutrient and oxygen diffusion and modulating cell-cell and cell-matrix interaction (Loh and Choong, 2013).

Therefore, the research presented in this thesis focuses on the development and use of a decellularised dental pulp matrix (DDP) as a novel strategy to facilitate vascularisation and support dental pulp regeneration. The findings of the present

research demonstrated pro-angiogenic and pro-odontogenic properties in the developed DDP. Seeding of hDPSCs onto the DDP resulted in progressive cell repopulation of the DDP's matrix and vasculature, enhanced expression of markers involved in angiogenesis and odontogenesis in hDPSCs and improved DDP's *in vivo* vascularisation capacity. Furthermore, the developed DDP showed chemotactic activity enabling host cell migration and infiltration *in vivo*.

Bovine dental pulps were used in the present research, as a source for DDPs' development. The main advantages of utilising xenogeneic sources, such as bovine and swine dental pulps, for the preparation of DDPs are the wide availability, ease of obtaining tissues in abundant quantities as by-products of the food supply chain and clinical practicality. However, concerns regarding the risk of disease transmission from the donor tissues and the risk of adverse immune-mediated response by the host need to be addressed.

The concern regarding disease transmission by the donor tissues has been associated with the use of decellularised xenogeneic scaffolds. It should be noted that the donor tissues used for the manufacture of decellularised xenogeneic scaffolds are by-products of the food industry, and there is no evidence that a xenograft carries infectious agents transmissible to humans, beyond that which would occur via animal husbandry and abattoirs (Keane and Badylak, 2015). In addition, effective sterilisation of decellularised scaffolds has shown the potential to eliminate endotoxins and intact viral and bacterial DNA that may be present (Hodde and Hiles, 2002, Qiu *et al.*, 2009). Numerous decellularised xenogeneic scaffolds are currently available for clinical use in soft tissue repair and reconstruction, such as TissueMend[®] (decellularised bovine dermis), CopiOs[®] (decellularised bovine pericardium) and Restore[®] (decellularised porcine small intestine) (Badylak, 2014). These scaffolds are classified as medical devices by

the Food and Drug Administration (FDA) in the United States, and are required to meet a sterility assurance level appropriate for their intended clinical application (Keane and Badylak, 2015). Multiple sterilisation methods, including ethylene oxide exposure, gamma irradiation, electron beam irradiation and supercritical carbon dioxide, can be utilised for decellularised scaffolds' sterilisation (Crapo *et al.*, 2011). Further research is required to determine the optimal sterilisation method for the developed DDPs.

Host response to a decellularised scaffold is distinct from the response to whole tissue which contains donor cells (Badylak, 2014). The cells and nuclear materials of allogenic and xenogeneic tissues are, by definition, recognised as foreign by the recipient and therefore provoke an immune mediated rejection (Gilbert *et al.*, 2006). However, the extracellular matrix constituents are highly conserved among mammalian species and therefore expected to elicit a similar response when implanted as allogenic or xenogeneic scaffolds (Keane and Badylak, 2015, Cramer and Badylak, 2019). Further research is required to gain more insight into the host response to DDPs of xenogeneic and allogeneic origin to determine the optimal tissue source for DDPs' development.

Thorough decellularisation of the source tissues, with effective elimination of the cells and nuclear materials, is necessary to prevent an adverse immune-mediated response by the host (Crapo *et al.*, 2011, Keane *et al.*, 2015). In parallel, retention of the native extracellular matrix constituents, following tissue decellularisation, is crucial for the performance of the developed scaffolds (Hoshiba *et al.*, 2010). Retention of the extracellular matrix constituents following tissue decellularisation has been directly linked to the use of low concentrations of chemicals, in particular detergents, in addition to the use of protease inhibitors such as aprotinin (Knight *et al.*, 2008). It has been shown that the use of highly

concentrated detergents for a prolonged duration leads to extracellular matrix disruption and growth factors' elimination (Reing *et al.*, 2010), often resulting in cytotoxic scaffolds (Cebotari *et al.*, 2010). For this reason, a gentle decellularisation protocol, involving the low concentration of a single detergent (0.03% w/v SDS) in combination with a protease inhibitor, enzymatic agents and mild physical stress, was used in bovine dental pulp decellularisation. The protocol resulted in acellular dental pulp matrices retaining the native histoarchitecture, essential extracellular matrix components (collagen I and III, fibronectin, laminin and glycosaminoglycans) and multiple growth factors (VEGF-A, FGF-2, TGF- β 1 and BMP-2) of the dental pulp matrix. This is consistent with the findings reported by Matoug-Elwerfelli *et al.* following the use of the same protocol in human and rat dental pulp decellularisation (Matoug-Elwerfelli *et al.*, 2018, 2020). In contrast, loss of dental pulp matrix components was demonstrated following the use of a harsher decellularisation protocol involving a high concentration of dual detergents (1% w/v SDS / 1% w/v Triton X100) (Chen *et al.*, 2015). This suggests that the protocol used in the present research might be advantageous for future use in DDPs' development.

In the present research, bovine dental pulp decellularisation revealed preservation of the native vascular channels. This finding is consistent with several previous studies reporting retention of the native vascular channels following effective decellularisation of numerous tissues and organs (Ott *et al.*, 2008, Totonelli *et al.*, 2012, Maghsoudlou *et al.*, 2013, Bonandrini *et al.*, 2014). The retained vascular channels in the DDP could potentially anastomose with the host microvessels following *in vivo* implantation and establish blood flow through a process called inosculation (Laschke *et al.*, 2009). As explained previously in Chapter 6, inosculation involves the growth of vascular sprouts from the host

microvessels towards the connecting ends of the vascular channels retained in the DDP, or vice versa. These sprouts could connect eventually, forming continuous lumina and establishing blood flow. As the inosculation process is known to be directed by the endothelial cells located at the sprouts' tips (Gerhardt *et al.*, 2003), seeding these cells into the decellularised scaffolds has been attempted to facilitate inosculation, thus promoting the engineered constructs vascularisation. Despite the promising results achieved (Pellegata *et al.*, 2018), endothelial cells' use is highly limited due to the difficulties in culture expansion techniques and the insufficient number of cells available for seeding (Novosel *et al.*, 2011). Therefore, the use of mesenchymal stem cells, which have the potential to enhance angiogenesis in the scaffold, has been suggested (Zhao *et al.*, 2010, Liu *et al.*, 2011). These cells could contribute to the vascularisation process by differentiating into endothelial-like cells or releasing angiogenic growth factors.

In the present research, hDPSCs were selected as a cell source for DDP recellularisation as these cells are known to be an excellent candidate for dental pulp regeneration (Sloan and Waddington, 2009). The potential of hDPSCs to differentiate into endothelial-like cells and express certain angiogenic markers has been demonstrated in several studies (d'Aquino *et al.*, 2007, Marchionni *et al.*, 2009, Karbanová *et al.*, 2011, Aksel and Huang, 2017). Upon seeding of hDPSCs onto the DDP, the cells were able to attach, proliferate and migrate through the scaffold, demonstrating its suitability for cell binding and growth. Histological and immunohistochemical analyses of *in vitro* engineered tissues showed hDPSCs aligning along the luminal surface of the DDP's vasculature and exhibiting positive immunoreactivity to the CD31 antigen. Moreover, gene expression analysis of hDPSCs grown in the DDP, relative to similar cells grown

in two-dimensional and three-dimensional models, showed an increase in the expression of two angiogenic markers, namely KDR and PECAM-1. Interestingly, this enhancement of angiogenic markers' expression took place in the absence of specialised differentiation media. This suggests that the developed DDP, like many other reported decellularised scaffolds (Sun *et al.*, 2016, Rameshbabu *et al.*, 2018), is a pro-angiogenic scaffold characterised by the retention of several angiogenic growth factors in the matrix following decellularisation. Among growth factors that have demonstrated retention in the DDP are VEGF-A and FGF-2, two powerful angiogenic growth factors known to be effective in promoting microvascular formation. These growth factors, at least in part, are responsible for the migration and enhancement of angiogenic markers' expression in hDPSCs.

Seeding of hDPSCs onto the DDP revealed upregulation of two markers known to be involved in odontogenesis, namely DSPP and DMP-1. This finding links well with the results reported by Song *et al.* (2017) showing increased gene expression of DSPP and DMP-1 in apical papilla stem cells (SCAP) following seeding onto a decellularised dentine-pulp disk. While their study suggested that the odontogenic genes' upregulation is most likely due to the effect of growth and differentiation factors released from dentine walls of the decellularised dentine-pulp disk, the results of the present research demonstrated an obvious contribution of the decellularised dental pulp matrix since no dentine matrix exists and exogenous differentiation factors were used. Therefore, it could be hypothesised that the implantation of a DDP into a root canal may provide a synergistic effect on stem cells leading to enhanced odontoblast-like cell differentiation.

To begin investigating the *in vivo* vascularisation capacity of a DDP seeded with hDPSCs, a preliminary study was conducted in which DDPs were initially seeded with hDPSCs. Recellularised scaffolds were then implanted in human premolar root slices and transplanted into SCID mice, together with empty slices and slices containing unseeded DDPs. Observation of blood-perfused vessels, together with the absence of any obvious vacant human cell nuclei-lined vessels, suggests that inosculation may have taken place, resulting in blood flow from the host to the engineered tissue. However, this does not exclude the possibility that some of the observed blood-perfused vessels may be neovessels originating from the host. The immunohistochemical detection of human cell nuclei around the lumina of erythrocytes-containing vessels, together with the significant increase in blood-perfused vessel density in the group which received hDPSCs-seeded decellularised dental pulps as compared to the group which received unseeded decellularised dental pulps, indicated that hDPSCs had played a role in enhancing the vascularisation capacity of the DDP. hDPSCs might have contributed to vascularisation enhancement through their differentiation into endothelial-like cells and participation in the inosculation process or through the secretion of angiogenic growth factors. Further experiments are required to gain more insight into the role of hDPSCs in enhancing the vascularisation capacity of the DDP *in vivo*.

In vivo implantation of unseeded DDP revealed host cells' migration and infiltration. Several previous studies have shown that ECM components, such as collagen, when subjected to proteolytic degradation, release molecules that possess chemotactic activity enabling cell migration (Bellon *et al.* 2004, Tran *et al.* 2005). *In vitro* degradation of dental pulp matrix has been shown to result in products that possess chemotactic properties leading to cell migration (Smith *et*

al. 2012). Based on this, cell recruitment, which was observed following the *in vivo* implantation of unseeded DDPs, is most likely due to chemotactic breakdown products generated as the decellularised dental pulp matrix degraded and was remodelled by the host. DDP is composed of a naturally occurring extracellular matrix and is therefore expected to be responsive to the same proteases as the natural extracellular matrix (Beattie *et al.*, 2009). The findings of the present research suggest that the developed DDP might have the potential to recruit host cells from the periapical tissues during the process of dental pulp regeneration via a cell homing approach. Further investigations of the DDP remodelling process and its correlation with host cell recruitment, infiltration and new tissue formation are required.

The findings of the present research suggest that DDP seeded with hDPSCs could provide a promising vascularisation promoting strategy for dental pulp regeneration. Although recent studies reported the development of hydrogels consisting of DDPs of bovine and human origin (Bakhtiar *et al.*, 2020, Li *et al.*, 2020), the present research demonstrates the benefit of using DDPs in their intact form for a stem cell transplantation approach, where the retained vasculature could facilitate vascularisation. The use of a stem cell transplantation approach for dental pulp regeneration has shown immense potential for rebuilding the complex histological structure of the native pulp with a highly organised pattern (Xuan *et al.* 2018, Sui *et al.* 2019). This approach is becoming a well-accepted therapeutic strategy for functional dental pulp regeneration (Nakashima *et al.* 2017).

From a clinical translational perspective, decellularised dental pulps can be produced from a variety of xenogeneic dental pulp tissues (bovine or swine dental pulps), if proved safe for human use, or from human dental pulps. Converting the

decellularised dental pulps into cone-like forms could help deliver the scaffolds into the root canal system of recipient teeth.

8.2 Conclusions

The present research reports novel findings on the potential of a decellularised bovine dental pulp matrix (DDP) to facilitate vascularisation and support dental pulp regeneration. Bovine dental pulps represent a readily available source for DDPs development. Effective decellularisation of bovine dental pulps was shown possible using a gentle single detergent-based protocol. The developed DDP is a cytocompatible, pro-angiogenic and pro-odontogenic scaffold characterised by the retention of native histoarchitecture, vasculature, essential extracellular matrix components and angiogenic and odontogenic growth factors in the matrix following decellularisation. Seeding of hDPSCs onto the DDP led to progressive cell repopulation of the matrix and vasculature, enhanced expression of the markers involved in angiogenesis and odontogenesis in hDPSCs and improved *in vivo* vascularisation capacity of the DDP. Moreover, the DDP has a chemotactic activity *in vivo*, enabling host cells mobilisation and recruitment.

The findings of the present research suggest that a combination of DDP and hDPSCs could provide a promising vascularisation promoting strategy for dental pulp regeneration via cell transplantation. Furthermore, the use of DDP, in its acellular form, could provide a strategy for dental pulp regeneration via cell homing. This research forms a foundation for further future research towards translating the DDP for clinical use in regenerative endodontic therapy.

8.3 Future directions

Decellularised dental pulp matrix translation for clinical use in regenerative endodontic therapy requires further research in the following aspects:

- Bovine dental pulps were used as a source for decellularised scaffolds' development in the present research. This source could help in overcoming the supply limitation of human dental pulps. However, concerns regarding the risk of disease transmission from the donor tissues, as well as the risk of adverse immune-mediated response by the host, need to be addressed before attempting clinical translation. Further research is required to gain more insight into the host response to decellularised dental pulps of xenogeneic and allogeneic origin and to determine the optimal tissue source of decellularised dental pulp development. Further investigations are also required to determine the optimal sterilisation method for decellularised dental pulp matrices.
- Dental pulp stem cells were used in the present research as a cell source in decellularised dental pulp matrix recellularisation. However, the use of other mesenchymal stem cell sources, such as stem cells from exfoliated primary teeth (SHED), might be more feasible for the clinical translation of this approach, particularly in young patients. Further investigations are required to determine the optimal cell source for use in decellularised dental pulp matrix recellularisation.
- The vascularisation capacity of a decellularised dental pulp matrix, seeded with dental pulp stem cells, has been demonstrated in the present research. However, the role of dental pulp stem cells in enhancing the vascularisation capacity of the decellularised dental pulp is still not clear. Furthermore, the potential of a decellularised dental pulp matrix, seeded with dental pulp stem

cells to promote rapid vascularisation during dental pulp regeneration, warrants further research.

- The potential of a decellularised dental pulp matrix to promote odontoblast-like cell differentiation has been demonstrated *in vitro* in the present research. However, further characterisation of odontogenic cell differentiation is required. It is still unknown if the decellularised dental pulp matrix is capable of promoting odontoblast-like cell differentiation and mineralised matrix formation *in vivo*. Additionally, it will be interesting to investigate the potential of a decellularised dental pulp matrix to promote dental pulp lineage-specific differentiation of stem cells regardless of their origin (i.e. periodontal ligament, periapical tissues, bone marrow, etc.).
- The potential of a decellularised dental pulp matrix to mobilise and recruit host cells has been demonstrated in the present research. Further research is needed to gain more insight into the mechanism by which the decellularised dental pulp matrix promotes cell migration. Additionally, further research is required to investigate the remodelling process of the decellularised dental pulp matrix and its correlation with host cell recruitment, infiltration and new tissue formation.
- Decellularised dental pulp matrix can be used in an intact form or a hydrogel form. The preservation of the three-dimensional structure and vasculature in the intact form provides physical cues and a vascularisation route, in addition to the chemical cues provided by the extracellular matrix components. However, processing the decellularised dental pulp matrix into a hydrogel form offers an injectable delivery method, which is more attractive clinically. Further research is required to compare the regenerative potential of the two scaffold forms.

References

- Agarwal, N., Kumar, D., Anand, A. and Bahetwar, S.K. 2016. Dental implants in children: A multidisciplinary perspective for long-term success. *National journal of maxillofacial surgery*,. **7**(2), p122.
- Agarwal, T., Maiti, T.K. and Ghosh, S.K. 2019. Decellularized caprine liver-derived biomimetic and pro-angiogenic scaffolds for liver tissue engineering. *Materials Science and Engineering: C*. **98**, pp.939-948.
- Agmon, G. and Christman, K.L. 2016. Controlling stem cell behavior with decellularized extracellular matrix scaffolds. *Current Opinion in Solid State and Materials Science*. **20**(4), pp.193-201.
- Akhtar, K., Khan, S.A., Khan, S.B. and Asiri, A.M. 2018. Scanning Electron Microscopy: Principle and Applications in Nanomaterials Characterization. In: Sharma, S.K. ed. *Handbook of Materials Characterization*. Cham: Springer International Publishing, pp.113-145.
- Aksel, H. and Huang, G.T.-J. 2017. Human and swine dental pulp stem cells form a vascularlike network after angiogenic differentiation in comparison with endothelial cells: a quantitative analysis. *Journal of Endodontics*,. **43**(4), pp.588-595.
- Al-Jundi, S.H. 2004. Type of treatment, prognosis, and estimation of time spent to manage dental trauma in late presentation cases at a dental teaching hospital: a longitudinal and retrospective study. *Dental Traumatology*. **20**(1), pp.1-5.
- Alghilan, M., Windsor, L.J., Palasuk, J. and Yassen, G.H. 2017. Attachment and proliferation of dental pulp stem cells on dentine treated with different regenerative endodontic protocols. *International Endodontic Journal*. **50**(7), pp.667-675.
- Alghutaimel, H., Yang, X., Drummond, B., Nazzal, H., Duggal, M. and Raif, E. 2021. Investigating the vascularization capacity of a decellularized dental pulp matrix seeded with human dental pulp stem cells: in vitro and preliminary in vivo evaluations. *International Endodontic Journal*,. DOI: 10.1111/iej.13510.
- Alobaid, A.S., Cortes, L.M., Lo, J., Nguyen, T.T., Albert, J., Abu-Melha, A.S., Lin, L.M. and Gibbs, J.L. 2014. Radiographic and clinical outcomes of the treatment of immature permanent teeth by revascularization or apexification: a pilot retrospective cohort study. *Journal of Endodontics*,. **40**(8), pp.1063-1070.

Alqahtani, Q., Zaky, S., Patil, A., Beniash, E., Ray, H. and Sfeir, C. 2018. Decellularized Swine Dental Pulp Tissue for Regenerative Root Canal Therapy. *Journal of Dental Research*,. **97**(13), pp.1460-1467.

Alsousou, J., Thompson, M., Hulley, P., Noble, A. and Willett, K. 2009. The biology of platelet-rich plasma and its application in trauma and orthopaedic surgery: a review of the literature. *The Journal of Bone and Joint Surgery. British Volume*. **91**(8), pp.987-996.

Altaii, M., Richards, L. and Rossi-Fedele, G. 2017. Histological assessment of regenerative endodontic treatment in animal studies with different scaffolds: A systematic review. *Dental Traumatology*. **33**(4), pp.235-244.

Althumairy, R.I., Teixeira, F.B. and Diogenes, A. 2014. Effect of dentin conditioning with intracanal medicaments on survival of stem cells of apical papilla. *Journal of Endodontics*. **40**(4), pp.521-525.

Alvarèz Fallas, M.E., Piccoli, M., Franzin, C., Sgrò, A., Dedja, A., Urbani, L., Bertin, E., Trevisan, C., Gamba, P. and Burns, A.J. 2018. Decellularized diaphragmatic muscle drives a constructive angiogenic response in vivo. *International Journal of Molecular Sciences*,. **19**(5), p1319.

American Association of Endodontists. 2013. *Scope of Endodontics: Regenerative Endodontics Position Statement*. [Online]. [accessed October 2020]. Available from: <https://tinyurl.com/y6hoclcc>.

American Association of Endodontists. 2016. *Regenerative Endodontics: Clinical Considerations for a Regenerative Procedure*. [Online]. [Accessed October 2020]. Available from: <https://tinyurl.com/yyxc5dlk>.

Andreasen, F.M. and Kahler, B. 2015. Pulpal response after acute dental injury in the permanent dentition: clinical implications—a review. *Journal of Endodontics*. **41**(3), pp.299-308.

Andreasen, J.O., Farik, B. and Munksgaard, C. 2002. Long-term calcium hydroxide as a root canal dressing may increase risk of root fracture. *Dental Traumatology*. **18**(3), pp.134-137.

Arana-Chavez, V.E. and Massa, L.F. 2004. Odontoblasts: the cells forming and maintaining dentine. *The International Journal of Biochemistry and Cell Biology*,. **36**(8), pp.1367-1373.

Arhun, N., Arman, A., Ungor, M. and Erkut, S. 2006. A conservative multidisciplinary approach for improved aesthetic results with traumatised anterior teeth. *British Dental Journal*,. **201**(8), pp.509-512.

Arora, N.S., Ramanayake, T., Ren, Y.-F. and Romanos, G.E. 2009. Platelet-rich plasma: a literature review. *Implant Dentistry*,. **18**(4), pp.303-310.

Athirasala, A., Lins, F., Tahayeri, A., Hinds, M., Smith, A.J., Sedgley, C., Ferracane, J. and Bertassoni, L.E. 2017. A novel strategy to engineer pre-vascularized full-length dental pulp-like tissue constructs. *Scientific Reports*,. **7**(1), pp.1-11.

Avery, J.K., Cox, C.F. and Chiego Jr, D.J. 1980. Presence and location of adrenergic nerve endings in the dental pulps of mouse molars. *The Anatomical Record*. **198**(1), pp.59-71.

Badylak, S.F. 2002. The extracellular matrix as a scaffold for tissue reconstruction. *Seminars in Cell and Developmental Biology*,. **13**(5), pp.377-383.

Badylak, S.F. 2004. Xenogeneic extracellular matrix as a scaffold for tissue reconstruction. *Transplant Immunology*,. **12**(3-4), pp.367-377.

Badylak, S.F. 2007. The extracellular matrix as a biologic scaffold material. *Biomaterials*. **28**(25), pp.3587-3593.

Badylak, S.F. 2014. Decellularized allogeneic and xenogeneic tissue as a bioscaffold for regenerative medicine: factors that influence the host response. *Annals of Biomedical Engineering*,. **42**(7), pp.1517-1527.

Badylak, S.F. and Gilbert, T.W. 2008. Immune response to biologic scaffold materials. *Seminars in Immunology*,. **20**(2), pp.109-116.

Bakhtiar, H., Pezeshki-Modaress, M., Kiaipour, Z., Shafiee, M., Ellini, M.R., Mazidi, A., Rajabi, S., Benisi, S.Z., Ostad, S.N. and Galler, K. 2020. Pulp ECM-derived macroporous scaffolds for stimulation of dental-pulp regeneration process. *Dental Materials*. **36**(1), pp.76-87.

Bakland, L.K. and Andreasen, J.O. 2012. Will mineral trioxide aggregate replace calcium hydroxide in treating pulpal and periodontal healing complications subsequent to dental trauma? A review. *Dental traumatology*. **28**(1), pp.25-32.

Banchs, F. and Trope, M. 2004. Revascularization of immature permanent teeth with apical periodontitis: new treatment protocol?. *Journal of Endodontics*. **30**(4), pp.196-200.

Barthel, C., Levin, L., Reisner, H. and Trope, M. 1997. TNF- α release in monocytes after exposure to calcium hydroxide treated Escherichia coli LPS. *International Endodontic Journal*. **30**(3), pp.155-159.

Batur, Y.B., Erdemir, U. and Sancakli, H.S. 2013. The long-term effect of calcium hydroxide application on dentin fracture strength of endodontically treated teeth. *Dental Traumatology*,. **29**(6), pp.461-464.

Beattie, A.J., Gilbert, T.W., Guyot, J.P., Yates, A.J. and Badylak, S.F. 2009. Chemoattraction of progenitor cells by remodeling extracellular matrix scaffolds. *Tissue Engineering Part A*. **15**(5), pp.1119-1125.

Becerra, P., Ricucci, D., Loghin, S., Gibbs, J.L. and Lin, L.M. 2014. Histologic study of a human immature permanent premolar with chronic apical abscess after revascularization/revitalization. *Journal of Endodontics*. **40**(1), pp.133-139.

Bellon, G., Martiny, L. and Robinet, A. 2004. Matrix metalloproteinases and matrikines in angiogenesis. *Critical Reviews in Oncology and Hematology*,. **49**(3), pp.203-220.

Best, S., Ammons, C.L., Karunanayake, G.A., Saemundsson, S.R. and Tawil, P.Z. 2021. Outcome Assessment of Teeth with Necrotic Pulp and Apical Periodontitis Treated with Long-term Calcium Hydroxide. *Journal of Endodontics*. **47**(1), pp.11-18.

Bezgin, T., Yilmaz, A.D., Celik, B.N., Kolsuz, M.E. and Sonmez, H. 2015. Efficacy of Platelet-rich Plasma as a Scaffold in Regenerative Endodontic Treatment. *Journal of Endodontics*. **41**(1), pp.36-44.

Bjørndal, L. 2008. The caries process and its effect on the pulp: the science is changing and so is our understanding. *Pediatric Dentistry*,. **30**(3), pp.192-196.

Bodnar, E., Olsen, E., Florio, R. and Dobrin, J. 1986. Damage of porcine aortic valve tissue caused by the surfactant sodiumdodecylsulphate. *The Thoracic and Cardiovascular Surgeon*,. **34**(02), pp.82-85.

Bonandrini, B., Figliuzzi, M., Papadimou, E., Morigi, M., Perico, N., Casiraghi, F., Dipl, C., Sangalli, F., Conti, S. and Benigni, A. 2014. Recellularization of well-

preserved acellular kidney scaffold using embryonic stem cells. *Tissue Engineering Part A*. **20**(9-10), pp.1486-1498.

Bonte, E., Beslot, A., Boukpepsi, T. and Lasfargues, J.-J. 2015. MTA versus Ca(OH)₂ in apexification of non-vital immature permanent teeth: a randomized clinical trial comparison. *Clinical Oral Investigations*. **19**(6), pp.1381-1388.

Borum, M.K. and Andreasen, J.O. 2001. Therapeutic and economic implications of traumatic dental injuries in Denmark: an estimate based on 7549 patients treated at a major trauma centre. *International Journal of Paediatric Dentistry*. **11**(4), pp.249-258.

Bose, R., Nummikoski, P. and Hargreaves, K. 2009. A Retrospective Evaluation of Radiographic Outcomes in Immature Teeth With Necrotic Root Canal Systems Treated With Regenerative Endodontic Procedures. *Journal of Endodontics*,. **35**(10), pp.1343-1349.

Brennan, E.P., Tang, X.H., Stewart-Akers, A.M., Gudas, L.J. and Badylak, S.F. 2008. Chemoattractant activity of degradation products of fetal and adult skin extracellular matrix for keratinocyte progenitor cells. *Journal of Tissue Engineering and Regenerative Medicine*,. **2**(8), pp.491-498.

Bronckaers, A., Hilkens, P., Fanton, Y., Struys, T., Gervois, P., Politis, C., Martens, W. and Lambrichts, I. 2013. Angiogenic properties of human dental pulp stem cells. *Plos One*,. **8**(8), pe71104.

Brown, B., Lindberg, K., Reing, J., Stolz, D.B. and Badylak, S.F. 2006. The basement membrane component of biologic scaffolds derived from extracellular matrix. *Tissue Engineering*,. **12**(3), pp.519-526.

Brown, B.N. and Badylak, S.F. 2014. Extracellular matrix as an inductive scaffold for functional tissue reconstruction. *Translational Research*. **163**(4), pp.268-285.

Brown, B.N., Barnes, C.A., Kasick, R.T., Michel, R., Gilbert, T.W., Beer-Stolz, D., Castner, D.G., Ratner, B.D. and Badylak, S.F. 2010. Surface characterization of extracellular matrix scaffolds. *Biomaterials*. **31**(3), pp.428-437.

Brown, B.N., Valentin, J.E., Stewart-Akers, A.M., McCabe, G.P. and Badylak, S.F. 2009. Macrophage phenotype and remodeling outcomes in response to biologic scaffolds with and without a cellular component. *Biomaterials*. **30**(8), pp.1482-1491.

BS EN ISO 10993-5. 2009. Biological evaluation of medical devices–Part 5: Tests for in vitro cytotoxicity. [Online]. [accessed October 2020]. Available from: <https://www.iso.org/standard/36406.html>.

Bucchi, C., Marcé-Nogué, J., Galler, K.M. and Widbiller, M. 2019. Biomechanical performance of an immature maxillary central incisor after revitalization: a finite element analysis. *International Endodontic Journal*. **52**(10), pp.1508-1518.

Burk, J., Erbe, I., Berner, D., Kacza, J., Kasper, C., Pfeiffer, B., Winter, K. and Brehm, W. 2014. Freeze-thaw cycles enhance decellularization of large tendons. *Tissue Engineering Part C: Methods*. **20**(4), pp.276-284.

Butler, W.T., Brunn, J.C., Qin, C. and McKee, M.D. 2002. Extracellular matrix proteins and the dynamics of dentin formation. *Connective Tissue Research*,. **43**(2-3), pp.301-307.

Byzova, T.V., Goldman, C.K., Pampori, N., Thomas, K.A., Bett, A., Shattil, S.J. and Plow, E.F. 2000. A mechanism for modulation of cellular responses to VEGF: activation of the integrins. *Molecular Cell*,. **6**(4), pp.851-860.

Canoglu, H., Gungor, H.C. and Cehreli, Z.C. 2007. Management of cervical root fracture using orthodontic extrusion and crown reattachment: a case report. *Oral Surgery, Oral Medicine, Oral Pathology, Oral Radiology, and Endodontology*,. **104**(3), pp.e46-e49.

Carmeliet, P. and Jain, R.K. 2000. Angiogenesis in cancer and other diseases. *Nature*. **407**(6801), pp.249-257.

Casagrande, L., Demarco, F., Zhang, Z., Araujo, F., Shi, S. and Nör, J. 2010. Dentin-derived BMP-2 and odontoblast differentiation. *Journal of Dental Research*,. **89**(6), pp.603-608.

Causa, F., Netti, P.A. and Ambrosio, L. 2007. A multi-functional scaffold for tissue regeneration: The need to engineer a tissue analogue. *Biomaterials*,. **28**(34), pp.5093-5099.

Cebotari, S., Tudorache, I., Jaekel, T., Hilfiker, A., Dorfman, S., Ternes, W., Haverich, A. and Lichtenberg, A. 2010. Detergent decellularization of heart valves for tissue engineering: toxicological effects of residual detergents on human endothelial cells. *Artificial Organs*,. **34**(3), pp.206-210.

Chan, B. and Leong, K. 2008. Scaffolding in tissue engineering: general approaches and tissue-specific considerations. *European Spine Journal*. **17**(4), pp.467-479.

Charadram, N., Austin, C., Trimby, P., Simonian, M., Swain, M.V. and Hunter, N. 2013. Structural analysis of reactionary dentin formed in response to polymicrobial invasion. *Journal of Structural Biology*. **181**(3), pp.207-222.

Chen, G., Chen, J., Yang, B., Li, L., Luo, X., Zhang, X., Feng, L., Jiang, Z., Yu, M. and Guo, W. 2015. Combination of aligned PLGA/Gelatin electrospun sheets, native dental pulp extracellular matrix and treated dentin matrix as substrates for tooth root regeneration. *Biomaterials*. **52**, pp.56-70.

Chen, M.H., Chen, K.L., Chen, C.A., Tayebaty, F., Rosenberg, P. and Lin, L. 2012. Responses of immature permanent teeth with infected necrotic pulp tissue and apical periodontitis/abscess to revascularization procedures. *International Endodontic Journal*. **45**(3), pp.294-305.

Chen, X., Wang, Z. and Liu, S. 2003. Expression of basic fibroblast growth factor in dental pulp of immature permanent teeth. *Shanghai Journal of Stomatology*. **12**(1), pp.41-43.

Cheung, H.K., Han, T.T.Y., Marecak, D.M., Watkins, J.F., Amsden, B.G. and Flynn, L.E. 2014. Composite hydrogel scaffolds incorporating decellularized adipose tissue for soft tissue engineering with adipose-derived stem cells. *Biomaterials*. **35**(6), pp.1914-1923.

Chmilewsky, F., Jeanneau, C., Dejou, J. and About, I. 2014. Sources of dentin-pulp regeneration signals and their modulation by the local microenvironment. *Journal of Endodontics*,. **40**(4), pp.S19-S25.

Chueh, L.-H. and Huang, G.T.-J. 2006. Immature teeth with periradicular periodontitis or abscess undergoing apexogenesis: a paradigm shift. *Journal of Endodontics*. **32**(12), pp.1205-1213.

Colombo, J.S., Howard-Jones, R.A., Young, F.I., Waddington, R.J., Errington, R.J. and Sloan, A.J. 2015. A 3D ex vivo mandible slice system for longitudinal culturing of transplanted dental pulp progenitor cells. *Cytometry Part A*,. **87**(10), pp.921-928.

Conconi, M.T., Nico, B., Mangieri, D., Tommasini, M., Di Liddo, R., Parnigotto, P.P., Nussdorfer, G.G. and Ribatti, D. 2004. Angiogenic response induced by acellular aortic matrix in vivo. *The Anatomical Record Part A: Discoveries in*

Molecular, Cellular, and Evolutionary Biology: An Official Publication of the American Association of Anatomists. **281**(2), pp.1303-1307.

Conde, M., Chisini, L., Demarco, F., Nör, J., Casagrande, L. and Tarquinio, S. 2016. Stem cell-based pulp tissue engineering: variables enrolled in translation from the bench to the bedside, a systematic review of literature. *International Endodontic Journal.* **49**(6), pp.543-550.

Cordeiro, M.M., Dong, Z., Kaneko, T., Zhang, Z., Miyazawa, M., Shi, S., Smith, A.J. and Nör, J.E. 2008. Dental pulp tissue engineering with stem cells from exfoliated deciduous teeth. *Journal of Endodontics.* **34**(8), pp.962-969.

Couble, M.-L., Farges, J.-C., Bleicher, F., Perrat-Mabillon, B., Boudeulle, M. and Magloire, H. 2000. Odontoblast differentiation of human dental pulp cells in explant cultures. *Calcified Tissue International.* **66**(2), pp.129-138.

Couve, E. 1986. Ultrastructural changes during the life cycle of human odontoblasts. *Archives of Oral Biology.* **31**(10), pp.643-651.

Cramer, M.C. and Badylak, S.F. 2019. Extracellular matrix-based biomaterials and their influence upon cell behavior. *Annals of Biomedical Engineering.* **48**, pp.2132-2153.

Crapo, P.M., Gilbert, T.W. and Badylak, S.F. 2011. An overview of tissue and whole organ decellularization processes. *Biomaterials.* **32**(12), pp.3233-3243.

Cree, I. and Andreotti, P. 1997. Measurement of cytotoxicity by ATP-based luminescence assay in primary cell cultures and cell lines. *Toxicology in Vitro.* **11**(5), pp.553-556.

Crouch, S., Kozlowski, R., Slater, K. and Fletcher, J. 1993. The use of ATP bioluminescence as a measure of cell proliferation and cytotoxicity. *Journal of Immunological Methods.* **160**(1), pp.81-88.

Cvek, M. 1992. Prognosis of luxated non-vital maxillary incisors treated with calcium hydroxide and filled with gutta-percha. A retrospective clinical study. *Dental Traumatology.* **8**(2), pp.45-55.

d'Aquino, R., Graziano, A., Sampaolesi, M., Laino, G., Pirozzi, G., De Rosa, A. and Papaccio, G. 2007. Human postnatal dental pulp cells co-differentiate into osteoblasts and endotheliocytes: a pivotal synergy leading to adult bone tissue formation. *Cell Death and Differentiation.* **14**(6), pp.1162-1171.

Da Silva, L.A.B., Nelson-Filho, P., da Silva, R.A.B., Flores, D.S.H., Heilborn, C., Johnson, J.D. and Cohenca, N. 2010. Revascularization and periapical repair after endodontic treatment using apical negative pressure irrigation versus conventional irrigation plus triantibiotic intracanal dressing in dogs' teeth with apical periodontitis. *Oral Surgery, Oral Medicine, Oral Pathology, Oral Radiology, and Endodontology*. **109**(5), pp.779-787.

Dahl, S.L., Koh, J., Prabhakar, V. and Niklason, L.E. 2003. Decellularized native and engineered arterial scaffolds for transplantation. *Cell Transplantation*,. **12**(6), pp.659-666.

Daly, A.B., Wallis, J.M., Borg, Z.D., Bonvillain, R.W., Deng, B., Ballif, B.A., Jaworski, D.M., Allen, G.B. and Weiss, D.J. 2012. Initial binding and recellularization of decellularized mouse lung scaffolds with bone marrow-derived mesenchymal stromal cells. *Tissue Engineering Part A*. **18**(1-2), pp.1-16.

Damle, S., Bhattal, H. and Loomba, A. 2012. Apexification of anterior teeth: a comparative evaluation of mineral trioxide aggregate and calcium hydroxide paste. *Journal of Clinical Pediatric Dentistry*. **36**(3), pp.263-268.

Das, B. and Muthu, M.S. 2013. Surgical extrusion as a treatment option for crown–root fracture in permanent anterior teeth: a systematic review. *Dental Traumatology*,. **29**(6), pp.423-431.

Davis, G.E., Bayless, K.J., Davis, M.J. and Meininger, G.A. 2000. Regulation of Tissue Injury Responses by the Exposure of Matricryptic Sites within Extracellular Matrix Molecules. *The American Journal of Pathology*,. **156**(5), pp.1489-1498.

Davis, J.M. 1994. *Basic cell culture: a practical approach*. Oxford.

Del Fabbro, M., Lolato, A., Bucchi, C., Taschieri, S. and Weinstein, R.L. 2016. Autologous Platelet Concentrates for Pulp and Dentin Regeneration: A Literature Review of Animal Studies. *Journal of Endodontics*. **42**(2), pp.250-257.

Demarco, F.F., Casagrande, L., Zhang, Z., Dong, Z., Tarquinio, S.B., Zeitlin, B.D., Shi, S., Smith, A.J. and Nör, J.E. 2010. Effects of morphogen and scaffold porogen on the differentiation of dental pulp stem cells. *Journal of Endodontics*,. **36**(11), pp.1805-1811.

Diogenes, A., Henry, M.A., Teixeira, F.B. and Hargreaves, K.M. 2013. An update on clinical regenerative endodontics. *Endodontic Topics*. **28**(1), pp.2-23.

Diogenes, A. and Ruparel, N.B. 2017. Regenerative Endodontic Procedures: Clinical Outcomes. *Dental Clinics of North America*. **61**(1), pp.111-125.

Diogenes, A., Ruparel, N.B., Shiloah, Y. and Hargreaves, K.M. 2016. Regenerative endodontics: A way forward. *The Journal of the American Dental Association*. **147**(5), pp.372-380.

Dissanayaka, W. and Zhang, C. 2017. The role of vasculature engineering in dental pulp regeneration. *Journal of Endodontics*. **43**(9), pp.S102-S106.

Dissanayaka, W., Zhu, L., Hargreaves, K., Jin, L. and Zhang, C. 2014. Scaffold-free prevascularized microtissue spheroids for pulp regeneration. *Journal of Dental Research*,. **93**(12), pp.1296-1303.

Dissanayaka, W.L., Hargreaves, K.M., Jin, L., Samaranayake, L.P. and Zhang, C. 2015. The interplay of dental pulp stem cells and endothelial cells in an injectable peptide hydrogel on angiogenesis and pulp regeneration in vivo. *Tissue Engineering Part A*. **21**(3-4), pp.550-563.

Dissanayaka, W.L. and Zhang, C. 2020. Scaffold-based and Scaffold-free Strategies in Dental Pulp Regeneration. *Journal of Endodontics*. **46**(9), pp.S81-S89.

Dominici, M., Le Blanc, K., Mueller, I., Slaper-Cortenbach, I., Marini, F., Krause, D., Deans, R., Keating, A., Prockop, D. and Horwitz, E.J.C. 2006. Minimal criteria for defining multipotent mesenchymal stromal cells. The International Society for Cellular Therapy Position Statement. **8**(4), pp.315-317.

Dowthwaite, G.P., Bishop, J.C., Redman, S.N., Khan, I.M., Rooney, P., Evans, D.J.R., Houghton, L., Bayram, Z., Boyer, S., Thomson, B., Wolfe, M.S. and Archer, C.W. 2004. The surface of articular cartilage contains a progenitor cell population. *Journal of Cell Science*. **117**(6), pp.889-897.

Doyon, G.E., Dumsha, T. and von Fraunhofer, J.A. 2005. Fracture Resistance of Human Root Dentin Exposed to Intracanal Calcium Hydroxide. *Journal of Endodontics*,. **31**(12), pp.895-897.

Duggal, M., Tong, H.J., Al-Ansary, M., Twati, W., Day, P.F. and Nazzal, H. 2017. Interventions for the endodontic management of non-vital traumatised immature permanent anterior teeth in children and adolescents: a systematic review of the evidence and guidelines of the European Academy of Paediatric Dentistry. *European Archives of Paediatric Dentistry*. **18**(3), pp.139-151.

- Dziki, J.L., Sicari, B.M., Wolf, M.T., Cramer, M.C. and Badylak, S.F. 2016. Immunomodulation and mobilization of progenitor cells by extracellular matrix bioscaffolds for volumetric muscle loss treatment. *Tissue Engineering Part A*. **22**(19-20), pp.1129-1139.
- Egaña, J.T., Fierro, F.A., Krüger, S., Bornhäuser, M., Huss, R., Lavandero, S. and Machens, H.-G. 2009. Use of human mesenchymal cells to improve vascularization in a mouse model for scaffold-based dermal regeneration. *Tissue Engineering Part A*. **15**(5), pp.1191-1200.
- Egusa, H., Sonoyama, W., Nishimura, M., Atsuta, I. and Akiyama, K. 2012. Stem cells in dentistry—part I: stem cell sources. *Journal of Prosthodontic Research*,. **56**(3), pp.151-165.
- El Meligy, O.A. and Avery, D.R. 2006. Comparison of apexification with mineral trioxide aggregate and calcium hydroxide. *Pediatric Dentistry*,. **28**(3), pp.248-253.
- Elkins, K.M. 2012. *Forensic DNA biology: a laboratory manual*. Academic Press.
- Eltoum, I., Fredenburgh, J., Myers, R.B. and Grizzle, W.E. 2001. Introduction to the theory and practice of fixation of tissues. *Journal of Histotechnology*. **24**(3), pp.173-190.
- Emsley, J., Knight, C.G., Farndale, R.W. and Barnes, M.J. 2004. Structure of the integrin $\alpha 2\beta 1$ -binding collagen peptide. *Journal of Molecular Biology*,. **335**(4), pp.1019-1028.
- Eramo, S., Natali, A., Pinna, R. and Milia, E. 2018. Dental pulp regeneration via cell homing. *International Endodontic Journal*. **51**(4), pp.405-419.
- European Society of Endodontology. 2016. European Society of Endodontology position statement: revitalization procedures. *International Endodontic Journal*. **49**(8), pp.717-723.
- Fava, L. and Saunders, W. 1999. Calcium hydroxide pastes: classification and clinical indications. *International Endodontic Journal*,. **32**(4), pp.257-282.
- Frantz, C., Stewart, K.M. and Weaver, V.M. 2010. The extracellular matrix at a glance. *Journal of Cell Science*,. **123**(24), pp.4195-4200.
- French, K.M., Boopathy, A.V., DeQuach, J.A., Chingozha, L., Lu, H., Christman, K.L. and Davis, M.E. 2012. A naturally derived cardiac extracellular matrix

enhances cardiac progenitor cell behavior in vitro. *Acta Biomaterialia*,. **8**(12), pp.4357-4364.

Fu, R.-H., Wang, Y.-C., Liu, S.-P., Shih, T.-R., Lin, H.-L., Chen, Y.-M., Sung, J.-H., Lu, C.-H., Wei, J.-R. and Wang, Z.-W. 2014. Decellularization and recellularization technologies in tissue engineering. *Cell Transplantation*,. **23**(4-5), pp.621-630.

Galili, U. 2001. The α -gal epitope (Gal α 1-3Gal β 1-4GlcNAc-R) in xenotransplantation. *Biochimie*. **83**(7), pp.557-563.

Gallacher, A., Ali, R. and Bhakta, S. 2016. Dens invaginatus: diagnosis and management strategies. *British Dental Journal*. **221**(7), p383.

Galler, K. 2016. Clinical procedures for revitalization: current knowledge and considerations. *International Endodontic Journal*. **49**(10), pp.926-936.

Galler, K.M., Buchalla, W., Hiller, K.-A., Federlin, M., Eidt, A., Schiefersteiner, M. and Schmalz, G. 2015. Influence of root canal disinfectants on growth factor release from dentin. *Journal of Endodontics*. **41**(3), pp.363-368.

Galler, K.M., D'Souza, R.N. and Hartgerink, J.D. 2010. Biomaterials and their potential applications for dental tissue engineering. *Journal of Materials Chemistry*. **20**(40), pp.8730-8746.

Galler, K.M., D'souza, R., Hartgerink, J. and Schmalz, G. 2011a. Scaffolds for dental pulp tissue engineering. *Advances in Dental Research*. **23**(3), pp.333-339.

Galler, K.M., D'Souza, R.N., Federlin, M., Cavender, A.C., Hartgerink, J.D., Hecker, S. and Schmalz, G. 2011b. Dentin conditioning codetermines cell fate in regenerative endodontics. *Journal of Endodontics*,. **37**(11), pp.1536-1541.

Galler, K.M. and Widbiller, M. 2020. Cell-Free Approaches for Dental Pulp Tissue Engineering. *Journal of Endodontics*. **46**(9), pp.S143-S149.

Garibyan, L. and Avashia, N. 2013. Research techniques made simple: polymerase chain reaction (PCR). *The Journal of Investigative Dermatology*,. **133**(3), pe6.

Gathani, K.M. and Raghavendra, S.S. 2016. Scaffolds in regenerative endodontics: A review. *Dental Research Journal*,. **13**(5), p379.

Gerhardt, H. and Betsholtz, C. 2005. How do endothelial cells orientate? In: Clauss, M. and Breier, G. eds. *Mechanisms of Angiogenesis*. Basel: Birkhäuser Basel, pp.3-15.

Gerhardt, H., Golding, M., Fruttiger, M., Ruhrberg, C., Lundkvist, A., Abramsson, A., Jeltsch, M., Mitchell, C., Alitalo, K. and Shima, D. 2003. VEGF guides angiogenic sprouting utilizing endothelial tip cell filopodia. *The Journal of Cell Biology*,. **161**(6), pp.1163-1177.

Gilbert, T.W. 2012. Strategies for tissue and organ decellularization. *Journal of Cellular Biochemistry*,. **113**(7), pp.2217-2222.

Gilbert, T.W., Sellaro, T.L. and Badylak, S.F. 2006. Decellularization of tissues and organs. *Biomaterials*. **27**(19), pp.3675-3683.

Gilbert, T.W., Stewart-Akers, A.M., Simmons-Byrd, A. and Badylak, S.F. 2007. Degradation and remodeling of small intestinal submucosa in canine Achilles tendon repair. *The Journal of Bone & Joint Surgery*. **89**(3), pp.621-630.

Givan, A.L. 2011. Flow cytometry: an introduction. *Flow Cytometry Protocols*. Springer, pp.1-29.

Glendor, U. 2008. Epidemiology of traumatic dental injuries—a 12 year review of the literature. *Dental Traumatology*. **24**(6), pp.603-611.

Gomes-Filho, J.E., Tobias Duarte, P.C., Ervolino, E., Mogami Bomfim, S.R., Xavier Abimussi, C.J., Mota da Silva Santos, L., Lodi, C.S., Penha De Oliveira, S.H., Dezan, E. and Cintra, L.T.A. 2013. Histologic Characterization of Engineered Tissues in the Canal Space of Closed-apex Teeth with Apical Periodontitis. *Journal of Endodontics*. **39**(12), pp.1549-1556.

Gonçalves, S.B., Dong, Z., Bramante, C.M., Holland, G.R., Smith, A.J. and Nör, J.E. 2007. Tooth slice-based models for the study of human dental pulp angiogenesis. *Journal of Endodontics*,. **33**(7), pp.811-814.

Gronthos, S., Brahim, J., Li, W., Fisher, L., Cherman, N., Boyde, A., DenBesten, P., Robey, P.G. and Shi, S. 2002. Stem cell properties of human dental pulp stem cells. *Journal of Dental Research*,. **81**(8), pp.531-535.

Gronthos, S., Mankani, M., Brahim, J., Robey, P.G. and Shi, S. 2000. Postnatal human dental pulp stem cells (DPSCs) in vitro and in vivo. *Proceedings of the National Academy of Sciences*. **97**(25), pp.13625-13630.

Gu, K., Smoke, R.H. and Rutherford, R.B. 1996. Expression of genes for bone morphogenetic proteins and receptors in human dental pulp. *Archives of Oral Biology*,. **41**(10), pp.919-923.

Guan, J., Stankus, J.J. and Wagner, W.R. 2007. Biodegradable elastomeric scaffolds with basic fibroblast growth factor release. *Journal of Controlled Release*. **120**(1-2), pp.70-78.

Guest, D., Smith, M. and Allen, W. 2010. Equine embryonic stem-like cells and mesenchymal stromal cells have different survival rates and migration patterns following their injection into damaged superficial digital flexor tendon. *Equine Veterinary Journal*,. **42**(7), pp.636-642.

Hargreaves, K.M. and Berman, L.H. 2015. *Cohen's pathways of the pulp*. Elsevier Health Sciences.

Hargreaves, K.M., Diogenes, A. and Teixeira, F.B. 2013. Treatment options: biological basis of regenerative endodontic procedures. *Pediatric Dentistry*. **35**(2), pp.129-140.

Hargreaves, K.M., Giesler, T., Henry, M. and Wang, Y. 2008. Regeneration potential of the young permanent tooth: what does the future hold? *Pediatric Dentistry*. **30**(3), pp.253-260.

Harker, R. and Morris, J. 2003. *Children's Dental Health in England*. Office for National Statistics.

Harris, R. and Griffin, C. 1969. The fine structure of the mature odontoblasts and cell rich zone of the human dental pulp. *Australian Dental Journal*,. **14**(3), pp.168-177.

Hayat, M.A. 1993. *Stains and cytochemical methods*. Springer Science & Business Media.

He, Q., Zhao, Y., Chen, B., Xiao, Z., Zhang, J., Chen, L., Chen, W., Deng, F. and Dai, J. 2011. Improved cellularization and angiogenesis using collagen scaffolds chemically conjugated with vascular endothelial growth factor. *Acta Biomaterialia*,. **7**(3), pp.1084-1093.

Heptinstall, J. and Rapley, R. 2000. Spectrophotometric analysis of nucleic acids. *The nucleic acid protocols handbook*. Springer, pp.57-60.

- Hodde, J., Ernst, D. and Hiles, M. 2005. An investigation of the long-term bioactivity of endogenous growth factor in OASIS Wound Matrix. *Journal of Wound Care*,. **14**(1), pp.23-25.
- Hodde, J. and Hiles, M. 2002. Virus safety of a porcine-derived medical device: Evaluation of a viral inactivation method. *Biotechnology and Bioengineering*,. **79**(2), pp.211-216.
- Hodde, J., Record, R., Liang, H. and Badylak, S. 2001. Vascular endothelial growth factor in porcine-derived extracellular matrix. *Endothelium*. **8**(1), pp.11-24.
- Holland, G. 1990. Role of the odontoblast process. *Dynamic Aspects of Dental Pulp*,. Springer, pp.73-95.
- Holland, R., de Mello, W., Nery, M.J., Bernabe, P.F. and de Souza, V. 1977. Reaction of human periapical tissue to pulp extirpation and immediate root canal filling with calcium hydroxide. *Journal of Endodontics*,. **3**(2), pp.63-67.
- Hørsted, P., Östby, N. and Fejerskoy, O. 1978. Tissue formation in root canal after total pulpectomy and partial root filling. *Oral Surgery, Oral Medicine, Oral Pathology*. **46**(2), pp.275-282.
- Hoshiba, T., Lu, H., Kawazoe, N. and Chen, G. 2010. Decellularized matrices for tissue engineering. *Expert Opinion on Biological Therapy*,. **10**(12), pp.1717-1728.
- Howard, C., Murray, P.E. and Namerow, K.N. 2010. Dental pulp stem cell migration. *Journal of Endodontics*,. **36**(12), pp.1963-1966.
- Huang, G.-J., Gronthos, S. and Shi, S. 2009. Mesenchymal stem cells derived from dental tissues vs. those from other sources: their biology and role in regenerative medicine. *Journal of Dental Research*,. **88**(9), pp.792-806.
- Huang, G.T.-J. and Lin, L.M. 2008. Letter to the editor: Comments on the use of the term “revascularization” to describe. *Journal of Endodontics*. **34**(5), p511.
- Huang, G.T.-J., Liu, J., Zhu, X., Yu, Z., Li, D., Chen, C.-A. and Azim, A.A. 2020. Pulp/Dentin Regeneration: It Should Be Complicated. *Journal of Endodontics*. **46**(9), pp.S128-S134.
- Huang, G.T.-J., Sonoyama, W., Liu, Y., Liu, H., Wang, S. and Shi, S. 2008. The hidden treasure in apical papilla: the potential role in pulp/dentin regeneration and bioroot engineering. *Journal of Endodontics*. **34**(6), pp.645-651.

Huang, G.T.-J., Yamaza, T., Shea, L.D., Djouad, F., Kuhn, N.Z., Tuan, R.S. and Shi, S. 2010. Stem/progenitor cell-mediated de novo regeneration of dental pulp with newly deposited continuous layer of dentin in an in vivo model. *Tissue Engineering Part A*. **16**(2), pp.605-615.

Hudson, T.W., Liu, S.Y. and Schmidt, C.E. 2004. Engineering an improved acellular nerve graft via optimized chemical processing. *Tissue Engineering*,. **10**(9-10), pp.1346-1358.

Hynes, R.O. 1992. Integrins: Versatility, modulation, and signaling in cell adhesion. *Cell*. **69**(1), pp.11-25.

Iohara, K., Murakami, M., Takeuchi, N., Osako, Y., Ito, M., Ishizaka, R., Utunomiya, S., Nakamura, H., Matsushita, K. and Nakashima, M. 2013. A novel combinatorial therapy with pulp stem cells and granulocyte colony-stimulating factor for total pulp regeneration. *Stem Cells Translational Medicine*,. **2**(7), pp.521-533.

Iohara, K., Nakashima, M., Ito, M., Ishikawa, M., Nakasima, A. and Akamine, A. 2004. Dentin regeneration by dental pulp stem cell therapy with recombinant human bone morphogenetic protein 2. *Journal of Dental Research*,. **83**(8), pp.590-595.

Iop, L., Renier, V., Naso, F., Piccoli, M., Bonetti, A., Gandaglia, A., Pozzobon, M., Paolin, A., Ortolani, F. and Marchini, M. 2009. The influence of heart valve leaflet matrix characteristics on the interaction between human mesenchymal stem cells and decellularized scaffolds. *Biomaterials*. **30**(25), pp.4104-4116.

Islam, B., Khan, S.N. and Khan, A.U. 2007. Dental caries: from infection to prevention. *Medical Science Monitor*. **13**(11), pp.RA196-RA203.

Itoh, Y., Sasaki, J., Hashimoto, M., Katata, C., Hayashi, M. and Imazato, S. 2018. Pulp regeneration by 3-dimensional dental pulp stem cell constructs. *Journal of Dental Research*. **97**(10), pp.1137-1143.

Ivanyi, D. 1972. Nucleoli of human odontoblasts. *Archives of Oral Biology*. **17**(6), pp.931-IN935.

Iwaya, S.i., Ikawa, M. and Kubota, M. 2001. Revascularization of an immature permanent tooth with apical periodontitis and sinus tract. *Dental Traumatology*. **17**(4), pp.185-187.

Jadhav, G., Shah, N. and Logani, A. 2012. Revascularization with and without platelet-rich plasma in nonvital, immature, anterior teeth: a pilot clinical study. *Journal of Endodontics*,. **38**(12), pp.1581-1587.

Jamshidi, D., Homayouni, H., Moradi Majd, N., Shahabi, S., Arvin, A. and Ranjbar Omid, B. 2018. Impact and Fracture Strength of Simulated Immature Teeth Treated with Mineral Trioxide Aggregate Apical Plug and Fiber Post Versus Revascularization. *Journal of Endodontics*,. **44**(12), pp.1878-1882.

Javelet, J., Torabinejad, M. and Bakland, L.K. 1985. Comparison of two pH levels for the induction of apical barriers in immature teeth of monkeys. *Journal of Endodontics*,. **11**(9), pp.375-378.

Jeeruphan, T., Jantarat, J., Yanpiset, K., Suwannapan, L., Khewsawai, P. and Hargreaves, K.M. 2012. Mahidol study 1: comparison of radiographic and survival outcomes of immature teeth treated with either regenerative endodontic or apexification methods: a retrospective study. *Journal of Endodontics*. **38**(10), pp.1330-1336.

Junqueira, L.C.U., Bignolas, G. and Brentani, R.R. 1979. Picrosirius staining plus polarization microscopy, a specific method for collagen detection in tissue sections. *The Histochemical Journal*,. **11**(4), pp.447-455.

Kahler, B., Mistry, S., Moule, A., Ringsmuth, A.K., Case, P., Thomson, A. and Holcombe, T. 2014. Revascularization outcomes: a prospective analysis of 16 consecutive cases. *Journal of Endodontics*. **40**(3), pp.333-338.

Kaigler, D., Wang, Z., Horger, K., Mooney, D.J. and Krebsbach, P.H. 2006. VEGF scaffolds enhance angiogenesis and bone regeneration in irradiated osseous defects. *Journal of Bone and Mineral Research*,. **21**(5), pp.735-744.

Kapuscinski, J.J.B. 1995. DAPI: a DNA-specific fluorescent probe. *Biotechnic and Histochemistry*. **70**(5), pp.220-233.

Karbanová, J., Soukup, T., Suchánek, J., Pytlík, R., Corbeil, D. and Mokřý, J. 2011. Characterization of dental pulp stem cells from impacted third molars cultured in low serum-containing medium. *Cells Tissues Organs*. **193**(6), pp.344-365.

Kawasaki, K., Tanaka, S. and Ishikawa, T. 1979. On the daily incremental lines in human dentine. *Archives of Oral Biology*. **24**(12), pp.939-943.

- Keane, T.J. and Badylak, S.F. 2015. The host response to allogeneic and xenogeneic biological scaffold materials. *Journal of Tissue Engineering and Regenerative Medicine*,. **9**(5), pp.504-511.
- Keane, T.J., Londono, R., Turner, N.J. and Badylak, S.F. 2012. Consequences of ineffective decellularization of biologic scaffolds on the host response. *Biomaterials*. **33**(6), pp.1771-1781.
- Keane, T.J., Swinehart, I.T. and Badylak, S.F. 2015. Methods of tissue decellularization used for preparation of biologic scaffolds and in vivo relevance. *Methods*. **84**, pp.25-34.
- Kheir, E., Stapleton, T., Shaw, D., Jin, Z., Fisher, J. and Ingham, E. 2011. Development and characterization of an acellular porcine cartilage bone matrix for use in tissue engineering. *Journal of Biomedical Materials Research Part A*,. **99**(2), pp.283-294.
- Kim, J.Y., Xin, X., Moioli, E.K., Chung, J., Lee, C.H., Chen, M., Fu, S.Y., Koch, P.D. and Mao, J.J. 2010. Regeneration of dental-pulp-like tissue by chemotaxis-induced cell homing. *Tissue Engineering Part A*. **16**(10), pp.3023-3031.
- Kim, S. 1985. Microcirculation of the dental pulp in health and disease. *Journal of Endodontics*. **11**(11), pp.465-471.
- Kim, S. 1990. Neurovascular interactions in the dental pulp in health and inflammation. *Journal of Endodontics*. **16**(2), pp.48-53.
- Kim, S., Dörscher-Kim, J. and Liu, M. 1989. Microcirculation of the dental pulp and its autonomic control. *Proceedings of the Finnish Dental Society*. **85**(4-5), pp.279-287.
- Kim, S.-H., Turnbull, J. and Guimond, S. 2011. Extracellular matrix and cell signalling: the dynamic cooperation of integrin, proteoglycan and growth factor receptor. *Journal of Endocrinology*. **209**(2), pp.139-151.
- Kim, S.G. 2017. Biological molecules for the regeneration of the pulp-dentin complex. *Dental Clinics*. **61**(1), pp.127-141.
- Kim, S.G., Malek, M., Sigurdsson, A., Lin, L.M. and Kahler, B. 2018. Regenerative endodontics: a comprehensive review. *International Endodontic Journal*. **51**(12), pp.1367-1388.

Kim, S.G., Zhou, J., Solomon, C., Zheng, Y., Suzuki, T., Chen, M., Song, S., Jiang, N., Cho, S. and Mao, J.J. 2012. Effects of growth factors on dental stem/progenitor cells. *Dental Clinics*. **56**(3), pp.563-575.

Knight, R., Wilcox, H., Korossis, S., Fisher, J. and Ingham, E. 2008. The use of acellular matrices for the tissue engineering of cardiac valves. *Proceedings of the Institution of Mechanical Engineers, Part H: Journal of Engineering in Medicine*. **222**(1), pp.129-143.

Kontakiotis, E.G., Filippatos, C.G. and Agrafioti, A. 2014. Levels of evidence for the outcome of regenerative endodontic therapy. *Journal of Endodontics*. **40**(8), pp.1045-1053.

Koyuturk, A.E. and Malkoc, S. 2005. Orthodontic extrusion of subgingivally fractured incisor before restoration. A case report: 3-years follow-up. *Dental Traumatology*,. **21**(3), pp.174-178.

Kraus, N.A., Ehebauer, F., Zapp, B., Rudolphi, B., Kraus, B.J. and Kraus, D. 2016. Quantitative assessment of adipocyte differentiation in cell culture. *Adipocyte*. **5**(4), pp.351-358.

Kuang, R., Zhang, Z., Jin, X., Hu, J., Shi, S., Ni, L. and Ma, P.X. 2016. Nanofibrous spongy microspheres for the delivery of hypoxia-primed human dental pulp stem cells to regenerate vascularized dental pulp. *Acta Biomaterialia*,. **33**, pp.225-234.

Kumar, G. 2015. *Orban's oral histology and embryology*. Elsevier India.

Langer, R. and Vacanti, J. 1993. Tissue engineering. *Science*. **260**(5110), pp.920-926.

Laschke, M.W., Vollmar, B. and Menger, M.D. 2009. Inosculation: connecting the life-sustaining pipelines. *Tissue Engineering Part B: Reviews*. **15**(4), pp.455-465.

Lechner, J. and Kalnitsky, G. 1981. The presence of large amounts of type III collagen in bovine dental pulp and its significance with regard to the mechanism of dentinogenesis. *Archives of Oral Biology*. **26**(4), pp.265-273.

Ledermann, P., Hassell, T. and Hefti, A. 1993. Osseointegrated dental implants as alternative therapy to bridge construction or orthodontics in young patients: seven years of clinical experience. *Pediatric dentistry*,. **15**(5), pp.327-333.

Lee, S.-J., Monsef, M. and Torabinejad, M. 1993. Sealing ability of a mineral trioxide aggregate for repair of lateral root perforations. *Journal of Endodontics*,. **19**(11), pp.541-544.

Lee, S.-M., Zhang, Q. and Le, A.D. 2014. Dental stem cells: sources and potential applications. *Current Oral Health Reports*. **1**(1), pp.34-42.

Lei, L., Chen, Y., Zhou, R., Huang, X. and Cai, Z. 2015. Histologic and immunohistochemical findings of a human immature permanent tooth with apical periodontitis after regenerative endodontic treatment. *Journal of Endodontics*,. **41**(7), pp.1172-1179.

Lesot, H., Lisi, S., Peterkova, R., Peterka, M., Mitolo, V. and Ruch, J. 2001. Epigenetic signals during odontoblast differentiation. *Advances in Dental Research*. **15**(1), pp.8-13.

Levitan, M.E. and Himel, V.T. 2006. Dens evaginatus: literature review, pathophysiology, and comprehensive treatment regimen. *Journal of Endodontics*. **32**(1), pp.1-9.

Li, J., Parada, C. and Chai, Y. 2017. Cellular and molecular mechanisms of tooth root development. *Development*. **144**(3), pp.374-384.

Li, J., Rao, Z., Zhao, Y., Xu, Y., Chen, L., Shen, Z., Bai, Y., Lin, Z. and Huang, Q. 2020. A Decellularized Matrix Hydrogel Derived from Human Dental Pulp Promotes Dental Pulp Stem Cells Proliferation, Migration, and Induced Multidirectional Differentiation in vitro. *Journal of Endodontics*. **46**(10), pp.1438-1447.

Li, Y.Y., McTiernan, C.F. and Feldman, A.M. 2000. Interplay of matrix metalloproteinases, tissue inhibitors of metalloproteinases and their regulators in cardiac matrix remodeling. *Cardiovascular Research*,. **46**(2), pp.214-224.

Lin, J., Zeng, Q., Wei, X., Zhao, W., Cui, M., Gu, J., Lu, J., Yang, M. and Ling, J. 2017. Regenerative endodontics versus apexification in immature permanent teeth with apical periodontitis: a prospective randomized controlled study. *Journal of Endodontics*,. **43**(11), pp.1821-1827.

Linde, A. 1970. Glycosaminoglycans (mucopolysaccharides) of the porcine dental pulp. *Archives of Oral Biology*. **15**(11), pp.1035-1046.

Linde, A. 1972. Glycosaminoglycans of the rat incisor pulp. *Biochimica et Biophysica Acta -General Subjects*. **279**(3), pp.446-455.

Linde, A. 1973a. Glycosaminoglycan turnover and synthesis in the rat incisor pulp. *European Journal of Oral Sciences*. **81**(2), pp.145-154.

Linde, A. 1973b. A study of the dental pulp glycosaminoglycans from permanent human teeth and rat and rabbit incisors. *Archives of oral biology*. **18**(1), pp.49-59.

Linde, A. 1985. Session II: Cells and Extracellular Matrices of the Dental Pulp—CT Hanks, Chairman: The Extracellular Matrix of the Dental Pulp and Dentin. *Journal of Dental Research*. **64**(4), pp.523-529.

Linde, A., Johansson, S., Jonsson, R. and Jontell, M. 1982. Localization of fibronectin during dentinogenesis in rat incisor. *Archives of Oral Biology*. **27**(12), pp.1069-1073.

Linsuwanont, P., Sinpitaksakul, P. and Lertsakchai, T. 2017. Evaluation of root maturation after revitalization in immature permanent teeth with nonvital pulps by cone beam computed tomography and conventional radiographs. *International Endodontic Journal*. **50**(9), pp.836-846.

Lisi, S., Peterkova, R., Peterka, M., Vonesch, J., Ruch, J. and Lesot, H. 2003. Tooth morphogenesis and pattern of odontoblast differentiation. *Connective Tissue Research*. **44**(1), pp.167-170.

Liu, H., Li, W., Shi, S., Habelitz, S., Gao, C. and DenBesten, P. 2005. MEPE is downregulated as dental pulp stem cells differentiate. *Archives of Oral Biology*,. **50**(11), pp.923-928.

Liu, S., Zhang, H., Zhang, X., Lu, W., Huang, X., Xie, H., Zhou, J., Wang, W., Zhang, Y. and Liu, Y. 2011. Synergistic angiogenesis promoting effects of extracellular matrix scaffolds and adipose-derived stem cells during wound repair. *Tissue Engineering Part A*. **17**(5-6), pp.725-739.

Loh, Q.L. and Choong, C. 2013. Three-dimensional scaffolds for tissue engineering applications: role of porosity and pore size. *Tissue Engineering Part B: Reviews*,. **19**(6), pp.485-502.

Lovelace, T.W., Henry, M.A., Hargreaves, K.M. and Diogenes, A. 2011. Evaluation of the delivery of mesenchymal stem cells into the root canal space of necrotic immature teeth after clinical regenerative endodontic procedure. *Journal of Endodontics*,. **37**(2), pp.133-138.

- Lukinmaa, P.-L. and Waltimo, J. 1992. Immunohistochemical localization of types I, V, and VI collagen in human permanent teeth and periodontal ligament. *Journal of Dental Research*. **71**(2), pp.391-397.
- Luo, J., Korossis, S.A., Wilshaw, S.-P., Jennings, L.M., Fisher, J. and Ingham, E. 2014. Development and characterization of acellular porcine pulmonary valve scaffolds for tissue engineering. *Tissue Engineering Part A*. **20**(21-22), pp.2963-2974.
- Maghsoudlou, P., Georgiades, F., Tyraskis, A., Totonelli, G., Loukogeorgakis, S.P., Orlando, G., Shangaris, P., Lange, P., Delalande, J.-M. and Burns, A.J. 2013. Preservation of micro-architecture and angiogenic potential in a pulmonary acellular matrix obtained using intermittent intra-tracheal flow of detergent enzymatic treatment. *Biomaterials*. **34**(28), pp.6638-6648.
- Mangkornkarn, C. and Steiner, J.C. 1992. In vivo and in vitro glycosaminoglycans from human dental pulp. *Journal of Endodontics*. **18**(7), pp.327-331.
- Marchionni, C., Bonsi, L., Alviano, F., Lanzoni, G., Di Tullio, A., Costa, R., Montanari, M., Tazzari, P., Ricci, F. and Pasquinelli, G. 2009. Angiogenic potential of human dental pulp stromal (stem) cells. *International Journal of Immunopathology and Pharmacology*. **22**(3), pp.699-706.
- Martin, G., Ricucci, D., Gibbs, J.L. and Lin, L.M. 2013. Histological findings of revascularized/revitalized immature permanent molar with apical periodontitis using platelet-rich plasma. *Journal of Endodontics*. **39**(1), pp.138-144.
- Martinez, E. and Araujo, V. 2004. In vitro immunoexpression of extracellular matrix proteins in dental pulpal and gingival human fibroblasts. *International Endodontic Journal*. **37**(11), pp.749-755.
- Martinez, E.F., de Souza, S.O.M., Corrêa, L. and de Araújo, V.C. 2000. Immunohistochemical localization of tenascin, fibronectin, and type III collagen in human dental pulp. *Journal of Endodontics*. **26**(12), pp.708-711.
- Matoug-Elwerfelli, M., Duggal, M.S., Nazzal, H., Esteves, F. and Raif, E. 2018. A biocompatible decellularized pulp scaffold for regenerative endodontics. *International Endodontic Journal*. **51**(6), pp.663-673.
- Matoug-Elwerfelli, M., Nazzal, H., Raif, E.M., Wilshaw, S.-P., Esteves, F. and Duggal, M. 2020. Ex-vivo recellularisation and stem cell differentiation of a decellularised rat dental pulp matrix. *Scientific Reports*. **10**(1), p21553.

Matoug-Elwerfelli, M., Duggal, M., Nazzal, H., Esteves, F. and Raif, E. 2018. A biocompatible decellularized pulp scaffold for regenerative endodontics. *International Endodontic Journal*,. **51**(6), pp.663-673.

Matsushita, K., Motani, R., Sakutal, T., Yamaguchi, N., Koga, T., Matsuo, K., Nagaoka, S., Abeyama, K., Maruyama, I. and Torii, M. 2000. The role of vascular endothelial growth factor in human dental pulp cells: induction of chemotaxis, proliferation, and differentiation and activation of the AP-1-dependent signaling pathway. *Journal of Dental Research*,. **79**(8), pp.1596-1603.

Mauney, J., Olsen, B.R. and Volloch, V. 2010. Matrix remodeling as stem cell recruitment event: a novel in vitro model for homing of human bone marrow stromal cells to the site of injury shows crucial role of extracellular collagen matrix. *Matrix Biology*. **29**(8), pp.657-663.

McDevitt, C.A., Wildey, G.M. and Cutrone, R.M. 2003. Transforming growth factor- β 1 in a sterilized tissue derived from the pig small intestine submucosa. *Journal of Biomedical Materials Research Part A*. **67**(2), pp.637-640.

Melin, M., Joffre-Romeas, A., Farges, J.-C., Couble, M.-L., Magloire, H. and Bleicher, F. 2000. Effects of TGF β 1 on dental pulp cells in cultured human tooth slices. *Journal of Dental Research*,. **79**(9), pp.1689-1696.

Menon, N.G., Rodriguez, E.D., Byrnes, C.K., Giroto, J.A., Goldberg, N.H. and Silverman, R.P. 2003. Revascularization of human acellular dermis in full-thickness abdominal wall reconstruction in the rabbit model. *Annals of Plastic Surgery*,. **50**(5), pp.523-527.

Meryman, H.T. 2007. Cryopreservation of living cells: principles and practice. *Transfusion*. **47**(5), pp.935-945.

Mirsadraee, S., Wilcox, H.E., Korossis, S.A., Kearney, J.N., Watterson, K.G., Fisher, J. and Ingham, E. 2006. Development and characterization of an acellular human pericardial matrix for tissue engineering. *Tissue Engineering*,. **12**(4), pp.763-773.

Miura, M., Gronthos, S., Zhao, M., Lu, B., Fisher, L.W., Robey, P.G. and Shi, S. 2003. SHED: stem cells from human exfoliated deciduous teeth. *Proceedings of the National Academy of Sciences*. **100**(10), pp.5807-5812.

Mohammadi, Z. and Dummer, P.M.H. 2011. Properties and applications of calcium hydroxide in endodontics and dental traumatology. *International Endodontic Journal*,. **44**(8), pp.697-730.

Moore, K.L., Persaud, T.V.N. and Torchia, M.G. 2018. *The Developing Human: Clinically Oriented Embryology*. Elsevier Health Sciences.

Mullane, E.M., Dong, Z., Sedgley, C., Hu, J.-C., Botero, T., Holland, G. and Nör, J. 2008. Effects of VEGF and FGF2 on the revascularization of severed human dental pulps. *Journal of Dental Research*,. **87**(12), pp.1144-1148.

Murphy, C.M., Haugh, M.G. and O'Brien, F.J. 2010. The effect of mean pore size on cell attachment, proliferation and migration in collagen–glycosaminoglycan scaffolds for bone tissue engineering. *Biomaterials*,. **31**(3), pp.461-466.

Murray, P.E., Garcia-Godoy, F. and Hargreaves, K.M. 2007. Regenerative endodontics: a review of current status and a call for action. *Journal of Endodontics*. **33**(4), pp.377-390.

Muschler, G.F., Nakamoto, C. and Griffith, L.G. 2004. Engineering principles of clinical cell-based tissue engineering. *The Journal of Bone and Joint Surgery*. **86**(7), pp.1541-1558.

Na, S., Zhang, H., Huang, F., Wang, W., Ding, Y., Li, D. and Jin, Y. 2016. Regeneration of dental pulp/dentine complex with a three-dimensional and scaffold-free stem-cell sheet-derived pellet. *Journal of Tissue Engineering and Regenerative Medicine*,. **10**(3), pp.261-270.

Nagaoka, S., Miyazaki, Y., Liu, H.-J., Iwamoto, Y., Kitano, M. and Kawagoe, M. 1995. Bacterial invasion into dentinal tubules of human vital and nonvital teeth. *Journal of Endodontics*. **21**(2), pp.70-73.

Nagata, J.Y., Figueiredo de Almeida Gomes, B.P., Rocha Lima, T.F., Murakami, L.S., de Faria, D.E., Campos, G.R., de Souza-Filho, F.J. and Soares, A.d.J. 2014. Traumatized Immature Teeth Treated with 2 Protocols of Pulp Revascularization. *Journal of Endodontics*,. **40**(5), pp.606-612.

Nagy, M.M., Tawfik, H.E., Hashem, A.A.R. and Abu-Seida, A.M. 2014. Regenerative potential of immature permanent teeth with necrotic pulps after different regenerative protocols. *Journal of Endodontics*,. **40**(2), pp.192-198.

Nakashima, M. and Akamine, A. 2005. The application of tissue engineering to regeneration of pulp and dentin in endodontics. *Journal of Endodontics*,. **31**(10), pp.711-718.

Nakashima, M., Iohara, K., Bottino, M.C., Fouad, A.F., Nör, J.E. and Huang, G.T.-J. 2019. Animal models for stem cell-based pulp regeneration: foundation for

human clinical applications. *Tissue Engineering Part B: Reviews*. **25**(2), pp.100-113.

Nakashima, M., Iohara, K., Murakami, M., Nakamura, H., Sato, Y., Arijii, Y. and Matsushita, K. 2017. Pulp regeneration by transplantation of dental pulp stem cells in pulpitis: a pilot clinical study. *Stem Cell Research and Therapy*,. **8**(1), pp.1-13.

Nakayama, K.H., Batchelder, C.A., Lee, C.I. and Tarantal, A.F. 2010. Decellularized rhesus monkey kidney as a three-dimensional scaffold for renal tissue engineering. *Tissue Engineering Part A*. **16**(7), pp.2207-2216.

Nanci, A. 2017. *Ten Cate's Oral Histology: Development, Structure, and Function*. Elsevier Health Sciences.

Narang, I., Mittal, N. and Mishra, N. 2015. A comparative evaluation of the blood clot, platelet-rich plasma, and platelet-rich fibrin in regeneration of necrotic immature permanent teeth: a clinical study. *Contemporary clinical dentistry*,. **6**(1), p63.

Nasseri, B.A., Pomerantseva, I., Kaazempur-Mofrad, M.R., Sutherland, F.W., Perry, T., Ochoa, E., Thompson, C.A., Mayer Jr, J.E., Oesterle, S.N. and Vacanti, J.P. 2003. Dynamic rotational seeding and cell culture system for vascular tube formation. *Tissue Engineering*,. **9**(2), pp.291-299.

Nazzal, H. and Duggal, M. 2017. Regenerative endodontics: a true paradigm shift or a bandwagon about to be derailed?. *European Archives of Paediatric Dentistry*. **18**(1), pp.3-15.

Nicklas, J.A. and Buel, E. 2003. Quantification of DNA in forensic samples. *Analytical and Bioanalytical Chemistry*,. **376**(8), pp.1160-1167.

Nicoloso, G.F., Pötter, I.G., Rocha, R.d.O., Montagner, F. and Casagrande, L. 2017. A comparative evaluation of endodontic treatments for immature necrotic permanent teeth based on clinical and radiographic outcomes: a systematic review and meta-analysis. *International Journal of Paediatric Dentistry*,. **27**(3), pp.217-227.

Ning, L.-J., Zhang, Y.-J., Zhang, Y., Qing, Q., Jiang, Y.-L., Yang, J.-L., Luo, J.-C. and Qin, T.-W. 2015. The utilization of decellularized tendon slices to provide an inductive microenvironment for the proliferation and tenogenic differentiation of stem cells. *Biomaterials*. **52**, pp.539-550.

Novosel, E.C., Kleinhans, C. and Kluger, P.J. 2011. Vascularization is the key challenge in tissue engineering. *Advanced Drug Delivery Reviews*,. **63**(4-5), pp.300-311.

Novoseletskaya, E., Grigorieva, O., Efimenko, A.Y. and Kalinina, N. 2019. Extracellular matrix in the regulation of stem cell differentiation. *Biochemistry (Moscow)*. **84**(3), pp.232-240.

O'brien, F.J. 2011. Biomaterials & scaffolds for tissue engineering. *Materials Today*,. **14**(3), pp.88-95.

Östby, B. and Hjortdal, O. 1971. Tissue formation in the root canal following pulp removal. *European Journal of Oral Sciences*. **79**(3), pp.333-349.

Östby, B.N. 1961. The role of the blood clot in endodontic therapy an experimental histologic study. *Acta Odontologica Scandinavica*. **19**(3-4), pp.323-353.

Ott, H.C., Clippinger, B., Conrad, C., Schuetz, C., Pomerantseva, I., Ikonou, L., Kotton, D. and Vacanti, J.P. 2010. Regeneration and orthotopic transplantation of a bioartificial lung. *Nature Medicine*,. **16**(8), pp.927-933.

Ott, H.C., Matthiesen, T.S., Goh, S.-K., Black, L.D., Kren, S.M., Netoff, T.I. and Taylor, D.A. 2008. Perfusion-decellularized matrix: using nature's platform to engineer a bioartificial heart. *Nature medicine*. **14**(2), pp.213-221.

Paphangkorakit, J. and Osborn, J. 1998. Discrimination of hardness by human teeth apparently not involving periodontal receptors. *Archives of Oral Biology*. **43**(1), pp.1-7.

Parirokh, M. and Torabinejad, M. 2010. Mineral trioxide aggregate: a comprehensive literature review—part III: clinical applications, drawbacks, and mechanism of action. *Journal of Endodontics*. **36**(3), pp.400-413.

Pashley, D., Walton, R. and Slavkin, H. 2002. Histology and physiology of the dental pulp. *Endodontics 5th ed. Ingle JJ, Bakland LK. BC Decker Inc, Hamilton*. pp.25-60.

Pashley, D.H. 1996. Dynamics of the pulpo-dentin complex. *Critical Reviews in Oral Biology and Medicine*. **7**(2), pp.104-133.

Pellegata, A.F., Tedeschi, A.M. and De Coppi, P. 2018. Whole organ tissue vascularization: engineering the tree to develop the fruits. *Frontiers in Bioengineering and Biotechnology*,. **6**, p56.

Perniconi, B., Costa, A., Aulino, P., Teodori, L., Adamo, S. and Coletti, D. 2011. The pro-myogenic environment provided by whole organ scale acellular scaffolds from skeletal muscle. *Biomaterials*. **32**(31), pp.7870-7882.

Petrino, J. 2007. Revascularization of necrotic pulp of immature teeth with apical periodontitis. *Northwest Dentistry*. **86**(3), pp.33-35.

Petrino, J.A., Boda, K.K., Shambarger, S., Bowles, W.R. and McClanahan, S.B. 2010. Challenges in regenerative endodontics: a case series. *Journal of Endodontics*. **36**(3), pp.536-541.

Pitts, N., Chadwick, B. and Anderson, T. 2013. *Children's Dental Health Survey 2013. Report 2: Dental disease and damage in children England, Wales and Northern Island England. Health & Social Care Information Centre [Online]. [Accessed October 2020]. Available from: <https://tinyurl.com/y2h5dxob>.*

Piva, E., Silva, A.F. and Nör, J.E. 2014. Functionalized scaffolds to control dental pulp stem cell fate. *Journal of Endodontics*,. **40**(4), pp.S33-S40.

Pohanka, M. 2009. Monoclonal and polyclonal antibodies production-preparation of potent biorecognition element. *Journal of Applied Biomedicine*,. **7**, pp.115-121.

Pohto, P. and Antila, R. 1968. Demonstration of adrenergic nerve fibres in human dental pulp by histochemical fluorescence method. *Acta Odontologica Scandinavica*. **26**(1-2), pp.137-144.

Pradhan, D., Chawla, H., Gauba, K. and Goyal, A. 2006. Comparative evaluation of endodontic management of teeth with unformed apices with mineral trioxide aggregate and calcium hydroxide. *Journal of Dentistry for Children*. **73**(2), pp.79-85.

Prat-Vidal, C. and Bayes-Genis, A. 2020. Decellularized pericardial extracellular matrix: The preferred porous scaffold for regenerative medicine. *Xenotransplantation*,. **27**(1), pe12580.

Puchtler, H., Meloan, S.N. and Terry, M.S. 1969. On the history and mechanism of alizarin and alizarin red S stains for calcium. *Journal of Histochemistry and Cytochemistry*. **17**(2), pp.110-124.

Qiu, Q.Q., Leamy, P., Brittingham, J., Pomerleau, J., Kabaria, N. and Connor, J. 2009. Inactivation of bacterial spores and viruses in biological material using supercritical carbon dioxide with sterilant. *Journal of Biomedical Materials Research Part B: Applied Biomaterials* **91**(2), pp.572-578.

Rafter, M. 2005. Apexification: a review. *Dental Traumatology*. **21**(1), pp.1-8.

Rameshbabu, A.P., Bankoti, K., Datta, S., Subramani, E., Apoorva, A., Ghosh, P., Maity, P.P., Manchikanti, P., Chaudhury, K. and Dhara, S. 2018. Silk sponges ornamented with a placenta-derived extracellular matrix augment full-thickness cutaneous wound healing by stimulating neovascularization and cellular migration. *ACS Applied Materials and Interfaces*,. **10**(20), pp.16977-16991.

Ramos-Vara, J. 2005. Technical aspects of immunohistochemistry. *Veterinary Pathology*,. **42**(4), pp.405-426.

Ramos-Vara, J. and Miller, M. 2014. When tissue antigens and antibodies get along: revisiting the technical aspects of immunohistochemistry—the red, brown, and blue technique. *Veterinary Pathology*,. **51**(1), pp.42-87.

Ravindran, S. and George, A. 2015. Biomimetic extracellular matrix mediated somatic stem cell differentiation: applications in dental pulp tissue regeneration. *Frontiers in Physiology*,. **6**, p118.

Reing, J.E., Brown, B.N., Daly, K.A., Freund, J.M., Gilbert, T.W., Hsiong, S.X., Huber, A., Kullas, K.E., Tottey, S. and Wolf, M.T. 2010. The effects of processing methods upon mechanical and biologic properties of porcine dermal extracellular matrix scaffolds. *Biomaterials*. **31**(33), pp.8626-8633.

Ricard-Blum, S. and Salza, R. 2014. Matricryptins and matrikines: biologically active fragments of the extracellular matrix. *Experimental dermatology*. **23**(7), pp.457-463.

Richardson, T.P., Peters, M.C., Ennett, A.B. and Mooney, D.J. 2001. Polymeric system for dual growth factor delivery. *Nature Biotechnology*,. **19**(11), pp.1029-1034.

Rieder, E., Kasimir, M.-T., Silberhumer, G., Seebacher, G., Wolner, E., Simon, P. and Weigel, G. 2004. Decellularization protocols of porcine heart valves differ importantly in efficiency of cell removal and susceptibility of the matrix to recellularization with human vascular cells. *The Journal of Thoracic and Cardiovascular Surgery*,. **127**(2), pp.399-405.

- Robb, K.P., Shridhar, A. and Flynn, L.E. 2017. Decellularized matrices as cell-instructive scaffolds to guide tissue-specific regeneration. *ACS Biomaterials Science and Engineering*. **4**(11), pp.3627-3643.
- Roberts-Clark, D. and Smith, A. 2000. Angiogenic growth factors in human dentine matrix. *Archives of Oral Biology*. **45**(11), pp.1013-1016.
- Rodd, H.D., Davidson, L.E., Livesey, S. and Cooke, M.E. 2002. Survival of intentionally retained permanent incisor roots following crown root fractures in children. *Dental Traumatology*,. **18**(2), pp.92-97.
- Rosa, V., Zhang, Z., Grande, R.H.M. and Nör, J. 2013. Dental pulp tissue engineering in full-length human root canals. *Journal of Dental Research*. **92**(11), pp.970-975.
- Rosario, D.J., Reilly, G.C., Ali Salah, E., Glover, M., Bullock, A.J. and MacNeil, S. 2008. Decellularization and sterilization of porcine urinary bladder matrix for tissue engineering in the lower urinary tract. *Regenerative medicine*. **3**(2), pp.145-156.
- Rosenberg, B., Murray, P.E. and Namerow, K. 2007. The effect of calcium hydroxide root filling on dentin fracture strength. *Dental Traumatology*. **23**(1), pp.26-29.
- Ross, E.A., Williams, M.J., Hamazaki, T., Terada, N., Clapp, W.L., Adin, C., Ellison, G.W., Jorgensen, M. and Batich, C.D. 2009. Embryonic stem cells proliferate and differentiate when seeded into kidney scaffolds. *Journal of the American Society of Nephrology*. **20**(11), pp.2338-2347.
- Rouwkema, J., Rivron, N.C. and van Blitterswijk, C.A. 2008. Vascularization in tissue engineering. *Trends in Biotechnology*,. **26**(8), pp.434-441.
- Ruparel, N.B., Teixeira, F.B., Ferraz, C.C. and Diogenes, A. 2012. Direct effect of intracanal medicaments on survival of stem cells of the apical papilla. *Journal of Endodontics*. **38**(10), pp.1372-1375.
- Sadaghiani, L., Gleeson, H.B., Youde, S., Waddington, R.J., Lynch, C.D. and Sloan, A.J. 2016. Growth Factor Liberation and DPSC Response Following Dentine Conditioning. *Journal of Dental Research*. **95**(11), pp.1298-1307.
- Safavi, K.E. and Nichols, F.C. 1994. Alteration of biological properties of bacterial lipopolysaccharide by calcium hydroxide treatment. *Journal of Endodontics*,. **20**(3), pp.127-129.

Sahebi, S., Moazami, F. and Abbott, P. 2010. The effects of short-term calcium hydroxide application on the strength of dentine. *Dental Traumatology*,. **26**(1), pp.43-46.

Saito, T., Ogawa, M., Hata, Y. and Bessho, K. 2004. Acceleration effect of human recombinant bone morphogenetic protein-2 on differentiation of human pulp cells into odontoblasts. *Journal of Endodontics*,. **30**(4), pp.205-208.

Sakai, V., Zhang, Z., Dong, Z., Neiva, K., Machado, M.A.d.A.M., Shi, S., Santos, C.F.d. and Nör, J. 2010. SHED differentiate into functional odontoblasts and endothelium. *Journal of Dental Research*. **89**(8), pp.791-796.

Sakai, V.T., Cordeiro, M., Dong, Z., Zhang, Z., Zeitlin, B.D. and Nör, J.E. 2011. Tooth slice/scaffold model of dental pulp tissue engineering. *Advances in Dental Research*,. **23**(3), pp.325-332.

Salmivirta, K., Sorokin, L.M. and Ekblom, P. 1997. Differential expression of laminin α chains during murine tooth development. *Developmental dynamics: an official publication of the American Association of Anatomists*. **210**(3), pp.206-215.

Saoud, T.M.A., Zaazou, A., Nabil, A., Moussa, S., Aly, H.M., Okazaki, K., Rosenberg, P.A. and Lin, L.M. 2015. Histological observations of pulpal replacement tissue in immature dog teeth after revascularization of infected pulps. *Dental Traumatology*. **31**(3), pp.243-249.

Sarris, S., Tahmassebi, J.F., Duggal, M.S. and Cross, I.A. 2008. A clinical evaluation of mineral trioxide aggregate for root-end closure of non-vital immature permanent incisors in children-a pilot study. *Dental Traumatology*. **24**(1), pp.79-85.

Schmalz, G., Widbiller, M. and Galler, K.M. 2017. Signaling molecules and pulp regeneration. *Journal of Endodontics*,. **43**(9), pp.S7-S11.

Schmittgen, T.D. and Livak, K.J. 2008. Analyzing real-time PCR data by the comparative C T method. *Nature Protocols*,. **3**(6), p1101.

Schroder, U. 1971. Early reaction of intact human teeth to calcium hydroxide following experimental pulpotomy and its significance to the development of hard tissue barrier. *Odont Revy*. **22**, pp.379-396.

Scott, J.E. 1996. Alcian blue. Now you see it, now you don't. *European Journal of Oral Sciences*,. **104**(1), pp.2-9.

Seddon, A.M., Curnow, P. and Booth, P.J. 2004. Membrane proteins, lipids and detergents: not just a soap opera. *Biochimica et Biophysica Acta (BBA)-Biomembranes*. **1666**(1-2), pp.105-117.

Shabahang, S. and Torabinejad, M. 2000. Treatment of teeth with open apices using mineral trioxide aggregate. *Practical Periodontics and Aesthetic Dentistry*. **12**(3), pp.315-320.

Shi, S., Bartold, P., Miura, M., Seo, B., Robey, P. and Gronthos, S. 2005. The efficacy of mesenchymal stem cells to regenerate and repair dental structures. *Orthodontics and Craniofacial Research*. **8**(3), pp.191-199.

Shimizu, E., Jong, G., Partridge, N., Rosenberg, P.A. and Lin, L.M. 2012. Histologic observation of a human immature permanent tooth with irreversible pulpitis after revascularization/regeneration procedure. *Journal of Endodontics*. **38**(9), pp.1293-1297.

Shimizu, E., Ricucci, D., Albert, J., Alobaid, A.S., Gibbs, J.L., Huang, G.T.-J. and Lin, L.M. 2013. Clinical, radiographic, and histological observation of a human immature permanent tooth with chronic apical abscess after revitalization treatment. *Journal of Endodontics*. **39**(8), pp.1078-1083.

Shuttleworth, C., Ward, J. and Hirschmann, P. 1978. The presence of type III collagen in the developing tooth. *Biochimica et Biophysica Acta -Protein Structure*. **535**(2), pp.348-355.

Sigal, M., Aubin, J., Ten Cate, A. and Pitaru, S. 1984. The odontoblast process extends to the dentinoenamel junction: an immunocytochemical study of rat dentine. *Journal of Histochemistry and Cytochemistry*. **32**(8), pp.872-877.

Silujjai, J. and Linsuwanont, P. 2017. Treatment Outcomes of Apexification or Revascularization in Nonvital Immature Permanent Teeth: A Retrospective Study. *Journal of Endodontics*,. **43**(2), pp.238-245.

Silverman, J.D. and Kruger, L. 1987. An interpretation of dental innervation based upon the pattern of calcitonin gene-related peptide (CGRP)-immunoreactive thin sensory axons. *Somatosensory Research*. **5**(2), pp.157-175.

Silverman, R., Li, E., Holton, L., Sawan, K. and Goldberg, N. 2004. Ventral hernia repair using allogenic acellular dermal matrix in a swine model. *Hernia*. **8**(4), pp.336-342.

Simon, S., Rilliard, F., Berdal, A. and Machtou, P. 2007. The use of mineral trioxide aggregate in one-visit apexification treatment: a prospective study. *International Endodontic Journal*. **40**(3), pp.186-197.

Simon, S.R., Tomson, P.L. and Berdal, A. 2014. Regenerative Endodontics: Regeneration or Repair? *Journal of Endodontics*. **40**(4), pp.S70-S75.

Singh, S., Wu, B.M. and Dunn, J.C. 2011. Accelerating vascularization in polycaprolactone scaffolds by endothelial progenitor cells. *Tissue Engineering Part A*. **17**(13-14), pp.1819-1830.

Sloan, A. 2015. Chapter 29 - Biology of the Dentin-Pulp Complex. In: Vishwakarma, A., et al. eds. *Stem Cell Biology and Tissue Engineering in Dental Sciences*. Boston: Academic Press, pp.371-378.

Sloan, A. and Smith, A. 2007. Stem cells and the dental pulp: potential roles in dentine regeneration and repair. *Oral Diseases*. **13**(2), pp.151-157.

Sloan, A.J. and Waddington, R.J. 2009. Dental pulp stem cells: what, where, how? *International Journal of Paediatric Dentistry*. **19**(1), pp.61-70.

Smith, A., Murray, P., Sloan, A., Matthews, J. and Zhao, S. 2001. Trans-dentinal stimulation of tertiary dentinogenesis. *Advances in Dental Research*. **15**(1), pp.51-54.

Smith, A., Tobias, R., Plant, C., Browne, R., Lesot, H. and Ruch, J. 1990. In vivo morphogenetic activity of dentine matrix proteins. *Journal De Biologie Buccale*. **18**(2), pp.123-129.

Smith, A.J. 2003. Vitality of the dentin-pulp complex in health and disease: growth factors as key mediators. *Journal of Dental Education*. **67**(6), pp.678-689.

Smith, A.J., Duncan, H.F., Diogenes, A., Simon, S. and Cooper, P.R. 2016. Exploiting the bioactive properties of the dentin-pulp complex in regenerative endodontics. *Journal of Endodontics*. **42**(1), pp.47-56.

Smith, E.L., Colombo, J.S., Sloan, A.J. and Waddington, R.J. 2011. TGF-beta1 exposure from bone surfaces by chemical treatment modalities. *Eur Cells and Materials*,. **21**, pp.193-201.

Smith, J., Smith, A., Shelton, R. and Cooper, P. 2012. Recruitment of dental pulp cells by dentine and pulp extracellular matrix components. *Experimental Cell Research*,. **318**(18), pp.2397-2406.

Song, J., Takimoto, K., Jeon, M., Vadakekalam, J., Ruparel, N.B. and Diogenes, A. 2017. Decellularized human dental pulp as a scaffold for regenerative endodontics. *Journal of Dental Research*. **96**(6), pp.640-646.

Sonoyama, W., Liu, Y., Yamaza, T., Tuan, R.S., Wang, S., Shi, S. and Huang, G.T.-J. 2008. Characterization of the apical papilla and its residing stem cells from human immature permanent teeth: a pilot study. *Journal of Endodontics*. **34**(2), pp.166-171.

Stapleton, T.W., Ingram, J., Katta, J., Knight, R., Korossis, S., Fisher, J. and Ingham, E. 2008. Development and characterization of an acellular porcine medial meniscus for use in tissue engineering. *Tissue Engineering Part A*. **14**(4), pp.505-518.

Steiner, J. and Van Hassel, H. 1971. Experimental root apexification in primates. *Oral Surgery, Oral Medicine, Oral Pathology*. **31**(3), pp.409-415.

Stokes, D. 2008. *Principles and practice of variable pressure/environmental scanning electron microscopy (VP-ESEM)*. John Wiley & Sons.

Sui, B., Chen, C., Kou, X., Li, B., Xuan, K., Shi, S. and Jin, Y. 2019. Pulp Stem Cell–Mediated Functional Pulp Regeneration. *Journal of Dental Research*,. **98**(1), pp.27-35.

Sun, F., Jiang, Y., Xu, Y., Shi, H., Zhang, S., Liu, X., Pan, S., Ye, G., Zhang, W. and Zhang, F. 2016. Genipin cross-linked decellularized tracheal tubular matrix for tracheal tissue engineering applications. *Scientific reports*. **6**(1), pp.1-12.

Swinehart, I.T. and Badylak, S.F. 2016. Extracellular matrix bioscaffolds in tissue remodeling and morphogenesis. *Developmental Dynamics*. **245**(3), pp.351-360.

Syed-Picard, F., Ray Jr, H., Kumta, P. and Sfeir, C. 2014. Scaffoldless tissue-engineered dental pulp cell constructs for endodontic therapy. *Journal of Dental Research*. **93**(3), pp.250-255.

Thelen, D.S., Trovik, T.A. and Bårdsen, A. 2011. Impact of traumatic dental injuries with unmet treatment need on daily life among Albanian adolescents: a case–control study. *Dental Traumatology*. **27**(2), pp.88-94.

Thesleff, I. and Nieminen, P. 1996. Tooth morphogenesis and cell differentiation. *Current Opinion in Cell Biology*. **8**(6), pp.844-850.

Thibodeau, B., Teixeira, F., Yamauchi, M., Caplan, D.J. and Trope, M. 2007. Pulp revascularization of immature dog teeth with apical periodontitis. *Journal of Endodontics*. **33**(6), pp.680-689.

Thibodeau, B. and Trope, M. 2007. Pulp revascularization of a necrotic infected immature permanent tooth: case report and review of the literature. *Pediatric Dentistry*,. **29**(1), pp.47-50.

Tomlinson, M.J., Dennis, C., Yang, X.B. and Kirkham, J. 2015. Tissue non-specific alkaline phosphatase production by human dental pulp stromal cells is enhanced by high density cell culture. *Cell and Tissue Research*. **361**(2), pp.529-540.

Tong, H.J., Rajan, S., Bhujel, N., Kang, J., Duggal, M. and Nazzal, H. 2017. Regenerative Endodontic Therapy in the Management of Nonvital Immature Permanent Teeth: A Systematic Review—Outcome Evaluation and Meta-analysis. *Journal of Endodontics*. **43**(9), pp.1453-1464.

Torabinejad, M., Hong, C., McDonald, F. and Ford, T.P. 1995a. Physical and chemical properties of a new root-end filling material. *Journal of Endodontics*,. **21**(7), pp.349-353.

Torabinejad, M., Hong, C.-U., Lee, S.-J., Monsef, M. and Ford, T.R.P. 1995b. Investigation of mineral trioxide aggregate for root-end filling in dogs. *Journal of Endodontics*,. **21**(12), pp.603-608.

Torabinejad, M., Nosrat, A., Verma, P. and Udochukwu, O. 2017. Regenerative endodontic treatment or mineral trioxide aggregate apical plug in teeth with necrotic pulps and open apices: a systematic review and meta-analysis. *Journal of Endodontics*. **43**(11), pp.1806-1820.

Torabinejad, M., Walton, R.E. and Fouad, A. 2014. *Endodontics: Principles and practice*. Elsevier Health Sciences.

Totonelli, G., Maghsoudlou, P., Garriboli, M., Riegler, J., Orlando, G., Burns, A.J., Sebire, N.J., Smith, V.V., Fishman, J.M. and Ghionzoli, M. 2012. A rat decellularized small bowel scaffold that preserves villus-crypt architecture for intestinal regeneration. *Biomaterials*. **33**(12), pp.3401-3410.

Toyono, T., Nakashima, M., Kuhara, S. and Akamine, A. 1997. Expression of TGF- β superfamily receptors in dental pulp. *Journal of Dental Research*. **76**(9), pp.1555-1560.

- Tran, K.T., Lamb, P. and Deng, J.-S. 2005. Matrikines and matricryptins: Implications for cutaneous cancers and skin repair. *Journal of Dermatological Science*,. **40**(1), pp.11-20.
- Tran-Hung, L., Laurent, P., Camps, J. and About, I. 2008. Quantification of angiogenic growth factors released by human dental cells after injury. *Archives of Oral Biology*,. **53**(1), pp.9-13.
- Tran-Hung, L., Mathieu, S. and About, I. 2006. Role of human pulp fibroblasts in angiogenesis. *Journal of Dental Research*,. **85**(9), pp.819-823.
- Traphagen, S.B., Fourligas, N., Xylas, J.F., Sengupta, S., Kaplan, D.L., Georgakoudi, I. and Yelick, P.C. 2012. Characterization of natural, decellularized and reseeded porcine tooth bud matrices. *Biomaterials*. **33**(21), pp.5287-5296.
- Twati, W., Wood, D., Liskiewicz, T., Willmott, N. and Duggal, M. 2009b. An evaluation of the effect of non-setting calcium hydroxide on human dentine: a pilot study. *European Archives of Paediatric Dentistry*. **10**(2), pp.104-109.
- Uygun, B.E., Soto-Gutierrez, A., Yagi, H., Izamis, M.-L., Guzzardi, M.A., Shulman, C., Milwid, J., Kobayashi, N., Tilles, A. and Berthiaume, F. 2010. Organ reengineering through development of a transplantable recellularized liver graft using decellularized liver matrix. *Nature Medicine*,. **16**(7), pp.814-820.
- Vacanti, J.P. and Langer, R. 1999. Tissue engineering: the design and fabrication of living replacement devices for surgical reconstruction and transplantation. *The lancet*. **354**, pp.S32-S34.
- Van Amerongen, J., Lemmens, I.G. and Tonino, G. 1983. The concentration, extractability and characterization of collagen in human dental pulp. *Archives of Oral Biology*. **28**(4), pp.339-345.
- Villalona, G.A., Udelsman, B., Duncan, D.R., McGillicuddy, E., Sawh-Martinez, R.F., Hibino, N., Painter, C., Mirensky, T., Erickson, B. and Shinoka, T. 2010. Cell-seeding Techniques in Vascular Tissue Engineering,. *Tissue Engineering Part B: Reviews*,. **16**(3), pp.341-350.
- Vo, T.N., Kasper, F.K. and Mikos, A.G. 2012. Strategies for controlled delivery of growth factors and cells for bone regeneration. *Advanced Drug Delivery Reviews*,. **64**(12), pp.1292-1309.
- Vos, T., Abajobir, A.A., Abate, K.H., Abbafati, C., Abbas, K.M., Abd-Allah, F., Abdulkader, R.S., Abdulle, A.M., Abebo, T.A. and Abera, S.F. 2017. Global,

regional, and national incidence, prevalence, and years lived with disability for 328 diseases and injuries for 195 countries, 1990–2016: a systematic analysis for the Global Burden of Disease Study 2016. *The Lancet*. **390**(10100), pp.1211-1259.

Voytik-Harbin, S.L., Brightman, A.O., Kraine, M.R., Waisner, B. and Badylak, S.F. 1997. Identification of extractable growth factors from small intestinal submucosa. *Journal of Cellular Biochemistry*,. **67**(4), pp.478-491.

Waddington, R.J., Youde, S.J., Lee, C.P. and Sloan, A.J. 2009. Isolation of distinct progenitor stem cell populations from dental pulp. *Cells Tissues Organs*,. **189**(1-4), pp.268-274.

Wang, Q., Lin, X., Lin, Z., Liu, G. and Shan, X. 2007. Expression of vascular endothelial growth factor in dental pulp of immature and mature permanent teeth in human. *Shanghai Journal of Stomatology*. **16**(3), pp.285-289.

Wang, X., Thibodeau, B., Trope, M., Lin, L.M. and Huang, G.T.-J. 2010. Histologic characterization of regenerated tissues in canal space after the revitalization/revascularization procedure of immature dog teeth with apical periodontitis. *Journal of Endodontics*. **36**(1), pp.56-63.

Wei, X., Ling, J., Wu, L., Liu, L. and Xiao, Y. 2007. Expression of mineralization markers in dental pulp cells. *Journal of Endodontics*,. **33**(6), pp.703-708.

Widbiller, M., Althumairy, R.I. and Diogenes, A. 2019. Direct and indirect effect of chlorhexidine on survival of stem cells from the apical papilla and its neutralization. *Journal of Endodontics*. **45**(2), pp.156-160.

Widbiller, M., Driesen, R.B., Eidt, A., Lambrichts, I., Hiller, K.-A., Buchalla, W., Schmalz, G. and Galler, K.M. 2018. Cell homing for pulp tissue engineering with endogenous dentin matrix proteins. *Journal of Endodontics*,. **44**(6), pp.956-962. e952.

Wilshaw, S.-P., Kearney, J.N., Fisher, J. and Ingham, E. 2006. Production of an acellular amniotic membrane matrix for use in tissue engineering. *Tissue Engineering*. **12**(8), pp.2117-2129.

Wilshaw, S.-P., Rooney, P., Berry, H., Kearney, J.N., Homer-Vanniasinkam, S., Fisher, J. and Ingham, E. 2012. Development and characterization of acellular allogeneic arterial matrices. *Tissue Engineering Part A*. **18**(5-6), pp.471-483.

Witherspoon, D.E., Small, J.C., Regan, J.D. and Nunn, M. 2008. Retrospective analysis of open apex teeth obturated with mineral trioxide aggregate. *Journal of Endodontics*,. **34**(10), pp.1171-1176.

Wittekind, D. 2003. Traditional staining for routine diagnostic pathology including the role of tannic acid. 1. Value and limitations of the hematoxylin-eosin stain. *Biotechnology and Histochemistry*,. **78**(5), pp.261-270.

Xu, H., Wan, H., Zuo, W., Sun, W., Owens, R.T., Harper, J.R., Ayares, D.L. and McQuillan, D.J. 2009. A porcine-derived acellular dermal scaffold that supports soft tissue regeneration: removal of terminal galactose- α -(1, 3)-galactose and retention of matrix structure. *Tissue Engineering Part A*. **15**(7), pp.1807-1819.

Xuan, K., Li, B., Guo, H., Sun, W., Kou, X., He, X., Zhang, Y., Sun, J., Liu, A. and Liao, L. 2018. Deciduous autologous tooth stem cells regenerate dental pulp after implantation into injured teeth. *Science Translational Medicine*. **10**(455).

Yadlapati, M., Bigueti, C., Cavalla, F., Nieves, F., Bessey, C., Bohluli, P., Garlet, G.P., Letra, A., Fakhouri, W.D. and Silva, R.M. 2017. Characterization of a vascular endothelial growth factor–loaded bioresorbable delivery system for pulp regeneration. *Journal of Endodontics*,. **43**(1), pp.77-83.

Yamauchi, N., Nagaoka, H., Yamauchi, S., Teixeira, F.B., Miguez, P. and Yamauchi, M. 2011. Immunohistological characterization of newly formed tissues after regenerative procedure in immature dog teeth. *Journal of Endodontics*. **37**(12), pp.1636-1641.

Yang, J., Yuan, G. and Chen, Z. 2016. Pulp regeneration: current approaches and future challenges. *Frontiers in Physiology*. **7**, p58.

Yang, S., Leong, K.-F., Du, Z. and Chua, C.-K. 2001. The design of scaffolds for use in tissue engineering. Part I. Traditional factors. *Tissue Engineering*,. **7**(6), pp.679-689.

Yassen, G.H. and Platt, J.A. 2013. The effect of nonsetting calcium hydroxide on root fracture and mechanical properties of radicular dentine: a systematic review. *International Endodontic Journal*. **46**(2), pp.112-118.

Yu, C. and Abbott, P.V. 2007. An overview of the dental pulp: its functions and responses to injury. *Australian Dental Journal*. **52**, pp.S4-S6.

Yuan, Z., Nie, H., Wang, S., Lee, C.H., Li, A., Fu, S.Y., Zhou, H., Chen, L. and Mao, J.J. 2011. Biomaterial selection for tooth regeneration. *Tissue Engineering Part B: Reviews*. **17**(5), pp.373-388.

Yuasa, K., Fukumoto, S., Kamasaki, Y., Yamada, A., Fukumoto, E., Kanaoka, K., Saito, K., Harada, H., Arikawa-Hirasawa, E. and Miyagoe-Suzuki, Y. 2004. Laminin $\alpha 2$ is essential for odontoblast differentiation regulating dentin sialoprotein expression. *Journal of Biological Chemistry*. **279**(11), pp.10286-10292.

Zantop, T., Gilbert, T.W., Yoder, M.C. and Badylak, S.F. 2006. Extracellular matrix scaffolds are repopulated by bone marrow-derived cells in a mouse model of achilles tendon reconstruction. *Journal of Orthopaedic Research*. **24**(6), pp.1299-1309.

Zeichner-David, M., Oishi, K., Su, Z., Zakartchenko, V., Chen, L.S., Arzate, H. and Bringas Jr, P. 2003. Role of Hertwig's epithelial root sheath cells in tooth root development. *Developmental dynamics: an official publication of the American Association of Anatomists*. **228**(4), pp.651-663.

Zhang, Q., Johnson, J.A., Dunne, L.W., Chen, Y., Iyyanki, T., Wu, Y., Chang, E.I., Branch-Brooks, C.D., Robb, G.L. and Butler, C.E. 2016. Decellularized skin/adipose tissue flap matrix for engineering vascularized composite soft tissue flaps. *Acta Biomaterialia*,. **35**, pp.166-184.

Zhang, W., Vazquez, B., Oreadi, D. and Yelick, P. 2017. Decellularized tooth bud scaffolds for tooth regeneration. *Journal of Dental Research*,. **96**(5), pp.516-523.

Zhang, X. and Dong, J. 2015. Direct comparison of different coating matrix on the hepatic differentiation from adipose-derived stem cells. *Biochemical and Biophysical Research Communications*. **456**(4), pp.938-944.

Zhao, S., Sloan, A.J., Murray, P.E., Lumley, P.J. and Smith, A.J. 2000. Ultrastructural Localisation of TGF- β Exposure in Dentine by Chemical Treatment. *The Histochemical Journal*,. **32**(8), pp.489-494.

Zhao, W., Han, Q., Lin, H., Sun, W., Gao, Y., Zhao, Y., Wang, B., Wang, X., Chen, B. and Xiao, Z. 2009. Human basic fibroblast growth factor fused with Kringle4 peptide binds to a fibrin scaffold and enhances angiogenesis. *Tissue Engineering Part A*. **15**(5), pp.991-998.

Zhao, Y., Zhang, S., Zhou, J., Wang, J., Zhen, M., Liu, Y., Chen, J. and Qi, Z. 2010. The development of a tissue-engineered artery using decellularized

scaffold and autologous ovine mesenchymal stem cells. *Biomaterials*. **31**(2), pp.296-307.

Zhu, X., Liu, J., Yu, Z., Chen, C.-A., Aksel, H., Azim, A.A. and Huang, G.T.-J. 2018. A miniature swine model for stem cell-based de novo regeneration of dental pulp and dentin-like tissue. *Tissue Engineering Part C: Methods*. **24**(2), pp.108-120.

Appendices

Appendix A: Ethical approvals

- I. Details of the ethical approval obtained from the Dental Research Ethics Committee at the University of Leeds (School of Dentistry Research Tissue Bank; Reference Number 060516/HA/204) for the isolation and use of human dental pulp stem cells from extracted human teeth are shown below.

	
Tissue Sample Form for School of Dentistry Research Tissue Bank	
Applicant: Hayat Alghutaimel	
DREC No: 060516/HA/204	
Research Tissue:	
<div style="border: 1px solid black; padding: 10px; margin: 10px auto; width: 80%;"><p>Bank ID No:.....</p><p>Age of patient (time of collection):.....</p><p>Sex:</p><p>Ethnic Origin:.....</p> <p>Signed (Recipient):</p><p>Signed (Supplier):.....</p><p>Date sample taken:.....</p></div>	
<p>Please ensure Bank ID number is recorded on all samples created from tissue received from the Tissue Bank.</p> <p>This is a requirement of the Human Tissue Act. By receiving tissue from the bank you are agreeing to abide by the HTA regulations.</p> <p>Useful links: http://www.hta.gov.uk/ Human Tissue Authority website http://www.opsi.gov.uk/acts/acts2004/ukpga_20040030_en_1 Human Tissue Act 2004</p>	

II. Details of the ethical approvals obtained from NHS Health Research Authority, East Midlands–Nottingham-2 Research Ethics Committee for the collection and use of extracted human teeth are shown below.



Dr H. Alghutaimel
Integrated PhD and MSc in Paediatric Dentistry
University of Leeds
Department of Paediatric Dentistry,
School of Dentistry
Level 6, Worsley Building,
Clarendon Way,
Leeds,
W. Yorkshire
LS29LU

Email: hra.approval@nhs.net

10 March 2017

Dear Dr H. Alghutaimel

Letter of HRA Approval

Study title:	Regenerative Endodontic Techniques for The Management of Non Vital Immature Permanent Teeth: Generation of Dental Pulp-like tissue Using Decellularized Natural Pulp tissue scaffold and Dental pulp stem cells – Feasibility Study
IRAS project ID:	212756
REC reference:	17/EM/0040
Sponsor	University of Leeds

I am pleased to confirm that **HRA Approval** has been given for the above referenced study, on the basis described in the application form, protocol, supporting documentation and any clarifications noted in this letter.

Participation of NHS Organisations in England

The sponsor should now provide a copy of this letter to all participating NHS organisations in England.

Appendix B provides important information for sponsors and participating NHS organisations in England for arranging and confirming capacity and capability. **Please read *Appendix B* carefully**, in particular the following sections:

- *Participating NHS organisations in England* – this clarifies the types of participating organisations in the study and whether or not all organisations will be undertaking the same activities
- *Confirmation of capacity and capability* - this confirms whether or not each type of participating NHS organisation in England is expected to give formal confirmation of capacity and capability. Where formal confirmation is not expected, the section also provides details on the time limit given to participating organisations to opt out of the study, or request additional time, before their participation is assumed.

Page 1 of 8



Health Research Authority

East Midlands - Nottingham 2 Research Ethics Committee

The Old Chapel
Royal Standard Place
Nottingham
NG1 6FS

Please note: This is the favourable opinion of the REC only and does not allow you to start your study at NHS sites in England until you receive HRA Approval

10 March 2017

Dr Hayat Alghutaimel
Integrated PhD and MSc in Paediatric Dentistry
UNIVERSITY OF LEEDS
Department of Paediatricdentistry,
School of Dentistry
Level6,
Worsley Building,
ClarendonWay,
LS29LU

Dear Dr Alghutaimel

Study title:	Regenerative Endodontic Techniques for The Management of Non Vital Immature Permanent Teeth: Generation of Dental Pulp-like tissue Using Decellularized Natural Pulp tissue scaffold and Dental pulp stem cells – Feasibility Study
REC reference:	17/EM/0040
IRAS project ID:	212756

Thank you for your submission of 27 February 2017 responding to the Proportionate Review Sub-Committee's request for changes to the documentation for the above study.

The revised documentation has been reviewed and approved by the sub-committee.

We plan to publish your research summary wording for the above study on the HRA website, together with your contact details. Publication will be no earlier than three months from the date of this favourable opinion letter. The expectation is that this information will be published for all studies that receive an ethical opinion but should you wish to provide a substitute contact point, wish to make a request to defer, or require further information, please contact please contact hra_studyregistration@nhs.net outlining the reasons for your request.

III. Details of the personal licence granted by the Home Office for performing regulated scientific procedures on mice and rats are shown below.

I2E7F18DE 21 May 2018	OFFICIAL - SENSITIVE
 Home Office	
No. I2E7F18DE	
ANIMALS (SCIENTIFIC PROCEDURES) ACT 1986	
PERSONAL LICENCE	
to	
carry out regulated procedures on living animals.	
In pursuance of the powers vested in him by the above Act, the Secretary of State hereby licenses	
Dr Hayat Al-Ghutaimel The University of Leeds Leeds LS2 9JT	
to apply regulated procedures of the category or categories specified below to animals of the species or groups specified below at places specified in authorised project licences subject to the restrictions and provisions contained in the Act, and subject also to the limitations and conditions contained in this licence and to such other conditions as the Secretary of State may from time to time prescribe:	
Description of animal(s)	
<ul style="list-style-type: none">• Mice• Rats	
Categories of regulated procedure:	
A. Minor/minimally invasive procedures not requiring sedation, analgesia or general anaesthesia B. Minor/minimally invasive procedures involving sedation, analgesia or brief general anaesthesia. Plus surgical procedures conducted under brief non-recovery general anaesthesia C. Surgical procedures involving general anaesthesia. Plus administration and maintenance of balanced or prolonged general anaesthesia	
This licence shall be in force until revoked by the Secretary of State and shall be periodically	
<small>The Home Office, in line with the rest of HMG, has implemented the Government Security Classification (GSC). Details of the GSC can be found at https://www.gov.uk/government/publications/government-security-classifications. Please note that documents and emails you receive may contain specific handling instructions. Handling Instructions: Contains personal sensitive information, subject to confidentiality requirements under the Data Protection Act. This should only be circulated in accordance with ASPA Guidance and stored in a locked secure location. All government information may be subject to an FOI request and subsequent assessment. UUID: 1983418 Page 2/6</small>	

Appendix B: Presentations and scientific awards

Presentations	
July 2017	<u>Hayat Alghutaimel</u> , Hani Nazzal, Monty Duggal, El Mostafa Raïf. Decellularisation and characterisation of bovine dental pulp tissue. Research day at the school of dentistry, University of Leeds (July 12 th , 2017), Leeds, United Kingdom. (Poster presentation)
June 2018	<u>Hayat Alghutaimel</u> , Hani Nazzal, Monty Duggal, Xuebin Yang, El Mostafa Raïf. Development of a biocompatible acellular bovine dental pulp tissue for potential use as a xenogeneic scaffold in regenerative endodontics. 14 th EAPD congress (June 20-23, 2018), Lugano, Switzerland. (Oral presentation)
July 2018	<u>Hayat Alghutaimel</u> , Hani Nazzal, Monty Duggal, Xuebin Yang, El Mostafa Raïf. Development of a biocompatible acellular bovine dental pulp tissue for potential use as a xenogeneic scaffold in regenerative endodontics. Research day at the school of dentistry, University of Leeds (July 12 th , 2018), Leeds, United Kingdom. (Oral presentation)
Sep. 2019	<u>Hayat Alghutaimel</u> , Xuebin Yang, Hani Nazzal, Bernadette Drummond, Monty Duggal, El Mostafa Raïf. Decellularised bovine dental pulp as a scaffold for regenerative endodontics: <i>in vitro</i> and <i>in vivo</i> studies. British society for oral and dental research congress (September 3-5, 2019), Leeds, United Kingdom. (Oral presentation)
Dec. 2019	<u>Hayat Alghutaimel</u> , Xuebin Yang, Hani Nazzal, Bernadette Drummond, Monty Duggal, El Mostafa Raïf. Decellularised bovine dental pulp as a scaffold for regenerative endodontics: <i>in vitro</i> and <i>in vivo</i> studies. TERMIS-AM conference (December 2-5, 2019), Orlando, United states. (Poster presentation)
July 2020	<u>Hayat Alghutaimel</u> , Xuebin Yang, Hani Nazzal, Bernadette Drummond, Monty Duggal, El Mostafa Raïf. Decellularised Bovine Dental Pulp as a Biological Scaffold for Regenerative Endodontic Therapy. 15 th EAPD virtual congress (July 3-4, 2020). (Oral Presentation)

Scientific awards

June 2018	<u>Young Scientist Research Award (joint 1st place)</u> . 14 th EAPD congress (June 20-23, 2018), Lugano, Switzerland.
July 2018	<u>Best Research Oral Presentation Award</u> . Research day at the school of dentistry, University of Leeds (July 12 th , 2018), Leeds, United Kingdom.
July 2018	<u>Research Booklet Image Award</u> . Research day at the school of dentistry, University of Leeds (July 12 th , 2018), Leeds, United Kingdom.
